NEW YORK STATE OF OPPORTUNITY. | NYSERDA

Assessment of an Urban Microgrid

Final Report

July 2017

NYSERDA's Promise to New Yorkers:

NYSERDA provides resources, expertise, and objective information so New Yorkers can make confident, informed energy decisions.

Mission Statement:

Advance innovative energy solutions in ways that improve New York's economy and environment.

Vision Statement:

Serve as a catalyst – advancing energy innovation, technology, and investment; transforming New York's economy; and empowering people to choose clean and efficient energy as part of their everyday lives.

Assessment of an Urban Microgrid

Final Report

Prepared for:

New York State Energy Research and Development Authority

Albany, NY

Prepared by:

Electric Power Research Institute

Palo Alto, CA

NYSERDA Contract 36660 July 2017

NOTICE

This report was prepared by Electric Power Research Institute in the course of performing work contracted for and sponsored by the New York State Energy Research and Development Authority (hereafter "NYSERDA"). The opinions expressed in this report do not necessarily reflect those of NYSERDA or the State of New York, and reference to any specific product, service, process, or method does not constitute an implied or expressed recommendation or endorsement of it. Further, NYSERDA, the State of New York, and the contractor make no warranties or representations, expressed or implied, as to the fitness for particular purpose or merchantability of any product, apparatus, or service, or the usefulness, completeness, or accuracy of any processes, methods, or other information contained, described, disclosed, or referred to in this report. NYSERDA, the State of New York, and the contractor make no representation that the use of any product, apparatus, process, method, or other information will not infringe privately owned rights and will assume no liability for any loss, injury, or damage resulting from, or occurring in connection with, the use of information contained, described, disclosed, or referred to in this report.

NYSERDA makes every effort to provide accurate information about copyright owners and related matters in the reports we publish. Contractors are responsible for determining and satisfying copyright or other use restrictions regarding the content of reports that they write, in compliance with NYSERDA's policies and federal law. If you are the copyright owner and believe a NYSERDA report has not properly attributed your work to you or has used it without permission, please email print@nyserda.ny.gov

Information contained in this document, such as web page addresses, are current at the time of publication.

ACKNOWLEDGMENTS

The following organizations, under contract to the Electric Power Research Institute (EPRI), assisted in the data collection, modelling, and analysis for this report:

- The University of Buffalo Energy Systems Integration Labs (ESI).
- The University of Texas at Austin
- Microgrid Labs, Inc.
- Industrial Economics, Inc.

The following Organizations participated in this project in a partnering capacity:

- Buffalo Niagara Medical Campus
- National Grid
- Kaleida Health
- The Roswell Park Cancer Institute
- The University of Buffalo
- The Hauptman-Woodward Institute (HWI)

Other contributing organization who were also involved in related efforts for the NY Prize Stage 1 effort include:

- Navigant Consulting
- CDH
- Wendell
- National Fuel

This report was written by EPRI.

ABSTRACT

This study was designed to support the continued growth of the Campus and Buffalo Niagara Region by exploring and evaluating distributed and renewable energy sources against the existing distribution system on-and-around the Campus to accomplish targeted grid modernization and to realize grid resiliency. The project determined the feasibility and best approaches to leverage grid modernization with end-user power technologies. It was intended to meet the needs of high-tech urban business campuses like the BNMC. The power system and power quality characteristics at various voltage levels were identified and used to benchmark the existing system's power quality and reliability. Realistic optimization possibilities for power quality and energy efficiency were identified throughout the power grid as well as within BNMC customer facilities. The benefit of innovative systems such as micro-grids and renewable energy sources toward improving the reliability, sustainability, and quality of the power system were determined along with the feasibility of implementing a self-sustainable energy hub for this area in the event of major utility outages or natural disasters.

Keywords
Microgrid

BNMC

New York Prize

Distributed Generation

DER

Assessment of an Urban Microgrid, NYSERDA Project Number: 36660

PRIMARY AUDIENCE: Those working with or interested in a microgrid capable of supporting its connected load as well as connecting to and islanding from the existing utility grid.

KEY RESEARCH QUESTION

What considerations are necessary for the design of a grid-connected microgrid capable of sustaining its own connected loads while connecting to and disconnecting from an existing utility grid.

RESEARCH OVERVIEW

The project determined the feasibility and best approaches to leverage grid modernization with end-user power technologies. It was intended to meet the needs of high-tech urban business campuses like the BNMC. The power system and power quality characteristics at various voltage levels were identified and used to benchmark the existing system's power quality and reliability. Realistic optimization possibilities for power quality and energy efficiency were identified throughout the power grid as well as within BNMC customer facilities. The benefit of innovative systems such as micro-grids and renewable energy sources toward improving the reliability, sustainability, and quality of the power system were determined along with the feasibility of implementing a self-sustainable energy hub for this area in the event of major utility outages or natural disasters.

KEY FINDINGS

- Monitored the power system characteristics for various voltage levels and benchmarked the existing power quality and reliability environment
- Identified power quality and energy efficiency optimization possibilities throughout the local power grid
- Determined the benefit of innovative systems such as microgrids and renewable energy sources to improve the reliability, sustainability, and quality of the power system
- Determined feasibility of implementing a self-sustainable energy hub

WHY THIS MATTERS

Self-sustaining systems such as micro-grids and renewable energy sources may significantly improve the reliability, sustainability, and quality of the power system in the event of major utility outages or natural disasters.

This publication is a corporate document that should be cited in the literature in the following manner:

Assessment of an Urban Microgrid, NYSERDA Project Number: 36660. EPRI, Palo Alto, CA: 2017.

CONTENTS

Electric Power Research Institute
3420 Hillview Avenue, Palo Alto, California 94304-1338 • PO Box 10412, Palo Alto, California 94303-0813 USA
800.313.3774 • 650.855.2121 • askepri@epri.com • www.epri.com

LIST OF FIGURES

Electric Power Research Institute
3420 Hillview Avenue, Palo Alto, California 94304-1338 • PO Box 10412, Palo Alto, California 94303-0813 USA
800.313.3774 • 650.855.2121 • askepri@epri.com • www.epri.com

Electric Power Research Institute
3420 Hillview Avenue, Palo Alto, California 94304-1338 • PO Box 10412, Palo Alto, California 94303-0813 USA
800.313.3774 • 650.855.2121 • askepri@epri.com • www.epri.com

LIST OF TABLES

1
EXECUTIVE SUMMARY

The Electrical Power Research Institute, National Grid, the University of Buffalo Energy Systems Integration (ESI) Lab, and the Buffalo Niagara Medical Campus received an award from NYSERDA to evaluate the electric grid in the BNMC and surrounding Allentown and Fruitbelt areas. This study was designed to support the continued growth of the Campus and Buffalo Niagara Region by exploring and evaluating distributed and renewable energy sources against the existing distribution system on-and-around the Campus to accomplish targeted grid modernization and to realize grid resiliency. The project determined the feasibility and best approaches to leverage grid modernization with end-user power technologies. It was intended to meet the needs of high-tech urban business campuses like the BNMC. The power system and power quality characteristics at various voltage levels were identified and used to benchmark the existing system's power quality and reliability. Realistic optimization possibilities for power quality and energy efficiency were identified throughout the power grid as well as within BNMC customer facilities. The benefit of innovative systems such as micro-grids and renewable energy sources toward improving the reliability, sustainability, and quality of the power system were determined along with the feasibility of implementing a self-sustainable energy hub for this area in the event of major utility outages or natural disasters.

Objective and Scope of Project

Specifically, the goals of the project were:

- Monitor the power system characteristics for various voltage levels and benchmark the existing power quality and reliability environment.
- Identify power quality and energy efficiency optimization possibilities throughout the local power grid and within BNMC customer facilities
- Analyze results in the context of improving electric power for end users by combining attributes of both the grid and distributed energy resources.
- Determine the benefit of innovative systems such as microgrids and renewable energy sources to improve the reliability, sustainability, and quality of the power system
- Determine feasibility of implementing a self-sustainable energy hub for the BNMC campus and surrounding areas

Project Benefits

This project provided a systematic approach to:

- evaluating a local urban electrical system regarding effective monitoring, monitor selection and placement
- gathering and analysis of data collected for such a system regarding reliability, power quality and energy efficiency

- identification of realistic improvements to the system as indicated by the data and economic analysis
- optimum location, sizing, rating, and control configuration of emerging advanced power system elements and solutions

For the state of New York, this study provides a model for other municipalities in the state and local areas within those municipalities to create similar energy hubs. The emerging advanced power system elements—photovoltaic arrays, wind generation, energy storage, etc.—could also serve in themselves to boost local economic development.

This study, a feasibility analysis, evaluates a tiered approach that builds upon the resiliency of its existing underground network, backup generation assets, distributed energy resources (DER), and energy-efficient facilities. As illustrated in the figure below, this microgrid strategy consists of three layers that would ultimately lead to a regional community microgrid enabling the service footprint of National Grid's Elm Street Substation, which includes the Campus, its surrounding neighborhoods, and greater Buffalo, to withstand a catastrophic weather event or system failure while also positioning itself to leverage 'blue-sky' monetization opportunities.

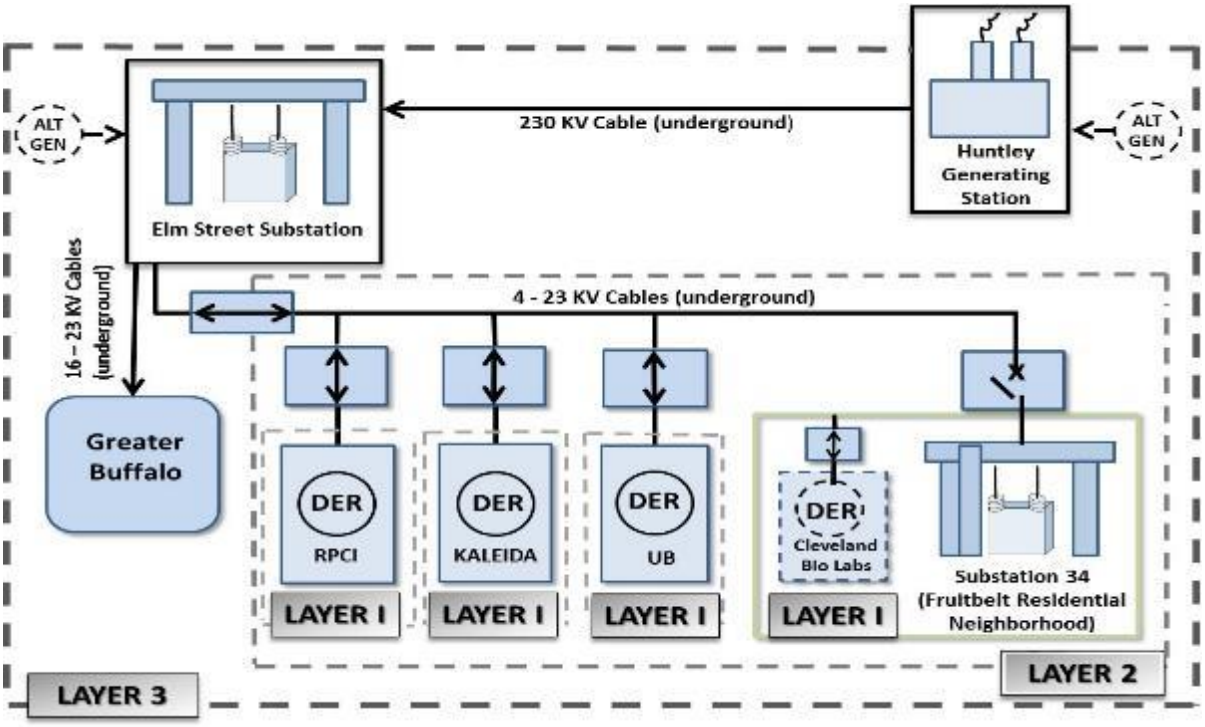

Figure 1-1. Proposed BNMC Community Grid Strategy for Greater Buffalo

The (3) layers of the proposed microgrid strategy consist of:

- **Layer 1**: As a precursor to a Campus-centric, dynamic portfolio, enabling each of the member institutions who employ emergency, back-up generation to disconnect, island, and optimize their facilities during weather or system-related events in order to maximize the capability of their back-up generating systems and other DER assets. This layer is characterized by maximizing the use of existing back-up generation assets (that electrically

cannot be paralleled with the grid), existing/planned DER's and optimizing the loading and control of individual member institution facilities. Existing and/or future generation assets could potentially serve facilities that are currently without back-up generation.

- **Layer 2**: Enabling the aggregate Campus to draw from on-site generation resources/DER at the individual member institution level or from common locations to disconnect during weather while also positioned to leverage 'blue-sky' monetization opportunities.
    - Layer 2 is characterized by installing individual interface equipment to connect the member institutions' back-up generation to the grid, making it available to others on the Campus, and potentially to the close to 2,000 residential and 500 commercial customers residing in Buffalo's Fruit Belt neighborhood who are served by National Grid's Substation 34, during grid outages. This layer also allows member institutions to self-generate and participate in energy markets (e.g. ISO markets, potential distribution level and future opportunities under the Distributed System Platform (DSP) model) under normal, grid-connected mode.
- **Layer 3**: Creating a regional community microgrid. Initially, this was proposed to be accomplished through installation of combined-cycle gas turbines either at the Huntley Generating Station or within National Grid's right-of-way at the Elm Street Substation. However, the Huntley facility is now closed leaving only the Elm Street Substation (supplied by Gardenville) available for this purpose. This new source would work in tandem with campus back-up generation and National Grid's existing infrastructure to ensure regional load served by the Elm Street Substation remains on-line during weather or system-related events.

In addition to enabling both the Campus and portions of the adjacent Fruit Belt residential neighborhood that share common infrastructure to endure weather-related or other adverse grid events, the proposed approach may enable member institutions to capitalize on available revenue and market opportunities for grid- paralleled generation during the vast majority of time.

Project Pre-Work (Phase 1)

The overall effort at the BNMC actually consisted of two phases. Funded solely by National Grid, the Phase 1 effort accomplished preliminary tasks that helped enable the success of the NYSERDA Urban Microgrid Project 36660 (Phase 2). Beginning in early 2013, EPRI worked with National Grid to begin to conceptualize a grid modernization and power quality study for the BNMC. This work ultimately included several tasks that were designed to directly support the overall Urban Microgrid project in which the project team was awarded in 2014. The Phase 1 project included three major tasks as noted below.

Task 1.1: Identification of Source Information

The purpose of this task was to identify the base-line information required to start the overall grid modernization project. These tasks included identifying the circuits inside and outside the site boundary areas. The initial circuit data and drawing information was exchanged between EPRI and National Grid. In this work, the sourcing substations were identified for both the medical center and residential center customers. Finally, the power quality monitoring hardware needs were discussed and identified.

Task 1.2: Identify Electrical System Load Information

In order to provide recommendations to modernize the overall grid feeding the BNMC and related residential areas, the breakout of the power users and load make-up needed to be understood. In this task, the metering load data was obtained from the feeding substations as well as the individual participant entities at the BNMC. The consumption and load shapes were identified. This information was compared against the total capacity of the existing electrical infrastructure that feeds the site to determine the potential for additional load growth within the context of the initial structure of the power distribution system.

Task 1.3: Determine Customer Load Information

This work involved determining the types of businesses in the survey area, the configuration of their electrical interconnection to the utility power system, related tariffs, and metering equipment that is already in place. The task also involved assessing BNMC campus tenants and a subset of residential customers to determine the types of specific loads within their premises that use electric power. Loads such as computers, chillers, compressors, lighting, motor controls and various medical surgical and diagnostic machines will be of specific interest. The sensitivity of specific equipment within the customer premises to anomalies on the grid was assessed based on the specific design and make-up of the system components, existing power quality data, and by site walk-downs and interviews with the member entities. The customer side assessments also included examination of any power quality and reliability protection strategies and practices already in-place. This work also included documenting the existing energy efficiency measures that have been adopted in the customer facilities. Facilities targeted in this effort included the Innovation Center, Cleveland BioLabs, Hauptman-Woodward Institute, the Kaleida Health (KH) Campus, Roswell Park Cancer Institute (RCPI), and the University of Buffalo (UB) facilities.

NYSERDA Urban Microgrid Project 36660 (Phase 2)

In this engineering study, the Electric Power Research Institute (EPRI), along with its partners the University of Buffalo, National Grid and the Buffalo Niagara Medical Campus (BNMC) conducted an assessment of microgrid options at BNMC. A systematic approach to evaluating a local urban microgrid options included the selection and placement of monitoring devices and controls; the gathering and analysis of data collected for such a system regarding reliability, power quality and energy efficiency; the identification of realistic improvements to the system as indicated by the data and economic analysis; the optimum location, sizing, rating, and control configuration of emerging advanced power system elements and solutions. It is intended that the methodologies and results of this study serve as a model for other municipalities in the state and local areas within those municipalities to create similar energy hubs and microgrids. With the effort officially kicking off in December, 2014, the project work by tasks and the overall findings of each task is summarized below. Detailed information may be found in the accompanying appendices at the end of this report.

Task 2.1: Economic Analysis and Tech Transfer Plan

An *Initial Economic Analysis and Tech Transfer Plan* was performed for the KH facility alone as an earlier part of the BNMC effort. This Task 2.1 Report by Industrial Economics, Incorporated was completed in October of 2015. The technology transfer plan was presented to NYSERDA in the Kickoff meeting held earlier in December 2014.

Subsequent to that earlier effort and being informed by it, the BNMC team decided to examine the microgrid concept at the community level. This later analysis is provided in Chapter 2, *NY Prize Feasibility Study Summary*. The feasibility study examined the Layer 2 concept consisting of the four Layer 1 entities and included a proposed CHP system to service both electrical and thermal loads. Among the many details of the analyses shown in Chapter 2, the benefit-cost ratio indicates that

- If the expected duration of major power outages is less than 0.3 days (7 hours) per year, the benefit-cost ratio will remain below 1.00.
- The benefit-cost ratio will rise to 1.00 if the expected duration of major outages is 0.3 days per year.
- The benefit-cost ratio will increase to 3.71 if the expected duration of major outages is seven days per year.

The BNMC microgrid was designed to operate for seven or more days. Considering the effects of Hurricane Irene in 2011 and Superstorm Sandy in 2012, the cost/benefit ratio of the BNMC microgrid may be even higher in the event of similar storms.

Task 2.2: Project Design and Planning

The microgrid project team created the design and plan for a comprehensive power system analysis and data monitoring effort to be implemented across the BNMC, Allentown and Fruitbelt electrical systems. The project team consolidated system circuit drawings into a common simulation platform, and developed the base-line circuit models to represent the power system in the study area. This task included the types of businesses in the survey area, their

major load types, electrical interconnections, related tariffs, and existing metering. The project team analyzed the area's equipment, including substations, feeder circuits, and any other relevant equipment, generation, or distributed energy resource. The project team determined the selection of appropriate measurement devices for the various locations and the data collection methods and consolidation tools to be used to gather and organize the information.

Findings:

The core BNMC project team (National Grid, BNMC Innovation Center, and EPRI) met regularly via conference call and webcast since the beginning of 2015 to brainstorm and design both the physical aspects of what the proposed microgrid may look like and the project design as well. In addition, this group discussed many logistical items such as scheduling subtasks, details of sub-agreements, obtaining needed datasets and drawings, communications to the larger group of member institutes, and scheduling project work. These discussions allowed the team to respond successfully to the New York Prize submittal resulting in an award: BNMC Community Microgrid Stage 1 - Feasibility Study Application. The microgrid strategy conceived during the weekly planning calls helped to facilitate the layered concept (see Figure 1-1 above and the descriptions that follow it) that was presented in the NY Prize proposal.

Task 2.3: Implementation of Data Collection System

The microgrid project team installed and gathered data to establish a base-line of power quality, reliability, and energy efficiency information used in the analysis and recommendations. The project team installed monitoring equipment throughout key locations in the electrical power systems and at customer metering locations and obtained the monitoring data for analysis.

Findings:

The BNMC monitoring project placed two varieties of power quality meters at two separate locations: the i-Sense (by Allen Bradley) and PQube3 (by Power Standards Labs). These are shown in Figure 1-2. The i-Sense devices monitored only voltage at a 480VAC panel while the PQube devices monitored both voltage and current from the PTs and CTs in RPCI's switchgear.

Figure 1-2

Power Quality Monitors
Left: iSense Monitors
PQube Monitors

The locations of the meters, at the Elm Street Substation and the switchgear for the Roswell Park Cancer Institute (RPCI)—about 1 mile apart—are shown below in Figure 1-3.

Figure 1-3
Location of BNMC PQ Monitors

EPRI undertook several studies over the years since around 1990 to document and to understand the power quality environment of the electrical system in the continental United States. These studies culminated in three reports known by the general titles DPQ I, DPQ II, and TPQ-DPQ III. These efforts examined power quality characteristics such as system average RMS-variation frequency index (SARFI), voltage distortion, voltage imbalance, and Flicker (both short-term and long-term). The most common voltage variation affecting electrical equipment is the voltage sag, a short-term reduction in voltage.

The above characteristics were examined for the BNMC electrical system:

Voltage deviation

The BNMC data, as illustrated in Figure 1-4, indicated that 5 events occurred over the span of time between 2/4/2016 through June 13, 2016 (around 120 days). These events were momentary reductions in voltage commonly known as *voltage sags*. According to the ITIC and SEMI F47 curves, only one voltage sag should have caused any upset of equipment with the others being within the upper and lower limits. Two events of the same magnitude and duration were measured on different feeders—one in April and one in June.

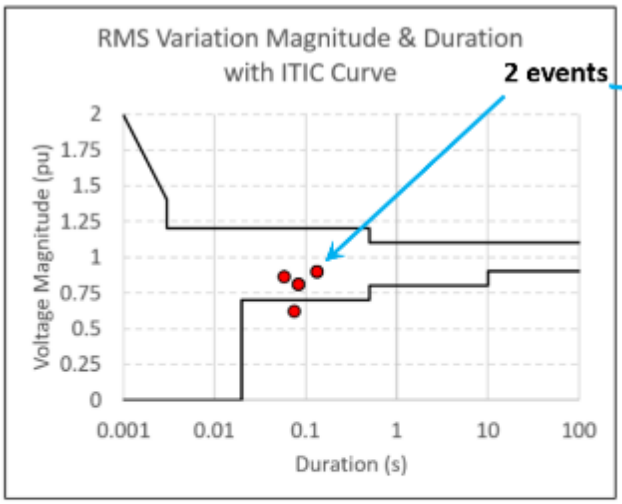

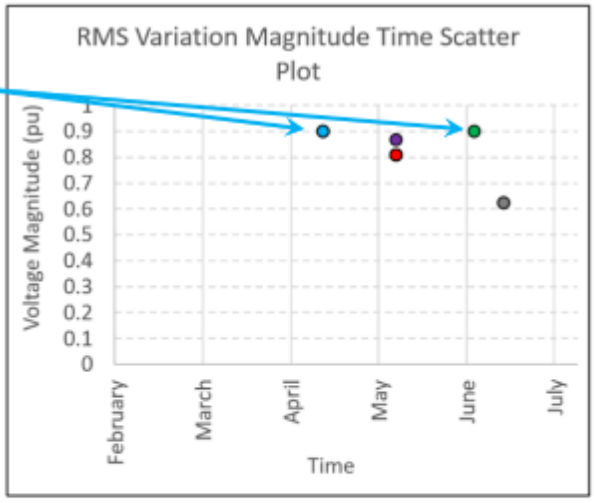

Site	Date and Time	Phase	Duration (s)	Magnitude (p.u.)
BNMC 15E	04/13/2016 01:29:20	CA	0.133	0.898
BNMC 14E	04/13/2016 01:29:20	CA	0.133	0.898
BNMC 12E	05/08/2016 01:16:29	AB	0.083	0.81
BNMC 11E	05/08/2016 01:16:30	AB	0.083	0.81
BNMC 15E	05/08/2016 01:17:14	AB	0.083	0.81
BNMC 14E	05/08/2016 01:17:21	AB	0.083	0.81
RPCI Srvc	05/08/2016 01:17:22	B	0.058	0.865
BNMC 12E	06/03/2016 17:23:08	BC	0.133	0.9
RPCI Panel	06/13/2016 22:16:17	A	0.075	0.621

Site	Monitoring Days
BNMC 11E	120
BNMC 12E	120
BNMC 14E	120
BNMC 15E	120
RPCI Srvc	120
RPCI Panel	120

Figure 1-4
BNMC Events

SARFI Events

The SARFI analysis of the BNMC events as recorded by the two meters compared to benchmark comparison data (BCD) taken from EPRI's TPQ-DPQ III study indicates that the BNMC average for this period of time was significant lower than that of the TPQ-DPQ III study. The BNMC/RPCI data ranged from 0 to 5.3 events per 365 days for all seven categories while the TPQ-DPQ III data ranged from 3.2 to 52.2 events for those same categories.

Voltage Distortion (THD)

The BNMC system had a much smaller range (CP 05 to CP 95) of voltage distortion than that of the TPQ-DPQ III study (under 0.8% difference vs. nearly 3.4% for TPQ-DPQ III). CP 50 was less than 1% for feeders 11E, 12E, 14E, and 15. The RPCI measurements were 1.1% for CP 50 while the TPQ-DPQIII data was 1.4%.

Voltage Imbalance

Similarly, the four E feeders had significantly less voltage imbalance than the TPQ-DPQ III data as did the RPCI Service; however, the RPCI_LPsub had a greater incidence of voltage imbalance compared to the TPQ-DPQ III data.

Flicker

For both short-term (Pst) and long-term (Plt) Flicker, the data for CP 05 and CP 50 for the four E feeders were significantly better, almost by half, than the TPQ-DPQ III data. The CP 95 data for the E feeders was one third of that for the TPQ-DPQ III study.

Conclusion

The BNMC system appears to be fairly robust on the utility side with no significant events occurring within the system either. Indeed, all the characteristics of the BNMC electrical system appear to be better than those of the TPQ-DPQ III study for the same voltage class.

Task 2.4: Data Analysis and Recommendations

The microgrid project team performed detailed power quality and energy efficiency analyses and provided recommendations for improvements to the power system and associated buildings. The project team performed transient analysis of the power quality data from the system against established reliability and power quality metrics. The project team established the actual performance of the grid in the study area to allow for comparison against the base-line model predictions. The project team developed recommendations and mitigation strategies for both the power system and customer facilities. The project team developed energy conservation measures for both grid-side and selected BNMC customer sites in the study area along with the supporting economic analysis.

Findings:

Project team examined individual member institutes, and identified specific areas of potential energy efficiency improvement, and power quality sensitivity.

Energy efficiency improvements to individual member institutes may result in these total savings and costs:

Member Institute	Estimated Annual Savings	Approximate Material Cost	Simple Payback
Total for All Members	**$194,649 to $197,884**	**$482,640 to $607,780**	**2.44 to 3.12 years**

Power quality sensitivity improvements to individual member institutes may result in these total costs to achieve or exceed compliance to PQ standards such as SEMI F47. The single-phase power quality technologies listed include the small, dynamic sag corrector (MiniDySC), the voltage dip compensator (VDC) and the constant voltage transformer (CVT).

Member Institute	Option 1: MiniDySC	Option 2: VDC	Option 3: CVT
Total for All Members	**$42,398 to $46,915**	**$54,356 to $57,586**	**$41,583 to $42,571**

Task 2.5: Advanced Power System Solutions

The microgrid project team developed an engineering study of the advanced power system solutions to increase system power quality and reliability while integrating renewable energy sources, energy storage, demand response, vehicle charging, and other microgrid technologies. The project team determined the optimum location, sizing, rating, and control configuration for implementing elements of the microgrid system. The project team developed both technical and economic factors considered in this analysis, and determined the feasibility of implementing a self-sustainable energy hub for the BNMC campus and the surrounding areas.

Findings:

Economic Analysis Report in Task 2.1 along with Project Design and Planning in Task 2.2: answered these questions.

Task 2.6: Technology Transfer

The microgrid project team developed technology transfer plan and conducted all technology transfer tasks.

Findings:

Technology transfer was an ongoing process beginning with the kick-off meeting in December 2014, extending through similar update meetings held in 2015 and 2016, and concluding with this final report.

Several webinars occurred from December 2nd, 2014 through 2015 and 2016.

Clay Burns of National Grid made a presentation at EPRI's Smart Distribution and Power Quality Conference in Columbus, Ohio on June 23, 2015 concerning the BNMC Microgrid. The presentation was entitled "A Multi-Layer Approach for Microgrid Implementation."

Presentation Abstract - A Multi-Layer Approach for Microgrid Implementation

Traditional microgrid concepts are based on a single-layer concept where the microgrid powers a local grid during a natural disaster. A multi-layered approach has been envisioned as a part of the NYSERDA project entitled "Assessment of an Urban Microgrid." In the new approach, upon examining existing infrastructure, an innovative three-layer strategy is envisioned that could offer redundancy and resiliency to a large medical and research campus, and the greater City of Buffalo, New York. This presentation will review the approach and discuss the engineering considerations for a regional community grid." Again, this concept was illustrated earlier in Figure 1-1.

Task 2.7 Final Written Document

The microgrid project team prepared a detailed, Final Written Document in the form of a report covering all aspects of the work performed.

- The report includes information on the following subjects with the information and findings understandable and actionable:
    - Discussions of the observations and findings and recommendations from all tasks, and avenues for further improvements;
    - Discussions of the project results and lessons learned regarding configuration, capabilities, and benefits of the Project; and
    - Environmental, and economic benefits, and implementation scenarios associated with such.

Findings:

With this report—presented in the Chapters 2 through 6, Task 2.7 is complete, and with it, the "Assessment of an Urban Microgrid" Project.

2
NY PRIZE FEASIBILITY STUDY SUMMARY

Executive Summary

This feasibility analysis evaluates a broad, comprehensive strategic plan that seeks to meet the resiliency needs of individual Buffalo Niagara Medical Campus ("BNMC" or "Campus") member institutions, the BNMC as a whole, and the Greater Buffalo Region through a tiered approach that builds upon the resiliency of its existing underground network, backup generation assets, distributed energy resources (DER), and energy-efficient facilities. As illustrated in Figure 2-1 below, this micro-grid strategy consists of three layers that would ultimately lead to a regional community micro-grid enabling the service footprint of National Grid's Elm Street Substation, which includes the Campus, its surrounding neighborhoods, and greater Buffalo, to withstand a catastrophic weather event or system failure while also positioning itself to leverage 'blue-sky' monetization opportunities.

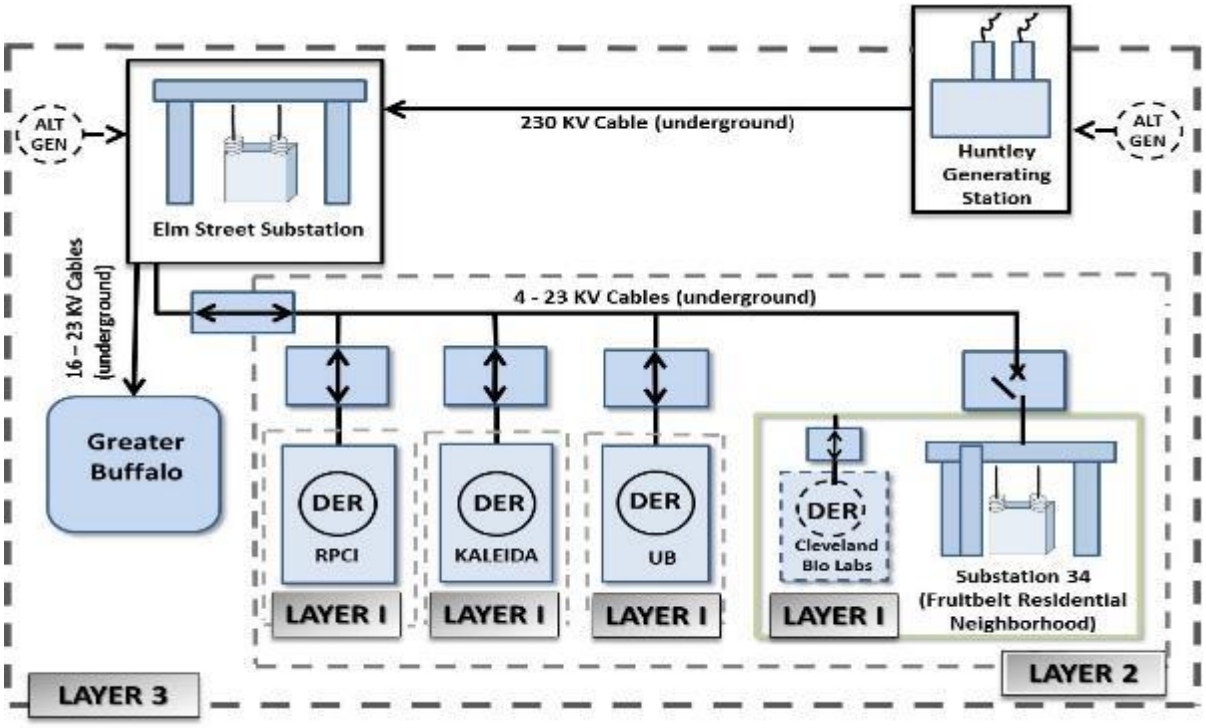

Figure 2-1
Proposed BNMC Community Grid Strategy for Greater Buffalo

The (3) layers of the proposed micro-grid strategy consist of:

- ***Layer 1:*** As a precursor to a Campus-centric, dynamic portfolio, enabling each of the member institutions who employ emergency, back-up generation to disconnect, island, and

optimize their facilities during weather or system-related events in order to maximize the capability of their back-up generating systems and other DER assets.

  - This layer is characterized by maximizing the use of existing back-up generation assets (that physically cannot be paralleled with the grid), existing/planned DER's and optimizing the loading and control of individual member institution facilities. Facilities that are currently without back-up generation could potentially be served by existing and/or future generation assets.

- ***Layer 2:*** Enabling the aggregate Campus to draw from on-site generation resources/DER at the individual member institution level or from common locations to disconnect during severe weather or system-related events while also positioned to leverage 'blue-sky' monetization opportunities.
  - Layer 2 is characterized by installing individual interface equipment to connect the member institutions' back-up generation to the grid, making it available to others on the Campus, and potentially to the close to 2,000 residential and 500 commercial customers residing in Buffalo's Fruit Belt neighborhood, who are served by National Grid's Substation 34, during grid outages. This layer also allows member institutions to self-generate and participate in energy markets (e.g. ISO markets, potential distribution level and future opportunities under the Distributed System Platform (DSP) model) under normal, grid-connected mode.
- ***Layer 3:*** Creating a regional, community micro-grid. Design proposes the installation of combined-cycle gas turbines within National Grid's right-of-way at the Elm Street Substation that work in tandem with Campus back-up generation and National Grid's existing infrastructure to ensure all regional load served by the Elm Street Substation remains on-line during weather or system-related events.

While the plan outlines three (3) layers of increasing complexity, the work described here, as part of the Feasibility Assessment, seeks to evaluate the feasibility of Layer 2. Layer 1 feasibility is being evaluated in a parallel effort funded by NYSERDA and National Grid.[1] Once complete, it will be possible to have portions of Layers 1 and 2 operating concurrently as well as redundantly. In addition to enabling both the Campus and portions of the adjacent Fruit Belt residential neighborhood[2] that share common infrastructure to endure weather-related events, the proposed approach would also enable member institutions to capitalize on available revenue and market opportunities for grid-paralleled generation during the vast majority of time that the greater grid is operating normally.

[1] *Assessment of an Urban Micro-grid*, NYSERDA Project #: 36660.

[2] This neighborhood is also the location of a PSC-approved, National Grid REV Demonstration Project.

Modeling Tool: DER-CAM

The Distributed Energy Resource Customer Adoption Model (DER-CAM) is a techno-economic tool that simulates DER adoption for buildings and microgrids. It determines the lowest cost combination and operation of DERs and grid electricity (if grid-tied) to supply microgrid load. DER-CAM is the product of over a decade of development at a US national laboratory—development began in 2000 at the Lawrence Berkeley National Lab (LBNL) and continues today. In that time, multiple versions, or branches, have been developed and are available—a free non-commercial version (WebOpt) and an investment/planning and operations branch of the full DER-CAM tool. This report covers the investment/planning branch, which is the primary version. LBNL provides a detailed description of DER-CAM versions on the DER-CAM website. DER-CAM is available open source for academic use with a collaboration license agreement, while commercialization (for use with a GUI and not open source) is ongoing.

DER-CAM works by optimizing DER adoption and hourly operation for a customer's facility over the first year of operation. It is written as a mixed integer linear program in the General Algebra Modeling System (GAMS) and minimizes a combination of system costs and/or emissions. Key inputs to the model include aggregated end-use loads, available DER technologies, site-specific parameters (such as location and space constraints), and local energy and fuel costs. DER-CAM has an internal library of DERs that includes many conventional generators (reciprocating engines, gas turbines, microturbines), thermal units (solar thermal, heat pumps, hot and cold storage, absorption chillers), renewables such as solar photovoltaics (PV), and emerging technologies such as energy storage, electric vehicles (EVs). The library also includes combined heat and power (CHP) systems and quantifies the flow of energy, heat, and emissions from generation through end consumption.

DER-CAM is an economic tool built on the monetization of energy and emission flows. It has been developed in great detail to quantify a customer's economic benefit from installing and operating DERs. That benefit is the difference in the customer's total energy cost had he/she remained a utility service customer. Other potential sources of microgrid revenue—such as from improved reliability via the value of lost load or ancillary service participation—can be considered but are coarsely developed at present.

DER-CAM can simulate new and existing microgrids and can perform sensitivity analyses. It is highly configurable and therefore suitable for case study analysis. It also lends itself well to systematic studies, in which input parameters vary over time, such as with changes to technology performance or cost, energy policies, and/or market parameters.

Campus Description

The Buffalo Niagara Medical Campus (BNMC) is made up of several, large member institutions (each with several buildings) as well as individual corporations that occupy single buildings.

The BNMC Microgrid Layer 2 Concept (herein referred to as "the microgrid") encompasses a subset of campus buildings that make up the bulk of the thermal and electric loads on campus. Table 2 below outlines the microgrid buildings, the affiliated member institution, and the electrical and thermal interconnections.

Table 2-1 Building Considered in Layer 2 BNMC Microgrids

#	Building	Institution	Electrical Interconnection	Thermal Interconnection
1	Buffalo General Hospital	KH	4.16 kV KH Substation	KH Steam + Chilled Water Loops
2	Gates Vascular Institute	KH	4.16 kV KH Substation	KH Steam + Chilled Water Loops
3	High Pointe on Michigan	KH	4.16 kV KH Substation	KH Steam + Chilled Water Loops
4	Clinical & Translational Research Center	UB	4.16 kV KH Substation	KH Steam + Chilled Water Loops
5	HighPointe on Michigan	KH	4.16 kV KH Substation	KH Steam + Chilled Water Loops
6	John R. Oishei Children's Hospital	KH	4.16 kV KH Substation	RPCI Steam + Chilled Water Loops
7	Main Hospital	RPCI	4.16 kV RPCI Substation	RPCI Steam + Chilled Water Loops
8	Gratwick Basic Science Building	RPCI	4.16 kV RPCI Substation	RPCI Steam + Chilled Water Loops
9	Administrative Services Building	RPCI	4.16 kV RPCI Substation	RPCI Steam + Chilled Water Loops
10	Cell & Virus Building	RPCI	4.16 kV RPCI Substation	RPCI Steam + Chilled Water Loops
11	Grace Center Drug Center	RPCI	4.16 kV RPCI Substation	RPCI Steam + Chilled Water Loops
12	Clinical Science Center	RPCI	4.16 kV RPCI Substation	RPCI Steam + Chilled Water Loops
13	University of Buffalo School of Medicine	UB	23 kV Elm Street Substation	*Independent Boiler System*
14	Cleveland BioLabs	*Independent*	5 kV Seneca Substation	*Independent Boiler System*
15	Fruitbelt Residential Neighborhood	*Independent*	5 kV Seneca Substation	*Household Boilers*

Kaleida Health (KH) and Roswell Park (RPCI) are two major campus institutions each with its own "utilities plant" which houses all the major electrical and thermal equipment needed to serve its buildings. Both institutions are fed off of four 23 kV feeders (11E, 12E, 14E, 15E) originating from Elm Street Substation. The respective utility plants each house four 23-to-4.16 kV

transformers. Individual mesh networks are then formed at the 4.16 kV level, allowing electricity to flow freely between all switchgears, bus bars, loads, etc. within each institution. KH's 4.16 kV network serves all KH buildings plus the University of Buffalo (UB) Clinical & Translational Research Center. RPCI's 4.16 kV network serves all RPCI buildings except the Center for Genetic & Pharmacology and no external buildings.

There are individual steam plants and distribution systems at Roswell and Kaleida. These central steam systems supply most of the buildings owned on their respective campuses. Each campus also has some buildings that use hot water boilers or other gas-fired systems within each building. Both Roswell and Kaleida also have chilled water loops on their campuses supplying most of their buildings. For Roswell, chilled water for the north campus is supplied from chillers in the utilities plant with a total capacity of 6,400 tons, while chilled water for the south campus is supplied from chillers in the Cancer Cell Center with a total capacity of 3,500 tons. The chillers in the Kaleida utilities plant total 6,100 tons of capacity. A few other buildings on the campus have separate cooling from within the building, including many air-cooled chillers, packaged rooftop units, and water loop heat pumps.

The Roswell Park utilities plant contains three steam boilers that normally run on natural gas. Each boiler has a capacity of 70,000 lb/h, resulting in total plant capacity of 210,000 lb/h. Each boiler has its own stack economizer. There is also a full-condensing economizer to pre-heat feedwater for the entire boiler system that is primarily used in the winter.

The Kaleida utilities plant contains three water-tube packaged steam boilers with a combined capacity of 150,000 lb/h. Two boilers installed in 1968 run on either natural gas or fuel oil, and a third smaller boiler installed in 1985 that can now only use natural gas. Only the third boiler has a feedwater boiler economizer. Updated oxygen trim controls were added in 2001.

The proposed CHP system will offset some of the thermal needs on the campus that are currently being served by the boilers at each site. When the CHP system is installed, a steam connection between the campus will allow loads to offset on both campuses. Some or all of the existing boilers will remain on campus to serve the remainder of the load and to provide redundancy.

With the Huntley Generation Station, a coal-fired power plant, now closed, Gardenville now feeds Elm Street Substation. Elm Street Substation steps down the voltage from 230 kV to 23 kV and acts as the central distribution point for most the BNMC campus buildings. Four 23 kV feeders (11E, 12E, 14E, 15E) serve the three largest loads on campus – Kaleida Health, Roswell Park Cancer Institute, and the University of Buffalo School of Medicine. Elm Street Substation also feeds Station 49, which in turn feeds the Hauptman-Woodward Medical Research Institute, the Research Institute on Addictions (UB), and the BNMC Innovation Center via 5 kV underground feeders. Finally, Elm Street Substation provides direct feeds to the Gateway Building (UB) and the Center for Genetic & Pharmacology (RPCI), with the Excellence in Bioinformatics & Life Sciences (UB) sub-metered.

At the east end of campus, Seneca Substation supplies an intermediate substation—Station 34—via 115 kV underground feeders. Station 34 subsequently feeds two loads of interest, Cleveland BioLabs and the Fruitbelt Residential Neighborhood.

Note: Figure 2.4 of the New York Prize Feasibility Study of March 2016 represents all the loads that will be considered under the BNMC 3-layer microgrid concept. However, this NY Prize

Stage 1 feasibility study considers only loads at the layer 2 level, which is shown in Figure 2.6 of the feasibility study.

The proposed microgrid includes 5 main loads – KH, RPCI, U.B. School of Medicine, Cleveland BioLabs, and Fruitbelt Neighborhood. The microgrid is separated into two groups—Group 1 and Group 2. Group 1 constitute loads normally fed via feeders 11E, 12E, 14E, and 15E from the Elm Street substation which are KH, RPCI, and U.B. School of Medicine. Group 2 constitutes loads normally fed from Station 34 i.e. Cleveland BioLabs and Fruitbelt neighborhood. Through Station 34, Group 1 and Group 2 loads may be interconnected by four existing circuit breakers for redundancy or other purposes (e.g. maintenance).

Thermal loop extension

While the thermal loads at both Roswell and Kaleida are fairly large with significant base loads in the summer, there would be additional benefit to further combine the thermal loads onto a common distribution system. This, combined with a central CHP plant, could efficiently and cost effectively serve these loads.

Figure 2-2 below shows the geographical mapping of the main BNMC campus, with the existing electrical distribution system feeders as well as the existing and proposed thermal (steam infrastructure).

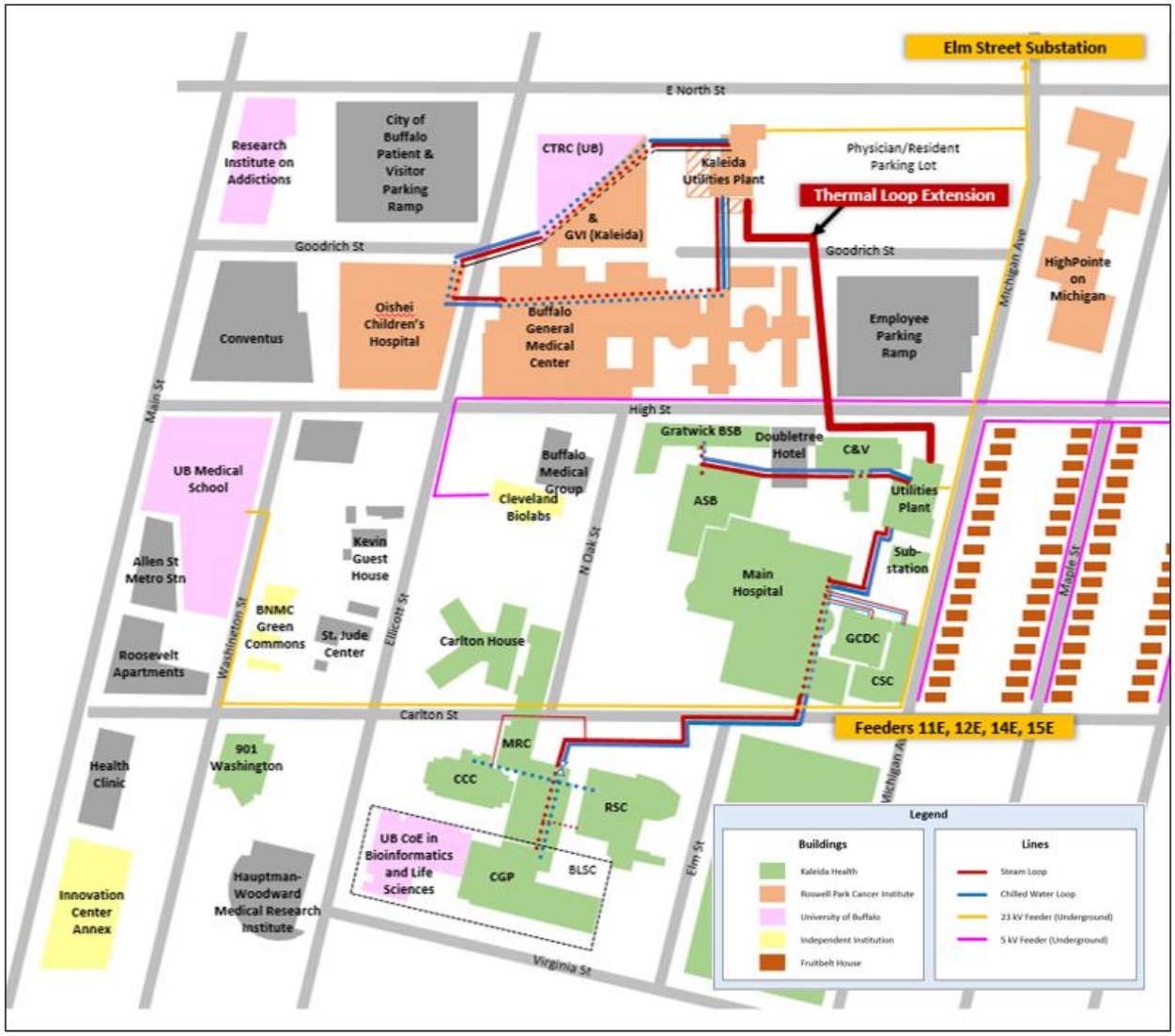

Figure 2-2
BNMC Main Campus

Study Results

Proposed DER Assets

Table 2-2 below lists the distributed energy resources that were ultimately chosen to be part of the proposed microgrid from the DER-CAM modeling effort. Selection was based on a variety of factors—size & dispatch modeling (i.e. economic optimization), technology characteristics & use cases, electrical & thermal infrastructure interconnection, communications, maintenance, operations, past experience with technology, general engineering judgement, physical/space constraints, policy and regulations (e.g. NYISO market participation, emissions, commercial arrangement), etc.

Table 2-2. Proposed Microgrid Distributed Energy Resources

Distributed Energy Resource	Nameplate Capacity	Energy Source	Location
Gas Combustion Turbine (Combined Heat & Power)	7,692 kW	Natural Gas	Roswell Park Cancer Institute
Internal Combustion Engine #1	5,000 kW	Natural Gas	Kaleida Health
Internal Combustion Engine #2	5,000 kW	Natural Gas	Kaleida Health
BNMC PV System #1	320 kW_{DC}	Solar	Kaleida Health – Children's Hospital
BNMC PV System #2	260 kW_{DC}	Solar	U.B. School of Medicine
Fruitbelt Distributed PV Systems	500 kW_{DC} – Total	Solar	Fruitbelt Neighborhood
Li-Ion Battery #1	50 kW / 200 kWh	Storage	Fruitbelt Neighborhood
Li-Ion Battery #2	50 kW / 200 kWh	Storage	Kaleida Health – Children's Hospital
Li-Ion Battery #3	50 kW / 200 kWh	Storage	UB School of Medicine

Significant electrical redundancy opportunities exist in the loading at each building on the medical campus. Most buildings are also equipped with building energy management systems (BEMS) wherein load shedding schemes within a microgrid may be implemented. The microgrid local controller that will be deployed at the BNMC campus will enable the coordination of load shedding.

We estimate that approximately 20% of the BNMC campus load can be categorized as "non-critical." A significant amount of the following buildings' loads may be estimated as being non-critical:

- High Pointe on Michigan—mostly outpatient procedures
- Grace Cancer Drug Center
- Cell & Virus Building
- Gratwick Basic Science Building
- Administrative Services Building

A more detailed load characterization should be conducted as part of the Detailed Design to more accurately determine which specific end-use loads may be shed with minimal detriment to facility operations as well as how fast the load may be shed.

Through existing and further build out of building energy management systems at each building, these non-critical loads may provide for fast load shedding. Fast load shedding may be used to account for any unexpected changes in load or generation and may act as operating reserve for

the microgrid in islanded mode. Provisions to implement load shedding may be programmed within the microgrid controller.

The li-ion battery at Fruitbelt and the flywheel storage system at BNMC campus will provide for fast response to minimize demand response requirements due to PV variability. Furthermore, accurate load forecasting and PV forecasting should further minimize the frequency of demand response requirements.

Demand response can be provided by temporally adjusting or shifting building temperature set points (e.g. allow building temperature to rise to offset electric cooling load), shutting off non-critical lighting within certain areas, water pumps, etc.

These types of non-critical load shedding should be of minimal and/or temporary impact to building inhabitants and/or operations. Critical loads such as building ventilation, life-support devices, operating rooms, lab refrigeration, data servers, and security systems will not be part of the load shedding demand response. Detailed demand response capacity and capabilities at each building will be further explored in the design stage.

Figure 2-3 then outlines the load vs generation & storage capacity balance in the proposed microgrid. Including existing diesel generating and demand response capability, the total capacity is approximately 70% greater than the total load.

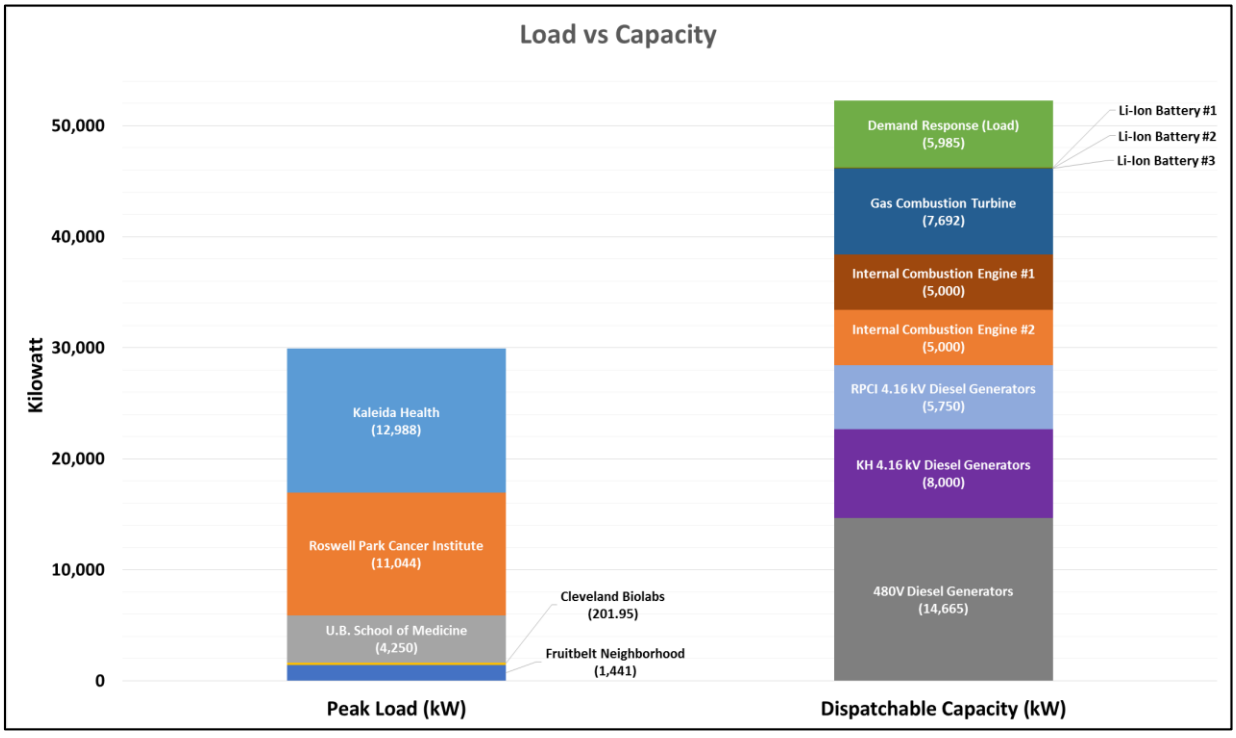

Figure 2-3
Load vs. Capacity

Microgrid Infrastructure

Table 2-3 below outlines the total estimated electrical, thermal, and communications/controls infrastructure upgrade costs for the proposed microgrid.

Table 2-3
Total Infrastructure Upgrades & Costs

Infrastructure Category	Estimated Installed Cost
Electrical	$3,280,000
Thermal	$1,000,000
Controls & Communications	$300,000
Total	$4,580,000

Microgrid Operations

Grid Connected

Table 2-4 outlines the annual electric load and generation breakdown for the base case (i.e. no microgrid) and the investment case (i.e. proposed microgrid) during grid-connected, "blue sky" operations. The creation of the microgrid would aggregate the electric loads at KH, RPCI, and UB Med School such that any electric import/export would occur behind one "master meter" (commercial and financial arrangements to be detailed in Task 3). Annual grid sales are quite low because the campus has a large amount of base load that cannot be met with on-site DERs instead (i.e. still significant amount of grid purchase).

Note: During grid-connected operations of the microgrid the four breakers between Elm Street substation and Station 34 are open, therefore no power flows from Group 1 DERs to Group 2 loads, vice versa.

Table 2-4
Annual electric load and generation breakdown with and without microgrid, grid-connected

	Base Case (kWh/yr.)	Invest Case (kWh/yr.)
Electric Load (Total)	**153,467,801.31**	**153,472,554.45**
- KH	66,862,520.52	147,360,456.67
- RPCI	56,442,694.02	
- UB Med School	24,050,488.99	
- Cleveland BioLabs	710,494.37	710,494.37
- Fruitbelt	5,401,603.41	5,401,603.41
Grid Purchase (Total)	**152,885,963.78**	**19,016,169.24**
- KH	66,862,521.21	13,485,909.99
- RPCI	56,442,694.95	
- UB Med School	24,050,488.37	
- Cleveland BioLabs	710,503.39	710,503.39

- Fruitbelt	4,819,755.86	4,819,755.86
Grid Sales (Total)	**0.00**	**11,526.83**
On-Site Generation (Total)	**581,848.62**	**134,588,644.69**
- 7692 KW CT CHP	n/a	63,919,399.03
- 2 x 5000 kW ICE	n/a	69,412,451.31
- 260 kW PV System (UB Med School)	n/a	302,561.88
- 320 kW PV System (KH)	n/a	372,383.85
- PV system @ Fruitbelt	581,848.62	581,848.62
- 50 kW/ 200 kWh Li-Ion battery	n/a	0
- 50 kW/ 200 kWh Li-Ion battery	n/a	0
- 50 kW/ 200 kWh Li-Ion battery	n/a	0

Similarly, Table 2-5 below outlines the annual heating load and generation breakdown for the base case (i.e. no microgrid) and the investment case (i.e. proposed microgrid) during grid-connected, "blue sky" operations. The extension of the steam loop from KH to RPCI would aggregate the heating loads at the two institutions thereby allowing more efficient operation of the central boilers at both each institution's utilities plant as well as allow the steam generated by the Combined Heat and Power unit (7692 kW combustion turbine) to be shared. On an annual basis the CHP unit provides for approximately 47% of the heating load, offsetting boiler operation. The remaining heating systems at the UB School of Medicine, Cleveland BioLabs, and within individual Fruitbelt residential houses remain unchanged.

Table 2-5
Annual thermal load and generation breakdown with and without microgrid, grid-connected

	Base Case (kWh/yr.)	Invest Case (kWh/yr.)
Heating Load (Total)	**163,505,221.66**	**163,505,238.69**
- KH	61,590,184.75	153,455,959.98
- RPCI	91,865,758.19	
- UB Med	9,893,645.23	9,893,645.23
- Cleveland BioLabs	155,633.49	155,633.49
- Fruitbelt	n/a	n/a
On-Site Generation (Total)	**n/a**	**76,689,678.65**
- 7692 KW CT CHP	n/a	76,689,678.65
Boiler (Total)	**163,505,358.31**	**86,815,695.76**
- KH	61,590,185.89	76,766,282.79
- RPCI	91,865,759.45	
- UB Med	9,893,645.84	9,893,645.84
- Cleveland BioLabs	155,767.13	155,767.13
- Fruitbelt	n/a	n/a

Table 2-6 below outlines the annual fuel consumption breakdown for the base case (i.e. no microgrid) and the investment case (i.e. proposed microgrid) during grid-connected as outlined above.

Table 2-6
Annual fuel consumption breakdown with and without microgrid, grid-connected

	Base Case	Invest Case
Natural Gas (Total)	**661,328.75**	**1,536,811.92**
- Boiler	661,328.75	351,142.71
- 7692 KW CT CHP	n/a	1,185,669.21
- 2 x 5000 kW ICE	n/a	

Figure 2-4 below shows sample dispatch profiles for summer and winter seasons.

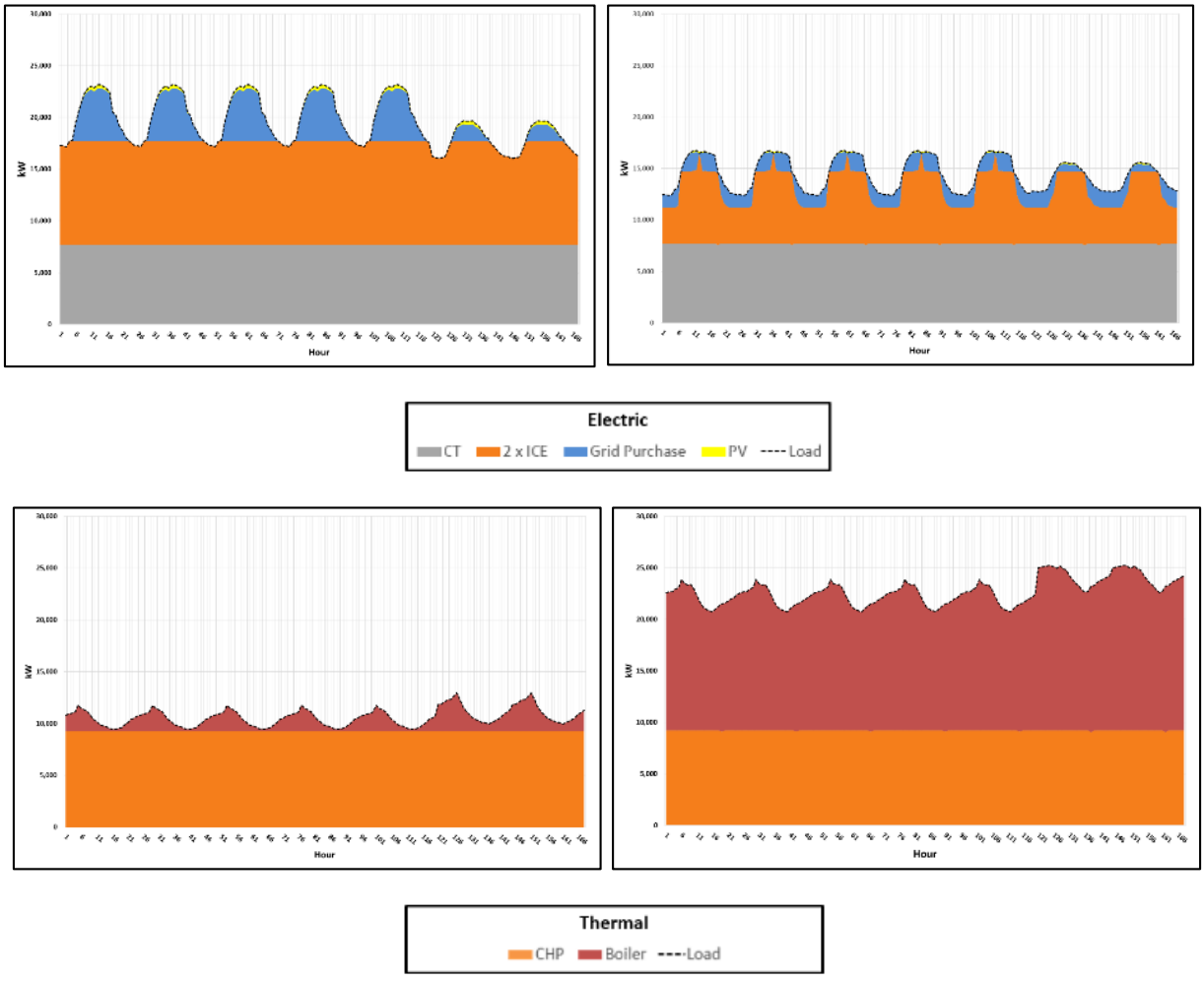

Figure 2-4
Top: Grid-Connected, Electric Dispatch (Summer, Winter)
Bottom: Grid-Connected, Thermal Dispatch (Summer, Winter)

Islanded Operations

Table 2-7 below outlines the annual electric load and generation breakdown for the base case (i.e. no microgrid) and the investment case (i.e. proposed microgrid) during islanded operations. The creation of the microgrid would allow all electric loads, both Group 1 and Group 2, to be served by microgrid DERs.

Table 2-7
Electric load and generation breakdown with and without microgrid, islanded mode

	Base Case (kWh/yr.)	Invest Case (kWh/yr.)
Electric Load (Total)	**3,477,809.40**	**3,477,810.00**
- KH	1,567,700.00	3,477,810.00
- RPCI	1,314,640.00	
- UB Med School	497,198.00	
- Cleveland BioLabs	17,564.00	
- Fruitbelt	80,707.40	
On-Site Generation (Total)	**1,016,712.00**	**3,477,809.45**
- 7692 KW CT CHP	n/a	1,292,256.00
- 5000 kW ICE #1	n/a	840,000.00
- 5000 kW ICE #2	n/a	812,603.00
- PV system @ BNMC	n/a	24,401.61
- PV system @ Fruitbelt	0.00	16,921.84
- 50 kW/ 200 kWh Li-Ion battery	n/a	0.00
- 50 kW/ 200 kWh Li-Ion battery	n/a	0.00
- 200 kW Flywheel	n/a	0.00
- Diesel Generators (KH)	399,156.00	268,795.00
- Diesel Generators (RPCI)	412,761.00	222,832.00
- Diesel Generators (UB Med School)	182,247.00	0.00
- Diesel Generator (Cleveland BioLabs)	22,548.00	0.00
Unmet Load (Total)	**2,466,081.40**	**0.00**
- KH	1,168,544.00	0.00
- RPCI	901,879.00	0.00
- UB Med	314,951.00	0.00
- Cleveland BioLabs	0.00	0.00
- Fruitbelt	80,707.40	0.00

Similarly, Table 2-8 below outlines the annual heating load and generation breakdown for the base case (i.e. no microgrid) and the investment case (i.e. proposed microgrid) during peak week outage operations. The heat generated by the CHP unit is able to meet approximately 60% of the heating load, offsetting boiler operation. The remaining heating systems at the UB School of Medicine, Cleveland BioLabs, and within individual Fruitbelt residential houses remain unchanged.

Table 2-8
Thermal load and generation breakdown with and without microgrid, islanded mode

	Base Case (kWh/yr.)	Invest Case (kWh/yr.)
Heating Load (Total)	2,285,403.00	2,285,402.00
- KH	917,431.00	2,115,558.00
- RPCI	1,198,128	
- UB Med	169,698.00	169,698.00
- Cleveland BioLabs	146.00	146.00
- Fruitbelt	n/a	n/a
On-Site Generation (Total)	**n/a**	**1,367,402.00**
- 7692 KW CT CHP	n/a	1,367,402.00
Boiler (Total)	**2,285,403.00**	**918,000.00**
- KH	917,431.00	748,156.00
- RPCI	1,198,128	
- UB Med	169,698.00	169,698.00
- Cleveland BioLabs	146.00	146.00
- Fruitbelt	n/a	n/a

Table 2-9 below outlines the annual fuel consumption breakdown for the base case (i.e. no microgrid) and the investment case (i.e. proposed microgrid) during peak week outage operations.

Table 2-9
Annual fuel consumption breakdown with and without microgrid, grid-connected

	Base Case	Invest Case
Natural Gas (Total)	**282,236.07 m^3**	**903,308.07 m^3**
- Boiler	282,236.07 m^3	113,369.07 m^3
- KH	113,298.00 m^3	92,394.00 m^3
- RPCI	147,963.00 m^3	
- UB Med	20,957.00 m^3	20,957.00 m^3
- Cleveland BioLabs	18.07 m^3	18.07 m^3
- Fruitbelt	n/a	n/a
- 7692 KW CT CHP	n/a	407,694.00 m^3
- 5000 kW ICE #1	n/a	193,932.00 m^3
- 5000 kW ICE #2	n/a	188,313.00 m^3
Diesel	**295,437.00 Liters**	**138,332.00 Liters**
- KH	115,976.40 Liters	73,344.00 Liters
- RPCI	118,139.70 Liters	64,988.00 Liters
- UB Med	54,544.00 Liters	0.00 Liters
- Cleveland BioLabs	6,776.90 Liters	0.00 Liters
- Fruitbelt	n/a	n/a

Electricity usage at the campus peaks during the summer when cooling loads are high; therefore, the worst-case outage scenario is a grid outage during the summer (i.e. when electric chillers are consistently operated). In the base case (i.e. no microgrid), with the currently existing diesel generator capacity and on-site fuel storage, a one-week summer interruption would amount to a total loss of 1,236,031 kilowatt-hours across all loads within the microgrid boundary. This is equivalent to 68% of unmet load during the outage week.

Figure 2-5 and Figure 2-6 below show the electric and thermal dispatch for the peak outage week with the microgrid.

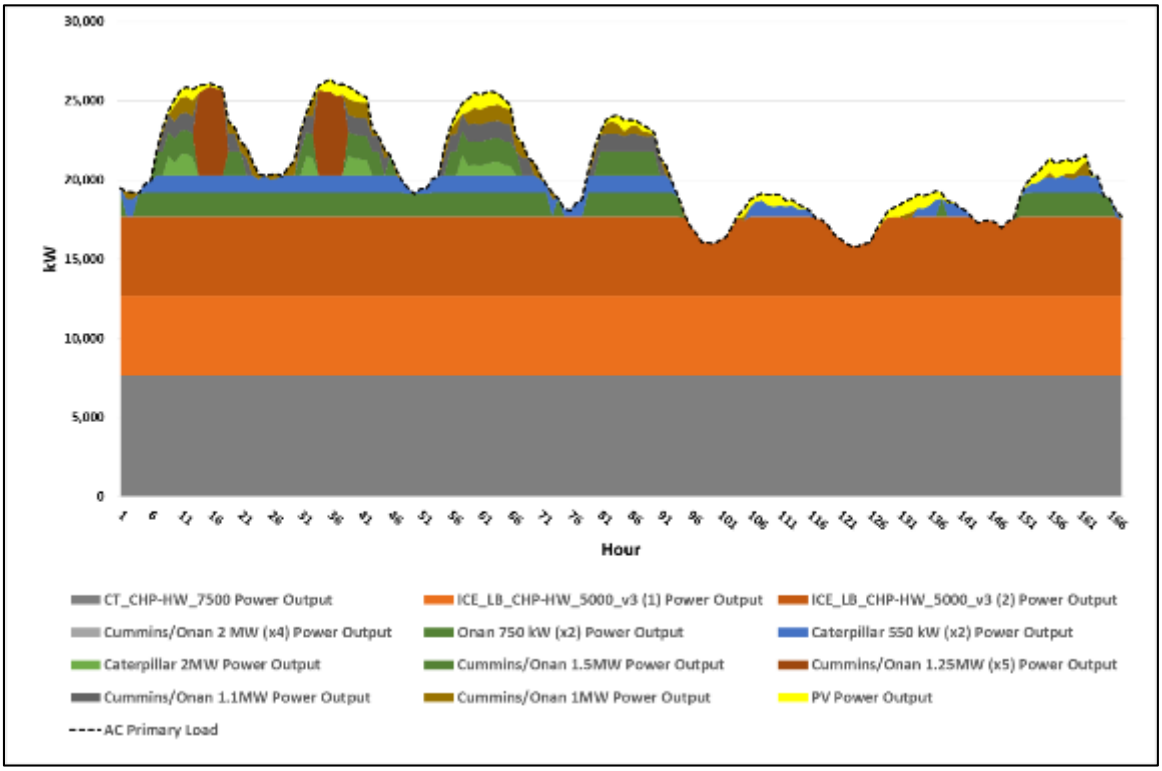

Figure 2-5
Islanded, Electric Dispatch (Peak Outage)

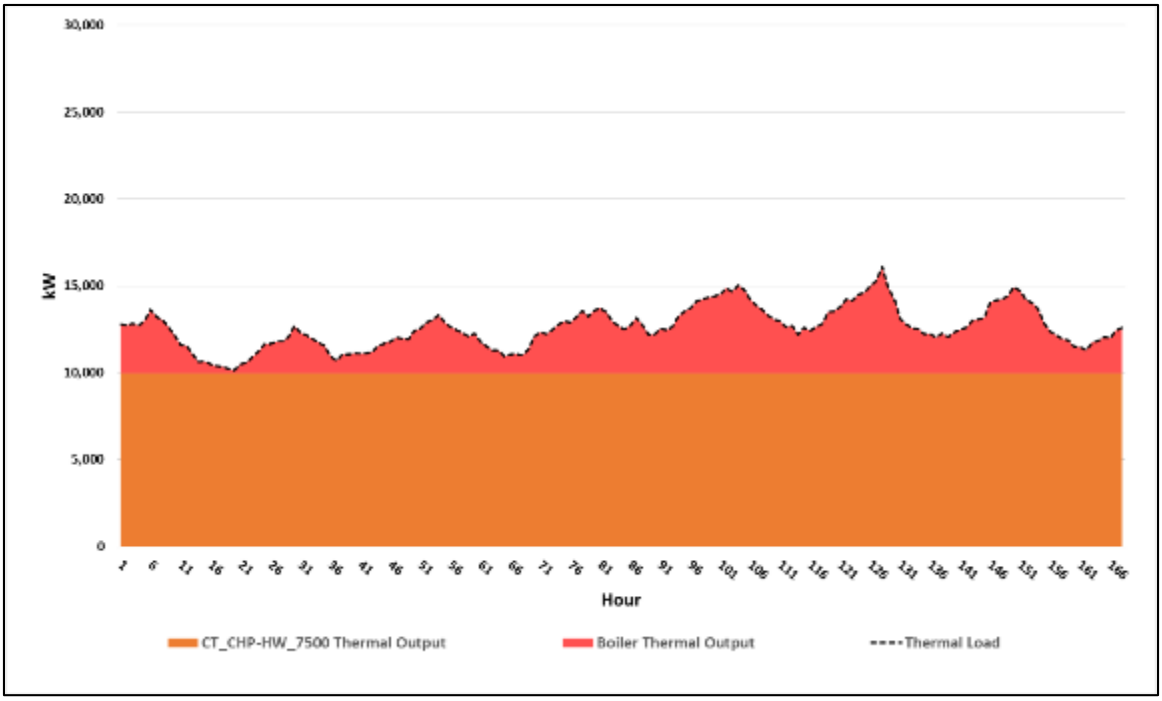

Figure 2-6
Islanded, Electric Dispatch (Peak Outage)

Cost & Benefit Analysis

Table 2-10 below provides the overall cost/benefit breakdown, in terms of net present as well as annualized values, for the proposed BNMC microgrid. Assuming no outages over the 20-year study period, the overall project cost/benefit ratio is 0.91 with an internal rate of return of 0.21%. The biggest benefit categories under this scenario are reduction in central generation, fuel savings from utilization of combined heat and power (i.e. waste heat utilization), and emissions reduction. The largest cost factors are capital investments in DER and electrical/thermal infrastructure upgrades, fuel purchase, and emissions damages. Note that avoided emissions damages (i.e. reduction in central generation dispatch) exceeds microgrid emissions damages; that is, the creation of the microgrid yields an overall emissions reduction for serving the same loads.

Table 2-10
Cost/Benefit Summary Table (No Outage Scenario)

Cost or Benefit Category	Present Value Over 20 Years (2014$)	Annualized Value (2014$)
Costs		
Initial Design and Planning	$328,000	$28,935
Capital Investments	$34,841,600	$3,073,645
Fixed O&M	$1,271,854	$112,200
Variable O&M (Grid-Connected Mode)	$15,553,839	$1,372,124
Fuel (Grid-Connected Mode)	$94,503,942	$8,336,919
Emission Control	$0	$0
Emissions Allowances	$0	$0
Emissions Damages (Grid-Connected Mode)	$85,306,281	$5,566,915
Total Costs	**$231,805,515**	**$18,490,738**
Benefits		
Reduction in Generating Costs	$74,807,225	$6,599,320
Fuel Savings from CHP	$24,700,216	$2,178,996
Generation Capacity Cost Savings	$16,437,498	$1,450,078
Distribution Capacity Cost Savings	$2,277,171	$200,887
Reliability Improvements	$1,796,307	$158,871
Power Quality Improvements	$3,035,015	$267,742
Avoided Emissions Allowance Costs	$45,455	$4,010
Avoided Emissions Damages	$88,251,774	$5,759,131
Major Power Outage Benefits	$0	$0
Total Benefits	**$211,350,661**	**$16,619,036**
Net Benefits	**-$20,454,855**	**-$1,871,702**
Benefit/Cost Ratio	**0.91**	
Internal Rate of Return	**0.21%**	

Table 2-11 shows the overall cost/benefit breakdown assuming an outage scenario of 7.6 hours (0.3 days) per year over the same study period. In this case, the overall project cost/benefit ratio is 1.00 with an internal rate of return of 8.2%. In general, the BNMC microgrid was designed for and is capable of riding through long-term outages lasting 7 days or more. Therefore, under severe outage conditions, such as those endured during Hurricane Irene and Superstorm Sandy in the Northeast, the cost/benefit ratio for the microgrid should be significantly higher (as IEc's final results illustrate).

Table 2-11
Cost/Benefit Summary Table (Outage Scenario – 0.3 days/year)

Cost or Benefit Category	Present Value Over 20 Years (2014$)	Annualized Value (2014$)
Costs		
Initial Design and Planning	$328,000	$28,900
Capital Investments	$34,800,000	$3,070,000
Fixed O&M	$1,270,000	$112,000
Variable O&M (Grid-Connected Mode)	$15,600,000	$1,370,000
Fuel (Grid-Connected Mode)	$94,500,000	$8,340,000
Emission Control	$0	$0
Emissions Allowances	$0	$0
Emissions Damages (Grid-Connected Mode)	$85,300,000	$5,570,000
Total Costs	**$232,000,000**	**$18,500,000**
Benefits		
Reduction in Generating Costs	$74,800,000	$6,600,000
Fuel Savings from CHP	$24,700,000	$2,180,000
Generation Capacity Cost Savings	$16,400,000	$1,450,000
Distribution Capacity Cost Savings	$2,280,000	$201,000
Reliability Improvements	$1,800,000	$159,000
Power Quality Improvements	$3,040,000	$268,000
Avoided Emissions Allowance Costs	$45,500	$4,010
Avoided Emissions Damages	$88,300,000	$5,760,000
Major Power Outage Benefits	$25,400,000	$2,240,000
Total Benefits	**$237,000,000**	**$18,900,000**
Net Benefits	**$4,940,000**	**$371,000**
Benefit/Cost Ratio	**1.0**	
Internal Rate of Return	**8.2%**	

The results indicate that the benefits of the proposed project would equal or exceed its costs if the project enabled the facilities it would serve to avoid an average of 0.3 days—or approximately seven hours—per year without power. Should the average annual duration of the outages the microgrid serves to prevent be less than this figure, the costs of the microgrid are projected to exceed its benefits.

3
MICROGRID DESIGN ANALYSIS OVERVIEW

Traditional distribution system planning aims to provide cost-effective, reliable, and quality power supply to the customers. With the advent of new types of generation in the distribution grid, the planning problem has expanded in order to accommodate the new possibilities and the associated concerns. One of the new design considerations is the ability of the distribution grid to function as an islanded microgrid system. The microgrid design evaluations should ensure that the islanded grid can reliably serve the load demand by conforming to the protection and power quality requirements of utilities. Further, the transition from grid-tied to islanded mode is also an important consideration for the successful operation of the microgrid. This study aims to bring out various design requirements and evaluate a microgrid at the Buffalo region in New York.

EPRI, in partnership with National Grid team, have identified a few microgrid configurations within Buffalo region to meet the resiliency needs of individual Buffalo Niagara Medical Campus (BNMC) institutions, the BNMC as a whole, and the Greater Buffalo region. Before actual implementation of the microgrid in BNMC region, a thorough analysis is required. Therefore, this study was initiated to model and analyze the feasibility of the microgrid scenarios carried out by extensive simulations including steady-state, transient, dynamic analysis, and protection studies. This chapter focuses on evaluating the performance of the overall microgrid system and distributed energy resource (DER) assets in grid-tied and islanded modes of operation.

Microgrid Configuration

A microgrid is a local energy grid containing loads and distributed energy resources—such as distributed generators (DG), storage devices, solar photovoltaic (PV) panels—that normally operate connected to a centralized grid but may also disconnect and function autonomously if required depending on internal and external conditions. Hence, the components of microgrid need to function in a structured and controlled manner without largely changing the existing electrical components. This creates the need to develop, understand, and analyze the different microgrid configurations.

A tiered approach is proposed that builds upon the resiliency of its existing underground network, backup generation assets, distributed energy resources (DER), and energy-efficient facilities. This microgrid strategy consists of three layers that would ultimately lead to a regional community microgrid enabling the service footprint of National Grid's Elm Street Substation which includes the Campus, its surrounding neighborhoods, and greater Buffalo. The plan outlines three (3) layers of increasing complexity (as shown in Figure 3-1).

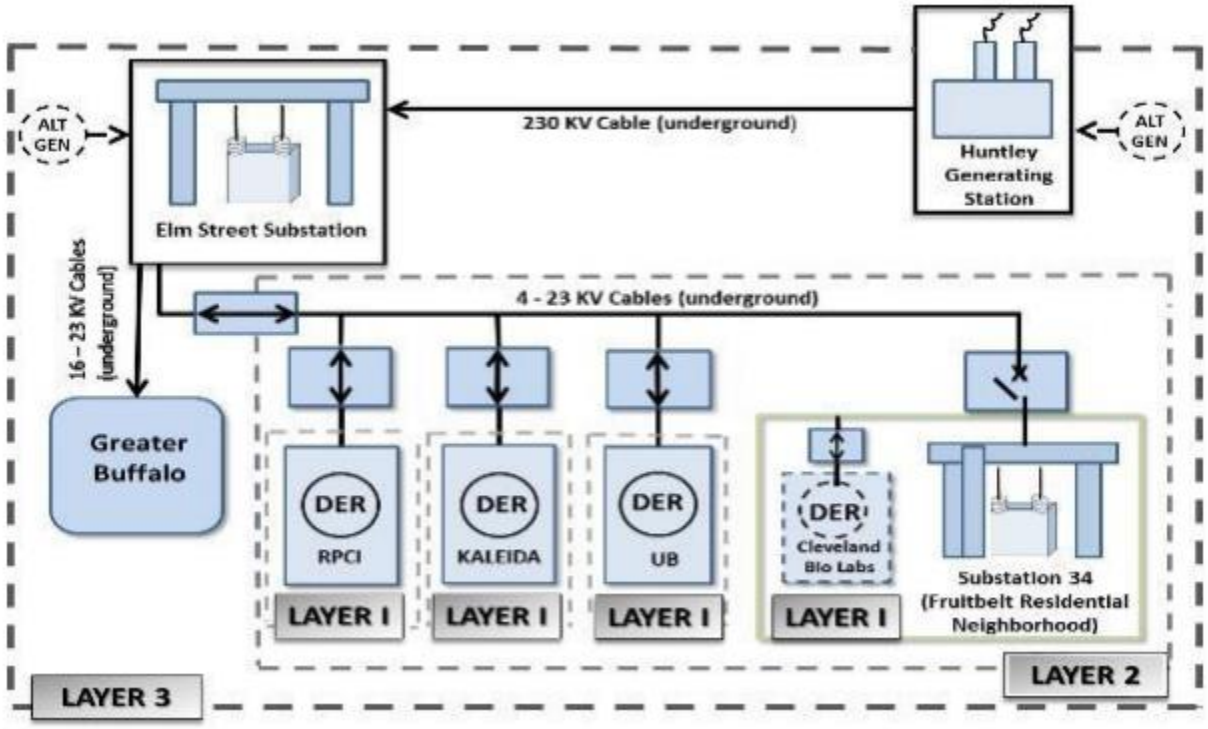

Figure 3-1
BNMC community grid strategy for Greater Buffalo

BNMC Microgrid Strategy Layers

The three layers of the microgrid strategy and their member institutions are detailed in the following sub-sections.

Layer 1

Layer 1 is each one of the individual member institution owned buildings. There are four layer 1 buildings such as,

- Kaleida Health (KH): Buffalo General Hospital, Gates Vascular Institute, High Pointe on Michigan, Women and Children's Hospital (currently under construction)
- Roswell Park Cancer Institute (RPCI): Main hospital complex, Gratwick Basic Science Building, Administrative Services Building, Cell and Virus Building, and Grace Cancer Drug Center
- State University of New York at Buffalo (UB): Clinical and Translational Research Center and the School of Medicine (SOM)
- Cleveland BioLabs and portions of the adjacent Fruitbelt residential neighborhood that share common electric infrastructure with the Campus

This layer is characterized by maximizing the use of existing back-up generation assets, existing/planned DER's and optimizing the loading and control of individual member institution facilities. Existing and/or future generation assets could potentially serve facilities that are currently without back-up generation.

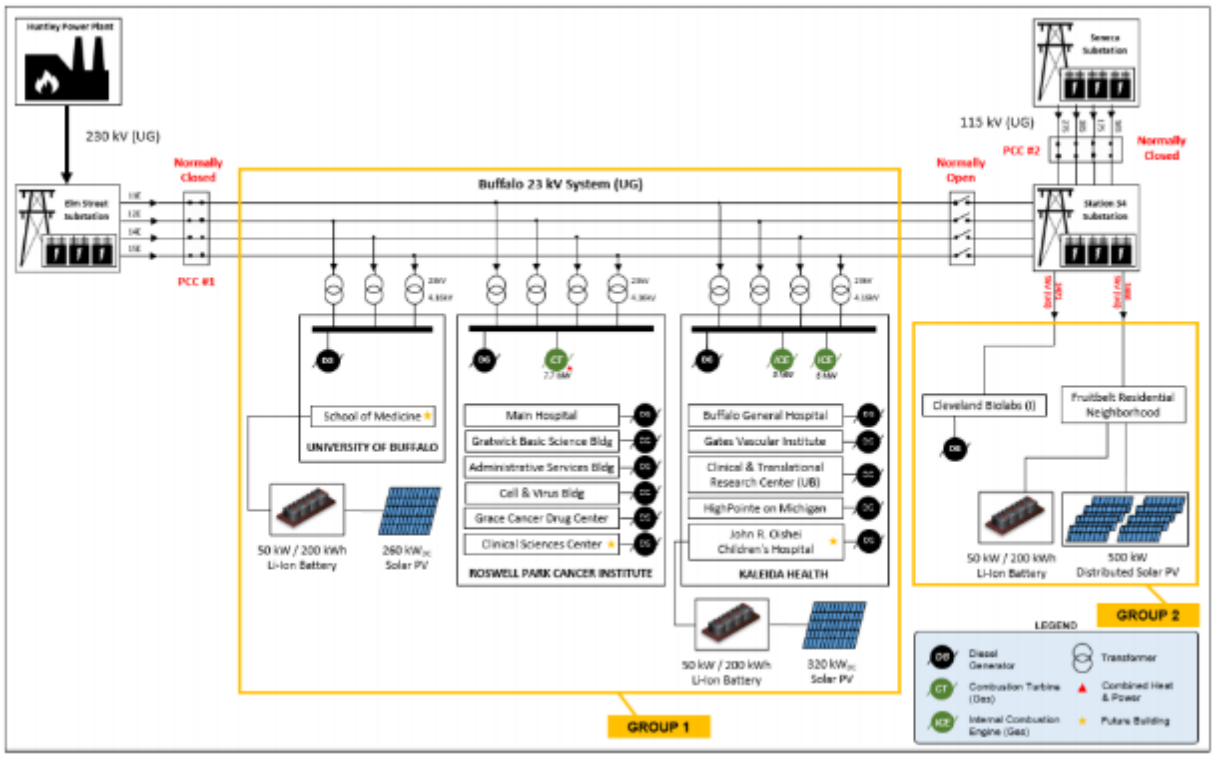

Figure 3-2
Simplified electrical one line – BNMC microgrid – Layer 2 microgrid

Layer 2

Layer 2 of the BNMC microgrid strategy includes the member institution owned buildings (RPCI, KH, UB) within the Campus and its surrounding area (Cleveland and Fruitbelt neighborhood). Layer 2 microgrid is separated into two groups – Group 1 and Group 2 (as shown in Figure 3-2). Group 1 constitutes KH, RPCI, and UB/ SOM loads normally fed via feeders 11E, 12E, 14E, and 15E from Elm Street substation. Group 2 constitutes loads normally fed from Station 34 i.e., Cleveland BioLabs and the Fruitbelt neighborhood.

Layer 2 is characterized by installing individual interface equipment to connect the member institutions' back-up generation to the grid. The generation can support potentially close to 2,000 residential and 500 commercial customers residing in Buffalo's Fruit Belt neighborhood who are served by National Grid's Substation 34, during grid outages. This layer also allows member institutions to participate in energy markets (e.g. ISO markets, potential distribution level and future opportunities under the Distributed System Platform (DSP) model) under normal grid-connected mode.

Layer 3

Layer 3 of the BNMC microgrid strategy includes creating a regional community microgrid through the proposed installation of combined cycle gas turbines within National Grid's right-of-way at the Elm Street Substation. The layer would work in tandem with campus backup generation and National Grid's existing infrastructure. The layer ensures that the regional loads served by the Elm Street Substation are always powered even during weather-related or system-

related events. This study is not focused on Layer 3 microgrid strategy. The feasibility studies on only Layer 1 and 2 microgrids are analyzed in detail.

Existing and New Generation Assets

An economic and environmental model of customer DER adoption (DER - CAM) was used to determine the technology type, mix and respective capacities of the generation source in the BNMC microgrid. Table 3-1 lists the existing and planned future assets in the buildings in the campus. It may be observed that the primary generation source capacity is not entirely diesel-fueled generators. Other DER technologies such as dual fuel natural gas/diesel generators (IC engines), CHP generators, solar PV and battery energy storage are included in the microgrid.

Table 3-1
List of existing and future electrical assets in each building

Buildings	Existing/New asset	Asset	Total Size
KH	Existing	9 Diesel generator	11.36 MW
	New	2 IC Engines	10 MW
		PV system	0.32 MW (DC)
		Li-Ion Battery	0.05 MW (200 kWh)
RPCI	Existing	13 Diesel generator	13.725 MW
	New	Gas combustion turbine (CHP)	7.69 MW
UB/SOM	Existing	1 Diesel generator	2.5 MW
	New	PV system	0.260 MW (DC)
		Li-Ion Battery	0.05 MW (200 kWh)
Cleveland BioLabs	Existing	2 Diesel generator	0.825 MW
Fruitbelt	New	PV system	0.5 MW (DC)
		Li-Ion Battery	0.05 MW (200 kWh)

500 kW of PV will be installed in the Fruitbelt neighborhood as part of National Grid's Fruit Belt Neighborhood Solar initiative which is a REV Demonstration Project. The 7 MW CHP unit and the two 5 MW internal combustion engines will be interconnected with the electrical grid and operate in parallel during normal operations. The CHP unit will be connected on the customer side of the point of common coupling (PCC) at Roswell Park Cancer Institute, and the internal combustion engines will be connected on the customer side of the PCC at Kaleida Health.

Modes of Operation:

The microgrid can be operated in two modes of operation i.e., grid-tied and islanded modes, depending on the source of the electric supply to the loads.

Grid-tied Operation

The utility source at Elm St. Station and Station 34 supplies the loads in grid-tied mode of operation. Figure 3-3 shows the system configuration and breaker conditions during grid-tied mode of operation. There are two utility points of interconnection related to the microgrid – PCC #1 and PCC #2. Group 1 circuit components are connected to the grid at PCC#1 and Group 2 circuit components are connected to the grid at PCC#2. PCC#1 are four breakers between Elm Street and Station 34 substations. PCC#2 are four breakers between Seneca and Station 34 substations.

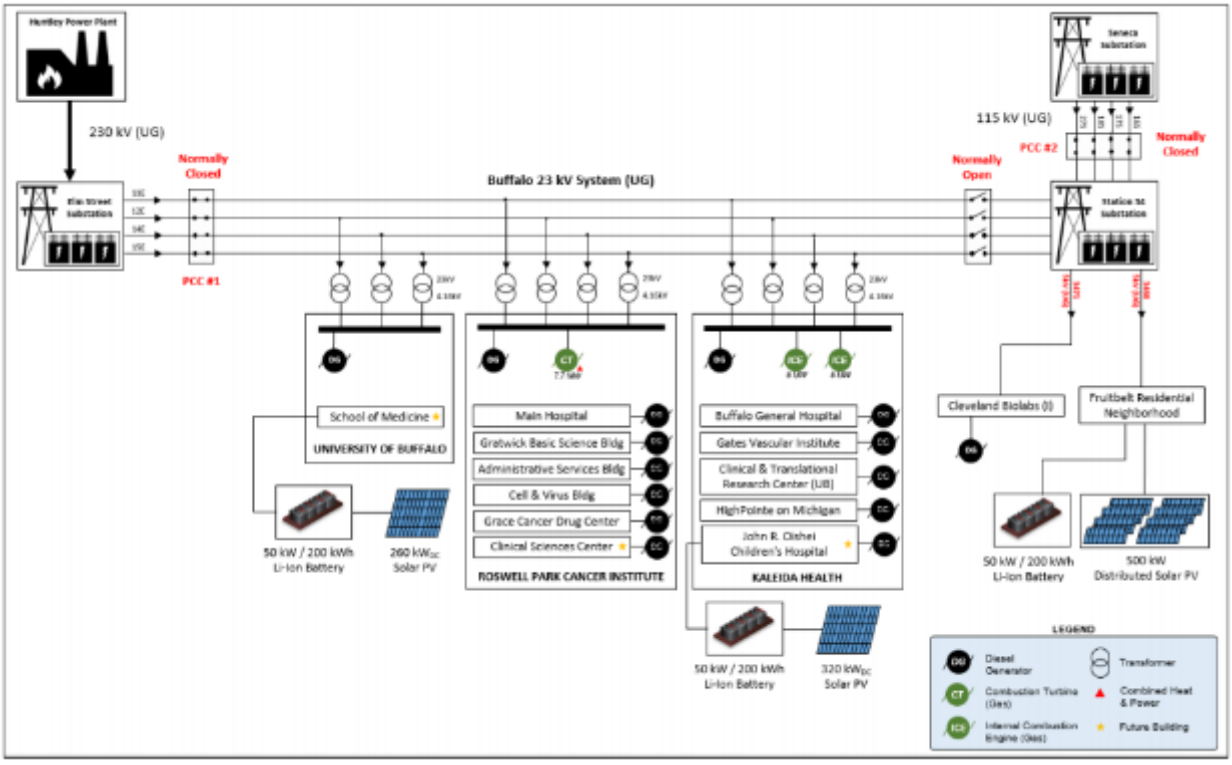

Figure 3-3
Simplified electrical one-line diagram – BNMC Microgrid in Grid Connected state

Kaleida Health, Roswell Park Cancer Institute (excluding Genetic & Pharmacology), and UB Medical School buildings are fed from the Elm Street substation. Cleveland BioLabs and the Fruitbelt residential neighborhood are normally fed from the Seneca substation (via feeders 16S, 17S, 18S, and 27S) through Station 34. From Station 34, the Fruitbelt neighborhood and Cleveland BioLabs are fed via feeders 3466 and 3471 respectively. In this study, only a subset of the Fruitbelt area is considered (one out of three feeders). Station 34 breakers for the four feeders connected to the Elm Street substation are normally open. During grid-connected operation, CHP, ICE, PV and battery are operational, but are not allowed to regulate the voltage at their terminal.

Islanded operation

The microgrid may operate in islanded mode either due to planned intentional islanding or unplanned intentional islanding. Two islanded cases are considered for the study i.e., Layer 1 and 2 islands. The first islanding scenario is where Layer 1 buildings as shown earlier in Figure 3-1 operate in islanded mode. The other islanded scenario is where Layer 2 buildings operate independently. In this scenario, building loads between Elm Street substation and Station 34 (i.e. Kaleida Health, Roswell Park, and UB Medical School) will be automatically transferred via breakers located near the Elm Street substation. The sequence of steps is shown in Figure 3-4 and Figure 3-5. The initial islanding state is illustrated in Figure 3-4. Group 1 buildings are separated from Elm St. Station by opening of PCC #1. Generation at the Group 1 building is sufficient to support the net load in the network. Since Group 2 buildings do not have sufficient generation, generators at Group 1 building should support the entire island. The final islanding state is illustrated in Figure 3-5 where PCC #2 is open and the normally open switch between the Group 1 and 2 buildings is closed.

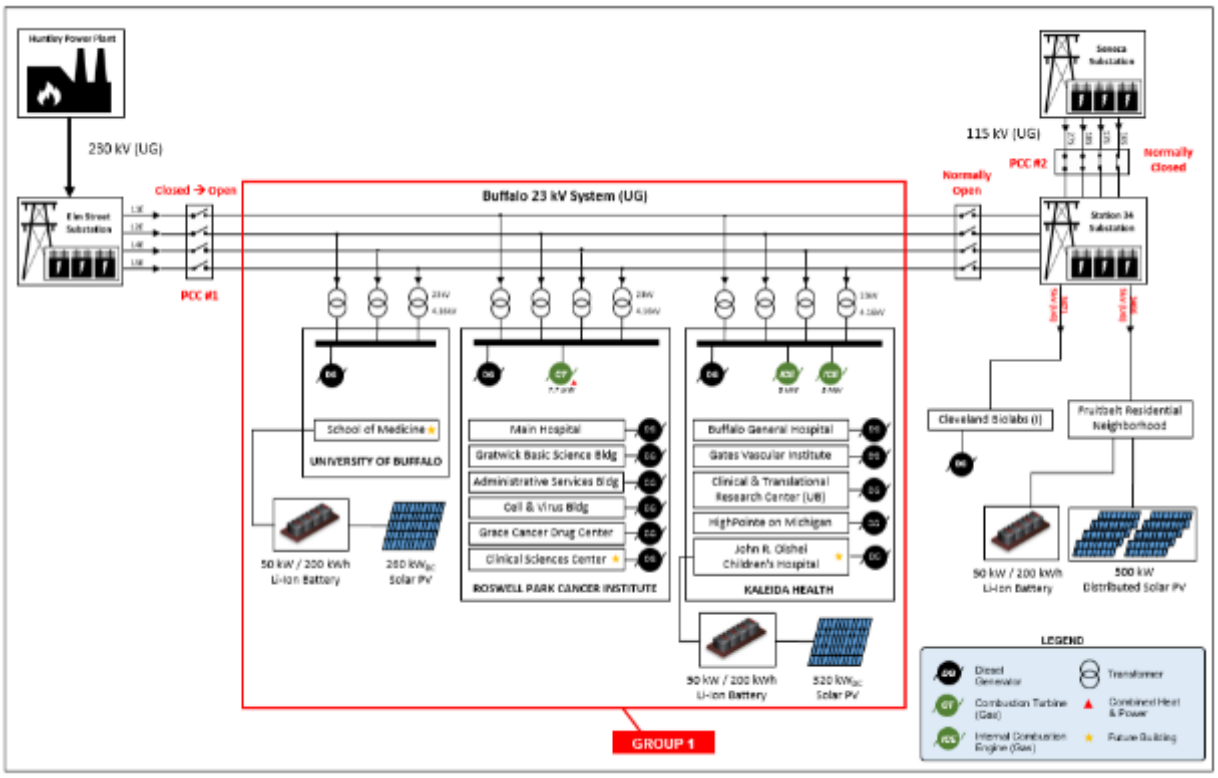

Figure 3-4
Simplified Electrical One-Line – BNMC Microgrid in Initial Islanding State (Layer 2, Group 1)

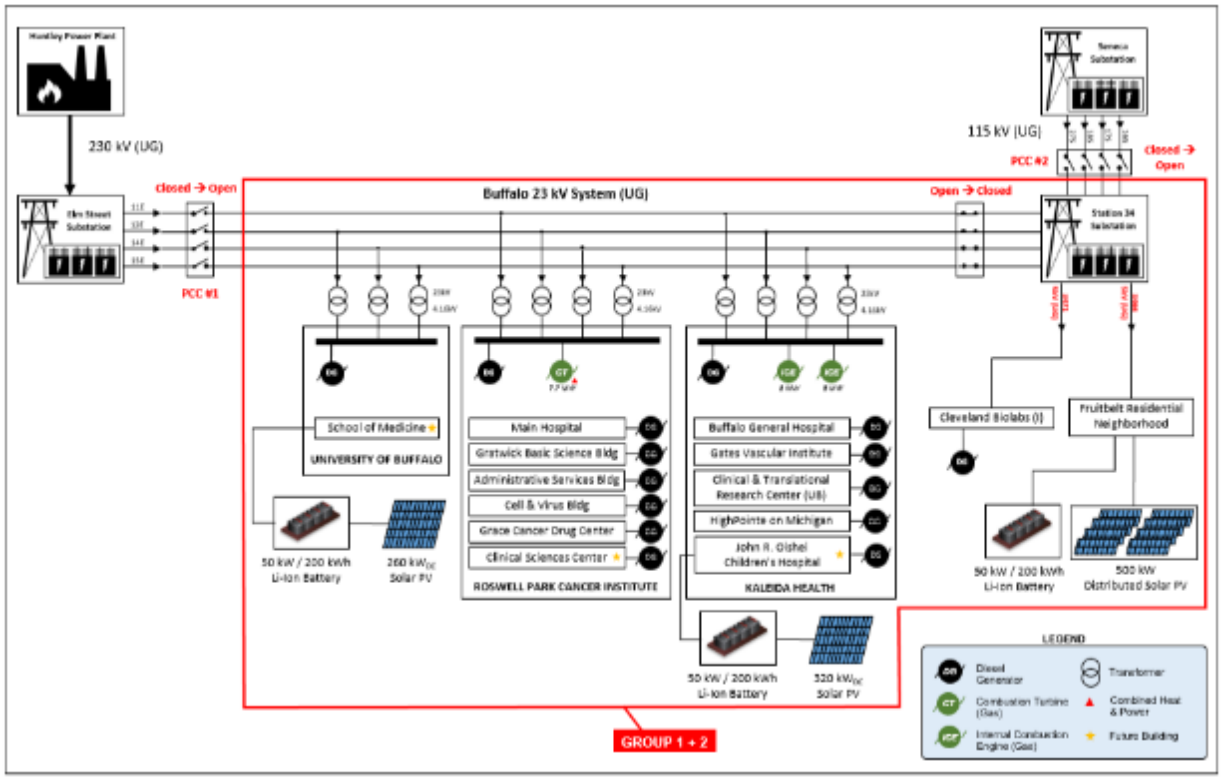

Figure 3-5
Simplified Electrical One-Line – BNMC Microgrid, Final Islanding State (Layer 2, Group 1+2)

Description of the Desired Functional Objectives of the Microgrid and Key Findings

Typical functions of the distribution grid include coordination with supervisory control and data acquisition (SCADA), distribution management system (DMS) to regulate voltage at the customer locations, to maintain generation adequacy by load shed, and to detect faults and to protect from outages. The desired functions of the grid are expanded when DERs are integrated in it. The objectives of the grid are detailed in the following sections according to the mode of operation i.e., grid-tied and islanded mode.

Grid-tied Functions

The primary function of the microgrid in grid-tied mode is to maintain voltage of the grid within limits specified by ANSI C84-1, i.e., the steady-state voltage should be maintained between 0.95 pu and 1.05 pu at the PCC. Steady-state load flow analysis of the BNMC microgrid in grid-tied mode of operation is carried out to evaluate the performance of the microgrid. The voltage range on a peak-load day is determined when the local generation—such as DGs, CHP and IC engines—are not operating. Assuming that the substation voltage is at 1 pu, the voltage at the grid is calculated to be between 0.95 and 0.99 pu. There is a maximum voltage drop of 0.05 pu; however, it is within the ANSI limits.

Another grid tied function is to allow the member institutions to self-generate and to participate in energy markets (e.g. ISO markets, potential distribution level and future opportunities under

the Distributed System Platform (DSP) model). The grid-tied condition where all the local generators are operating is simulated. The microgrid has sufficient generation capacity to provide on-site power for the loads and to export to the external grid (see Table 3-1). Steady-state load flow analysis on a peak day has shown a maximum reverse power flow of about 28.18 MW and 0.77 MW towards Elm St. Station and Station 34, respectively. Under these conditions, voltage rise occurred and the range was recorded between 0.99 and 1.02 pu, which is again within the ANSI limits.

Other functions of the grid include determination of the available kW and ensuring generation adequacy at all times. Further, sufficient generation should always be maintained by the grid for a seamless transition to an islanded mode during emergency.

Islanded Functions

The objective of the islanded mode of operation is to reliably serve power to physically separated critical facilities (the identified institutions in Section 0 within BNMC campus), on loss of the utility source.

The primary requirement of the controllers in the islanded mode is to maintain voltage and frequency of the island within ANSI standards. For single generators, voltage control is relatively straight forward but when multiple generators are involved, control of voltage becomes more complicated. For that reason, in the BNMC microgrid, it is assumed that the diesel generators (DG) at each building have automatic voltage regulators (AVR) to maintain voltage within limits. Whereas, the other generators such as IC engines and CHPs are assumed not to actively regulate the voltage at the building. Further, all the generators are assumed to participate in droop-based frequency control. Thereby, frequency of the microgrid is maintained at 1 pu.

In addition to steady-state voltage and frequency control, other voltage characteristics are also important. The local generation should also provide a stiff enough source to limit voltage unbalance, harmonics, and voltage flicker. Each of these is a function of the stiffness of the generation relative to the size of the load. During resiliency support, voltages with higher-than-normal excursions are likely to be tolerated, but problems will be limited if steady-state voltage, unbalance, harmonics, and voltage flicker can be restrained as much as possible. Sizing generators to have enough voltage support capability for the load is required.

Steady-state simulations of various islanded configurations were carried out to ensure that the voltage and frequency remain within the safe operating region as specified by ANSI standards. Some of the islanded configurations such as Layer 1 islands of SOM and Fruitbelt buildings require load sheds to match the generation with the net load for better voltage and frequency control within the microgrid.

Synchronization and Reconnection

When connecting an islanded microgrid to a utility distribution system or two islands of a microgrid together, an important consideration is synchronization of the two systems with minimal transients and disturbances during reconnection. The objective is to demonstrate successful synchronization of two separated islands and synchronization of microgrid and utility distribution system with minimal disturbance in the system. Synchronization of microgrid and utility is demonstrated by connecting islanded Group 1 microgrid with Elm St Station. So, the

microgrid changes from islanded mode of operation to grid-tied mode of operation. Successful synchronization of two islands is presented by connecting islanded Layer 1 (RPCI) with rest of Group 1 microgrid operating in islanded mode. The instantaneous and rms plots of voltages and current along with frequency and power (active and reactive) plots are used to study the transients during the synchronization process.

Active synchronization is possible if the voltage and frequency can be controlled sufficiently. The microgrid controller should align the voltage, frequency and phase angle of the islanded microgrid to that of the utility power system or the system to which it is connected for synchronization to be done without any significant disturbances. Another way to avoid disturbances is by de-energizing the microgrid and then reconnecting it to the utility power system. Once reconnected, the distributed generation can be restarted if desired. This is the easiest and least expensive option for grid reconnection, but the impacts to loads should be considered (refer to synchronization limits from IEEE 1547-2003). The ability to synchronize is dependent on how well the microgrid can control voltage and frequency.

Islanded Operation – Disconnection

When grid connected, the controller in the microgrid manages the local resources (e.g. generation and/or energy storage) to ensure high power quality and readiness to island. The objective is to demonstrate the ability of the microgrid to island and identify the desirable islanding conditions. The intentional islanding can be due to planned or unplanned scenarios.

The microgrid should be able to form an intentional island due to planned or unplanned scenarios. The islanding scenarios are detailed as follows.

Planned Intentional Islanding

When disconnecting a microgrid connected to a utility distribution system, or when disconnecting a portion of the microgrid from the rest of the system, an important consideration is to island with minimal transients. Also, the island formed has to be stable and must be able to function independently. Planned intentional islanding is demonstrated by islanding the grid-connected Group 1 microgrid (connected to Elm St Station initially). The Group 1 microgrid changes from grid-tied mode of operation to islanded mode of operation. Similar to synchronization analysis, transients caused due to islanding were studied using voltage, current, frequency, and power plots.

For successful islanding, each island to be formed should have sufficient generation capacity to meet its own load demand. For the islanding process to be smooth and have minimal transients, it is preferred not to have any power flow through the point of interconnection before islanding. This requirement can be achieved when the total generation in each individual island to be formed matches the total load in that island before islanding. When the islanding is planned, the microgrid controller can adjust the generation of different machines to meet the above requirement.

Unplanned/Unscheduled Intentional Islanding

When the islanding is unplanned or unscheduled, the power balance requirement along with having no power flow through the point of interconnection requirement may not be achievable.

Hence, in this case, there may be power flow through the point of interconnection before islanding and the total generation of each island to be formed would not match the total load in that island. This scenario is demonstrated by islanding Layer 1 (RPCI) from Group 1 microgrid operating in islanded mode. Voltage, current, frequency and power plots were analyzed to study the transients caused in this case.

Islanding in this scenario causes more disturbances and the larger transients compared to planned intentional islanding. The transient disturbances in voltage and frequency would be much larger than that seen in the case where there is no power flow through the point of interconnection before islanding. However, the voltage and frequency would eventually settle at a value close to 1 pu at steady state because the generators would adjust the power produced to match the load.

Black Start and Motor Starting

Black start is the ability of an islanded microgrid to energize from a de-energized state. The objective of this analysis is to demonstrate energizing a de-energized busbar and loading it. Key issues associated with black starting are cold-load pickup and inrush current requirement of the motor-based loads. Cold-load pickup is the condition where increase in load demand is experienced immediately after a service interruption. Inrush current is the high starting current of the motor-based loads. A utility source is normally stiffer than local generation within a microgrid but when black start is performed, the microgrid must be stiff enough to provide sufficient torque to start motors within the microgrid.

For successful black start with negligible disturbance, the main generator has to be brought to its spinning state (normal operation at no load) using some source of power such as small diesel generator before connecting the generator to the de-energized bus. The generator in the microgrid should be sized to handle the black start condition for a reliable islanded operation. If the generator is not sized to handle the load requirement, the microgrid controller should control the load to be brought online in steps so that the generator can support the load.

The objective of motor starting analysis is to study the starting characteristics of motors of different sizes in a small and weak microgrid. Motor starting analysis was performed by starting motors of various sizes at Layer 1 UB/SOM building. Motors of size up to 1.1 MW could be started where the available generation at UB/SOM was 2.6 MVA. Motor starting will be successful when the microgrid can supply the required inrush current required to start the motor without severe voltage drop at the motor terminals. A motor may fail to start when the electrical torque produced during this motor starting period is less than the torque required to start the motor. One option is to prevent large motors from starting during black start or ensure that such motors have a soft enough start for the microgrid. This can be done by using additional controls and implementing motor starting techniques.

Requirements for Coordination of Protection Settings

The design of protection schemes for a microgrid involves performing load flow and short-circuit analysis to determine maximum loading, minimum and maximum fault current levels across the microgrid system. As the microgrid can be operated in grid-tied and islanded modes, the protection system must respond in both these modes as desired.

In grid-tied mode, usually the fault current levels are higher compared to the islanded mode. Normally, the utility supplies a stiff source that has significant fault current available. As such, the microgrid protection design becomes similar to that of utility distribution systems. If the fault levels are high enough, the conventional overcurrent protection schemes generally work well if the connectivity of the microgrid circuit is radial. Then the desired protection system response can be obtained by careful selection of pickup current and time-dial settings. For microgrids having tapped lines, protection schemes based on other protection principles such as differential current may be needed to ensure good selectivity.

In islanded mode, the fault current levels in the microgrid can become very low depending upon the type and size of generation available. If the microgrid has mostly inverter-based generation, the overcurrent protection may not be suitable as the inverter-based generators generally do not provide sufficient fault currents. In such cases, fault detection based on over/undervoltage measurement may be suitable for detection of faults. These protection systems measure the sequence voltages at selected buses to distinguish between fault and non-fault conditions and trip appropriate breakers in case of faults.

In Layer 1 of the BNMC system, the microgrids—namely, Roswell Park Cancer Institute (RPCI), University of Buffalo/School of Medicine (SOM), Kaleida Health (KH)—are present in Group 1. Each of these microgrids operate separately in islanded mode. In Group 2, Fruitbelt (FB) and Cleveland BioLabs (CL) microgrids operate together in islanded mode. The existing protection system includes non-directional and directional overcurrent relays in these microgrids. As synchronous generators are available in all these microgrids, sufficient fault levels are available in both grid-tied and islanded modes for the existing overcurrent protection (ANSI code 50/51, 50N/51N) to work well. Therefore, overcurrent protection settings ensuring fault detection and quick isolation of faults are prepared for the overcurrent relays in each individual microgrid in Group 1. For Group 2 Layer 1 protection, the ground faults on the 4.16 kV Fruitbelt bus cannot be detected by the overcurrent relay in CL as the fault current does not propagate from Fruitbelt to CL because of the wye grounded-delta connection of the transformers. Furthermore, since Fruitbelt has inverter-based generation only with low fault current availability, fault detection is not possible by overcurrent measurement. Therefore, undervoltage (27) and residual overvoltage protections (59G) are proposed for detection of 3LG and SLG faults, respectively. Upon the detection of faults in Fruitbelt, these relays isolate the synchronous generator in Cleveland. Thus, overcurrent protection is sufficient for Layer 1 Group 1. Undervoltage and residual overvoltage protections are needed in addition to the overcurrent protection for Layer 1 Group 2 to ensure reliable fault detection.

The 23 kV feeders in Layer 2 are tapped lines (T sections). For providing sensitive protection to these T sections, a differential current protection scheme is proposed for both the Groups 1 and 2. Considering the T sections as protected zones, generic differential relay (ANSI code 87) settings may be provided for the proposed differential relays to allow them to remain stable for external faults and to detect all internal faults in grid-tied mode. Each differential relay detects the faults on one T section and isolates it during faults by tripping the breakers at the boundaries of the T section in grid-tied mode. This differential protection scheme provides the desired response for 3LG faults in islanded mode also for both Group 1 and Group 2. However, because the 23 kV system is connected to the delta side of the transformers, the ground faults in this

system do not produce overcurrent in islanded mode. Therefore, for the detection of ground faults in Groups 1 and 2, residual overvoltage protection (ANSI code 59G) is proposed. A wye grounded-delta connected voltage transformer installed at the Elm street substation bus provides open delta voltage input to the residual overvoltage ($3V_0$) relay to detect ground faults. When a ground fault is detected in the islanded mode, all the 23 kV breakers are tripped to isolate the fault. Thus, differential protection and residual overvoltage protections are needed for the Layer 2 protection for both Groups 1 and 2.

4
STEADY STATE LOAD FLOW ANALYSIS

A regional community microgrid that includes Buffalo Niagara Medical Campus (BNMC), its surrounding neighborhoods, and the greater Buffalo region in New York is being planned by EPRI in partnership with National Grid. The microgrid serves some critial loads such as medical facilities around the Buffalo region and a few residential customers. The aim of the microgrid is to establish high resiliency against any catastrophic weather events or system failures. The proposed approach to achieving high system reliability and resiliency involves increasing the generation assets and distributed energy resources (DER) in the microgrid (45.86 MW) by about twice the total load demand (28.27 MW) in the microgrid. The inclusion of huge proportions of renewable resources and distributed generation would change the distribution grid paradigm. Several studies have projected that deploying large percentages of distributed generation in the distribution grid may result in voltage, loading and protection-related concerns. Hence, a thorough analysis of various grid configurations is essential before the actual commissioning of the microgrid.

Objective and Analysis Approach

The objective of this chapter is to study the steady-state impacts of incorporating new generation assets and distributed energy resources in the microgrid. To ensure successful operation of the proposed microgrid, the concerns regarding the future operation of the microgrid should be evaluated. For this reason, a steady-state model of the BNMC microgrid was developed using DIgSILENT PowerFactory. Various microgrid configurations of both grid-tied and islanded modes of operation were identified. In this chapter, steady-state load flow analyses are carried out for all the defined microgrid configurations. The grid's operating conditions such as voltage, frequency, and power flows are recorded for each of the load flow analysis. From the results, the study aims to ensure that the microgrid has adequate equipment rating and to demonstrate that there are no voltage or thermal overload conditions during grid-tied and islanded modes of operation. In case of any violation, recommendations for a reliable operation of the microgrid are presented.

Analysis Tool and Microgrid Model

The analysis tool used for the study is DIgSILENT PowerFactory. PowerFactory is a leading power system analysis software that supports various advanced distribution system analysis capabilities. It supports sequential power flow (quasi-dynamic) simulations that are performed over successive time intervals typically over a day or a year with consideration to load and generator variations. Additionally, stability analysis functions (RMS) based on adaptive step-size algorithms to observe the impact of load/generator variations are also available. Other capabilities of the software include motor-starting functions, electromagnetic transients (EMT),

optimal power flow, and protection functions. Further, the software allows implementation of new user-defined calculation functions in the form of scripts.

Details on the planned microgrid in the Buffalo region are discussed briefly. The BNMC microgrid can operate in both grid-tied and islanded modes. During the grid-tied mode of operation, the network is currently supplied from the 230kV system and Seneca substation. Islanded modes of the BNMC microgrid are organized into three layers (layers 1, 2, and 3). This project focuses on layers 1 and 2 microgrids, which include five-member, institution-owned buildings within the campus and its surrounding area. The five buildings considered for the study along with their corresponding generation are represented in Figure 4-1. They are State University of New York at Buffalo/School of Medicine (UB/SOM), Kaleida health (KH), Roswell Park Cancer Institute (RPCI), Cleveland BioLabs and portions of adjacent Fruitbelt residential neighborhood.

Layer 1 is a microgrid arrangement where each of the individual main buildings operate in an islanded mode. The Layer 2 arrangement is a microgrid comprised of all the five member-owned buildings. Layer 2 is comprised of two groups – Group 1 and 2 as shown in Figure 4-1. Group 1 buildings include UB/SOM, RPCI and KH. They are currently fed from Gardenville through the 230 kV transmission system to the Elm Street substation. Group 2 buildings that include Fruitbelt and Cleveland BioLabs are fed from Station 34. The two groups are connected by a normally-open switch. They can operate separately or together by opening or closing the normally-open switch.

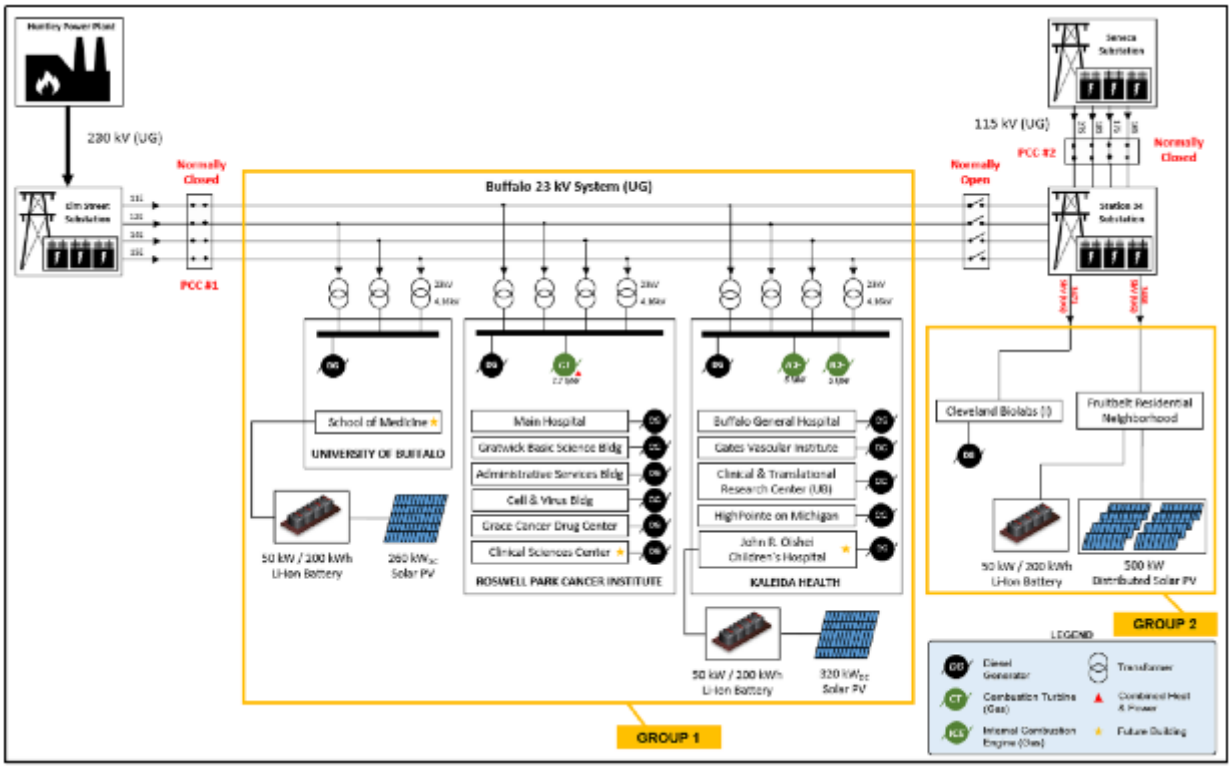

Figure 4-1
Simplified electrical one-line diagram – BNMC layer 2 microgrid with Group 1 and 2

For the purpose of conducting feasibility studies on the microgrid, the proposed BNMC community microgrid is modeled in PowerFactory. The specifics of the modeling process is presented in detail. Since the study is focused on determining the reliability of the network at the distribution side (4.16 kV), the electric network at the 230-kV voltage level is represented by the corresponding Thevenin equivalent source. The equivalent sources of Elm Street station and Station 34 are included at 23 kV in the west and east end of the model as shown in Figure 4-2. Unlike the Elm Street station, the Station 34 has 4 busbars with equivalent sources. Four 23-kV feeders (11E, 12E, 14E and 15E) from Elm Street station are connected to Station 34 through a normally-open switch. Each Group 1 building is fed from four 23-kV feeders through transformers as shown in Figure 4-2. Figure 4-2 also shows that Group 2 buildings are fed from Station 34 through two transformers. All the building loads and generators are modeled at 4.16 kV and are connected to the transmission lines through 23/4.16 kV transformers. Steady-state models of loads, generators, transformers, and other DER are also included in the microgrid.

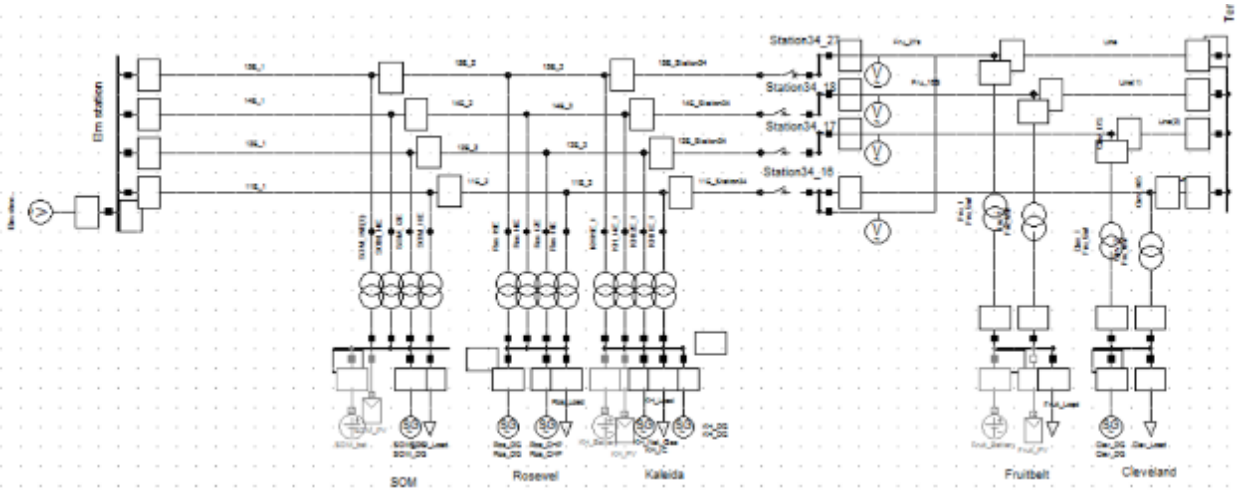

Figure 4-2
BNMC microgrid modeled in DIgSILENT PowerFactory

The actual short-circuit currents of the microgrid at the substation and along the 23 kV feeders are available for validation. The corresponding values from the developed PowerFactory model are compared and presented in Table 4-1. The maximum difference between the actual and the calculated short-circuit currents for both single line-to-ground and three phase faults is only 1.5%. Therefore, the developed simplified model can be considered to be accurate at the 23 kV voltage level.

Table 4-1
Short circuit validation of the model at 23 kV

Bus	Three phase short circuit current (kA)		Difference (%)	Single phase short circuit current (kA)		Difference (%)
	Actual	PF		Actual	PF	
Elm station	28.85	28.85	-0.01	7.27	7.27	-0.01
15E_1	6.12	6.13	0.19	3.82	3.86	0.99

15E_2	6.07	6.08	0.20	3.78	3.82	0.96
15E_3	5.99	6.01	0.24	3.71	3.75	0.93
Station 34_15E	4.24	4.18	-1.40	1.34	1.33	-0.53

Furthermore, circuits at 4.16 kV level are modeled. The first element at 4.16-kV is a transformer, so the transformers are designed first in PowerFactory. All the transformers are considered to be delta connected at the 23-kV side and wye grounded at the 4.16-kV voltage side. The ratings and impedances of the transformers at the individual buildings are summarized in Table 4-2. All the four transformers at each Group 1 building and two transformers at Group 1 building are rated similarly.

Table 4-2
Transformer rating and impedances

Buildings	MVA rating	% impedance
UB/SOM	5	7.16
KH	3.5	5.66
RPCI	5	7.16
Fruit belt	2.5	8.14
Cleveland	2.5	8.14

Next, the loads and generators at each building are modeled. All the loads and generators are assumed to be at the 4.16-kV voltage level. Details on the corresponding capacities at each building are summarized in Table 4-3. A column on generation adequacy at each building is also provided. It is to be noted that the total generation in Group 1 is sufficient to support all the buildings in the Layer 2 microgrid, whereas total generation in Group 2 buildings is not self-sufficient to support the total load in Group 2 buildings. Also, UB/SOM building of Group 1 and Fruitbelt neighborhood in Group 2 are not self-sufficient to support their individual building loads.

Table 4-3
Load and generation data

Buildings		Load (peak) MW	Generation (MW)	Generation adequacy
Group 1	UB/SOM	4.25	DG: 2.5MW, PV: 0.26 MW, Storage: 0.05 MW	1.75 MW deficit
	RPCI	11.04	CHP: 7.7 MW and DG: 13.72 MW	10.38 MW excess
	KH	12.98	IC engine: 10 MW, DG: 11.36 MW PV: 0.32 MW Storage: 0.05 MW	8.38 MW excess

Total in Group 1 buildings		28.27	DG, IC and CHP: 45.28 PV: 0.58 MW Storage: 0.10 MW	17.01 MW excess
Group 2	Fruitbelt	1.4	PV: 0.5 MW Storage: 0.05 MW	0.85 MW deficit
	Cleveland	0.2	DG: 0.8 MW	0.6 MW excess
Total in Group 2 buildings		1.6	DG: 0.8 MW, PV: 0.5, Storage: 0.05	0.3 MW deficit

All the loads are modeled as constant P and Q demands. The real power demand is specified above in Table 4-3. The reactive power of the loads is calculated based on the assumption that the loads operate at 0.9 p.f. (lag) in the analysis. The generation capacity at each building is also tabulated in Table 4-3. Since only MW ratings of the generators are known, the machines are rated (MVA rating) 5% more than the actual MW rating (i.e., operated at 0.95 power factor). All the generators are considered to be synchronous machines. The machines are modeled internally in PowerFactory as an equivalent voltage source behind the synchronous reactance as shown in Figure 4-3. The impedance parameters for diesel generators (DG) and combined heat and power plant (CHP) are provided in Table 4-4. PowerFactory provides appropriate closed-loop control to make the source function as a synchronous generator during load flow analysis.

Table 4-4
Generator impedances

Parameters	DG and IC engine	CHP
Synchronous reactance (xd)	1.79	2
Synchronous reactance (xq)	1.71	2
Zero sequence reactance (x0)	0.002	0.2327
Zero sequence resistance (r0)	0.13	0.002
Negative sequence reactance (x0)	0.13	0.2327
Negative sequence resistance (x0)	0.002	0.002

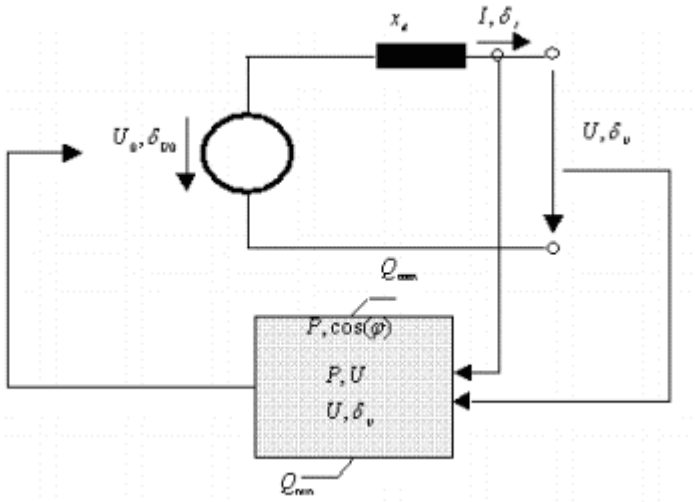

Figure 4-3
Load flow model of the synchronous machine

The active and reactive power control settings of synchronous machines are discussed briefly. The generators are locally controlled to keep the power factor constant. The corresponding control is known as ‘constant-Q’ control. Yet, the reactive power generation by the generators is defined by the capability curve as depicted in Figure 4-4. The x and y axes of Figure 4-4 are the reactive and real power generated by the machine respectively in pu. The real power is always positive; however, the reactive power can be either positive or negative. The reason for the nature of the capability curve is that real power can only be generated by the machine, whereas the reactive power can be either absorbed or generated by the synchronous machine. The maximum magnitude of the reactive power is about ±0.5 pu. Figure 4-4 indicates that the reactive power generation capability of the generator decreases with the increase in real power generation.

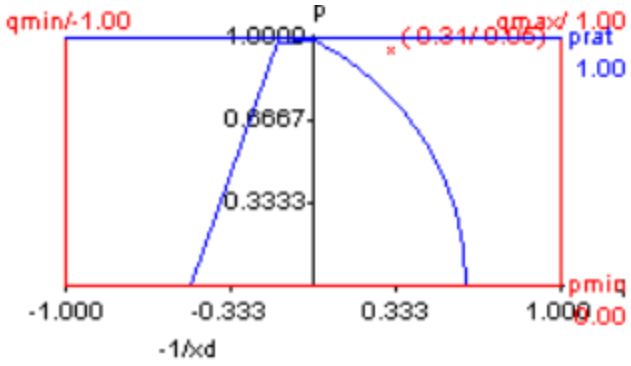

Figure 4-4
Capability curve of synchronous generators

The active power control is effected by an external secondary controller. The active power at each generator is defined by Eq. 2-1,

$$\boldsymbol{P = P_0 + K\,\Delta P_{sco}} \qquad \textbf{Eq. 4-1}$$

where P is the actual active power of the machine in MW, P_0 is the active power setpoint in MW, K is the participation factor, and ΔP_{SCO} is the total active power deviation of all units controlled by the respective power frequency controller.

Further, PowerFactory has many built-in standard models of turbine-governor and automatic voltage regulator (AVR). All the generators in the simulation are defined with the Woodward diesel governor where a droop control is used with either throttle or electric power feedback. Only the diesel generators in the grid are defined with the AVR model called 1968 IEEE type 1 excitation system. DGs are responsible for regulating the voltage at the respective buildings.

BNMC Microgrid Load Profile

The yearly load profile at each building is available from January 1st 2013 to January 1st 2014. Neglecting losses, the load demand at the Elm street station transformer would be the sum of load demands at all the Group 1 buildings. Figure 4-5 shows the substation's load demand for the whole year in 2013. The peak load demand at the substation transformer is observed on September 5th at 1 pm when it reached 24.64 MW. The load demands recorded on September 5th at each of Group 1 buildings and at the Elm Street station are also shown earlier in Figure 2-6. To study the impact of daily load variations, the peak load day is chosen for the analysis. Steady-state load flow analyses are carried out for the day.

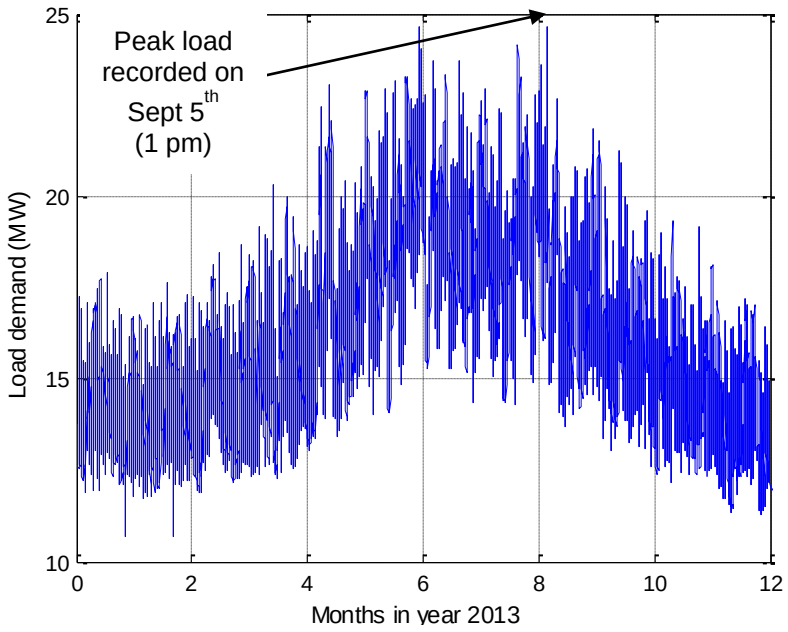

Figure 4-5
Load demand at the Elm street station transformer

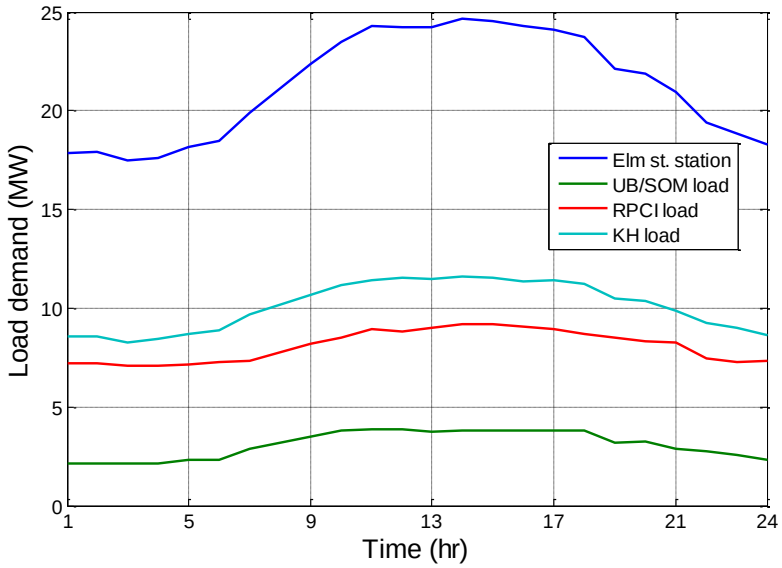

Figure 4-6
Load demand at the Elm street station and Group 1 buildings on Sept. 5th 2013

Similarly neglecting losses, the load demand at the Station 34 transformer is calculated as the sum of loads at Fruitbelt neighborhood and Cleveland BioLabs. The peak load of about 1.5 MW is recorded on August 12th at 4 am. Load flow analysis for the peak load day is carried out to study the daily variation in Group 2 buildings.

During islanded mode, it is possible that the Group 1 and Group 2 buildings may operate together. Therefore, it is necessary to find total load demands of all buildings in the microgrid. Peak load demand of the microgrid is about 25.25 MW which again occurs on September 5th at 1 pm. The coincident peak on September 5th at Group 1 and 2 buildings are 24.64 MW and 0.599 MW respectively. The load demands at Group 1 buildings on the peak load-demand day are represented in Figure 4-6. Group 2 buildings are also assigned load profile as recorded on September 5th.

Load Flow Analysis in PowerFactory

Steady-state load flow analysis of the BNMC microgrid is carried out both in grid-connected and islanded modes of operation using DIgSILENT PowerFactory. The simulations are carried out for an entire day on September 5th and August 12th as discussed in the earlier section. The daily load flow analysis for the study is accomplished either by using Quasi-dynamic or RMS/EMT simulations in PowerFactory. This section elaborates on the two simulation tools available for the analysis.

The Quasi-dynamic simulation tool is designed to perform a series of steady-state load flow simulations typically over a day or year. The simulation considers daily/yearly variations in loads and generators. Daily load profiles that are calculated in the earlier section may be assigned to each individual building loads in the simulation. The generation from the DGs and other local generators are determined by the external secondary control i.e., the power frequency controller and other plant controls (governor turbine and AVR control) that are defined in the grid.

The other simulation tool is the RMS/EMT that help analyze the dynamic behavior of small systems in the time domain. Though the dynamic simulation for the daily time series study may take more computational effort than the quasi-dynamic simulation, the variations in the grid parameters (voltage and frequency) on small time scales (seconds) can be investigated. To reduce the total time necessary to carry out the dynamic simulation, the 24-hour simulation is scaled down to 7200 seconds. Every hour corresponds to 300 seconds. The time scale is chosen because, it typically takes 300 seconds for all the transients due to load/ generation variations to settle down. The load variations in the study are implemented by step changes. Loads are stepped up at every 300 seconds. The explicitly-modeled generator controllers such as the turbine governors, AVR controls, and secondary controls determine the generator output.

The results of the daily simulation carried out using the two simulation tools are compared. For the grid-tied mode, the results from quasi-dynamic simulation and RMS/EMT simulations are similar. Whereas for the islanded simulation mode, there are some discrepancies in the results from both the methods. The results for Layer 2 islanded scenario with Group 1 buildings is presented in Figure 4-7 below. The voltage profiles at each building from both quasi-dynamic and RMS/EMT simulation can be compared in Figure 4-7. It may be observed that the voltage at the RPCI building is always held constant at 1 pu, whereas the corresponding voltage profile is varying in the RMS/EMT simulation. The reason for the 1 pu. voltage profile in the quasi-dynamic simulation is because the generator with the highest generation capacity is considered as the reference/slack bus for the load flow analysis. For this reason, the voltage at RCPI is always at 1 pu. The RMS/EMT simulations seem to provide reasonable voltage variations. The voltage at Elm Street Station is always at 1 pu as there is no power flow from the substation to the grid during the islanded mode of simulation. Therefore, the rest of the simulations in the study are carried out using the RMS simulation tool. The “transient spikes” in Figure 4-7 are transients that are observed during RMS/EMT simulations when the load changes from one level to the other.

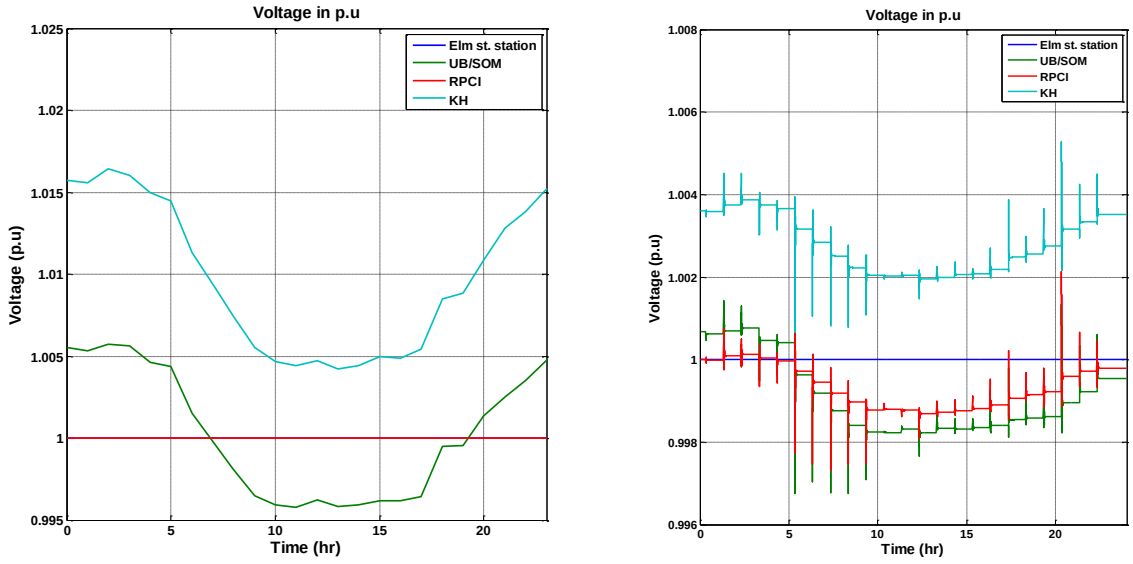

Figure 4-7
Voltage profile in Quasi-dynamic and RMS/EMT simulation

Study Scenarios

The BNMC microgrid can be operated in various islanded and grid-tied modes of operation. In this section, the simulated study scenarios and their corresponding assumptions are detailed. The study scenarios are enumerated below,

1. **Base-case scenario:** A grid-tied scenario with no local generations (such as DG, PV, and energy storage sources) in operation is considered as the base-case study. Peak load-demand day as observed at Elm Street Station and Station 34 are used for the simulation. The results of the scenario are used as reference quantities to compare those from other scenarios.

2. **Grid-tied with local generations:** Again, a grid-tied scenario is simulated, but with the local generations in service (only diesel generators operate. PV and energy storage are not in service). The peak loads as observed at Elm Street Station and Station 34 are used as the loading conditions. The objective of the study is to measure the maximum reverse power flow and the impacts of it on the voltage and frequency.

3. **Layer 1 island:** Each building is islanded from the rest of the grid and operated at peak loads from the perspective of each island. Local generation meets the load demand. If the generation is insufficient, load shed may be necessary. The scenario is conducted to study the ability of each island to operate independently in terms of voltage and frequency variations. Also, the required load shed is estimated.

4. **Layer 2 island with Group 1:** A scenario where Group 1 buildings in Layer 2 operate as an island. The island is operated at the peak-load day of the entire Group 1 buildings. The objective of the study is compare the voltage and frequency profiles with the base-case scenario. The ability of the Group 1 buildings to operate in island is determined.

5. **Layer 2 island with Group 1 and 2:** All the Layer 2 buildings i.e., Group 1 and 2 buildings, operate together as an island. The island is operated at the peak load day of the entire Group 1 and 2 buildings together. The ability of the buildings to operate in island is determined.

Assumptions

- PV and storage are not in service because the total generation capacity of the renewable sources is very much less compared to the total synchronous based generation capacity (only 1.99%).
- All the loads are assumed to be operated at 0.9 lagging power factor.
- The MVA ratings of the generators are fixed at 1.05% of the rated real power output of the machine (assumed to operate at 0.95 power factor).
- In case of insufficient generation, it is assumed that non-critical loads will be shed in such a way to match the total load with the generation capacity in the grid.
- There is a power-frequency controller for the secondary control in the microgrid. It is a droop control based algorithm that adjusts the generation based on each generator’s participation factor.

- All the generators in the simulation are equipped with a Woodward diesel governor, where the droop control is used with either throttle or electric power feedback.
- All the diesel generators (DG) in the grid are defined with the AVR model called 1968 IEEE Type 1 excitation system. The DGs are responsible for maintaining the voltage at each building.

Base-case Scenario

A typical grid-tied operation of distribution grid without any local generation is considered as a base-case scenario. The objective of the study is to measure the voltage, frequency and power flows at each bus for the base-case study. The parameters are used as reference quantities to compare with those from other case studies. The loading conditions for the simulation correspond to the days when peak loads are observed by the Elm Street Station and Station 34 respectively. The peak loads occur on September 5th and August 12th at Elm Street Station and Station 34 respectively in the year 2013.

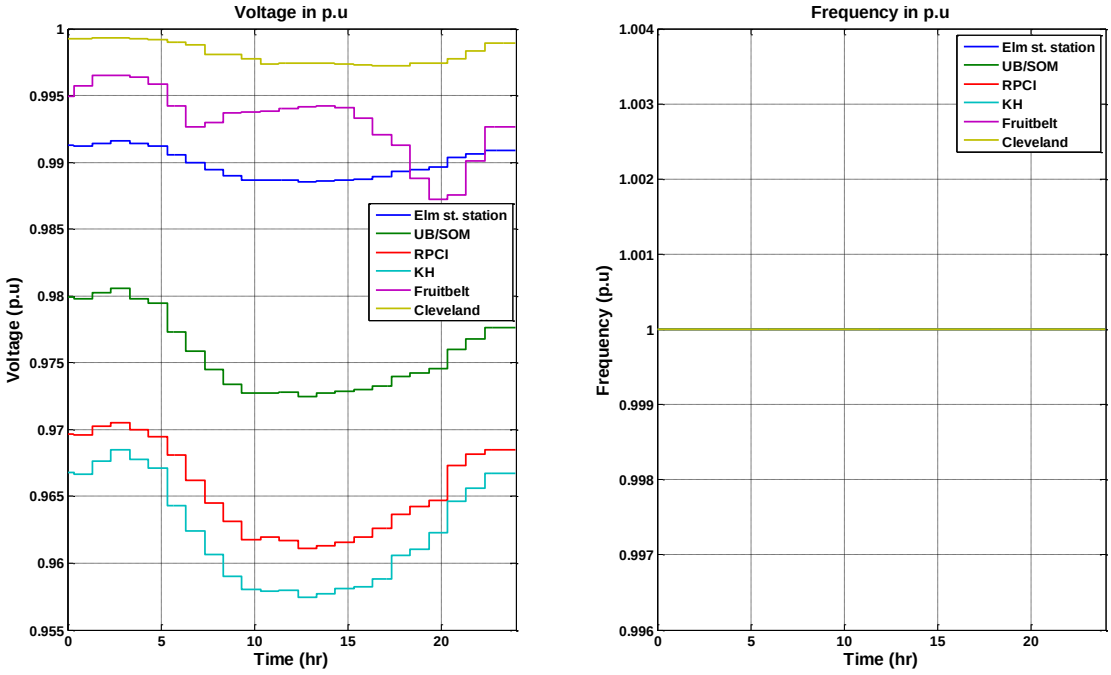

Figure 4-8
Base-case: Voltage and frequency profile at each building

Voltage and frequency at each building is shown in Figure 4-8. Elm Street Station has a voltage closer to 1 pu, whereas, the buildings that are fed from Elm Street Station have a voltage drop which is proportional to the electrical distance from the substation. It can be observed that the range of voltage during the day is between 0.95 pu and 0.99 pu for Group 1 buildings. Similarly, the voltage range for Group 2 buildings is between 0.98 pu and 0.99 pu. The voltages at the Group 2 buildings are closer to 1 pu, because of shorter distribution lines and therefore less voltage drop across the lines. The frequency at the buildings is always at 1 pu, as the total load demand in the grid is always satisfied.

The real and reactive power flows from Elm Street Station for the base case are measured and depicted below in Figure 4-9. The maximum active and reactive power flows from Elm Street Station are 24.64 MW and 12.5 Mvar, respectively. Power demand at each Group 1 building is also shown in Figure 4-9. The power demands correspond to the peak load data on September 5th 2013 as shown earlier in Figure 4-6. In addition, the real and reactive power losses are plotted in Figure 4-9. It can be observed that no real power losses occur, but peak reactive power losses appear to be about 1.5 Mvar. The reactive power losses are primarily due to the losses in transformers.

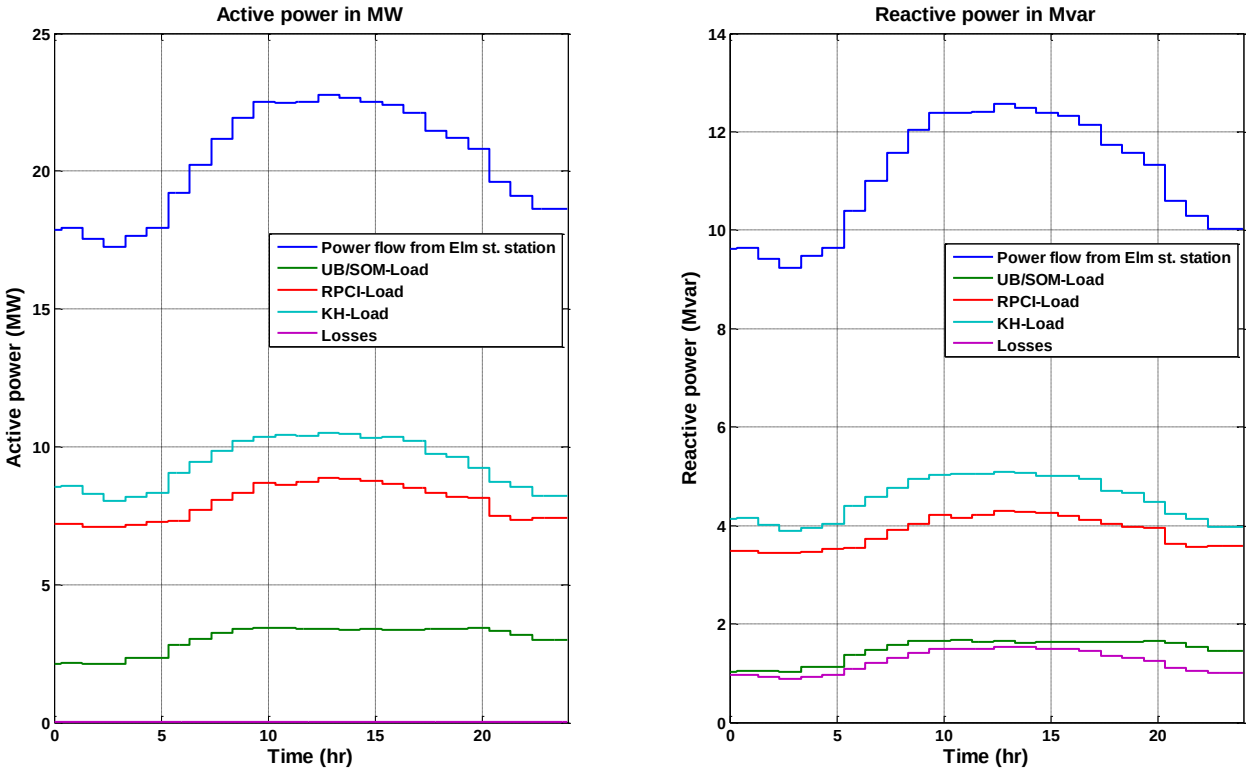

Figure 4-9
Base case: Real and reactive power flow and demand at Group 1 buildings

Similarly, real and reactive power flows at Station 34 are represented in Figure 4-10 below. The peak real and reactive powers are 1.1 MW and 0.55 Mvar respectively. The corresponding load demand at each Group 2 building is also plotted in Figure 4-10. Load demands correspond to the load profiles recorded on August 12th 2013, as the peak load demand was observed on that day at Station 34. The peak losses in the Group 2 buildings are relatively smaller (3.6% of total peak reactive power flow) compared to the Group 1 buildings (12% of total peak reactive power flow), due to the lesser number of transformers in Group 2 buildings.

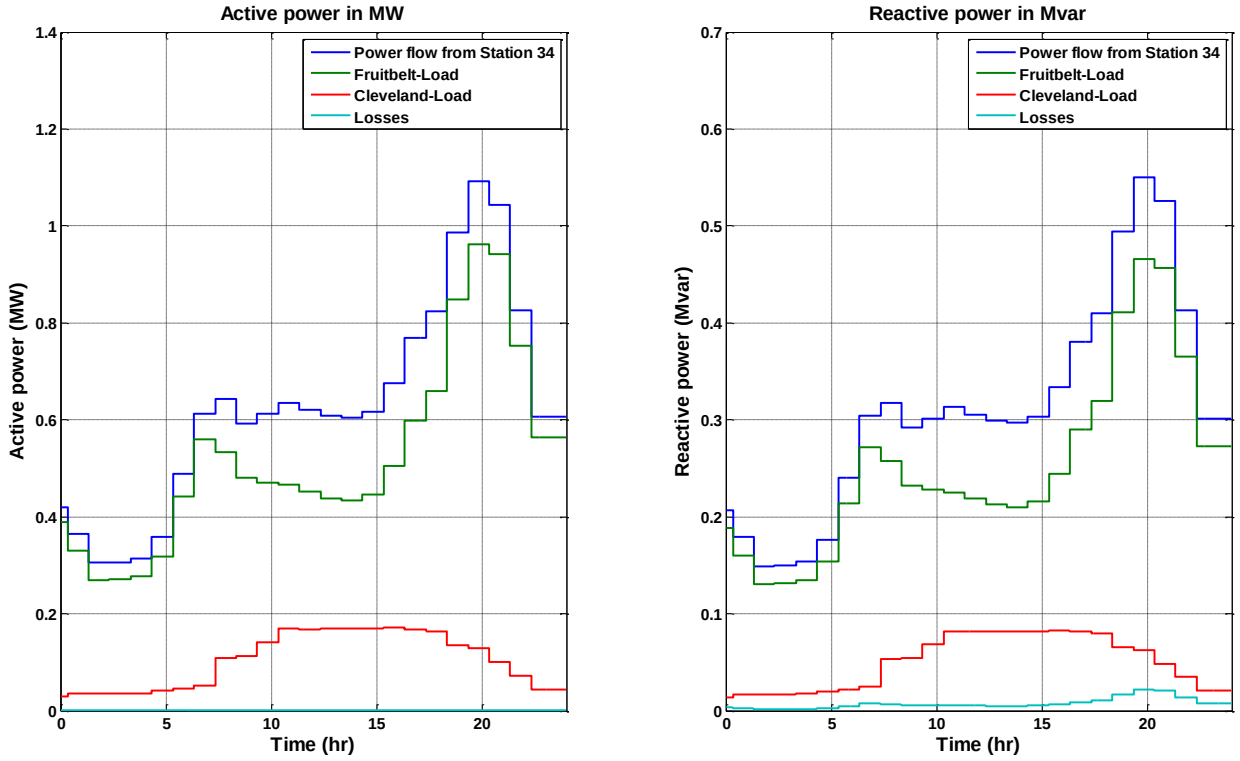

Figure 4-10
Base case: Real and reactive power flow and demand at Group 2 buildings

The peak load of the Group 1 and 2 buildings are 24.6 MW, 12.5 Mvar and 1.1 MW, 0.55 Mvar, respectively. The demand is met by the power flow from the corresponding substations in this scenario. The voltage range for base-case scenario for Group 1 buildings falls between 0.95 and 0.99 pu. Similarly, the voltage range for Group 2 buildings falls between 0.98 and 0.99 pu. In Sections 2-4-2 to 2-4-5, various grid configurations are analyzed. The power flows and voltage ranges for each of the scenarios are evaluated and compared with those of the base-case study.

Grid-tied with Local Generation

Another grid-tied scenario with all local generation (except PVs and energy storage) in operation is considered. The purpose of this scenario is to investigate the maximum reverse power flow that may be experienced in the grid and to study the maximum voltage rise in such conditions. Peak load-demand day is considered for this analysis as well. The load profiles correspond to the load demand observed on September 5th and August 12th 2013 for Group 1 and 2 buildings respectively. With local generation in service, the generation adequacy at each bus is studied. If the generation is insufficient, the power exchange between individual building groups and substation are analyzed. In addition, the voltage and frequency profiles at each building during the grid-tied building operation are recorded.

The voltage profile observed at each building is plotted in Figure 4-11 below. The range of voltage magnitude falls between 1.002 pu and 1.016 pu for Group 1 buildings. Similarly, the range of voltage magnitudes for Group 2 buildings falls between 0.99 pu and 1.018 pu. The voltage range is generally more than the value that is observed for the base-case scenario. Individual comparisons of the building voltage profiles are also presented in Figure 4-12. The reason for the increase can be attributed to the reverse power flow due to local generation at each building.

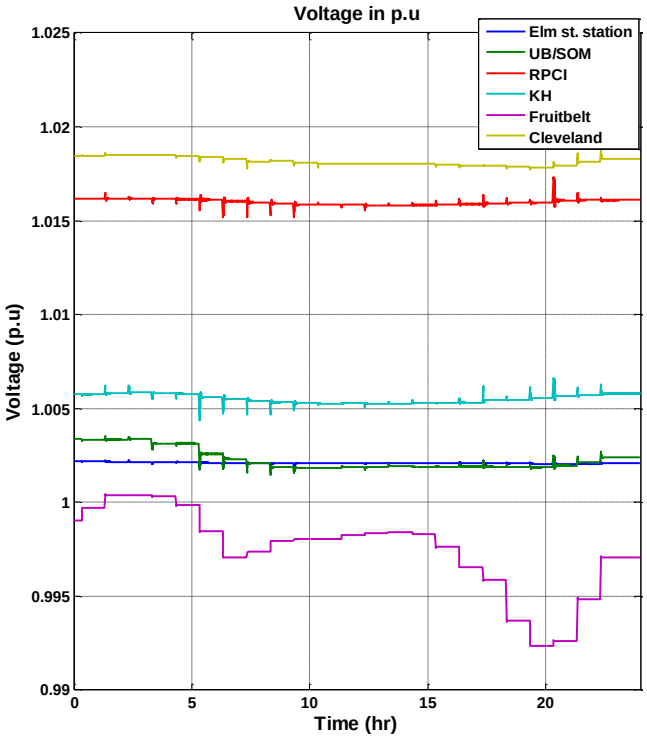

Figure 4-11
Grid-tied with local generations at rated capacity: Voltage profile at each individual building

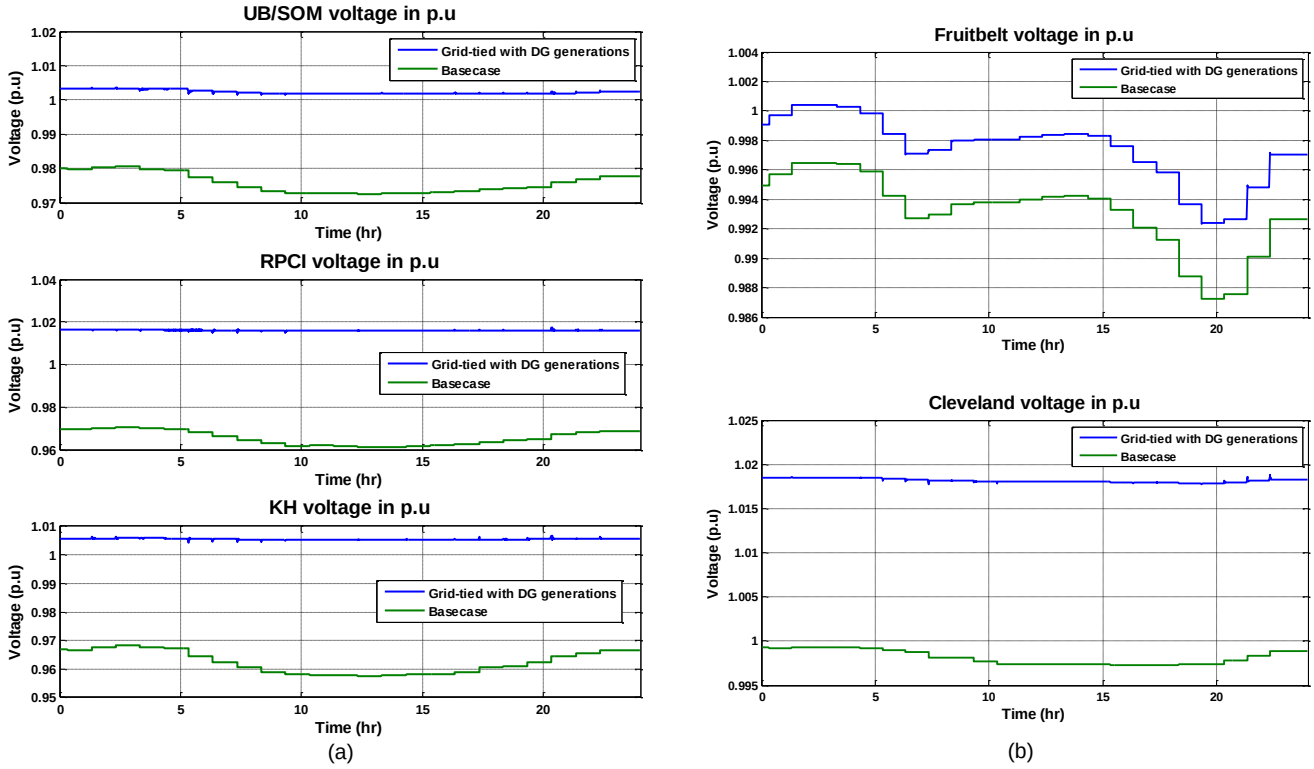

Figure 4-12
Voltage profiles of grid-tied with local generation scenario and base-case scenario (a) Group 1 buildings (b) Group 2 buildings

The power flow at each building is presented in Figure 4-13 to Figure 4-15. All the generators are assumed to be generating at its rated power at 0.95 power factor during the simulation. The results of the simulation are analyzed building-wise.

The power flow at UB/SOM building is plotted in Figure 4-13. It may be observed that the peak generation is 2.5 MW, whereas the peak load is about 3.5 MW. So it is evident that the total generation at the SOM building is insufficient to support the total real and reactive power demand at the building. About 1 MW and 1 Mvar of real and reactive power flows from RPCI and KH buildings. Since the power to SOM building does not flow from Elm Street Station through the 11E, 12E, 14E, and 15E feeders, the associated losses and voltage drop are absent. Therefore, it may be observed in Figure 4-12 (a) above that the voltage at the UB/SOM building is close to 1 pu compared to the base-case voltage profile. The study signifies the importance of local generation in a distribution grid.

The power flow at RPCI and KH buildings in Figure 4-13 and Figure 4-14 show excess generation at these buildings. The peak reverse power flow totally from RPCI and KH buildings is about 27.6 MW and 4.14 Mvar. Besides serving the deficit power at UB/SOM, the rest of the power is fed back to the Elm Street Station. The peak reverse power flow at the Elm Street Station is 28.1 MW and 1.9 Mvar. The power flow at the Elm Street Station in Figure 4-14 may be observed to have a negative sign because of the reversal of the power flow direction.

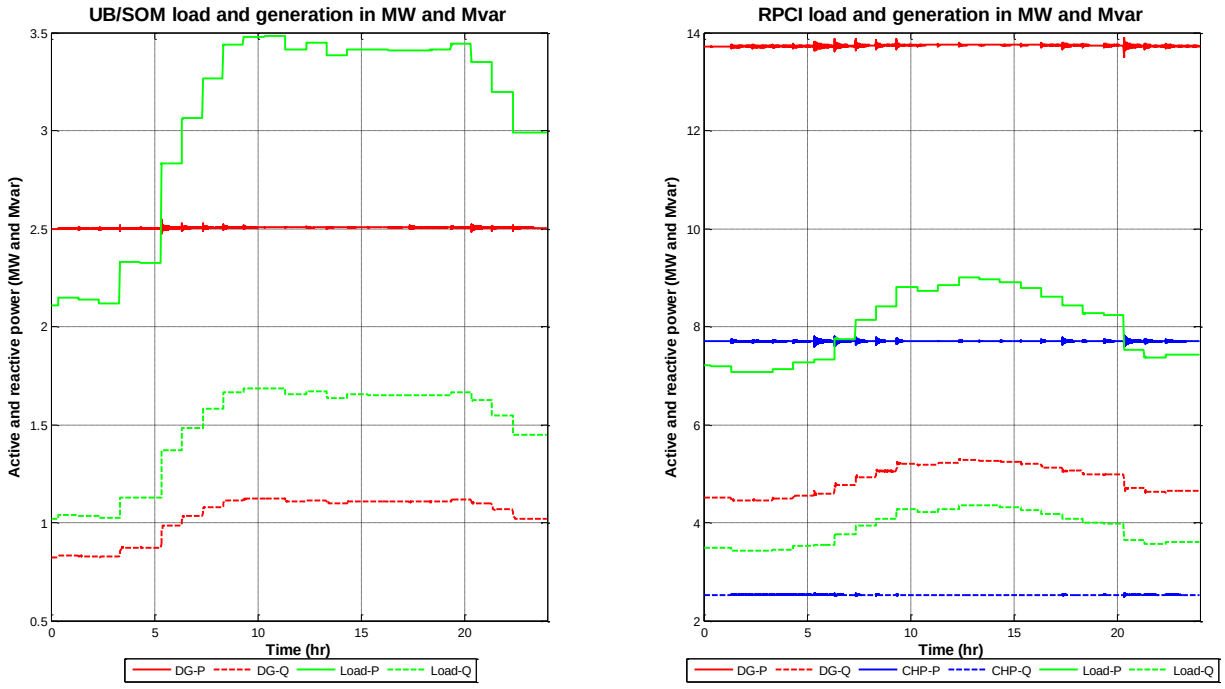

Figure 4-13
Grid-tied with local generations: Active and reactive power generation and load demand in SOM and RPCI buildings.

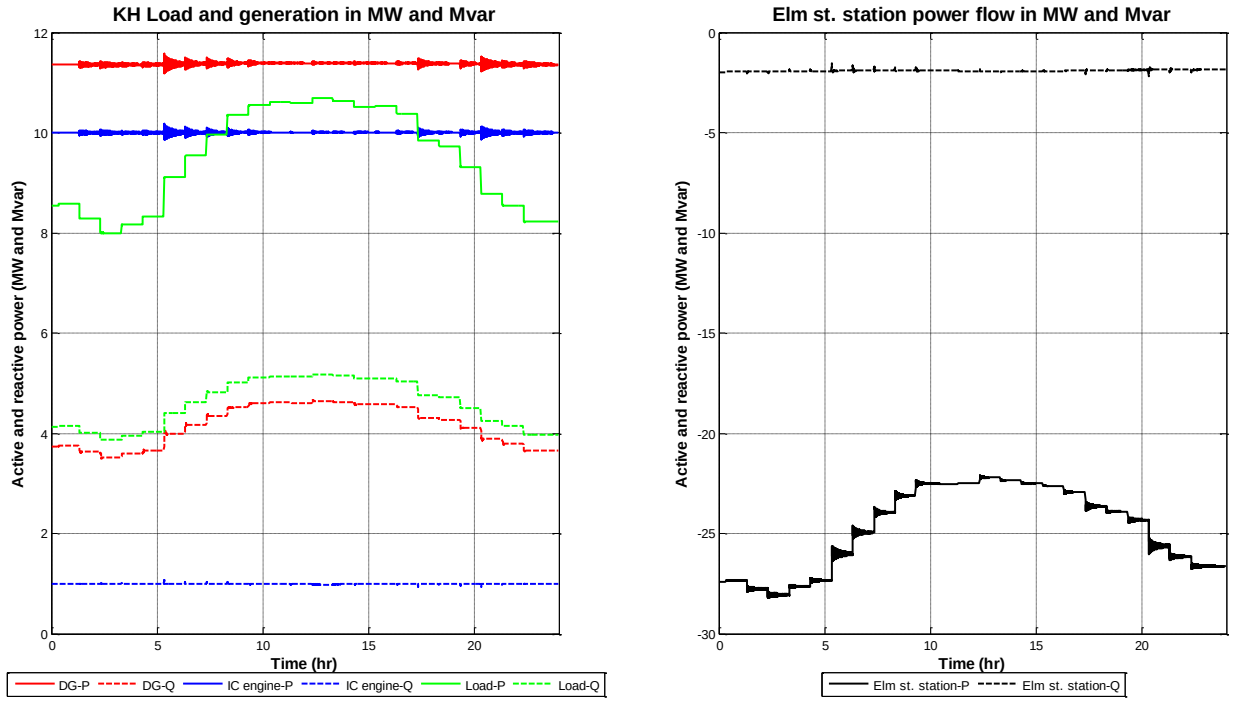

Figure 4-14
Grid-tied with local generations: Power flows in KH building and at Elm St. Station.

Similarly, the power flows at Group 2 buildings is shown in Figure 4-15. There is no local generation at Fruitbelt. All the load demand of the building is satisfied from either the Cleveland BioLab building or from Station 34. Cleveland BioLabs, however, is self-sufficient and can operate without any support from Station 34. The maximum reverse power flow from the Cleveland BioLab building is 0.49 MW.

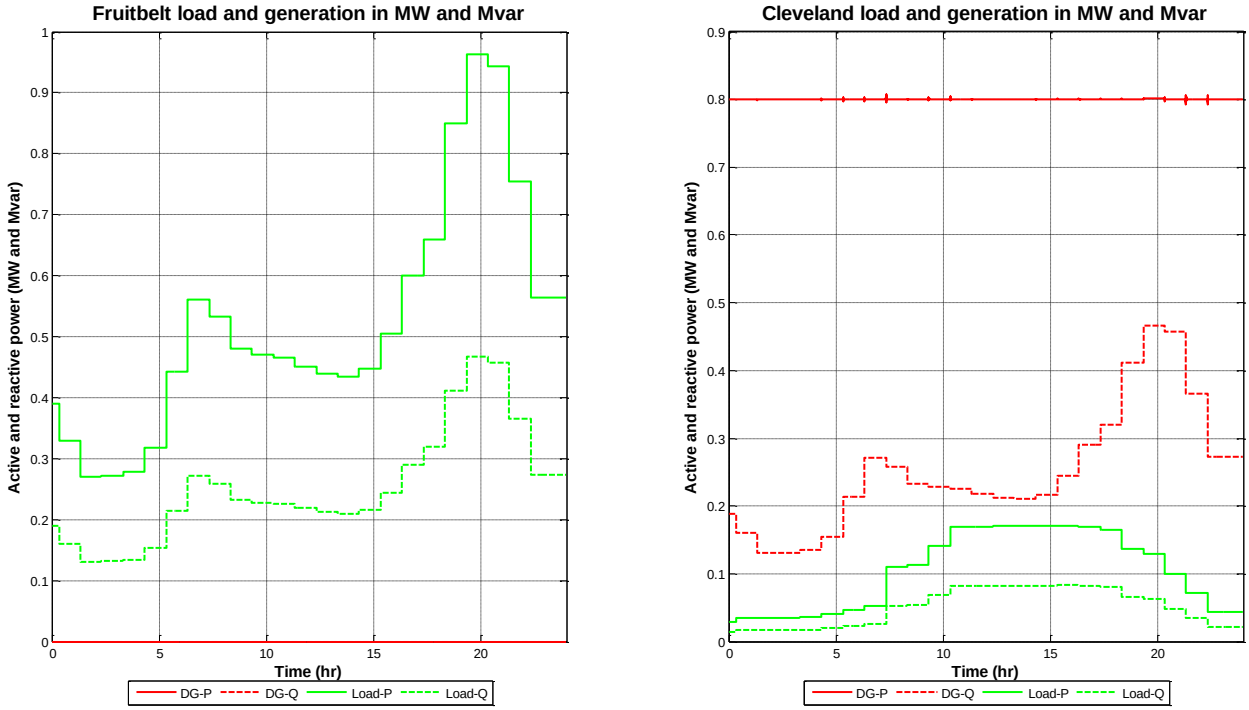

Figure 4-15
Grid-tied with local generations: Power flows in Fruitbelt and Cleveland buildings

The peak generation at Group 1 and 2 buildings are 45.83 MW, 14.57 Mvar and 0.8 MW, 0.45 Mvar respectively. The grid-tied scenario with all the local generation in operation results in back feed towards the substation. The maximum back feed towards Elm Street Station and Station 34 is 28.18 MW, 2.18 Mvar and 0.77 MW, 0.49 Mvar respectively. There is sufficient generation at the microgrid, with voltages and frequency at the buildings close to 1 pu. The voltage profiles indicate that the scenario with local generation is better compared to the base-case scenario.

Islanded Scenario: Layer 1

The first islanded study scenario examines the Layer 1 microgrids. Each building is operated as an isolated island from the rest of the grid. The aim of the scenario is to analyze the ability of each building to operate as a separate island. The load demands at each building are assumed to be equal to individual building peaks. For some of the buildings, e.g., UB/SOM and Fruitbelt, the peak load demand is more than the peak generation available at the building. Load shed is necessary in those buildings and the corresponding load shed is determined in this study. It is assumed that an appropriate load shed algorithm is implemented in the buildings so that a balance between the total generation and load demand is maintained. Based on the assumption, this study simulates the load shed and ensures reliable operation of the island.

There are four Layer 1 islands in the microgrid such as (i) UB/SOM, (ii) RPCI (iii) KH and (iv) the combined Fruitbelt neighborhood and Cleveland BioLab buildings. Details of each of the Layer 1 microgrids are elaborated in this section. Load flow analysis of each island on their corresponding peak day is carried out. The bus voltage and frequency variations due to hourly load change are recorded and presented for each of the buildings. Since the generation is sufficient in the island, the frequency at the microgrid is maintained at 1 pu.

First Layer 1 island that is considered for the analysis is the UB/SOM building. The load profile and the corresponding generations are plotted in Figure 4-16. The load at UB/SOM has been scaled down such that the peak demand is less than the generation capacity of 2.5 MW. It may be observed that the generation follows the total load demand in the building. Voltage profile at the building at the islanded condition is compared with that of the base-case scenario. The voltage is closer to 1 pu compared to the base-case scenario. The reason is due to the absence of distribution lines and the corresponding voltage drop. Also the generator has AVR control that tries to maintain the voltage profile closer to 1 pu.

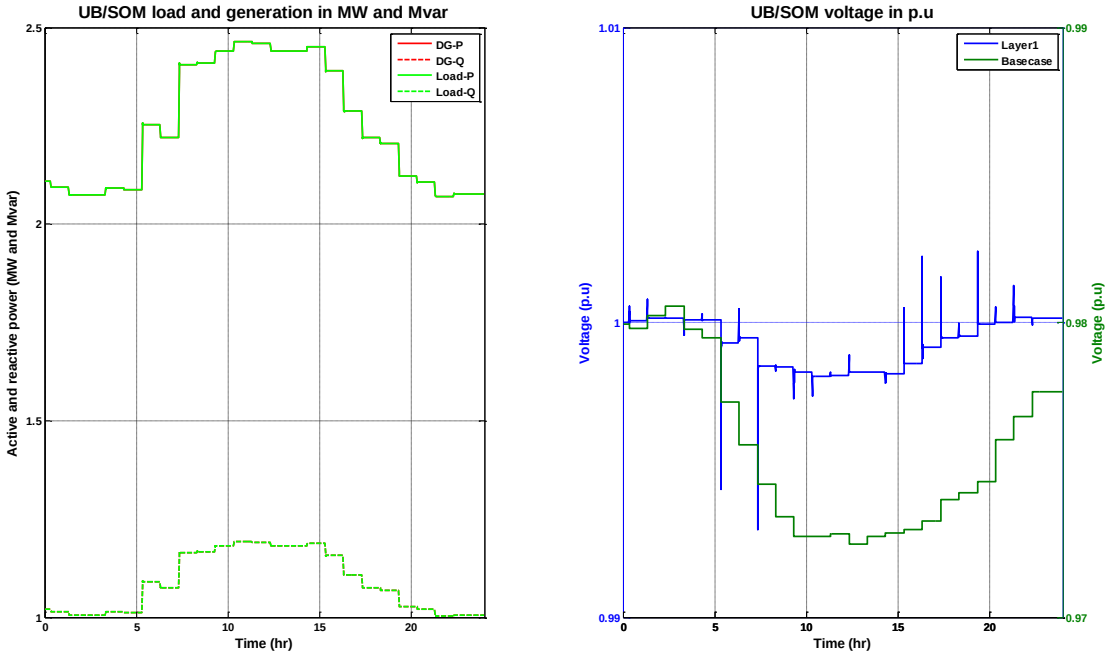

Figure 4-16
Islanded scenario: Layer 1 UB/SOM building. Power flows and voltage profile.

Similarly, the load, generation, and voltage profile at Layer 1 islands of the KH and RPCI buildings are presented in Figure 4-17 and Figure 4-18, respectively. The generation at the buildings in Figure 4-17 and Figure 4-18 may be observed to adjust their real and reactive power output according to their participation factors (K) in the power frequency control. Also, the voltage at the terminals remains close to 1 pu.

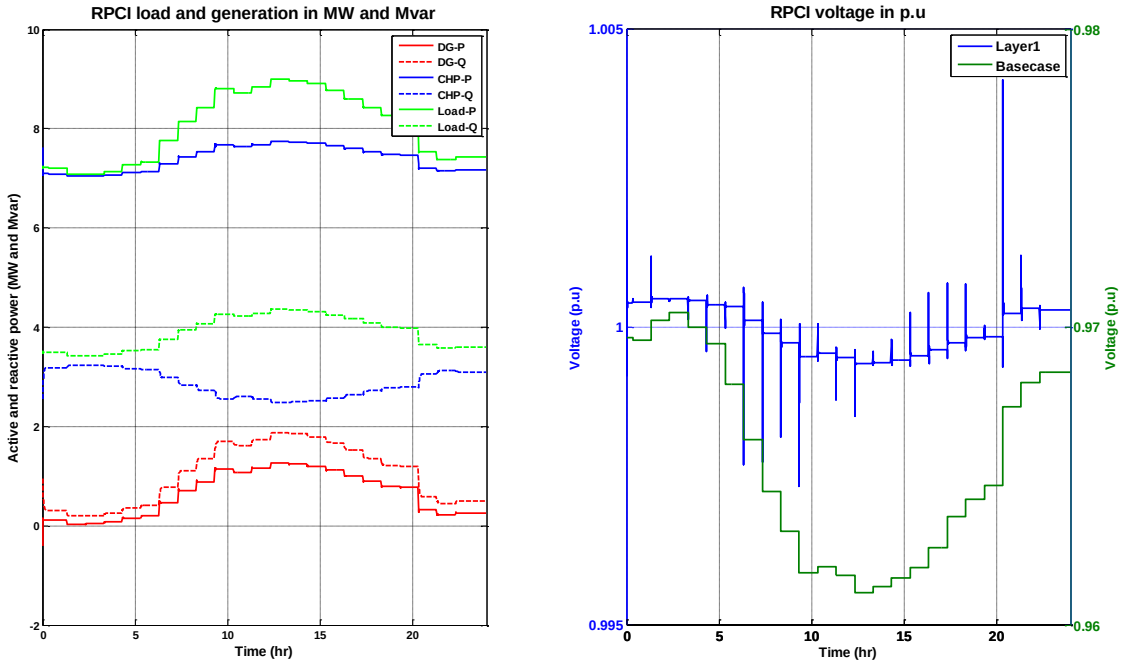

Figure 4-17
Islanded scenario: Layer 1 RPCI building. Power flows and voltage profile.

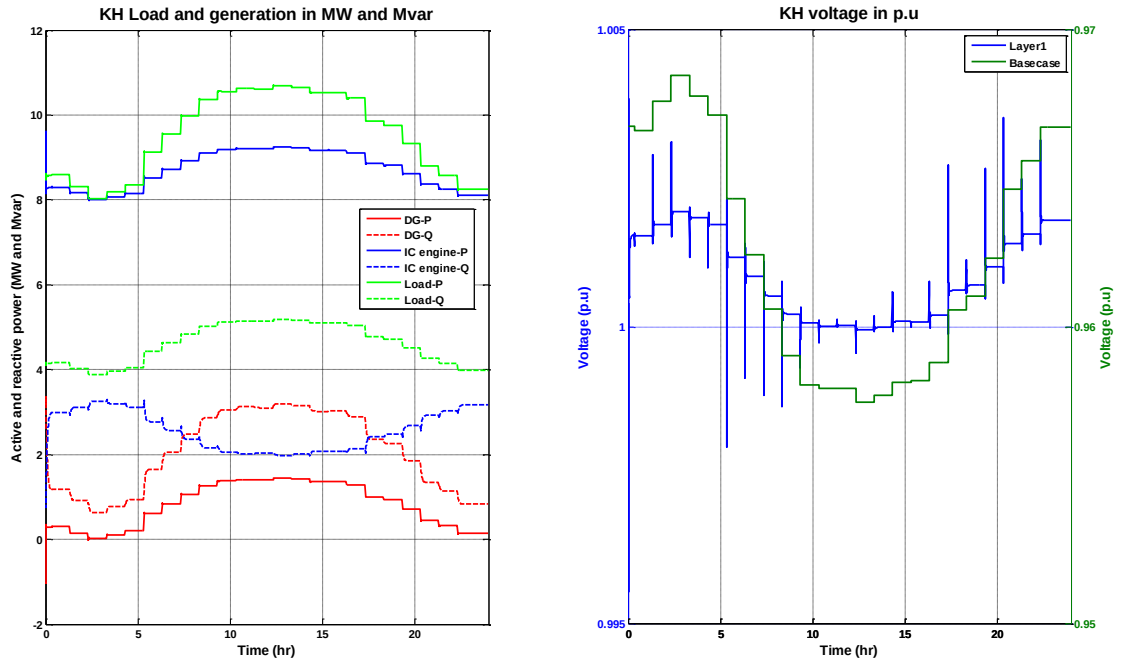

Figure 4-18
Islanded scenario: Layer 1 KH building. Power flows and voltage profile.

The last Layer 1 island is Fruitbelt and Cleveland BioLab buildings operating together. Non-critical loads at the Fruitbelt building are shed such that the total demand (Fruitbelt and Cleveland BioLabs) at the island is less than the DG capacity at Cleveland (0.8 MW). In this study, the PV at the Fruitbelt building is assumed not to be in service, so the real and reactive power output of PV seen earlier in Figure 2-19 is zero. The voltage profile at the Fruitbelt building is plotted in Figure 4-19. The voltage is closer to 1 pu compared to the base-case scenario. It is to be noted that unlike other buildings the voltage at Fruitbelt building is never above 1 pu during the day. This is because no generation is assigned to the Fruitbelt building in this study.

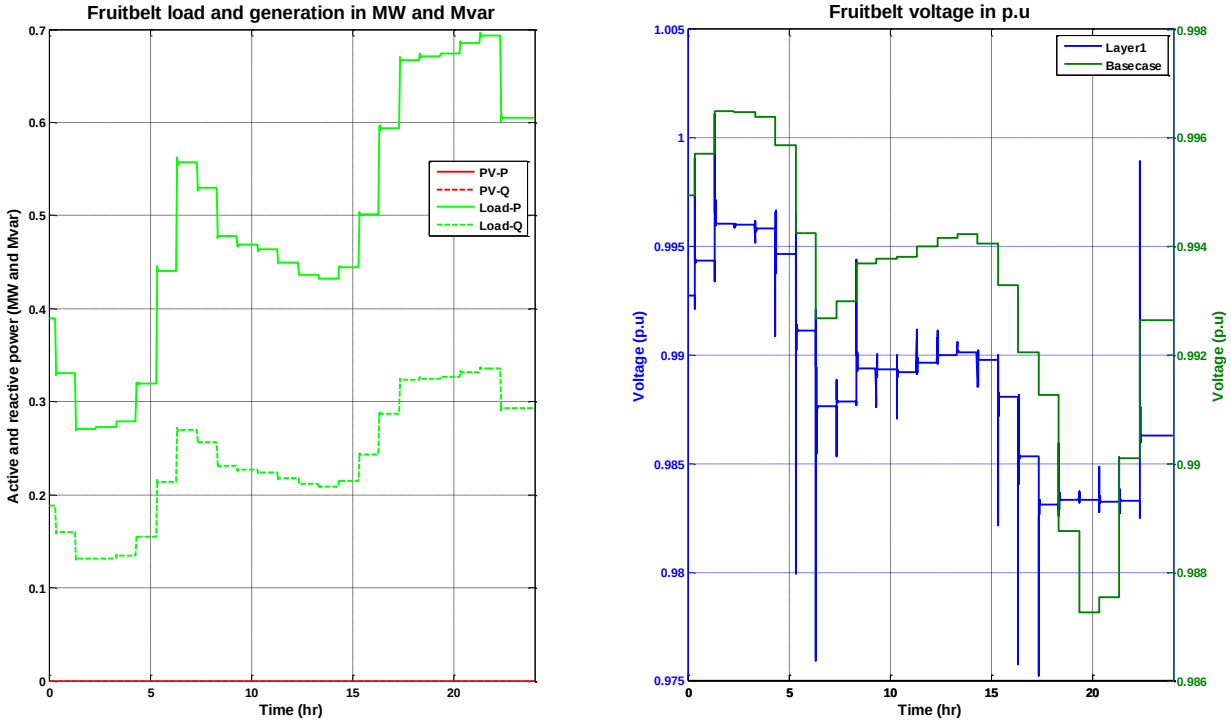

Figure 4-19
Islanded scenario: Layer 1 Fruitbelt building. Power flows and voltage profile.

The generation and load profile at Group 2 building is shown below in Figure 4-20. It may be observed that excess generation occurs at the building to support the load demand at Fruitbelt building. The voltage profile at the building is close to 1 pu. compared to the base-case profile.

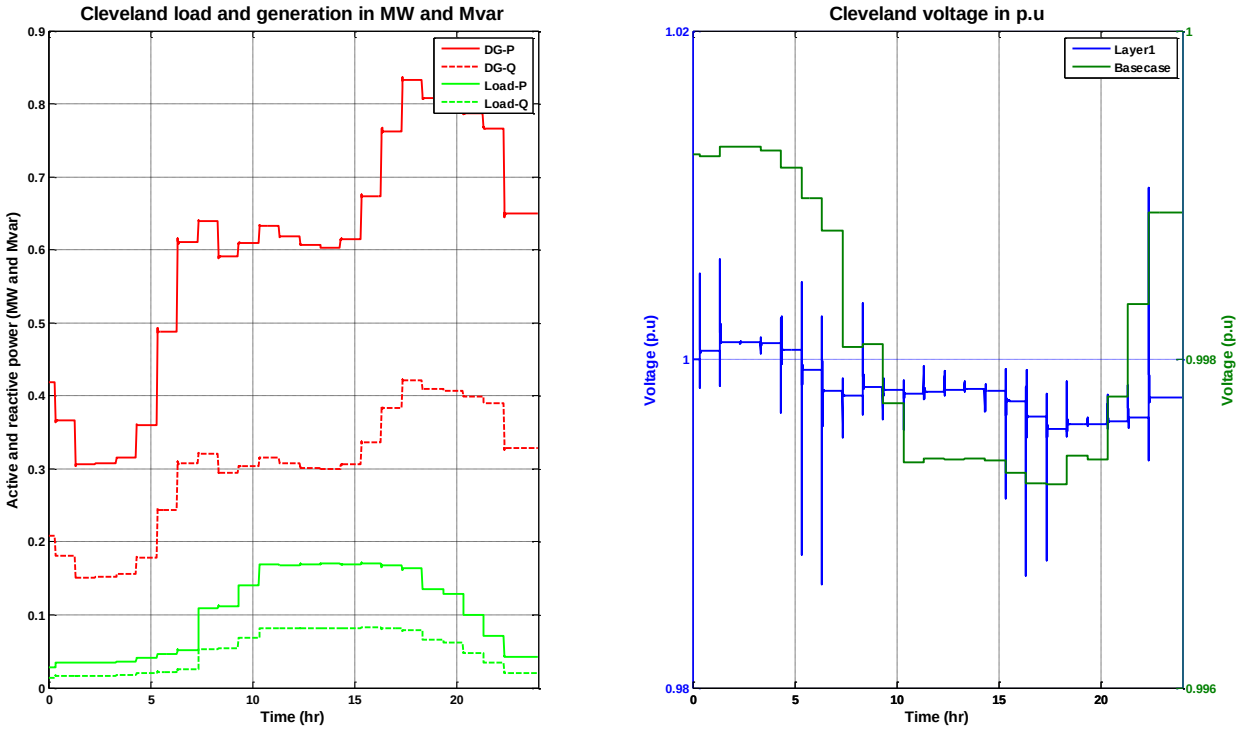

Figure 4-20
Islanded scenario: Layer 1 Cleveland BioLabs building. Power flows and voltage profile.

The operation of Layer 1 islands is studied in detail for the corresponding peak load day in the year 2013. For reliable operation, the UB/SOM island and Group 2 islands should undergo load shed such that total demand is met by total generation in the building. The corresponding load shed is calculated in the study. The load flow analysis with the respective load sheds indicate that the voltage and frequency at each island is maintained at 1 pu and the voltage profiles are better compared to the base-case scenario.

Islanded Scenario: Layer 2 with Group 1

Another islanded scenario where all Group 1 buildings, as marked in Figure 4-1, are operated in isolation from the rest of the grid. The objective of the scenario is to study the reliable operation of the microgrid on a peak load-demand day. Appropriate load shed algorithms are implemented to ensure the generation adequacy on the day. In addition, voltage and frequency fluctuation are estimated and compared with that of base-case scenario. The load profiles in the analysis correspond to the day when peak load demand of the entire Group 1 buildings is observed. As discussed previously in Section 0, the peak demand of 24.6 MW is recorded at Elm Street Station on September 5th. The load profiles as observed on September 5th are assigned to all buildings for the simulation. The generations at Group 1 building are sufficient to support all the loads in the island. Therefore, no load shed is required in the simulation. The bus voltage and frequency variations at the buildings are recorded and compared with the corresponding base-case scenario values in this section.

The voltage profiles at each of Group 1 building are plotted in Figure 2-21. The voltage at KH building may be observed to exceed that of the rest of the buildings. The reason for the voltage difference is due to the reactive power flow—reactive power flows from KH building to the other buildings. The voltage at the Elm Street Station remains at 1 pu since no power flows from the substation.

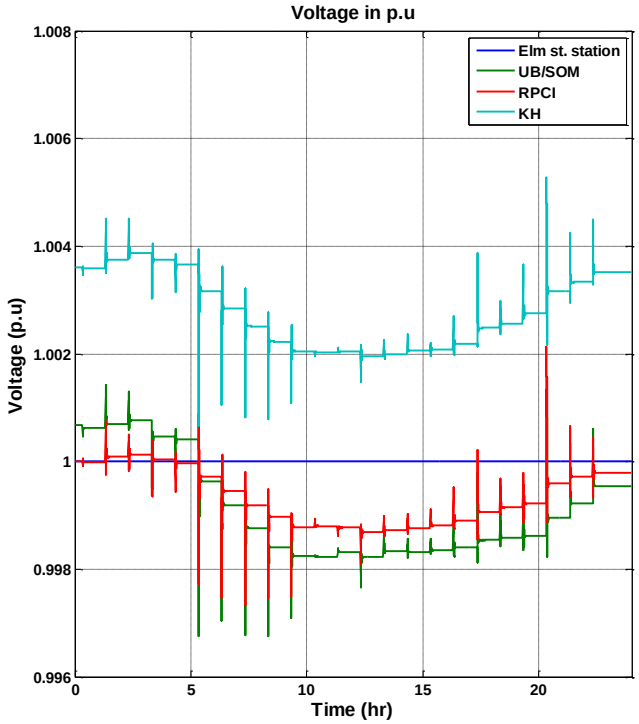

Figure 4-21
Islanded scenario: Layer 2 Group 1 – Voltage profiles.

The voltage and frequency profiles at each building are compared with the corresponding base-case scenario in Figure 4-22 below. The voltage and frequency at the buildings are maintained closer to 1 pu. compared to the base-case scenario.

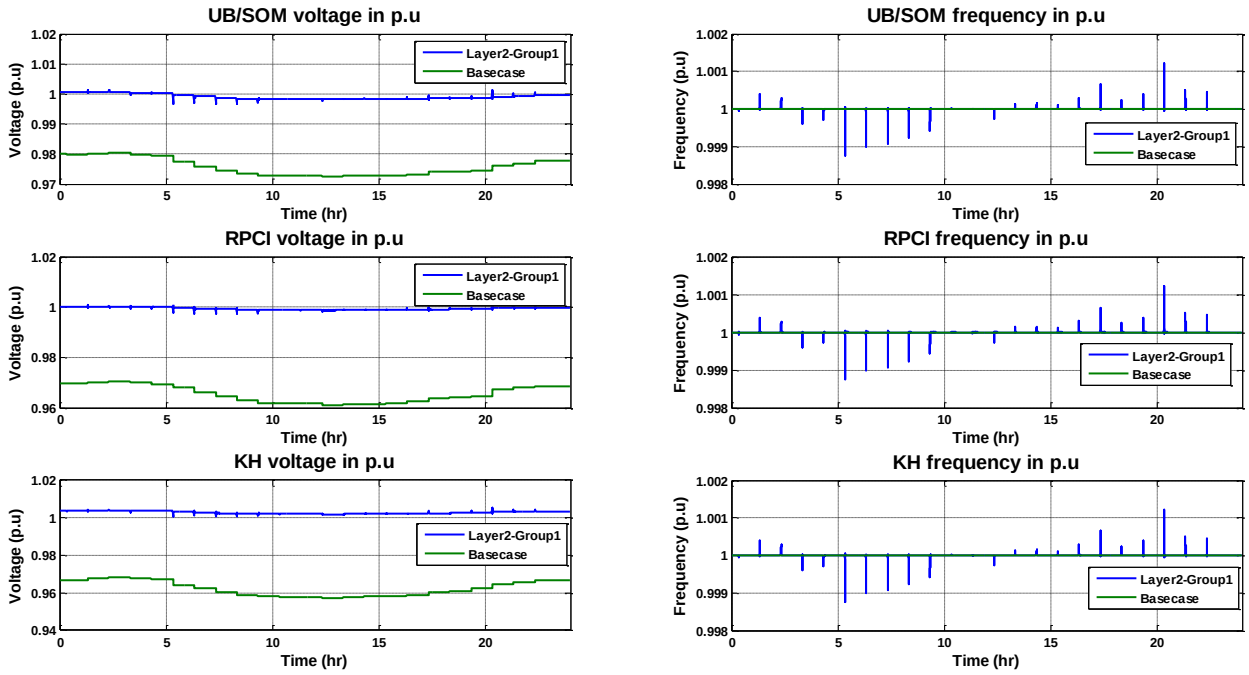

Figure 4-22
Islanded scenario: Layer 2 Group 1 and base-case – Voltage and frequency profiles.

Next, the power flow in the islanded Group 1 buildings is analyzed in Figure 4-23 and Figure 4-24. All the buildings are self-sufficient except UB/SOM building. The peak load is 3.5 MW at SOM building and the generator output is only 1.25 MW (see Fig 2-23), the rest of the active power (2.16 MW) flows from KH (1.96 MW) and RPCI buildings (0.18 MW). Peak reactive power of about 0.6 Mvar flows from KH building to SOM (0.36 Mvar) and RPCI building (0.24 Mvar).

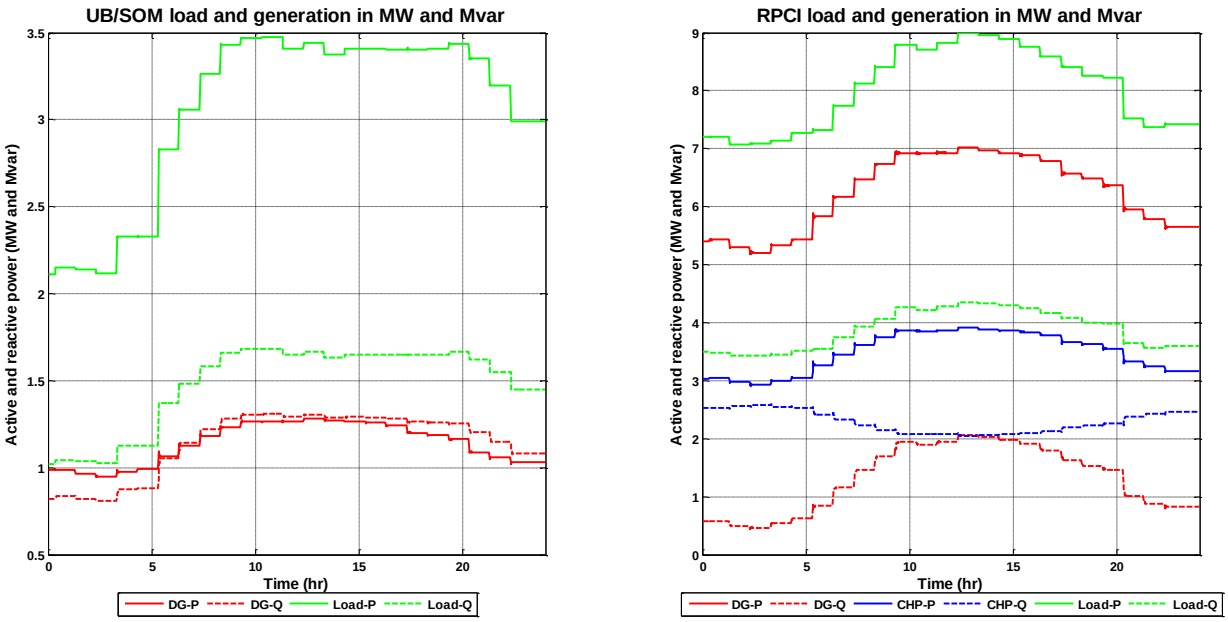

Figure 4-23
Islanded scenario: Layer 2 Group 1 – Power flows at UB/SOM and RPCI building.

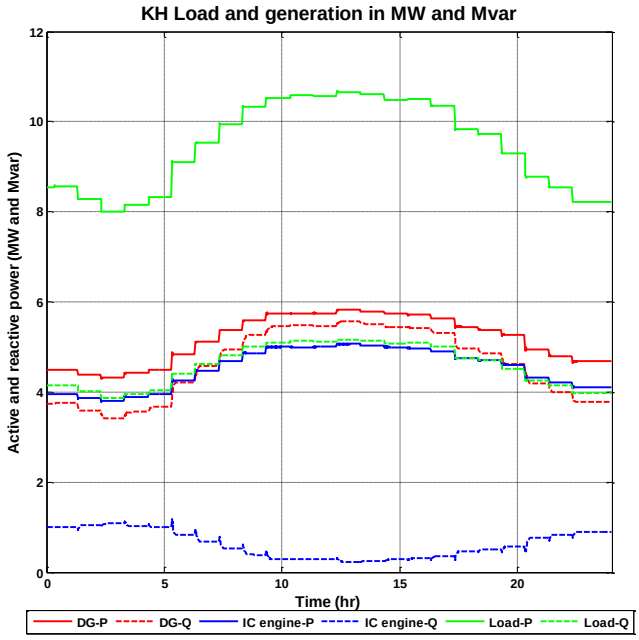

Figure 4-24
Islanded scenario: Layer 2 Group 1 – Power flows at KH building.

The Group 1 microgrid is operated on peak load demand day as observed on September 5th 2013. The microgrid has sufficient generation that it can reliably operate without any load shed. The voltage and frequency profiles in the microgrid are maintained close to 1 pu.

Islanded Scenario: Layer 2 with Groups 1 and 2

The last islanded scenario includes operation of all Group 1 and 2 buildings isolated from the rest of the grid. The objective of the scenario is to ensure reliable operation of the microgrid on a peak load-demand day. To ensure generation adequacy, required load shed in the grid is estimated. The voltage and frequency profiles and power flow between the buildings are evaluated. The load profiles in the analysis correspond to the day when peak load demand of all Group 1 and 2 buildings is observed. As discussed previously in Section 0 the peak demand of 25.25 MW is recorded at the Elm Street Station on September 5th 2013. The corresponding load profiles are assigned to all buildings for the simulation. The generation at Group 1 building is sufficient to support all the loads in the island, while Group 2 is not self-sufficient. But the combined operation of both groups of buildings make the generation self-sufficient. Therefore, no load shed is required in the simulation. The bus voltage and frequency variations at the buildings are recorded and compared with the corresponding base-case scenario values in this section.

The voltage profiles at each of Group 1 building are plotted in Figure 4-25. Again the voltage at KH building can be observed to be higher than those at the rest of the buildings. The reason for the voltage difference is that the reactive power flows from KH building to the other buildings. Similarly, the voltage at Cleveland BioLabs is higher than Fruitbelt because reactive power flows from Cleveland BioLabs to Fruitbelt.

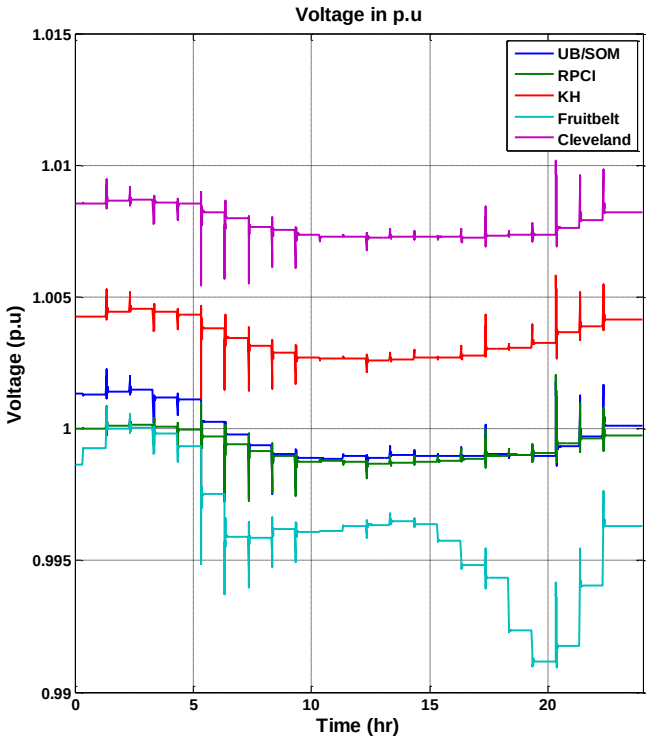

Figure 4-25
Islanded scenario: Layer 2 Group 1+2 – Voltage profiles.

The voltage profile is also compared with the corresponding base-case scenario in Figure 4-26 and Figure 4-27. The voltage and frequency at the buildings are maintained closer to 1 pu. compared to the base-case scenario.

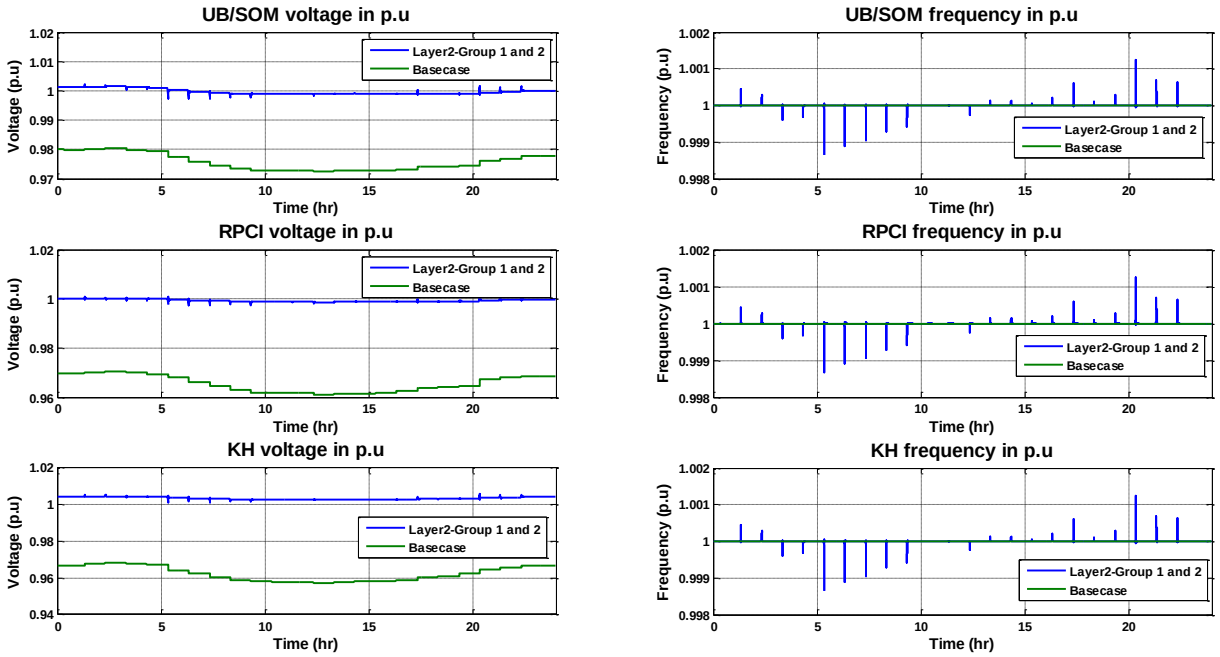

Figure 4-26
Islanded scenario: Layer 2 Group 1+2 and base-case – Voltage and frequency profiles of Group 1 buildings.

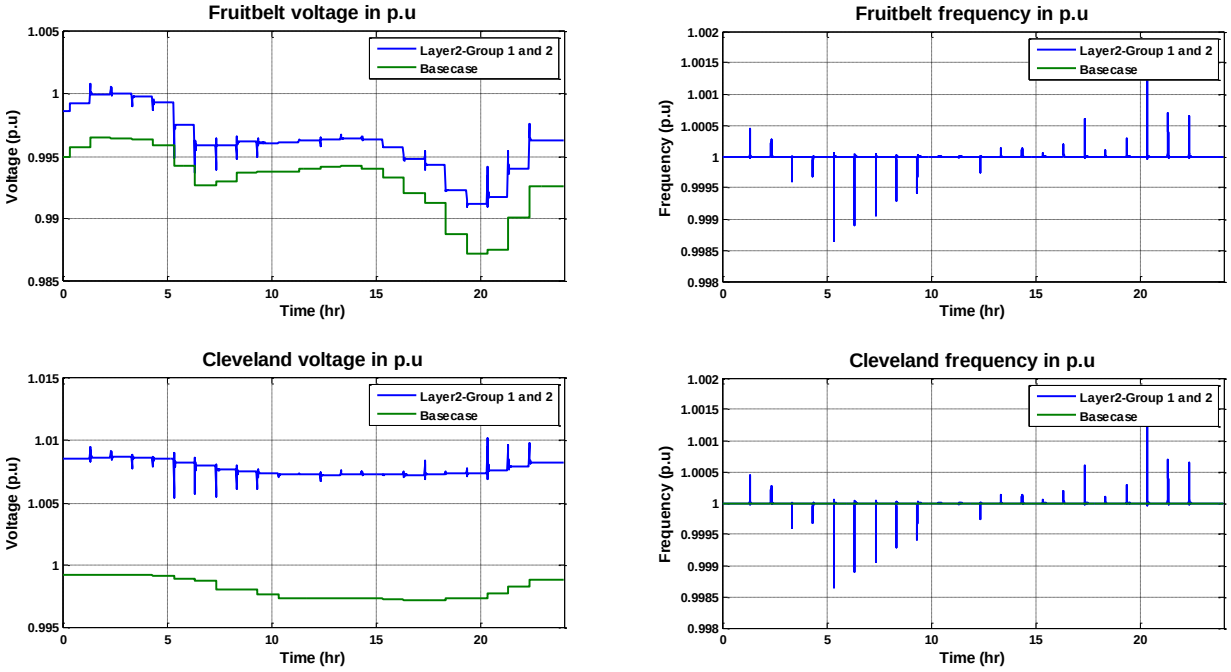

Figure 4-27
Islanded scenario: Layer 2 Group 1+2 and base-case – Voltage and frequency profiles of Group 2 buildings.

Next, the power flow in the island is analyzed building-wise in Figure 4-28 to Figure 4-30. All the buildings are self-sufficient except UB/SOM building and Fruitbelt. As in the previous Section 2-4-4, there is deficit of 2.16 MW power at SOM building. The required active power (2.16 MW) flows from RPCI (1.96 MW) and KH buildings (0.18 MW). Also, there is reactive power exchanged between the buildings. The peak reactive power flows from KH building to SOM and RPCI building are 0.36 Mvar and 0.24 Mvar respectively.

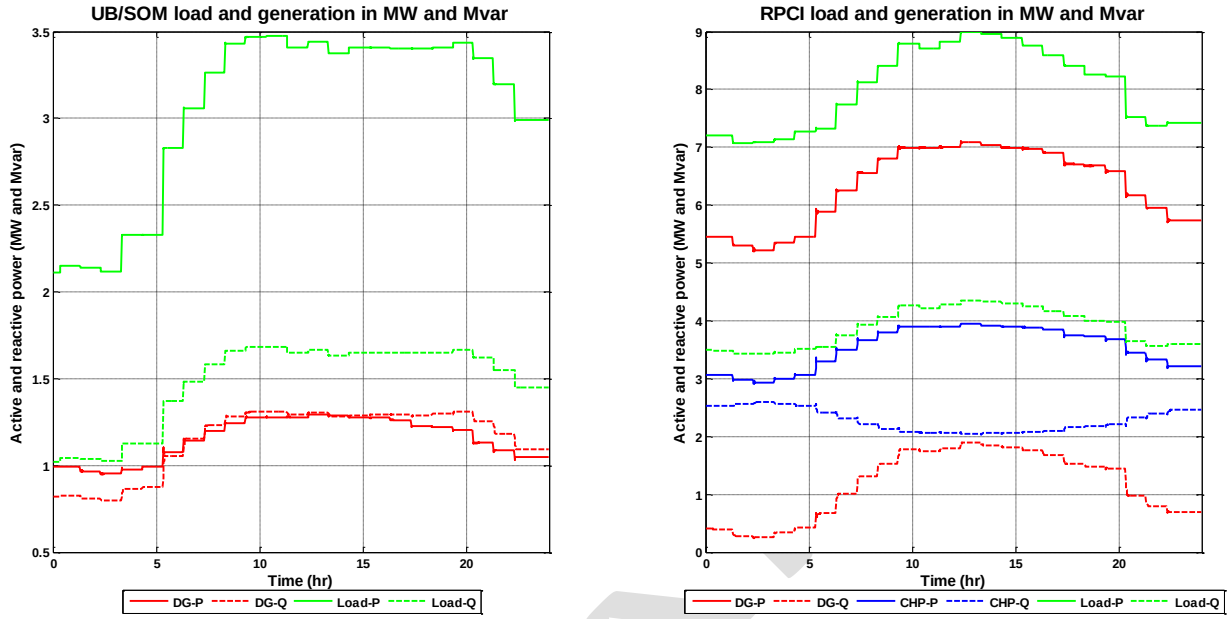

Figure 4-28
Islanded scenario: Layer 2 Group 1+2 and base-case – Power flows in UB/SOM and RPCI

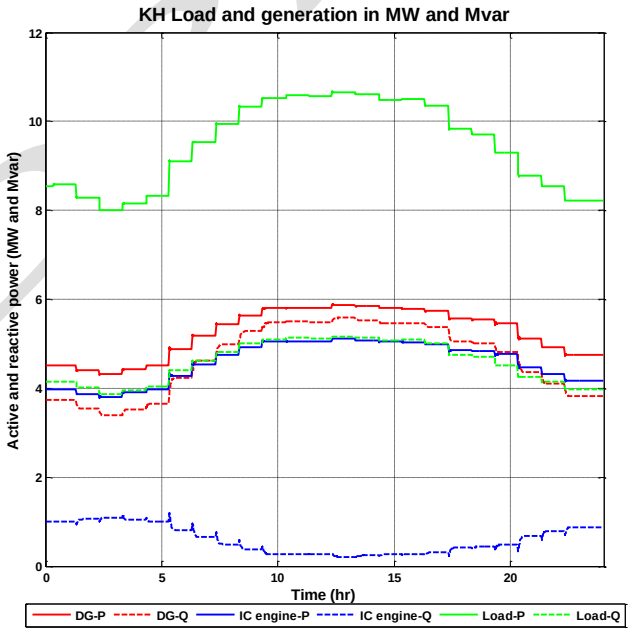

Figure 4-29
Islanded scenario: Layer 2 Group 1+2 and base-case – Power flows in KH building

The power flow in Group 2 buildings is shown in Figure 4-30. Maximum deficit at Group 2 buildings is about 0.7 MW. The required active power flows from the Group 1 buildings.

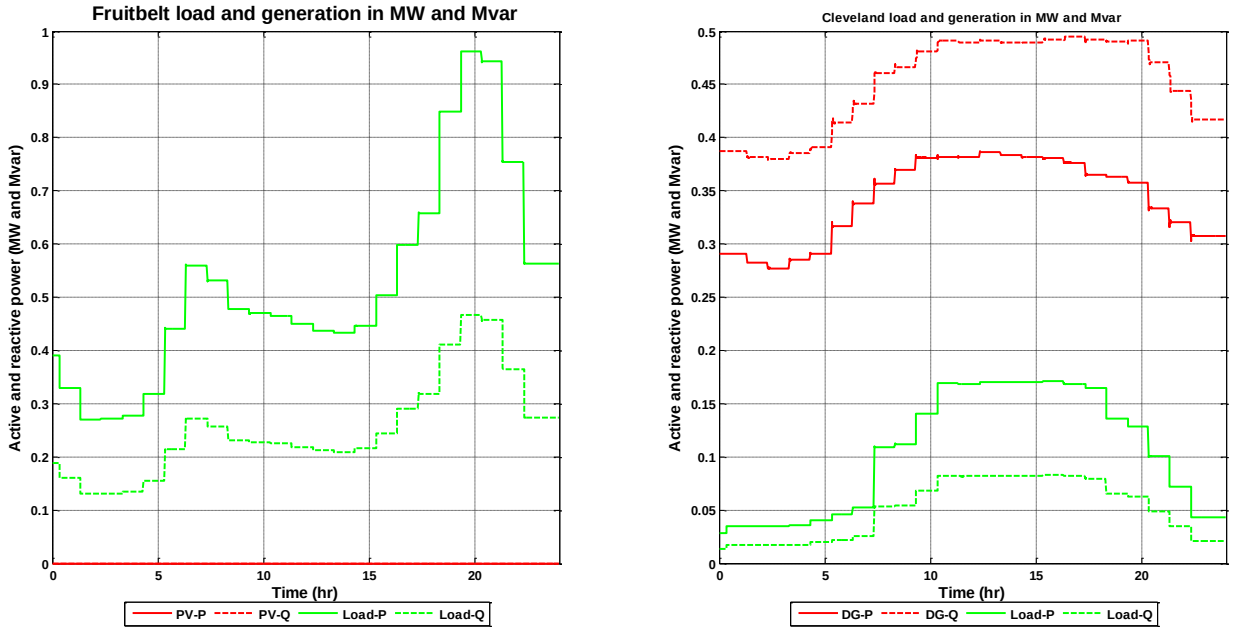

Figure 4-30
Islanded scenario: Layer 2 Group 1+2 and base-case – Power flows at Fruitbelt and Cleveland buildings

The Group 1 and 2 microgrids are operated on peak load demand day as observed on September 5th 2013. There is no load shed required for the scenario, as the load deficits in Group 2 building is supported by generation in Group 1 building. The voltage and frequency are also maintained close to 1 pu.

Key Findings

In this chapter, various microgrid configurations are analyzed using the PowerFactory simulation tool. A typical grid-tied scenario where no local generation units are in service is considered as the base-case scenario. Other grid-tied and islanded grid configurations are identified for the analysis. The grid parameters such as voltage, frequency, and power flow for each grid configurations are studied and compared with that of base-case scenario. Based on the analysis, the following conclusions are drawn:

1. For reliable operation, some of the islanded scenarios require load shed, since the net generation is less than the total load demand in the microgrid. They are Layer 1 islands of Fruitbelt building and UB/SOM building. A load-shed algorithm is needed in those two buildings when they are to be operated in islanded mode.
2. The load flow analysis is carried out for respective peak load-demand day. The voltage ranges during the day for each scenario is shown in Figure 4-31. The voltage profiles with the local generation, at both grid-tied and islanded modes of operation, are closer to 1 pu than the corresponding base-case profiles.

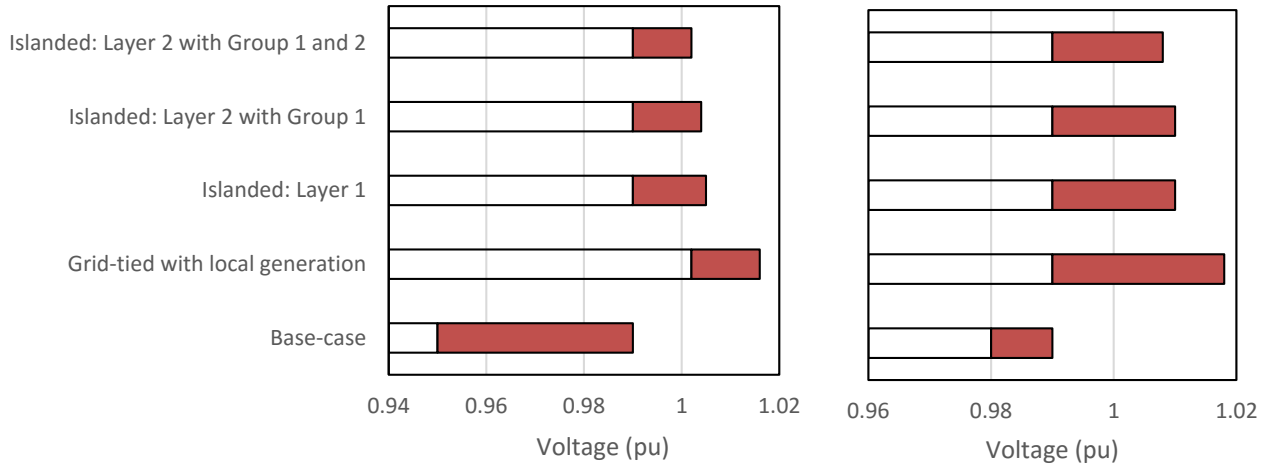

Figure 4-31
Voltage profile of Group 1 and 2 buildings for the simulated study scenarios

3. Frequency of the buildings for all scenarios are always at 1 pu. This is because it is made sure that there is always sufficient generation to meet the total load demand in this study.
4. The local generation units at the buildings are assumed to be controlled by secondary controllers, and explicitly defined turbine governors and AVR controls. The generation dispatch can be optimized according to power flow objectives such as power loss, cost of generation by the local generators and nodal electricity price.

5
SHORT-CIRCUIT AND PROTECTION ANALYSIS

Objectives and Approaches

One of the important aspects of the microgrid planning effort is the design of its short-circuit protection system. As opposed to the utility distribution system protection, the key challenge in the microgrid protection system is that it must detect and interrupt short-circuit fault currents in the shortest amount of time during both grid-tied and islanded modes of operation. The fault levels in the microgrid system can dramatically vary between these two modes. Such a variation must be considered while designing the microgrid protection schemes. In general, the fault levels in an islanded mode can be very low depending upon the type of generation available which may necessitate employing protection schemes relying on principles other than conventional overcurrent protection. Additionally, the transformer connections can influence the fault current propagation in the system, making the fault detection not possible by a conventional overcurrent (OC) protection approach in some cases. As such, protection schemes relying on other protection principles such as current differential and residual overvoltage protections may also be needed.

This chapter focuses on the design of protection systems for the BNMC microgrid to provide protection in both grid-tied and islanded modes of operation. The objective is to demonstrate that the existing protection in conjunction with the proposed protections can work well in both grid-tied and islanded modes. The protection systems are designed for each microgrid in Layer 1 and Layer 2. The current magnitudes for three phase-to-ground (3LG) and single line-to-ground (SLG) faults are obtained from short-circuit calculation in both grid-tied and islanded modes. These fault currents are used in conjunction with the maximum demand current to design the protection system settings. Based on the existing protection devices available, additional protection devices (circuit breakers and relays) required to operate the BNMC microgrid are identified and documented.

Some of the key assumptions in this study are given below:

- The transformers are solidly grounded on 4.16 kV side and the generators in the 4.16 kV network are wye connected and solidly grounded.
- It is assumed that the communications links required for the line differential current protection to work are available.
- It is assumed that the space is available in the field to install the proposed protection devices.

For the overcurrent protection design of Layer 1 microgrids, the synchronous generator is considered as the primary source of supply. During fault conditions, the overcurrent relay in the line connecting the synchronous generator should trip to interrupt the fault. If more than one synchronous generator is available, conservatively, the smaller generator is assumed to be in service for less fault current availability.

Overview of Overcurrent, Differential Current and Residual Overvoltage Protections

For the protection of BNMC microgrid, protection schemes based on overcurrent, differential current, and residual overvoltage are proposed. In this section, an overview of these protection principles is provided.

Overcurrent Protection

Overcurrent (OC) protection scheme is a common form of protection in the utility distribution systems. In this scheme, the current in the protected element is measured by the overcurrent relay. If it is above the preset pickup value of current, the relay sends a trip signal to the circuit breaker to cause it to open. The time of relay operation depends on the time overcurrent (TOC) characteristic curve and the time multiplier setting (TMS) or time-dial setting (TDS). The standard TOC characteristics are standard inverse, very inverse, and extremely inverse. The pickup current setting for a phase overcurrent relay should be above the maximum load current and below the minimum fault current so that the relay does not respond to the normal load currents and can detect all fault conditions. In practice, a pickup value of 1.5 to 3 times the maximum steady-state load current is chosen [1]. For ground overcurrent relays, the pickup current should be above the maximum expected unbalance current in the system. For most of the utility distribution feeders, the ground overcurrent relay pickup current setting ranges from 0.25 to 0.5 times the phase overcurrent relay pickup current setting [2]. The ANSI device numbers for non-directional phase and ground time overcurrent relays are 51 and 51N, respectively.

In addition to the TOC element, overcurrent relays may also use instantaneous overcurrent (IOC) protection elements for quick isolation of faults. The IOC elements can be reliably used only when the current during the faults is substantially higher than the normal loading conditions or if the fault current varies significantly as the fault location varies from closest to the breaker to the far-end of the line [2]. The operating time of these relay elements can also vary significantly. It may be as low as 0.016 s or as high as 0.1 s. The ANSI device numbers for non-directional phase and ground instantaneous overcurrent relays are 50 and 50N, respectively.

Differential Current Protection

Differential protection is a form of unit protection wherein the protected zone is clearly defined. The faults within the protected zone are internal faults, while the faults outside of the protected zone are external faults. In current differential protection, the currents at the boundaries of the protected zone are compared to discriminate between internal and external faults. The line current differential protection principle is illustrated in Figure 5-1. The line connected between two ends A and B is in the protected zone. The currents at both ends are measured using current transformers (CT) installed at each end. A typical line differential protection scheme computes two quantities from the current inputs, namely differential and stabilizing currents. The differential current is the vector sum of the currents while the stabilizing current is the product of the arithmetic sum of individual current magnitudes and a multiplier 'k' as given below:

$$Differential\ current, I_{diff} = |\overline{I_1} + \overline{I_2}| \quad \textbf{Eq. 5-1}$$

$$Stabilizing\ current, I_{stab} = k(|\overline{I_1}| + |\overline{I_2}|) \quad \textbf{Eq. 5-2}$$

The multiplier ‘k’ in Eq. 5-2 is typically chosen such that the stabilizing current becomes the average of currents entering and leaving the protected zone. For example, for a protection application having two current inputs to the stabilizing current computation, Eq. 5-2 gives the average of currents when ‘*k*’ is equal to 0.5. When the number of CT inputs is ‘*n*’, the ‘*k*’ value can be chosen as *1/n*. Scaling factor ‘*k*’ can be other values as well. The ANSI device number for differential relay is 87.

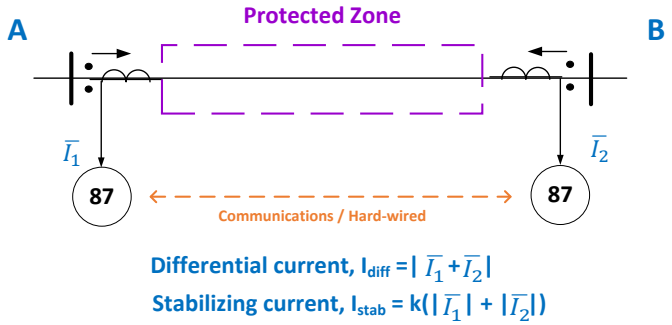

Figure 5-1
Illustration of differential protection principle

Figure 5-2 shows a dual-slope differential relay characteristic wherein the ‘operate’ and ‘stable’ regions are marked. The relay operates and issues a trip command when the differential current exceeds a given differential current threshold and is more than the stabilizing current. Under ideal measuring conditions, the differential current is zero for non-fault conditions. However, due to finite measurement errors, a differential current (although low) can be observed during non-fault conditions. To keep the relay stable, a differential current threshold is provided below which the relay does not operate even if the differential current is higher than the stabilizing current. At high current levels, the CT performance mismatches become pronounced because of the saturation of CT cores. As such, the differential current becomes higher at higher current levels. The stabilizing current is useful to improve the stability of the relay at high current levels. The stabilizing current also improves the sensitivity of the differential relay for internal faults and stability of the relay for external faults.

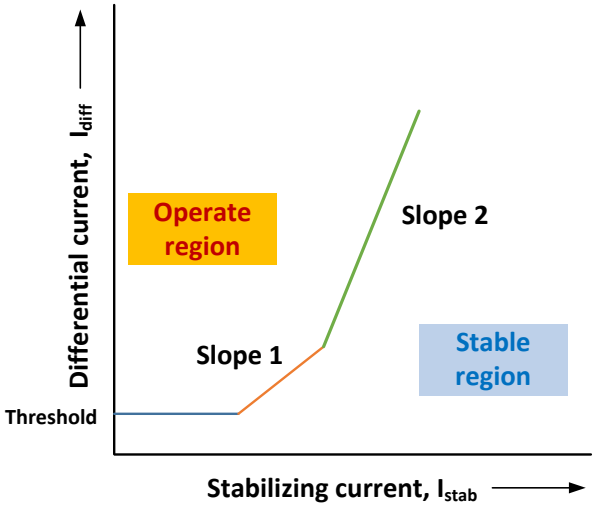

Figure 5-2
Dual-slope differential relay characteristic

Residual Overvoltage Protection

In ungrounded systems, such as delta connected or ungrounded wye connected systems, ground faults do not produce high fault currents as there is no path available for the zero-sequence current to flow to the ground. As such, the ground overcurrent protection cannot detect the faults as there is no overcurrent during the ground faults. For such systems, the ground fault detection may be done by measuring the neutral displacement/residual overvoltage. This functionality is represented by ANSI code 59G. The residual voltage is the vector sum of the phase-to-ground voltages as given below:

$$Residual\ voltage, V_{res} = 3V_0 = V_A + V_B + V_C \quad \textbf{Eq. 5-3}$$

The residual voltage may be measured indirectly by measuring phase-to-ground voltages of phases A, B, and C and then summing them up. Alternatively, the residual voltage can be measured directly by using a grounded-wye, delta-connected voltage transformer (VT) as shown in Figure 5-3. During normal operating conditions, the residual voltage is very low and during SLG fault conditions, it becomes very high indicating a ground fault. The residual overvoltage protection can be applied to systems with high-impedance grounded systems as well.

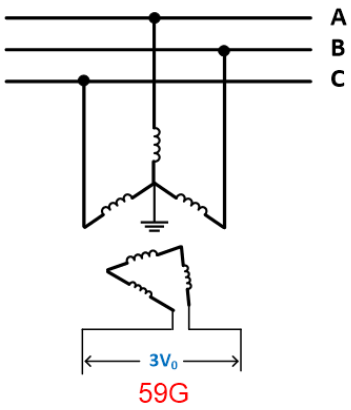

Figure 5-3
Illustration of residual voltage measurement using a grounded-wye, delta-connected voltage transformer

Layer 1 Protection Scheme Overview

The protection system design for each island of BNMC in Layer 1 is discussed in this section. The BNMC microgrid proposes four Layer 1 islands operating together: Roswell Park Cancer Institute (RPCI), University of Buffalo/School of Medicine (SOM), Kaleida Health (KH), Fruitbelt (FB) and Cleveland BioLabs (CL). These islands are highlighted in red in Figure 5-4. The generators and loads in each island are connected to a 4.16 kV bus and these four islands are connected to the external grid through grounded-wye, delta-connected 4.16 kV/23 kV transformers with a wye-grounded connection on the 4.16 kV side. The one-line diagrams of the islands indicate that the existing protection system in each island comprises of overcurrent relays for protecting the lines connecting the generators (diesel generator, gas combustion turbine generator, and internal combustion engine generator). Each overcurrent relay is equipped with two time overcurrent (TOC) elements, one for phase overcurrent protection and the other for ground overcurrent protection. The relays also have two instantaneous overcurrent (IOC) elements, i.e., for phase and ground instantaneous overcurrent protections.

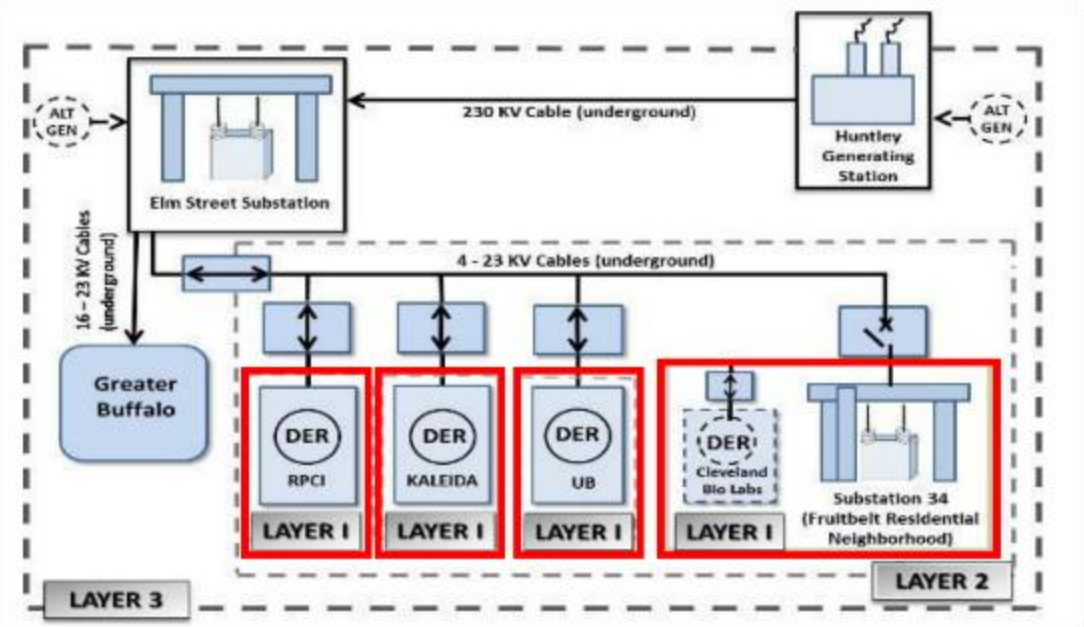

Figure 5-4
Islands in BNMC Layer 1

Assumed Device Protections for Photovoltaic and Battery Energy Storage Systems

It is proposed that UB/SOM and the combined Fruitbelt and Cleveland BioLabs microgrids will have photovoltaic (PV) and battery energy storage systems (BESS). The inverters of the PV systems typically have two main protections to respond to utility-side electrical disturbances. These protection systems measure the voltage and frequency at the point of interconnection (POI) and isolate the PV system. Table 5-1 shows the guidelines for undervoltage protection trip times for different levels of undervoltage [1]. Note that the details in this table indicate that the PV systems trip very quickly upon the detection of undervoltage during faults. Since the sizes and the fault current contributions of PV and BESS are very small compared to the other synchronous generators, and that quick isolation of inverter-based generation occurs during faults, it is assumed in this study that PV and BESS systems are equipped with the standard undervoltage protection to isolate them during faults.

Table 5-1
Undervoltage protection of photovoltaic system inverters

Voltage (at PCC)	Maximum trip time
V < 60 (V < 50%)	6 cycles
60 ≤ V < 106 (50% ≤ V < 88%)	120 cycles
106 ≤ V < 132 (88% ≤ V < 110%)	Normal operation
132 < V < 165 (110% < V < 137%)	120 cycles
165 ≤ V (137% ≤ V)	2 cycles

Overcurrent Protection Modeling and Criteria for Protection Settings

For overcurrent protection design of each island in Layer 1, the synchronous generator is considered as the primary source of supply. During fault conditions, the overcurrent relay in the line connecting the synchronous generator should trip to interrupt the fault currents. For example, in the RPCI island shown in Figure 5-5, the overcurrent relay R1 should trip the 7.7-MW combustion turbine upon detection of faults. A major concern in employing overcurrent protection in islanded mode is low fault current levels. Therefore, in this scenario the 7.7 MW combustion turbine is assumed to be in service—conservatively, as this is the smaller source compared to the 13.72 MW DG—resulting in low fault current availability at the 4.16 kV RPCI bus. The load in this Layer 1 microgrid is also reduced to 7.7 MW to match the available generation from the 7.7 MW combustion turbine. The same approach is followed for protection design of the other Layer 1 microgrids also.

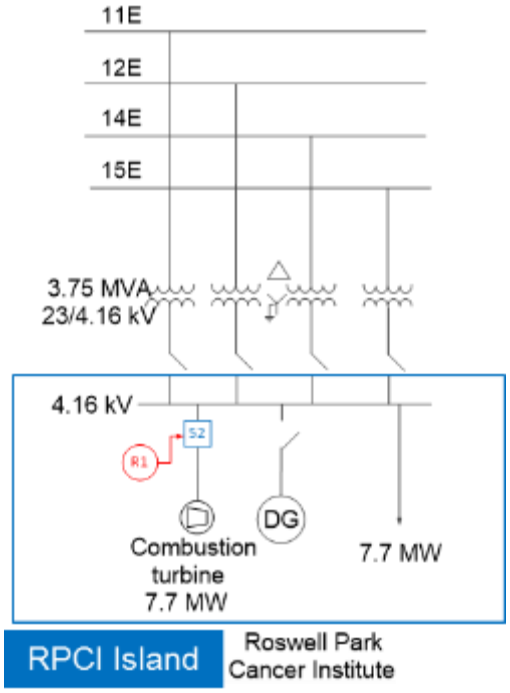

Figure 5-5
Roswell Park Cancer Institute (RPCI) Island

For the overcurrent protection modeling, a generic relay model available in the DIgSILENT PowerFactory is used. This relay model has two TOC elements and two IOC elements as described in Section 0 for phase overcurrent and ground overcurrent protections. The time overcurrent elements are assumed to follow the standard inverse TOC curve. The equation for this curve is given below:

$$\boldsymbol{t = TMS \times \frac{0.14}{I_r^{0.02}-1}} \qquad \textbf{Eq. 5-4}$$

where $I_r = I_{fault}/I_{pickup}$, and TMS = Time multiplier setting or time-dial setting

The relay pickup current settings (I_{pickup}) and the observed fault currents (I_{fault}) are specified in terms of primary values to avoid dependency on the current transformer (CT) ratio.

In this study, the phase overcurrent relay pickup current is selected to be about 2 times the maximum normal load current. The time-dial setting is fixed to a low value of 0.1 s for both phase and ground overcurrent relays to keep low relay operating time for 3LG and SLG faults, respectively. Furthermore, because the fault current levels are low in all Layer 1 microgrids, the instantaneous overcurrent elements are not used as primary protection. They will only support the time overcurrent elements to limit the relay operating time in case of very high short-circuit fault currents. Accordingly, the pickup current is selected as a few times higher than the time overcurrent pickup current setting. This ensures that instantaneous relay elements do not operate for the normal range of fault currents in the system and let the other overcurrent relay elements respond for these fault currents. A fixed time setting of 0.035 s is selected to keep the operating time very low for the IOC relay elements. Note that 0.035 s is the default value for this element in PowerFactory. The criteria for the preparation of overcurrent relay settings is summarized in the Table 5-2.

Table 5-2
Criteria for overcurrent relay protection settings in BNMC

Parameter	Criteria
AC time phase overcurrent relay pickup setting (I_p)	Selected as about 2 times the maximum normal load current. For some relays, it is adjusted to improve the relay operating time for a 3LG fault current in both grid-tied and islanded modes
AC time phase overcurrent relay time dial setting (T)	Fixed to a low value of 0.1 s to keep low relay operating time for a 3LG fault
AC time ground overcurrent relay pickup setting (I_{pg})	Selected as about 0.5 times the maximum normal load current. For some relays, it is adjusted to improve the relay operating time for SLG fault current in both grid-tied and islanded modes
AC time ground overcurrent relay time dial setting (T_g)	Fixed to a low value of 0.1 s to keep low relay operating time for an SLG fault
AC instantaneous phase/ground overcurrent relay pickup settings	Selected to a high value to keep the relay operating time on the AC inverse time curve for a 3LG/SLG faults
AC instantaneous phase/ground overcurrent time dial settings	A low value of 0.035 s is selected to keep very low relay operating time

BNMC Layer 1 Protection Systems

Figure 5-6 and Figure 5-7 depict the system connectivity of microgrids RPCI, SOM, and KH in islanded and grid-tied modes respectively to be considered for overcurrent protection in Layer 1. Note that the circuit breakers on the 4.16-kV wye side of the transformers i.e., those associated with the relays R2-R5, R7-R10, R12-R15 are opened in the islanded mode.

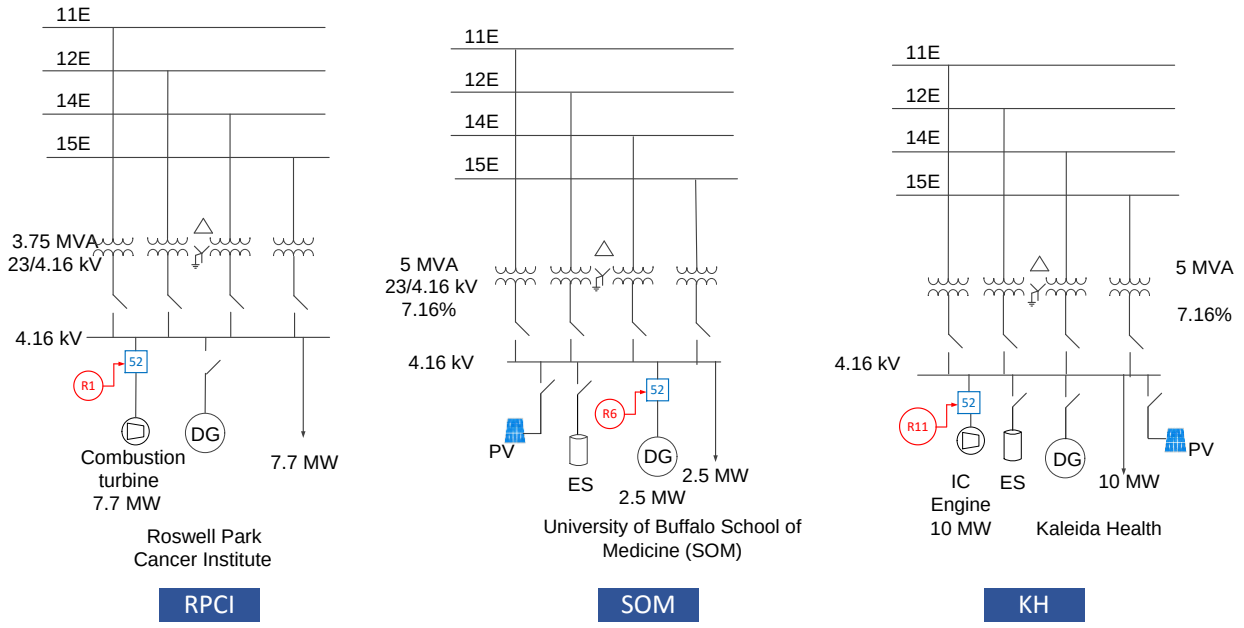

Figure 5-6
System connectivity in islanded mode for microgrids RPCI, SOM, and KH in Layer 1

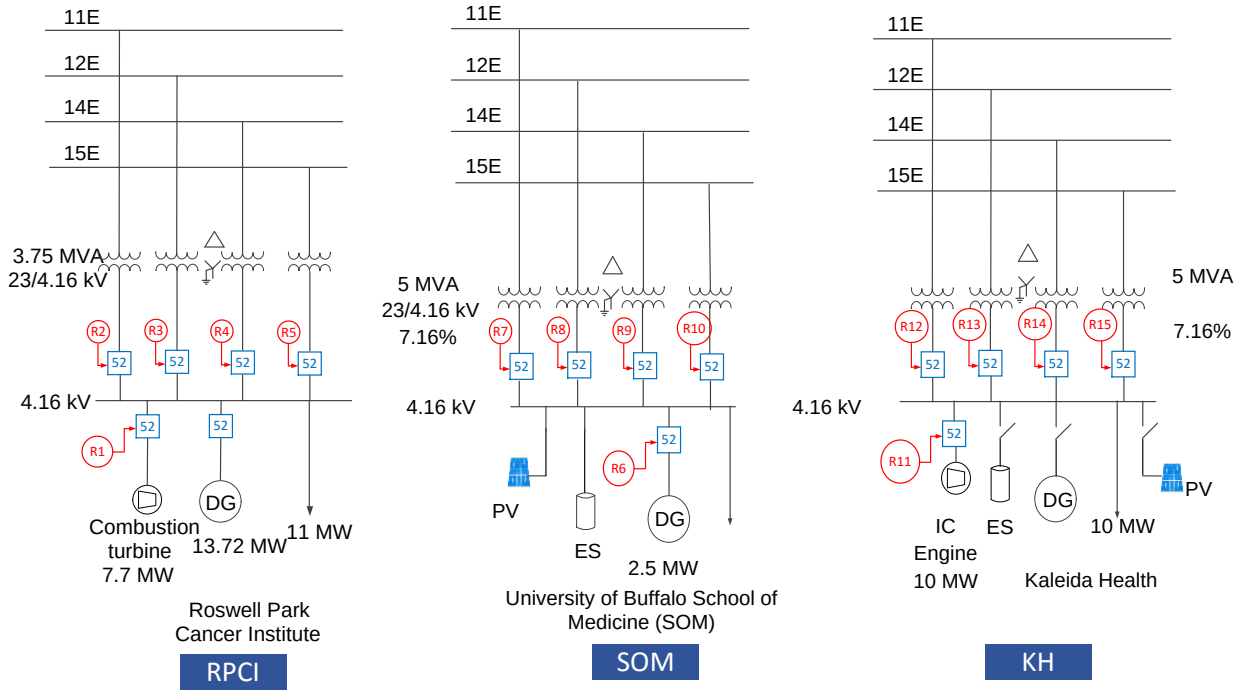

Figure 5-7
System connectivity in grid-tied mode for microgrids RPCI, SOM, and KH in Layer 1

For selecting the relay settings, the maximum load current through relays R1, R6 and R11 are noted during peak load conditions in the islanded mode. Using this information, the pickup and time-dial settings of these relays are then chosen based on the criteria specified in Table 5-1. The

phase and ground overcurrent relay response is observed for 3LG and SLG faults simulated on the 4.16 kV bus of each island in both grid-tied and islanded modes. These settings are slightly adjusted as needed to give satisfactory relay operation performance in both operating modes. The relays should *not* operate during the peak load condition and trip with low operating time during fault conditions already addressed by another setting.

The system conditions and simulation case description in grid-tied and islanded modes of operation for the RPCI island are shown in Table 5-3. The overcurrent relay R1 settings and the relay response to 3LG and SLG faults on the 4.16 kV bus in both grid-tied and islanded modes are shown in Table 5-4. It is observed that relay R1 does not respond during normal operating conditions. However, it will trip the associated circuit breaker during the 3LG and SLG fault conditions on the 4.16 kV bus.

Table 5-3
System conditions and description of cases for evaluating protection response in RPCI

Mode	System Conditions	Case Description
Islanded	**System Conditions:** In islanded mode, the breakers associated with R2, R3, R4, R5 are opened so that the RPCI island separates from the system **Fault cases:** 3LG and SLG faults are created on wye side of transformer, that is, on 4.16 kV bus to check the operation of DG side overcurrent relays. The overcurrent relay response under normal loading, 3LG, SLG fault conditions are checked.	**Case 1** - Normal loading conditions: In islanded mode of RPCI, only CHP is in service. No DG is in service. Thus, the fault current contribution is minimum. The load is reduced to 7.7 MW to match the available generation from CHP at 7.7 MW. **Case 2 -** 3LG fault on 4.16 kV RPCI bus **Case 3 -** SLG fault on 4.16 kV RPCI bus
Grid-tied	**System Conditions:** In grid-tied mode, Group 1 and Group 2 are supplied by Elm Street and Station 34, respectively. Peak load condition is considered. To check the protection response of the generation within each island, all the generators and storage (DG, CHP, PV, Battery) are generating their rated powers. **Fault cases:** 3LG and SLG faults are simulated on 4.16 kV bus to check the operation of DG side overcurrent relays. The overcurrent relay response under normal loading, 3LG, SLG fault conditions are checked.	Same as above except that the load in RPCI is at 11.04 MW (peak load)

Table 5-4
Overcurrent relay settings and response in RPCI Island

Protection	Relay	Fault location	Relay settings	Protection Response					
				Islanded mode			Grid-tied mode		
				Normal loading	3LG	SLG	Normal loading	3LG	SLG
51, 51N	R1	On 4.16 kV RPCI bus	**Time overcurrent**: Ip: 2000 A T: 0.1 sec Ipg: 500 A Tg: 0.1 sec **Instantaneous overcurrent:** Ip: 10000 A T: 0.035 sec Ipg: 8000 A Tg: 0.035 sec	Relay current: Ir = 1.07 kA Relay response: 51 - **No trip** 51G - **No trip**	Relay current: Ir = 3.46 kA Relay response: 51 - **Trip time 1.27 sec** 51G - **No trip**	Relay current: Ir = 2.5 kA Relay response: 51 - **Trip time 3.06 sec** 51G - **Trip time 0.43 sec**	Relay current: Ir = 1.07 kA Relay response: 51 - **No trip** 51G - **No trip**	Relay current: Ir = 3.35 kA Relay response: 51 - **Trip time 1.35 sec** 51G - **No trip**	Relay current: Ir = 1.26 kA Relay response: 51 - **Trip time 1.44 sec** 51G - **Trip time 0.75 sec**

Relay R1 operating characteristic with the chosen settings is shown in Figure 5-8. Both phase and ground element characteristics are shown on the same plot. The vertical line represents the current seen by relay R1 during a normal loading condition. Note that each relay characteristic includes both the time overcurrent (TOC) characteristic (the curved portion) and instantaneous overcurrent (IOC) characteristic (the straight line). The IOC characteristic cuts the TOC characteristic of the corresponding relay element. For example, the TOC curve of the phase overcurrent relay in Figure 5-8 is cut at the pickup current setting (10,000 A) of the IOC relay characteristic. Similarly, the TOC characteristic of the ground OC relay is cut at 8,000 A by the corresponding IOC relay characteristic.

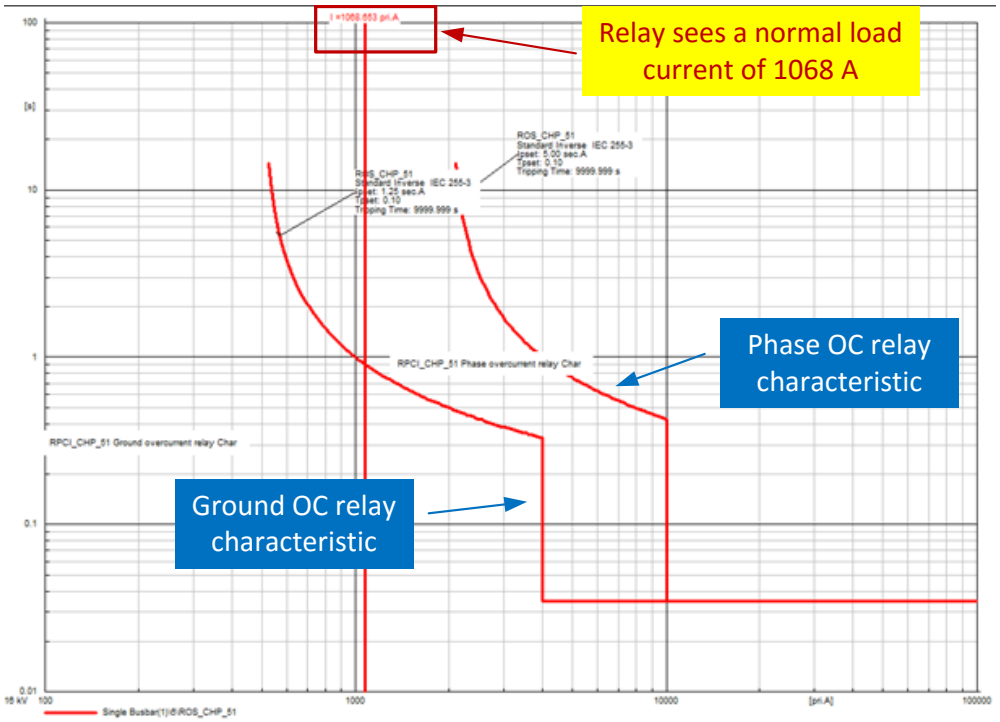

Figure 5-8
Overcurrent relay R1 response during normal loading conditions operating in islanded mode

Relay R1 response during 3LG and SLG faults are shown in Figure 5-9 and Figure 5-10, respectively. Note that relay R1 sees phase overcurrent of 3.46 kA and ground overcurrent of 2.5

kA during 3LG and SLG faults, respectively. These results along with corresponding relay operating times are shown earlier in Table 5-4.

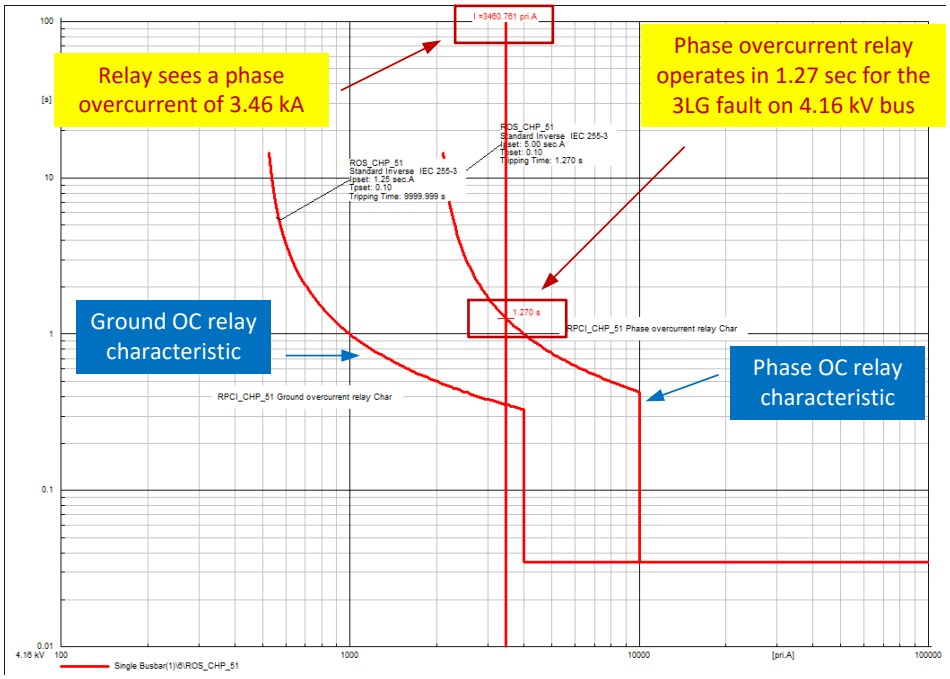

Figure 5-9
Overcurrent relay R1 response for a 3LG fault on 4.16 kV RPCI bus operating in islanded mode

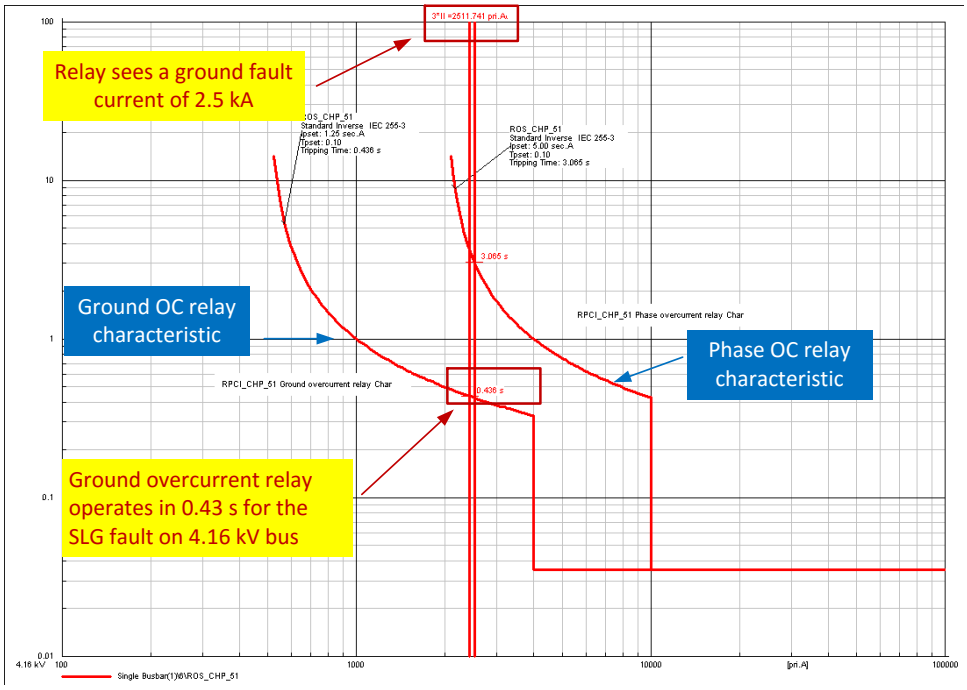

Figure 5-10
Overcurrent relay R1 response for an SLG fault on 4.16 kV RPCI bus operating in islanded mode

The system conditions, description of study cases, overcurrent relay settings and the relay responses (of R6 and R11) for SOM and KH microgrids operating in islanded and grid-tied modes are shown in Table 5-5 through Table 5-8.

Table 5-5
System conditions and description of cases for evaluating protection response in SOM

Mode	System Conditions	Case Description
Islanded	**System Conditions:** In islanded mode, the breakers associated with R7, R8, R9, R10 are opened so that the SOM island separates from the system **Fault cases:** 3LG and SLG faults are created on wye side of transformer, that is, on 4.16 kV bus to check the operation of DG side overcurrent relays. The overcurrent relay response under normal loading, 3LG, SLG fault conditions are evaluated.	**Case 1 -** Normal loading conditions: In islanded mode of SOM, only DG is in service. The PV and Battery are not in service. Thus, the fault current contribution is minimum. The load is reduced to 2.5 MW to match the available generation from DG at 2.5 MW. **Case 2 -** 3LG fault on 4.16 kV SOM bus **Case 3 -** SLG fault on 4.16 kV SOM bus
Grid-tied	**System Conditions:** In grid-tied mode, Group 1 and Group 2 are supplied by the Elm Street and Station 34, respectively. Peak load condition is considered. All the generators and storage (DG, PV, Battery) within each island are generating their rated powers. **Fault cases:** 3LG and SLG faults are simulated on 4.16 kV bus to check the operation of DG side overcurrent relays. The overcurrent relay response under normal loading, 3LG, SLG fault conditions are evaluated.	Same as above except that the load in SOM is at 4.25 MW

Table 5-6
Overcurrent relay settings and response in SOM Island

Protection	Relay	Fault location	Relay settings	Protection Response					
				Islanded mode			Grid-tied mode		
				Normal loading	3LG	SLG	Normal loading	3LG	SLG
51, 51N	R6	On 4.16 kV SOM bus	**Time overcurrent**: Ip: 800 A T: 0.1 sec Ipg: 300 A Tg: 0.1 sec **Instantaneous overcurrent:** Ip: 4000 A T: 0.035 sec Ipg: 3600 A Tg: 0.035 sec	Relay current: Ir = 361 A Relay response: 51 - **No trip** 51G - **No trip**	Relay current: Ir = 2.6 kA Relay response: 51 - **Trip time 0.6 sec** 51G - **No trip**	Relay current: Ir = 1.86 kA Relay response: 51 - **Trip time 0.82 sec** 51G - **Trip time 0.37 sec**	Relay current: Ir = 361 A Relay response: 51 - **No trip** 51G - **No trip**	Relay current: Ir = 2.5 kA Relay response: 51 - **Trip time 0.6 sec** 51G - **No trip**	Relay current: Ir = 1.01 kA Relay response: 51 - **Trip time 0.68 sec** 51G - **Trip time 0.57 sec**

Table 5-7
System conditions and description of cases for evaluating protection response in KH

Mode	System Conditions	Case Description
Islanded	**System Conditions:** In islanded mode, the breakers associated with R11, R12, R13, R14 are opened so that the KH island is isolated from the system **Fault cases:** 3LG and SLG faults are created on wye side of transformer, that is, on 4.16 kV bus to check the operation of DG side overcurrent relays. The overcurrent relay response under normal loading, 3LG, SLG fault conditions are evaluated.	**Case 1 -** Normal loading conditions: In islanded mode of KH, both natural gas internal combustion engines (total 10 MW) are in service. The DG, PV and Battery are not in service. Thus, the fault current contribution is minimum. The load is reduced to 10 MW to match the available generation from IC engines at 10 MW. **Case 2 -** 3LG fault on 4.16 kV KH bus **Case 3 -** SLG fault on 4.16 kV KH bus
Grid-tied	**System Conditions:** In grid-tied mode, Group 1 and Group 2 are supplied by Elm Street and Station 34, respectively. Peak load condition is considered. All the generators and storage (DG, PV, Battery) within each island are generating their rated powers. **Fault cases:** 3LG and SLG faults are simulated on 4.16 kV bus to check the operation of DG side overcurrent relays. The overcurrent relay response under normal loading, 3LG, SLG fault conditions are evaluated.	Same as above except that the load in KH is at 12.98 MW

Table 5-8
Overcurrent relay settings and response in KH Island

Protection	Relay	Fault location	Relay settings	Protection Response					
				Islanded mode			Grid-tied mode		
				Normal loading	3LG	SLG	Normal loading	3LG	SLG
51, 51N	R11	On 4.16 kV KH bus	**Time overcurrent**: Ip: 2800 A T: 0.1 sec Ipg: 1400 A Tg: 0.1 sec **Instantaneous overcurrent:** Ip: 14000 A T: 0.035 sec Ipg: 14000 A Tg: 0.035 sec	Relay current: Ir = 1388 A Relay response: 51 - **No trip** 51G - **No trip**	Relay current: Ir = 10.39 kA Relay response: 51 - **Trip time 0.53 sec** 51G - **No trip**	Relay current: Ir = 7.46 kA Relay response: 51 - **Trip time 0.70 sec** 51G - **Trip time 0.41 sec**	Relay current: Ir = 1445 kA Relay response: 51 - **No trip** 51G - **No trip**	Relay current: Ir = 9.99 kA Relay response: 51 - **Trip time 0.54 sec** 51G - **No trip**	Relay current: Ir = 4.53 kA Relay response: 51 - **Trip time 0.64 sec** 51G - **Trip time 0.59 sec**

In the Group 2 of the BNMC system, the combined Fruitbelt and Cleveland BioLabs circuits operate together in the islanded microgrid mode as shown in Figure 5-11. For Group 2 protection, the 0.8 MW DG in Cleveland BioLabs is the main generation source in the islanded mode. An overcurrent relay R18 is required to isolate the DG for 3LG and SLG faults on the 4.16 kV Cleveland BioLabs bus. However, because of the grounded-wye delta transformer connections, the faults on the 4.16 kV Fruitbelt bus cannot be detected by this overcurrent relay

R16. Furthermore, the Fruitbelt circuit does not have any synchronous generator-based generation. This results in low fault currents for 3LG faults on the 4.16 kV Fruitbelt bus. Therefore, an undervoltage relay (ANSI code 27) R17 and a residual overvoltage relay (ANSI code 59G) R18 are needed to detect 3LG and SLG faults respectively on the 4.16 kV Fruitbelt bus. These relays will send trip command to the breaker of 0.8 MW DG as shown in Figure 5-11. The system conditions, description of study cases, relay settings and the relay responses (of R16-R18) for the Group 2 Fruitbelt and Cleveland BioLabs combined system are shown in Table 5-9 and Table 5-10.

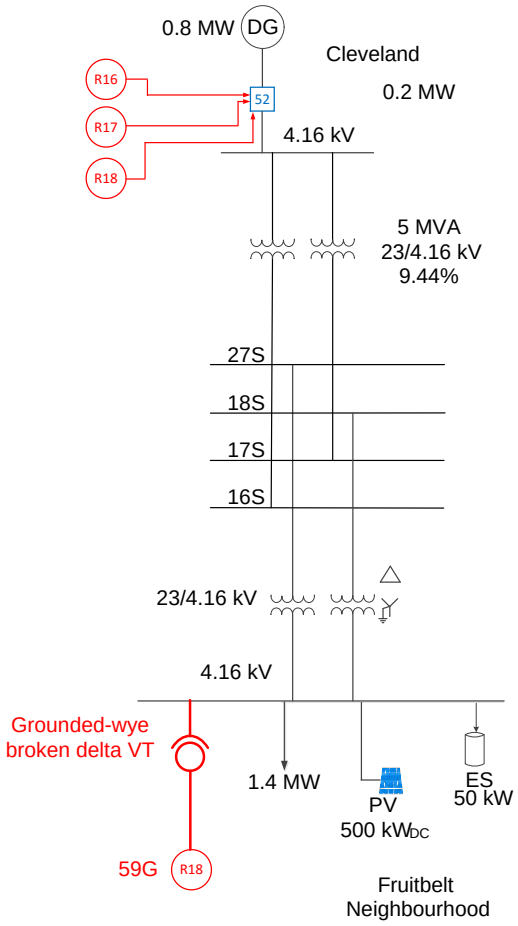

Figure 5-11
System connectivity in islanded mode for combined Fruitbelt and Cleveland BioLabs microgrid in Layer 1

Table 5-9
System conditions and description of cases for evaluating protection response in Group 2 Fruitbelt and Cleveland BioLabs combined system

Mode	System Conditions	Case Description
Grid-tied	**System Conditions:** In grid-tied mode, Group 1 and Group 2 are supplied by Elm Street and Station 34, respectively. Peak load condition is	**Case 1** - Normal loading conditions: In Grid-tied mode of CL, the DG in CL (0.8 MW) is in service.

	considered. Cleveland BioLabs (CL) DG is the main generation source in Group 2 microgrid. **Fault cases:** 3LG and SLG faults are simulated on 4.16 kV of CL bus to check the operation of the DG overcurrent relays. The overcurrent relay response under normal loading, 3LG, SLG fault conditions are evaluated.	**Case 2 -** 3LG fault on 4.16 kV CL bus **Case 3** - SLG fault on 4.16 kV CL bus **Case 4** - 3LG fault on 4.16 kV Fruitbelt bus **Case 5** - SLG fault on 4.16 kV Fruitbelt bus
Islanded	**System Conditions:** In islanded mode of Group 2, the Station 34 source in Group 2 are disabled. **Fault cases:** 3LG and SLG faults are created on 4.16 kV CL bus to check the operation of CL DG overcurrent relays. If this DG is tripped, then the fault will not be fed assuming the PV and the Battery have their own device protections which isolate them under fault conditions.	Same as above except the load in the Fruitbelt is 0.7 MW to match the available generation.

Table 5-10
Relay settings and response in in Group 2 Fruitbelt and Cleveland BioLabs combined system

Protection	Relay	Fault location	Relay settings	Protection Response					
				Islanded mode			Grid-tied mode		
				Normal loading	3LG	SLG	Normal loading	3LG	SLG
51, 51N	R16	On 4.16 kV CL bus	**Time overcurrent**: Ip: 280 A T: 0.1 sec Ipg: 40 A Tg: 0.1 sec **Instantaneous overcurrent:** Ip: 1200 A T: 0.035 sec Ipg: 600 A T: 0.035 sec	Relay current: Ir = 118 A Relay response: 51 - **No trip** 51G - **No trip**	Relay current: Ir = 834 A Relay response: 51 - **Trip time 0.63 sec** 51G - **No trip**	Relay current: Ir = 50 A Relay response: 51 - **Trip time 0.64 sec** 51G - **Trip time 2.9 sec**	Relay current: Ir = 118 A Relay response: 51 - **No trip** 51G - **No trip**	Relay current: Ir = 810 A Relay response: 51 - **Trip time 0.56 sec** 51G - **No trip**	Relay current: Ir = 334 A Relay response: 51 - **Trip time 0.77 sec** 51G - **Trip time 0.32 sec**
27, 59G	R17 (27), R18 (59G)	On 4.16 kV Fruitbelt bus	**Undervoltage protection (27):** V< 2 kV **Wye-broken-delta ground overvoltage protection (59G):** 3V0: 100 V	Relay voltages: V ≈ 2.14 kV 3V0 ≈ 0 V Relay response: 27 - **No trip** 59G - **No trip**	Relay voltages: V ≈ 0 V 3V0 ≈ 0 V Relay response: 27 - **Instantaneous trip** 59G - **No trip**	Relay voltages: Va ≈ 0∟0 V, Vb = 2.06∟-95.17 kV, Vc = 2.04∟92.86 kV 3V0 ≈ 287 V Relay response: 27 - **Instantaneous trip** 59G - **Instantaneous trip**	Relay voltages: V ≈ 2.14 kV 3V0 ≈ 0 V Relay response: 27 - **No trip** 59G - **No trip**	Relay voltages: V ≈ 0 V 3V0 ≈ 0 V Relay response: 27 - **Instantaneous trip** 59G - **No trip**	Relay voltages: Va ≈ 0 V, Vb = 2.31∟-148.09 kV, Vc = 2.25∟85.96 kV 3V0 ≈ 2.07 kV Relay response: 27 - **Instantaneous trip** 59G - **Instantaneous trip**

The summary of protection settings for Layer 1 of BNMC system is shown in Table 5-11.

Table 5-11
Summary of protection relay settings in Layer 1 of BNMC

Island	Protection	Relay	Relay settings			
			Time overcurrent	Instantaneous overcurrent	Undervoltage relay	Broken Wye-delta relay
Roswell (RPCI)	51, 51G	R1	Ip: 2000 A T: 0.1 sec Ipg: 500 A Tg: 0.1 sec	Ip: 10000 A T: 0.035 sec Ipg: 8000 A Tg: 0.035 sec	-	-
University of Buffalo SOM	51, 51G	R6	Ip: 800 A T: 0.1 sec Ipg: 300 A Tg: 0.1 sec	Ip: 4000 A T: 0.035 sec Ipg: 3600 A Tg: 0.035 sec	-	-
Kaleida Health (KH)	51, 51G	R11	Ip: 2800 A T: 0.1 sec Ipg: 1400 A Tg: 0.1 sec	Ip: 14000 A T: 0.035 sec Ipg: 14000 A Tg: 0.035 sec	-	-
Group 2: Cleveland+Fruitbelt	51, 51G,	R16, R17, R18	Ip: 280 A T: 0.1 sec Ipg: 40 A Tg: 0.1 sec	Ip: 1200 A T: 0.035 sec Ipg: 600 A Tg: 0.035 sec	R17: Vln < 2 kV	R18: 3V0 > 100 V

BNMC Layer 2 Protection Systems

The protection system design for Layer 2 of the BNMC system is done considering grid-tied mode of system operation and islanded mode operation of Group 1 and Group 2 combined system. Current differential protection is proposed for fault detection in the Layer 2 of BNMC in grid-tied mode. This protection can detect both 3LG and SLG faults on the 23 kV side in grid-tied mode. Because the transformer connection is delta on the 23 kV side, the 23 kV system is ungrounded in islanded mode of operation. As such, ground fault detection is not possible by the current differential protection. Therefore, the residual overvoltage protection approach is proposed for Layer 2 operating in islanded mode. These protection systems are discussed in this section.

Differential Protection in Layer 2 for Grid-tied Mode

Figure 5-12 shows the differential current protection scheme in Layer 2 of BNMC. The 23 kV lines of Group 1 i.e., 11E, 12E, 14E, and 15E are protected by differential relays R19 to R30 while that of Group 2 (16S, 17S, 18S, 27S) are protected by differential relays R31 to R34.

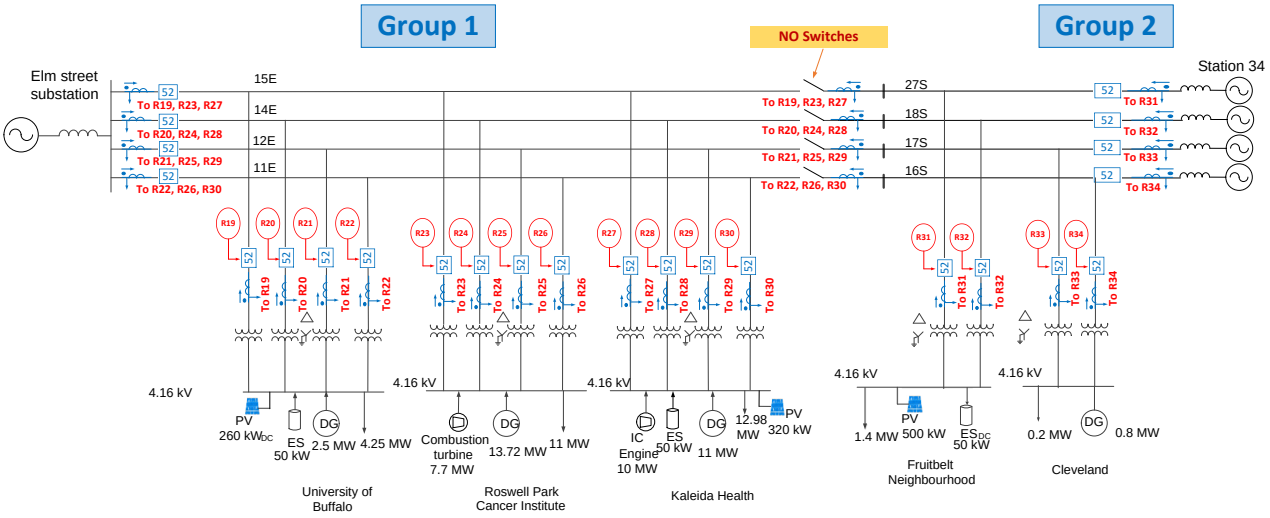

Figure 5-12
Differential protection scheme in Layer 2 of BNMC for Grid-tied mode

Each differential relay in Group 1 takes the inputs from three current transformers installed at the boundaries of the corresponding T section and protects the T section during the faults by tripping the circuit breakers installed at the boundaries of the T section. For the example shown in Figure 5-13, the protection zone of differential relay R19 along with associated protection devices are highlighted. Relay R19 receives current inputs from the CTs CT A, CT B, and CT C. Note that the CTs installed at Elm Street and Station 34 buses—CT B and CT C—provide current inputs to three relays R19, R23, and R27 as these CTs are at the boundaries of the protected zones of the relays R19, R23, and R27. Upon detection of a fault in the T section highlighted in yellow, the relay R19 trips the circuit breakers CB A, CB B and CB C. If the fault is on the 23 kV line 15E, the same fault is detected by the relays R23 and R27 which also trip their associated circuit breakers. Thus, the fault is isolated in Group 1 in islanded mode. The faults on the T sections of the other 23 kV lines in Group 1 and Group 2 are also isolated along the same lines.

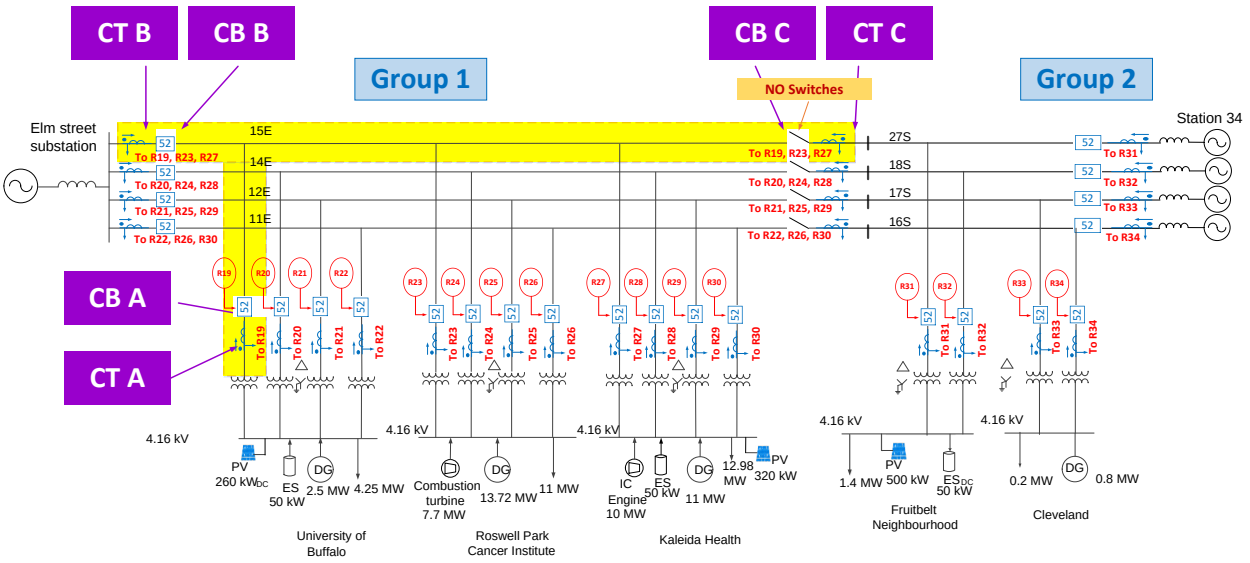

Figure 5-13
Illustration of Layer 2 differential protection scheme

Residual Overvoltage Protection in Layer 2 for Islanded Mode

Figure 5-14 shows the residual overvoltage protection scheme in Group 1+2 Layer 2 microgrid. A grounded-wye, delta-connected voltage transformer is installed at the 23 kV Elm Street Station bus which inputs the open-delta voltage to the ground overvoltage relay R35 (ANSI code 59G). This relay R35 will trip all 23 kV breakers upon detection of a ground fault using the residual overvoltage measurement. Thus, the ground faults will be isolated in Layer 2 in islanded mode.

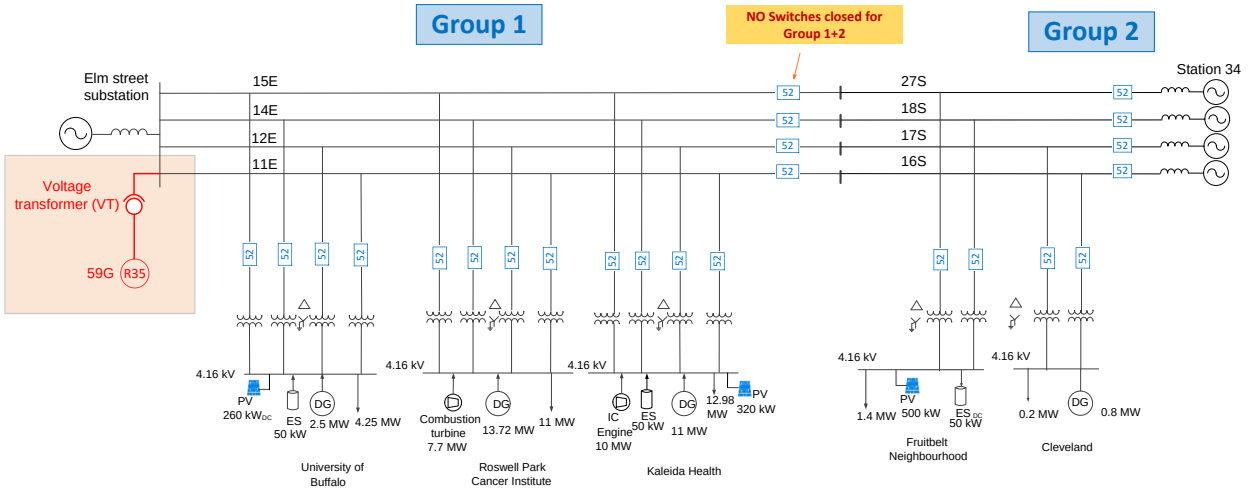

Figure 5-14
Illustration of Layer 2 residual overvoltage protection scheme

Layer 2 Protection Relay Settings and Relay Response

In this section, the protection relay settings and the relay response of Layer 2's Group 1 and Group 2 microgrids in both grid-tied and islanded modes are discussed. For all the differential relays R19 to R34, the settings shown in Table 5-12 are used. These settings are found to work well in keeping the relays stable for external faults while tripping for faults within their protected zones.

Table 5-12
Protection settings for differential relays in Layer 2

Parameter	Setting
Differential current threshold	800 A primary
Slopes	Slope 1: 20%, Slope 2: 80%

The response of differential relay R19 for a 3LG fault on the 23 kV line 15E in grid-tied mode is shown in Figure 5-15. The relay operating points in all the phases during the 3LG fault—marked by a circle—are in the relay operate region as the differential current of 6.85 kA is higher than the stabilizing current 3.43 kA in all the phases in the grid-tied mode. The relay will trip the breakers with an indication that all the phases are faulted.

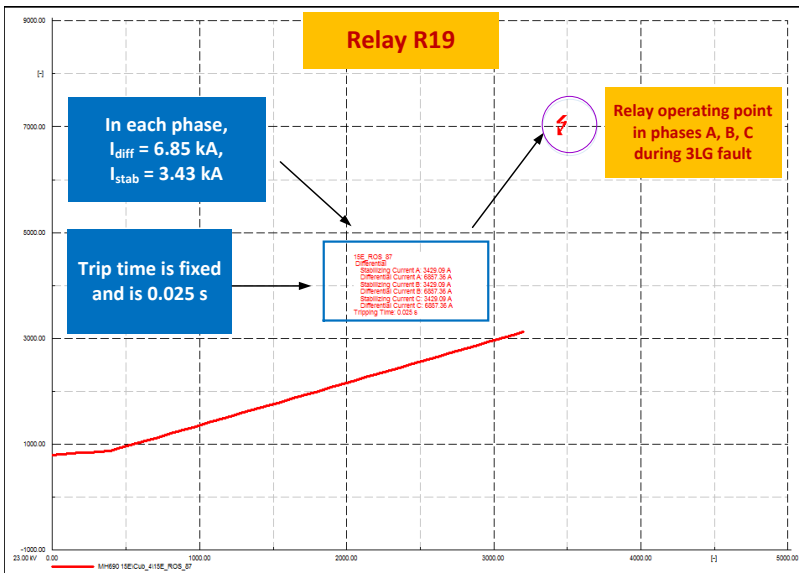

Figure 5-15
Differential relay R19 response for a 3LG fault on 23 kV line 15E operating in grid-tied mode

The differential relay R19 response for an SLG fault on the 23 kV line 15E is shown in Figure 5-16. The relay operating point in phase A is in the operate region as the differential current of 3.56 kA is higher than the stabilizing current of 1.78 kA in that phase. At the same time, the differential current is less than the differential threshold current setting of 800 A in phases B and C. Therefore, the relay operating point is in the stable region for phases B and C. The relay R19 will issue a trip command to the breakers with an indication that phase A is faulted. Figure 5-17

shows the response of relays R20, R21 and R22 during this SLG fault. Since the SLG fault is external to their protected zones, it is expected that these relays remain stable during the SLG fault. It can be observed in Figure 5-17 that the operating points of relays R20, R21 and R22 are in the stable region in all the phases as desired. Similarly, the other differential relays in the system for which the SLG fault on the 23 kV line 15E is external are observed to be stable during this short-circuit simulation.

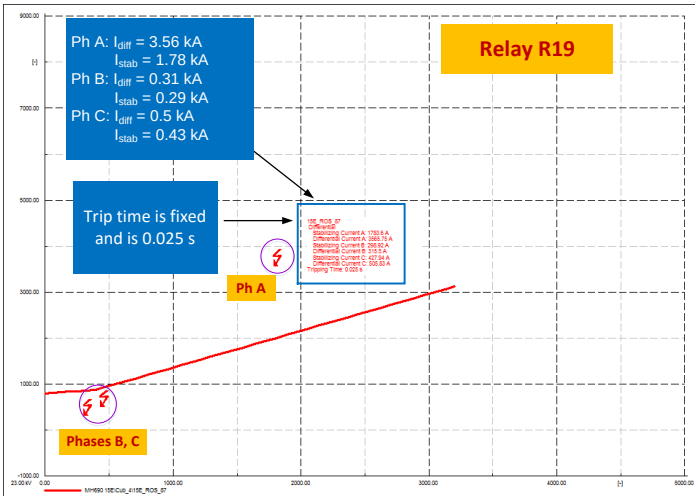

Figure 5-16
Differential relay R19 response for an SLG fault on 23 kV line 15E in grid-tied mode

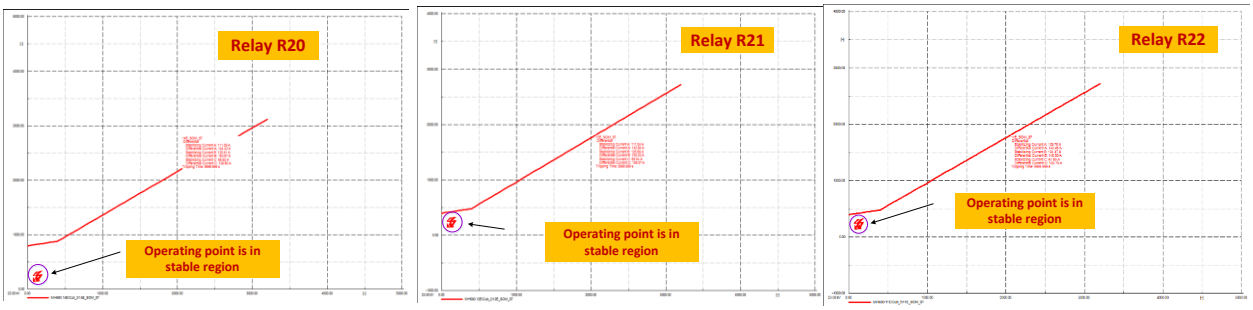

Figure 5-17
Response of differential relays R20, R21 and R22 during an SLG fault on 23 kV line 15E in grid-tied mode

The responses of differential relays for 3LG and SLG fault simulations on the 23 kV lines of Group 1 and Group 2 microgrids in the grid-tied mode are summarized in Table 5-13 and Table 5-14, respectively. It may be observed that the response of the differential relays is as desired with the relay settings given in Table 5-12.

Table 5-13
Summary of differential protection relay response in Layer 2, Group 1 in grid-tied mode

Fault location	Protection	Relay	Grid-tied mode						Relay Response
			Ph A		Ph B		Ph C		
			Idiff	Istab	Idiff	Istab	Idiff	Istab	
3LG fault on Line 15E	87	R19	6.85 kA	3.43 kA	6.85 kA	3.43 kA	6.85 kA	3.43 kA	Trip, Faulted phases: A,B,C
		R23	7.0 kA	3.5 kA	7.0 kA	3.5 kA	7.0 kA	3.5 kA	
		R27	7.06 kA	3.53 kA	7.06 kA	3.53 kA	7.06 kA	3.53 kA	
SLG fault on Line 15E	87	R19	3.56 kA	1.7 kA	0.31 kA	0.3 kA	0.5 kA	0.42 kA	Trip, Faulted phase: A
		R23	3.64 kA	1.83 kA	0.3 kA	0.3 kA	0.41 kA	0.47 kA	
		R27	3.65 kA	1.82 kA	0.29 kA	0.31 kA	0.44 kA	0.46 kA	
3LG fault on Line 14E	87	R20	6.85 kA	3.43 kA	6.85 kA	3.43 kA	6.85 kA	3.43 kA	Trip, Faulted phases: A,B,C
		R24	7.04 kA	3.52 kA	7.04 kA	3.52 kA	7.04 kA	3.52 kA	
		R28	7.06 kA	3.53 kA	7.06 kA	3.53 kA	7.06 kA	3.53 kA	
SLG fault on Line 14E	87	R20	3.56 kA	1.78 kA	0.32 kA	0.3 kA	0.5 kA	0.43 kA	Trip, Faulted phase: A
		R24	3.65 kA	1.83 kA	0.3 kA	0.3 kA	0.41 kA	0.48 kA	
		R28	3.64 kA	1.82 kA	0.29 kA	0.31 kA	0.44 kA	0.46 kA	
3LG fault on Line 12E	87	R21	6.85 kA	3.43 kA	6.85 kA	3.43 kA	6.85 kA	3.43 kA	Trip, Faulted phases: A,B,C
		R25	7.03 kA	3.52 kA	7.03 kA	3.52 kA	7.03 kA	3.52 kA	
		R29	7.06 kA	3.53 kA	7.06 kA	3.53 kA	7.06 kA	3.53 kA	
SLG fault on Line 12E	87	R21	3.56 kA	1.78 kA	0.32 kA	0.3 kA	0.5 kA	0.43 kA	Trip, Faulted phase: A
		R25	3.65 kA	1.83 kA	0.3 kA	0.3 kA	0.41 kA	0.48 kA	
		R29	3.64 kA	1.82 kA	0.29 kA	0.31 kA	0.44 kA	0.46 kA	
3LG fault on Line 11E	87	R22	6.86 kA	3.43 kA	6.86 kA	3.43 kA	6.86 kA	3.43 kA	Trip, Faulted phases: A,B,C
		R26	6.98 kA	3.5 kA	6.98 kA	3.5 kA	6.98 kA	3.5 kA	
		R30	7.06 kA	3.53 kA	7.06 kA	3.53 kA	7.06 kA	3.53 kA	
SLG fault on Line 11E	87	R22	3.56 kA	1.78 kA	0.32 kA	0.3 kA	0.5 kA	0.43 kA	Trip, Faulted phase: A
		R26	3.64 kA	1.83 kA	0.3 kA	0.3 kA	0.41 kA	0.47 kA	
		R30	3.64 kA	1.82 kA	0.29 kA	0.31 kA	0.44 kA	0.46 kA	

Table 5-14
Summary of differential protection relay responses in Layer 2, Group 2

Fault location	Protection	Relay	Grid-tied mode						Relay Response
			Ph A		Ph B		Ph C		
			Idiff	Istab	Idiff	Istab	Idiff	Istab	
3LG fault on Line Fru 27s	87	R31	2.9 kA	1.46 kA	2.9 kA	1.46 kA	2.9 kA	1.46 kA	Trip, Faulted phases: A,B,C
SLG fault on Line Fru 27s	87	R31	1.26 kA	0.6 kA	0 A	43 A	0 A	28 A	Trip, Faulted phase: A
3LG fault on Line Fru 18s	87	R32	2.9 kA	1.46 kA	2.9 kA	1.46 kA	2.9 kA	1.46 kA	Trip, Faulted phases: A,B,C
SLG fault on Line Fru 18s	87	R32	1.26 kA	0.6 kA	0 A	43 A	0 A	28 A	Trip, Faulted phase: A
3LG fault on Line CL 17s	87	R33	2.97 kA	1.48 kA	2.97 kA	1.48 kA	2.97 kA	1.48 kA	Trip, Faulted phases: A,B,C
SLG fault on Line CL 17s	87	R33	1.26 kA	0.6 kA	0 A	47 A	0 A	54 A	Trip, Faulted phase: A
3LG fault on Line CL 16s	87	R34	2.9 kA	1.46 kA	2.9 kA	1.46 kA	2.9 kA	1.46 kA	Trip, Faulted phases: A,B,C
SLG fault on Line CL 16s	87	R34	1.26 kA	0.6 kA	0 A	43 A	0 A	54 A	Trip, Faulted phase: A

For detection of ground faults in Layer 2 during islanded mode of the combined operation of Groups 1 and 2, a residual overvoltage protection scheme (59G) is proposed. For this, the residual overvoltage at the 23 kV Elm Street Station bus is measured during SLG fault conditions. The results are summarized in Table 5-15. Note that phase A is considered as the faulted phase for the SLG fault simulations. The results indicate that the voltage in the faulted phase becomes zero during the fault and that the voltage in the other two phases rises by about $\sqrt{3}$ times. As a result, a very high residual overvoltage ($3V_0$) is observed at the Elm Street Station bus during the SLG fault.

Table 5-15
Summary of residual overvoltage protection relay response in Layer 2 Groups 1+2

Bus	Fault location	Protection	Relay	Islanded Mode					Relay Response
				Va	Vb	Vc	V0	3V0	
23 kV Elm Station	SLG fault on Line 15E	59G	R35	0∟-91.18° kV	22.95∟-147.56° kV	22.95∟-152.44° kV	13.25∟-177.56° kV	39.75 kV	Trip, Phase A
	SLG fault on Line 14E			0∟88.22° kV	22.95∟-147.57° kV	22.95∟-152.43° kV	13.25∟-177.57° kV	39.75 kV	
	SLG fault on Line 12E			0∟77.80° kV	22.95∟-147.56° kV	22.95∟152.43° kV	13.25∟-177.57° kV	39.75 kV	
	SLG fault on Line 11E			0∟-83.64° kV	22.95∟-147.56° kV	22.95∟152.44° kV	13.25∟-177.56° kV	39.75 kV	

Key Findings

The design of protection system for microgrids is challenging as the protection system must satisfactorily respond in both grid-tied and islanded modes. As the fault levels in the islanded mode can be low depending on the type of generation in the microgrid and on the transformer connections, the fault levels require special attention in the design of the protection system. In the microgrids, overcurrent protection alone may not provide sufficient protection in meeting all these criteria. Differential current protection may be helpful in providing sensitive protection to a clearly defined zone and residual overvoltage protection is effective in detecting ground faults in ungrounded or high-impedance grounded systems. For the BNMC microgrid system, the protection schemes based on overcurrent, differential current and residual overvoltage principles are proposed. These protection schemes, relay settings, and the relay response for 3LG and SLG faults in both grid-tied and islanded modes of operation are discussed in this chapter.

The islands, namely Roswell Park Cancer Institute (RPCI), University of Buffalo/School of Medicine (SOM), Kaleida Health (KH), Fruitbelt (FB) and Cleveland BioLabs (CL) operating together, in Layer 1 of the BNMC have sufficient fault levels in both grid-tied and islanded modes for the overcurrent protection (ANSI code 50/51, 50N/51N) to work well. The existing protection system has overcurrent relays installed in these islands. Therefore, overcurrent protection settings providing desired protection response in Layer 1 for the existing overcurrent relays are documented.

Layer 2 has many tapped lines. For providing sensitive protection to these tapped lines, differential current protection scheme is proposed. The generic differential relay (ANSI code 87) settings provided for the proposed differential relays offer the desired relay response by keeping them stable for external faults while detecting all internal faults in grid-tied mode.

Because of the grounded-wye delta connection of the transformers, the 23 kV system becomes ungrounded in the islanded mode of operation. For ground fault protection on the 23 kV system of Layer 2 in islanded mode, residual overvoltage protection (ANSI code 59G) is proposed. This protection measures the residual voltage ($3V_0$) at the measurement point using a grounded-wye, delta-connected voltage transformer to detect ground faults. In the BNMC system, the residual voltage at the Elm Street Station bus may be measured to detect ground faults on the 23 kV system during the combined operation of Groups 1 and 2 microgrid in islanded mode. Upon the detection of a ground fault, the residual overvoltage relay will trip all the 23 kV breakers to isolate the ground fault.

Following are the key findings of this study:

1. The study results indicate that the existing overcurrent protection in conjunction with the proposed differential and under/overvoltage protections can detect faults in both grid-tied and islanded modes of operation of the BNMC microgrid.
2. The BNMC microgrid has sufficient fault levels in the four islands RPCI, SOM, KH and “Fruitbelt+Cleveland” due to the presence of synchronous generator-based generation to

utilize existing overcurrent protection in Layer 1. When a fault occurs in any of the islands in Layer 1, the overcurrent relay associated with the synchronous generator trips the associated circuit breaker.

3. Differential protection is needed to provide effective sensitive protection to the tapped sections on the 23 kV side in Layer 2 in the grid-tied mode of operation. The faults on the tapped sections are detected by the differential relays installed in that T section for fault isolation in grid-tied mode.
4. As the 23 kV system becomes ungrounded in the islanded mode of operation due to the grounded-wye delta transformer connections, the detection of ground faults is not possible with overcurrent protection or differential protection. For this scenario, residual overvoltage protection is needed.

6
DYNAMIC ANALYSIS

In Chapters 3 and 4 the system modeling and the circuit validation of the microgrid comprising mainly of the Buffalo Niagara Medical Campus (BNMC) were presented. The various elements present in the microgrid and the electrical parameters were also discussed in Chapter 4 along with circuit modeling. Chapter 4 analyzed the different microgrid configurations and performed load flow studies to examine the steady-state behavior of the system.

This chapter focusses on studying the dynamic behavior and transient characteristic of the system. This chapter concentrates on events which can cause power quality issues during microgrid operation. The most common switching scenario encountered by a microgrid which can cause a disturbance is during connecting two islands of a microgrid or connecting a microgrid operating in islanded mode to the grid. Similarly, islanding a grid-connected microgrid or forming independent islands from an interconnected microgrid can cause disturbances. When a microgrid is completely de-energized, having black start capability can help bring the microgrid back to operation without any help from an external source. Starting large motors in a weak microgrid may cause severe voltage sags and the motors may also fail to start. Therefore, this chapter demonstrates the process and requirements for a successful synchronization process and islanding process. This chapter also analyzes the black start and motor starting capability of the microgrid.

Objective and Analysis Approach

This chapter consists of four major sections where *synchronization*, *islanding*, *black start*, and *motor starting* are analyzed. The BNMC microgrid circuit modeled in DIgSILENT PowerFactory is used for performing various simulations. Electromagnetic Transient (EMT) simulations with a step size of 100 µs was used to study the system response characteristics. The motivation behind this analysis is to avoid disturbances which may occur when the microgrid undergoes transitions from one state to another. The objective of these analyses is to characterize the level of distribution support provided by the microgrid and the impact of these technologies on interconnected distribution systems.

Synchronization analysis involves studying the transient characteristics while interconnecting two separated islands or while interconnecting an island and an external grid. The objective is to demonstrate successful synchronization of two separated islands and synchronization of microgrid and utility distribution system with minimal disturbance in the system. When the islands meet the required necessary conditions for safe synchronization (which will be discussed in the next section), the two islands are interconnected by closing the breakers at the point of interconnection, or POI. The analysis presented in the upcoming sections demonstrates commonly encountered synchronization scenarios. The voltage, current, frequency and active power plots are provided to observe the system's dynamic characteristics during the process of synchronization as well as during the steady-state condition after the process of synchronization

has completed. The total generation and total load after synchronization are compared to ensure that the system is functioning as expected after the synchronization process.

Islanding analysis evaluates the transient characteristics while separating a microgrid into islands. The objective is to demonstrate the ability of the microgrid to island and to identify the desirable islanding conditions. This includes studying both islanding a grid-connected microgrid as well as islanding a smaller portion of a microgrid—itself operating in islanded mode. Similar to synchronization analysis, the voltage, current, frequency, and active power plots are presented for each case analyzed as well as the total generation and load after examining the islanding process(es).

Black start capability is the ability to start a microgrid from a de-energized state without the help of an external source. The objective of this analysis is to demonstrate and study energizing a de-energized busbar and loading it. Similarly, voltage, current and active power plots are presented.

Motor starting involves studying the capability of the microgrid to handle the starting requirements of a motor such as high inrush current and low bus voltage during the starting process. The objective is to study the starting characteristics of motors of different sizes in a small and weak microgrid. For this purpose, motors of various sizes were started on the weakest island and the results obtained were analyzed.

Synchronization

This section studies the process of interconnecting two power systems with little or no disturbance. A synchronization study includes connecting a microgrid operating in islanded mode to the utility grid as well as connecting an islanded Layer 1 group with the rest of the microgrid. Synchronization is a vital process as it interconnects two systems and helps exchange power between the two systems. Even though two systems may be stable independently, synchronization has to be done with care following the necessary requirements and precautions else it will lead to disrupting the stable islands upon reconnection. Table 6-1 presents the different synchronization analysis scenarios studied.

Table 6-1
Synchronization analysis scenarios

Case Number	Scenario
Case 1	Synchronizing islanded Group 1 with Elm Street Station Initial Condition: Group 1 microgrid is in islanded mode Microgrid changing from islanded mode to grid connected mode – Group 1
Case 2	Synchronizing islanded Layer 1(RPCI) with rest of Group 1 in islanded mode (not connected to Elm Street Station) Initial condition: Group 1 microgrid is in islanded mode and RPCI is disconnected from the island.

Case 1: Synchronizing Islanded Layer 2 – Group 1 With Elm Street Station

This case presents Layer 2 – Group 1 microgrid (see Figure 4-1) changing from islanded mode to grid-connected mode. The objective is to demonstrate a successful synchronization of islanded Group 1 microgrid and the Elm Street Station. Referring to the circuit description presented in Chapter 4, Layer 2 –Group 1 consists of the State University of New York at Buffalo and the School of Medicine (UB/SOM), Kaleida Health (KH) and Roswell Park Cancer Institute (RPCI). The microgrid may be connected to the Elm Street Station via four feeders (11E, 12E, 14E, and 15E) at the POI as shown in Figure 6-1.

Circuit Conditions

The Layer 2 – Group 1 microgrid is initially operating in an islanded mode. The total generation in Group 1 matches the total load in Group 1 microgrid. Group 1 microgrid at the POI and the Elm Street Station have the same frequency, voltage and phase angle before synchronization. Only synchronous machines were used for generation. PV and ES were not used as they are relatively very small in size and are also expected to function in a similar manner as the other machines. Hence, they do not impact the synchronization process much and are not used. All the generators in the simulation were defined with the Woodward diesel governor and only the diesel generators in the microgrid were equipped with the Automatic Voltage Regulator (AVR) model called 1968 IEEE Type 1 excitation system.

The load present in each building of Layer 2 – Group 1 microgrid corresponds to the load value at a time between 12 noon and 1 pm in islanded mode of operation of Layer 2 – Group 1 microgrid which was analyzed in Chapter 4 while studying load flow analysis. The loads at UB/SOM , RPCI, and KH are 3.4 MW, 9 MW, and 10.9 MW, respectively. The total load is 23.3 MW. The generations of SOM_DG, RPCI_DG, RPCI_CHP, KH_DG, and KH_Nat_Gas are 1.3 MW, 7.1 MW, 4.0 MW, 5.8MW, and 5.1 MW, respectively. The total generation is 23.3 MW. The circuit condition before synchronization is presented in Figure 6-1**.**

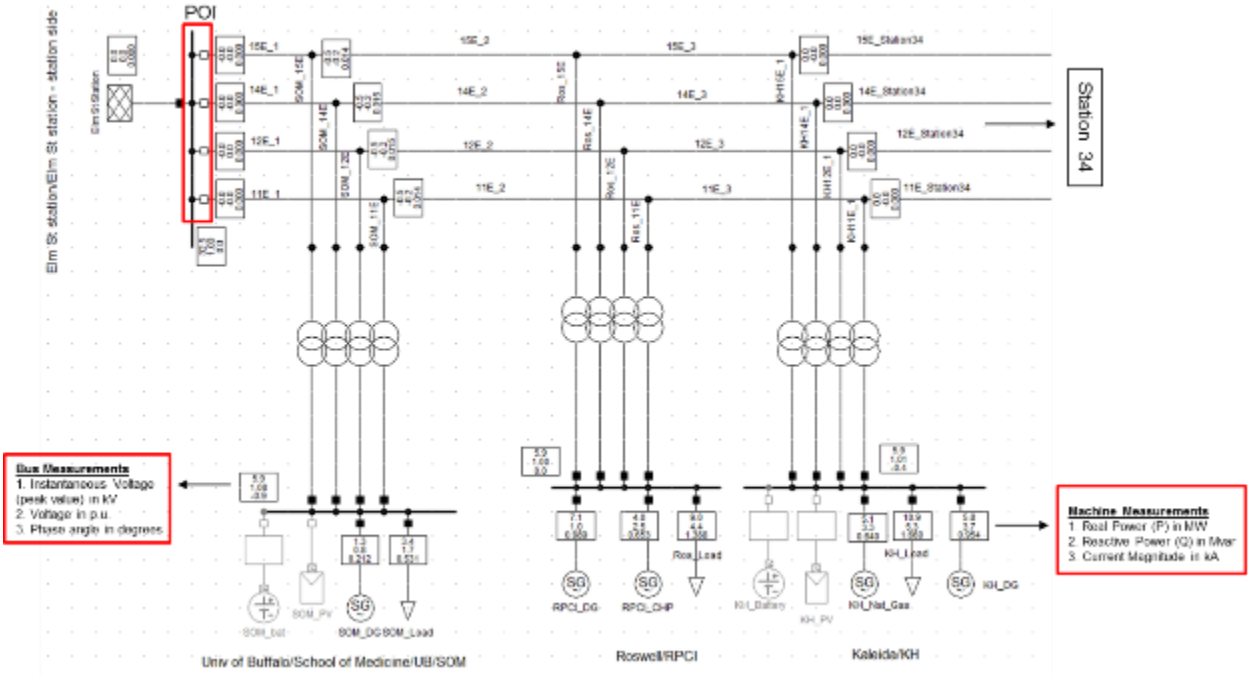

Figure 6-1
Synchronization Case 1: Initial circuit conditions

From Figure 6-1, it may be observed that all the bus voltages are close to 1 pu. Furthermore, the frequency of the system was also observed to be 1 pu because the generation in each building nearly matches the load in their respective buildings (UB/SOM imports 2.1 MW and 0.9 Mvar, RPCI exports 2.1 MW and imports 0.9 Mvar and KH exports only reactive power of 1.7Mvar). Notice there is not a very large transfer of power between buildings. KH has a slightly higher voltage than the other buses because it generates more reactive power and supplies it to other buildings. So, the system is stable in its present state before synchronization.

Breaker Timing

For synchronization, the breakers present at the POI must be closed to synchronize the islanded Layer 2 - Group 1 microgrid with the Elm Street Station. Elm Street Station and each of the four feeders (11E, 12E, 14E, and 15E) are connected using three-phase circuit breakers. The breakers are timed such that each phase of a three-phase circuit breaker closes one after the other so that any transients can be displayed clearly. Thus, all of the 3-phase circuit breakers present in 11E, 12E, 14E, and 15E operate one after the other in a similar manner as explained above. Table 6-2 shows the specified time for each breaker operation command.

Table 6-2
Synchronization Case 1: Breaker operation timings

Breaker Closing Operation	Time (seconds)
11E Breaker – Phase A	0.04
11E Breaker – Phase B	0.06
11E Breaker – Phase C	0.08
12E Breaker – Phase A	0.10
12E Breaker – Phase B	0.12
12E Breaker – Phase C	0.14
14E Breaker – Phase A	0.16
14E Breaker – Phase B	0.18
14E Breaker – Phase C	0.20
15E Breaker – Phase A	0.22
15E Breaker – Phase B	0.24
15E Breaker – Phase C	0.26

Event Analysis

Phase A of 11E breaker was timed to close at 0.04 seconds. The system at the point of interconnection is delta connected. Hence, no current flows after one phase of the breaker is closed. For current to start flowing, at least two phases of the breaker have to be closed. The voltage and current waveforms may be observed in Figure 6-2 and Figure 6-3. When phase C of the breaker is closed, current starts flowing in all the three breakers. The scale on the Y axes of the current plots are of the order of 0.01 kA. Hence, the current flowing through the breaker at the POI is negligible and almost 0 kA.

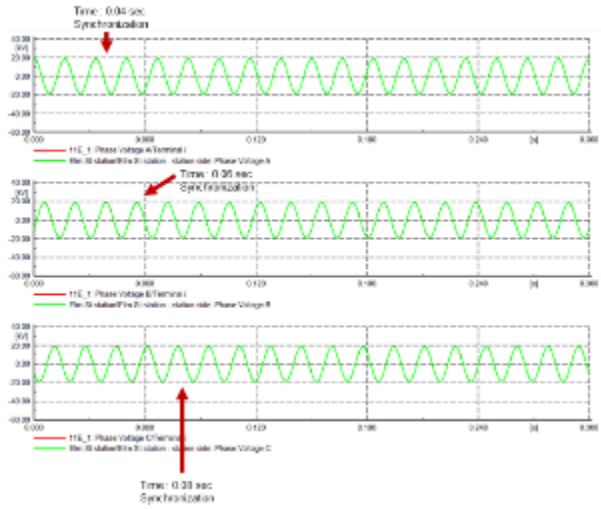

Figure 6-2
Synchronization Case 1: Instantaneous voltages in kV during synchronization at 11E breaker

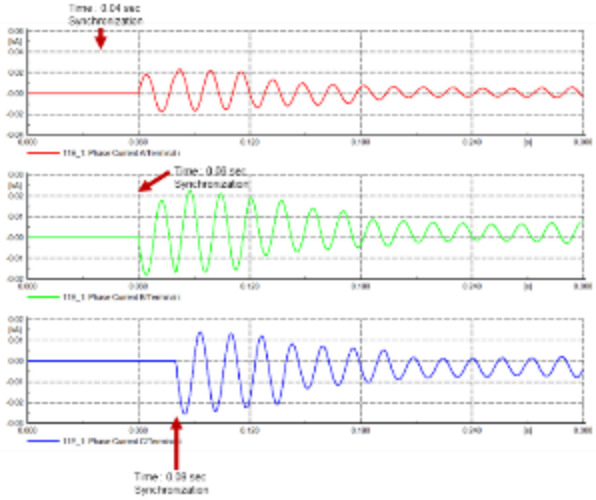

Figure 6-3
Synchronization Case 1: Instantaneous current in kA during synchronization at 11E breaker

Similar waveforms may be observed at 12E, 14E, and 15E breakers at the time of synchronization as shown in Figure 6-4 through Figure 6-9. In all these waveforms, it may be observed that current begins to flow when at least two phases of the circuit breaker are closed.

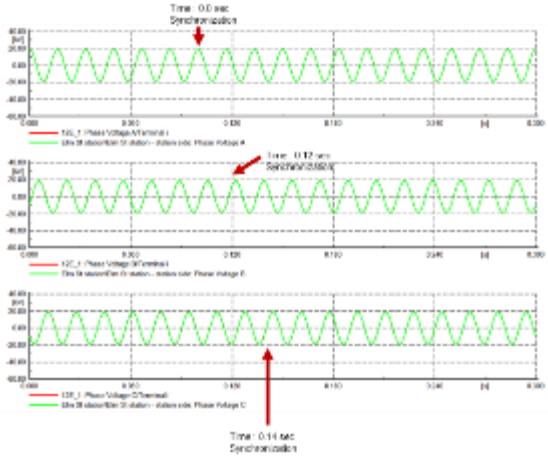

Figure 6-4
Synchronization Case 1: Instantaneous voltages in kV during synchronization at 12E breaker

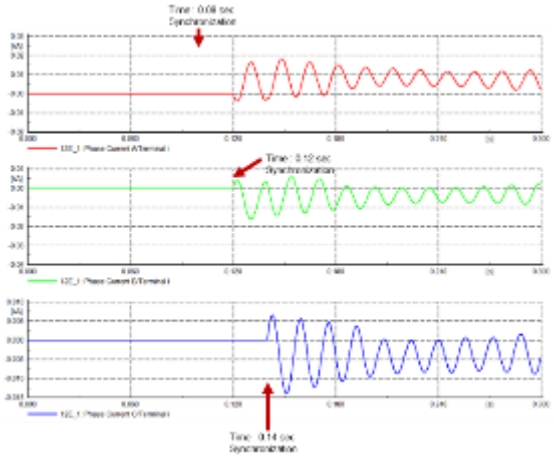

Figure 6-5
Synchronization Case 1: Instantaneous current in kA during synchronization at 12E breaker

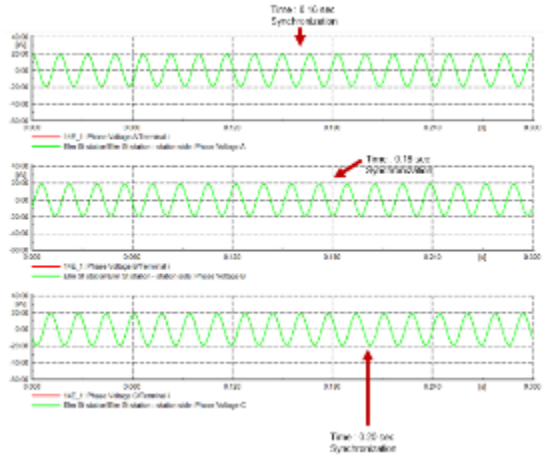

Figure 6-6
Synchronization Case 1: Instantaneous voltages in kV during synchronization at 14E breaker

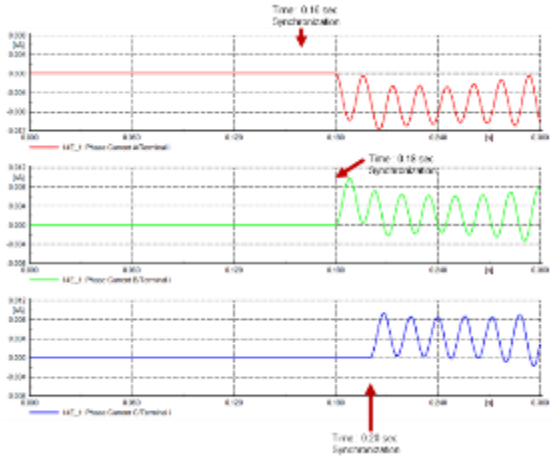

Figure 6-7
Synchronization Case 1: Instantaneous current in kA during synchronization at 14E breaker

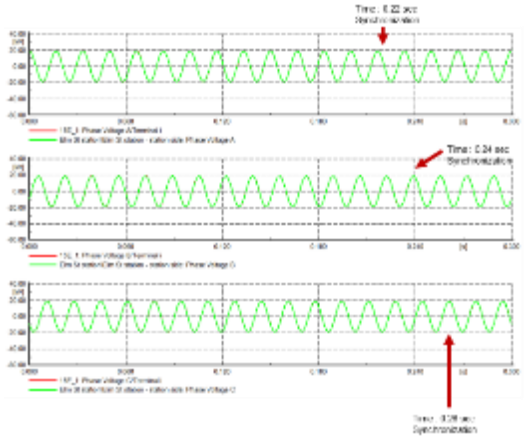

Figure 6-8
Synchronization Case 1: Instantaneous voltages in kV during synchronization at 15E breaker

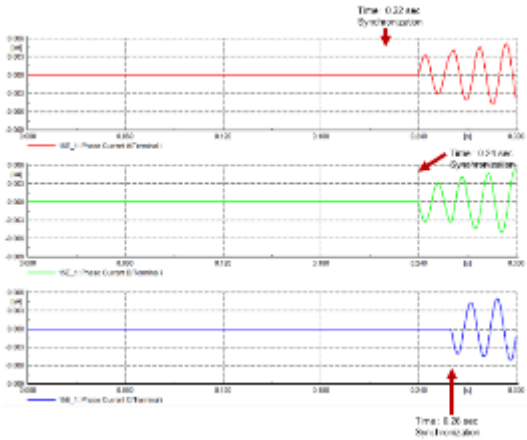

Figure 6-9
Synchronization Case 1: Instantaneous current in kA during synchronization at 15E breaker

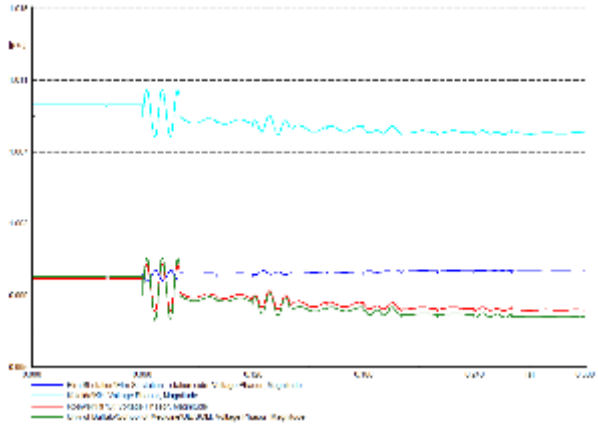

Figure 6-10
Synchronization Case 1: Voltages in pu during synchronization at different buses

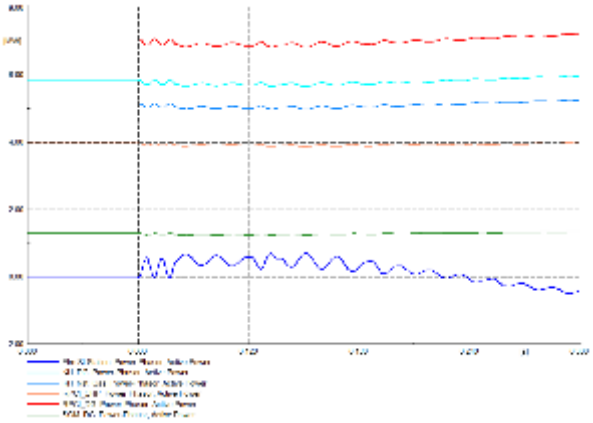

Figure 6-11
Synchronization Case 1: Active power supplied by various machines in MW during synchronization

The variation in the voltage is less than 0.004 pu when synchronization process occurs as can be seen in Figure 6-10. The transient is very small in magnitude and hence, synchronization process was successful without any disturbance. The small transient voltage variation arises because when the system is synchronized, Elm Street Station bus becomes the reference bus and stays at 1 pu voltage as it is the stronger bus. The other buses change their voltages accordingly for power flow transfer between different buildings. Eventually, voltage and current settle to new steady-state values.

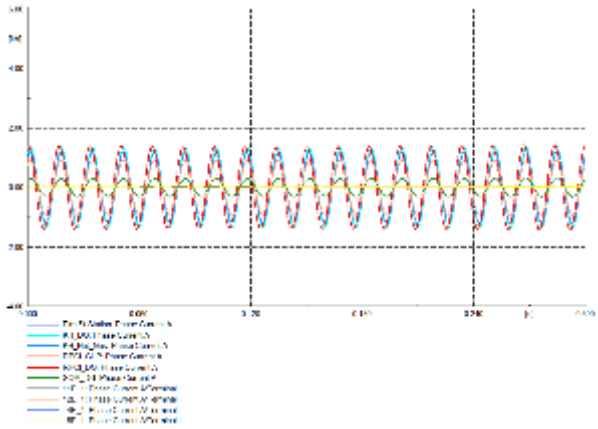

Figure 6-12
Synchronization Case 1: Instantaneous Phase A current in kA during synchronization

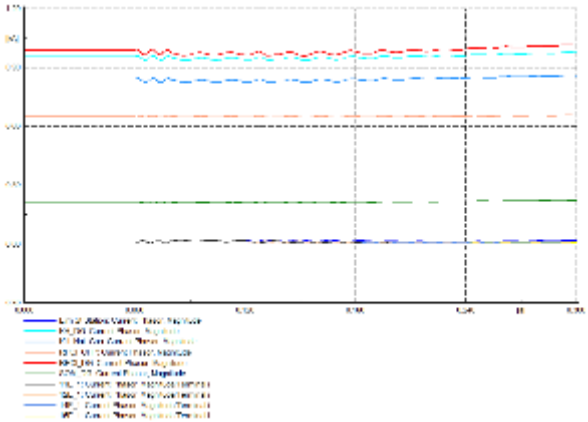

Figure 6-13
Synchronization Case 1: RMS current in kA during synchronization

In Figure 6-12, phase A currents of all the machines and at POI are shown. As the system is balanced, similar waveforms are expected for Phase B and Phase C. There is a small variation in active power generation during the transient period after synchronization. The active power and current plots of different machines eventually settle to similar values (values before synchronization) when they reach the steady-state condition. The settings for control of power in Elm Street Station are such that it does not supply or consume any real power from the microgrid in the steady-state condition. This may be observed in Figure 6-17 through Figure 6-20 showing the steady-state condition plots of the system after synchronization.

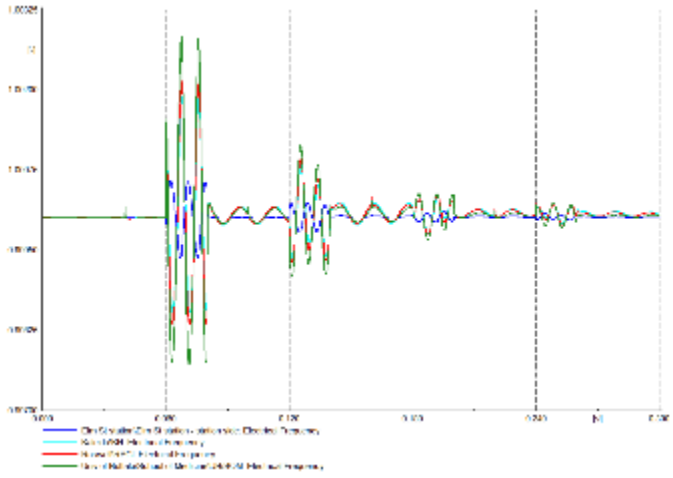

Figure 6-14
Synchronization Case 1: Frequency in pu during synchronization

From Figure 6-14, it may be seen that the variation in frequency is very small (0.998 pu to 1.003 pu). From the waveform, it may be observed that small variations in frequency occur when small current starts to flow in each beaker after synchronization (current starts to flow in 11E breaker at 0.06 s, similarly in 12E breaker at 0.12 s, 13E breaker at 0.18 s and 14E breaker at 0.24 s).

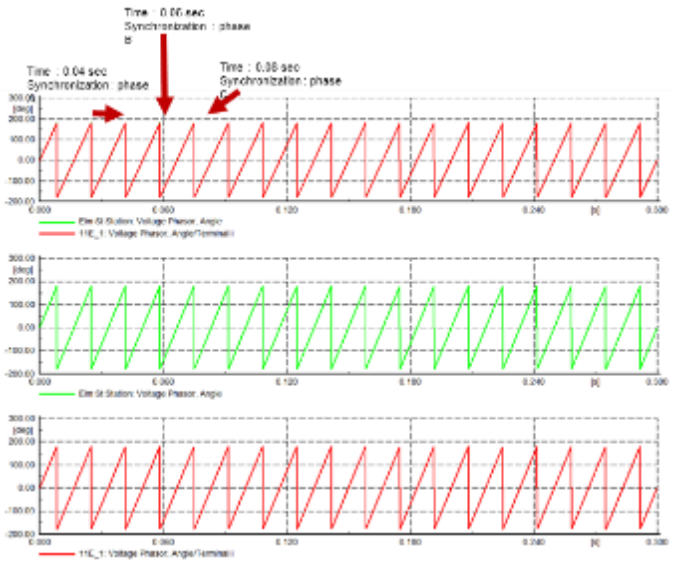

Figure 6-15
Synchronization Case 1: Voltage phase angle in degrees during synchronization

From Figure 6-10 through Figure 6-14, it may be observed that the transients were negligible during synchronization. This was because the total generation of the island matched the total load in that island before synchronization. Hence, there was negligible flow of current through the breakers when the breakers at the POI was closed as seen earlier in Figure 6-13. Also, the two systems had the same frequency and voltage at the point of interconnection before synchronization. The voltage phase angle of the two systems at the POI must also be same as shown in Figure 6-15 to have minimal transients.

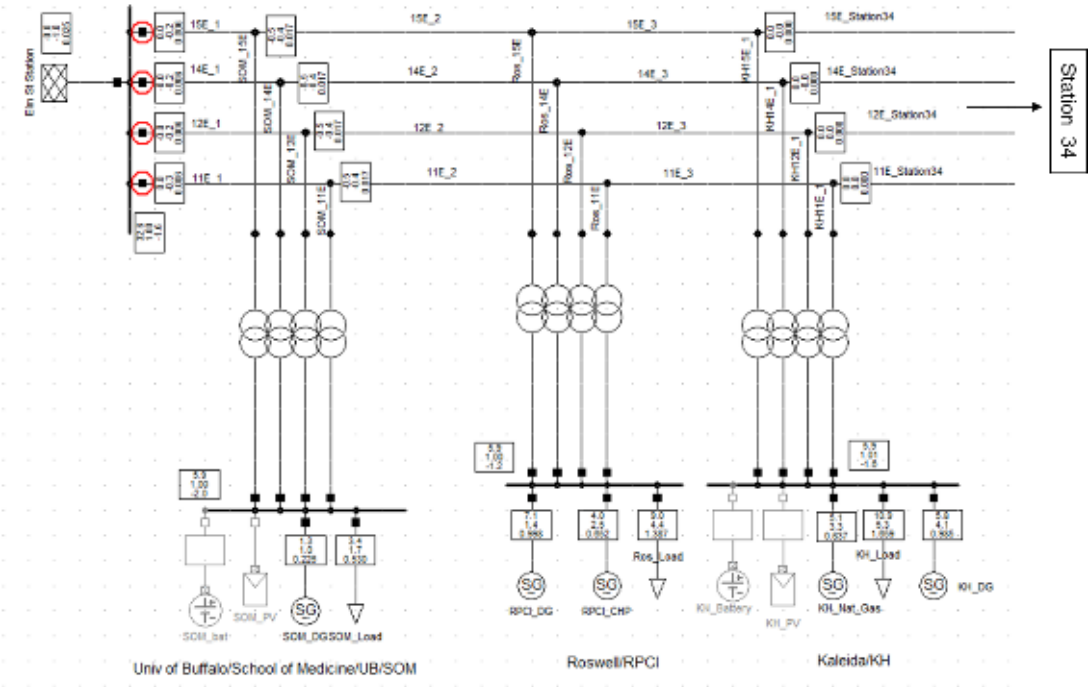

Figure 6-16
Synchronization Case 1: Circuit conditions after synchronization on reaching steady state

Figure 6-16 presents the state of the circuit on reaching steady state after synchronization. The loads have remained the same before and after synchronization. The real power generation has also remained the same because the controllers are programmed such that the Elm Street Station does not draw any real power after synchronization. From the steady-state graphs shown in Figure 6-17 and Figure 6-20, it can be observed that there is a small increase in voltage of all the buses. This is because, on synchronization, there is a small increase in reactive power generation of the synchronous machines and the excess reactive power is sent to the Elm Street Station.

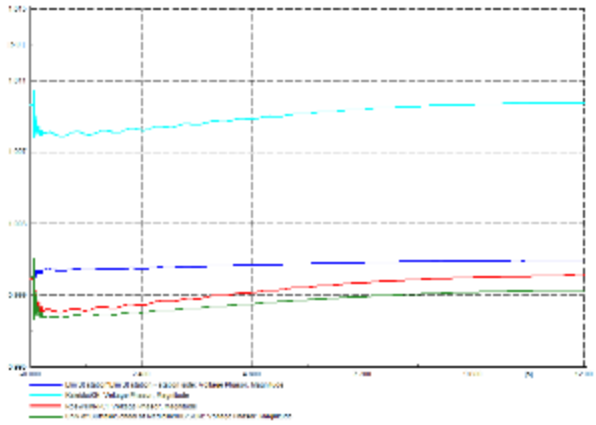

Figure 6-17
Synchronization Case 1: RMS Voltage in pu during synchronization (until steady state)

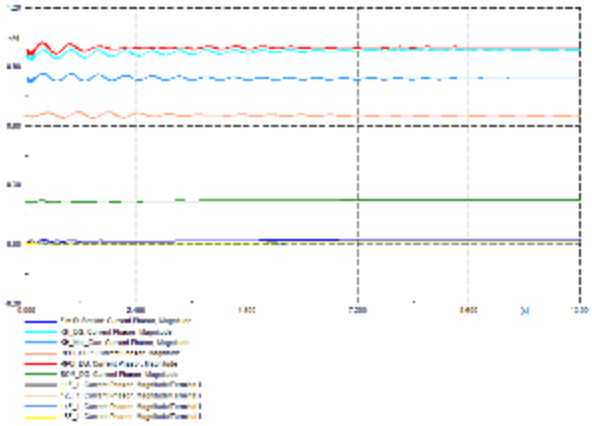

Figure 6-18
Synchronization Case 1: RMS current in kA during synchronization (until steady state)

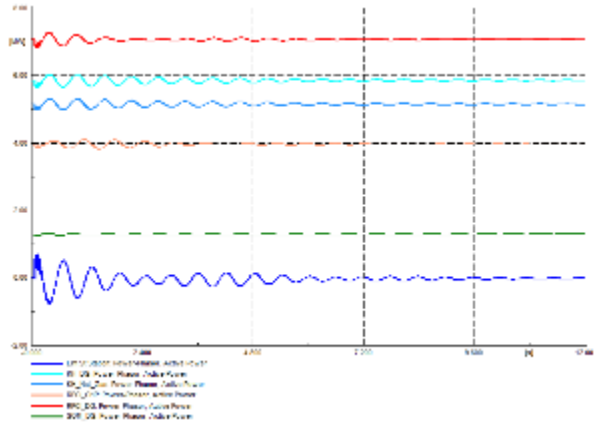

Figure 6-19
Synchronization Case 1: Active Power in MW during synchronization (until steady state)

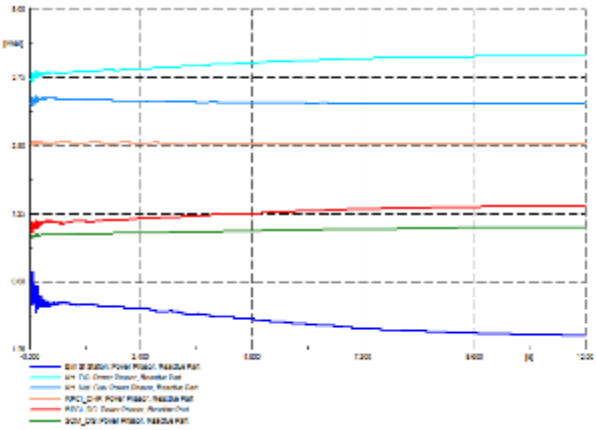

Figure 6-20
Synchronization Case 1: Reactive Power in Mvar during synchronization (until steady state)

From analyzing this case, it may be concluded that the synchronization process will be successful with minimal transients when the two systems have the same frequency, voltage, and phase angle at the POI before synchronization. It is assumed that controllers in each Layer 1 and Layer 2 groups ensure that the frequency, voltage, and phase angles match before synchronization.

Case 2: Synchronizing Islanded Layer 1(RPCI) With Rest of Layer 2 - Group 1 Microgrid in Islanded Mode

This case presents synchronizing of a Layer 1 building with the rest of Group 1 microgrid operating in islanded mode. The objective is to demonstrate successful synchronization of Layer 1 (RPCI building) with rest of Group 1 in islanded mode (UB/SOM and KH present together but without RPCI) to form the complete Group 1 island (UB/SOM, RPCI and KH together). The POI in this case is the 4 three-phase breakers present in the low voltage side of the distribution transformers connecting the feeders (11E, 12E, 14E, and 15E) and the RPCI building as shown in Figure 6-21.

Circuit Conditions

The Layer 2 – Group 1 microgrid is initially in islanded mode and Layer 1 (RPCI) is not part of the Group 1 microgrid. Hence, initially before synchronization, the Layer 2 – Group 1 consists of UB/SOM and KH only. Layer 1 (RPCI) at the POI and secondary of transformers connecting the feeders (11E, 12E, 14E, and 15E) to RPCI bus have the same frequency, voltage, and phase angle before synchronization. The load present in each building of the Layer 2 – Group 1 microgrid correspond to the load value at the time between 12 pm and 1 pm in the islanded mode of operation of the Layer 2 – Group 1 microgrid which was analyzed in Chapter 4 while studying load flow analysis. Only synchronous machines were used for generation. PV and ES were not used similar to the previous case.

Before synchronization, the load of 9 MW and 4.4 Mvar at RPCI is met only by the generation at RPCI (RPCI_DG and RPCI _CHP) and the load at SOM and KH are shared by SOM_DG, KH_DG and KH_Nat_Gas.

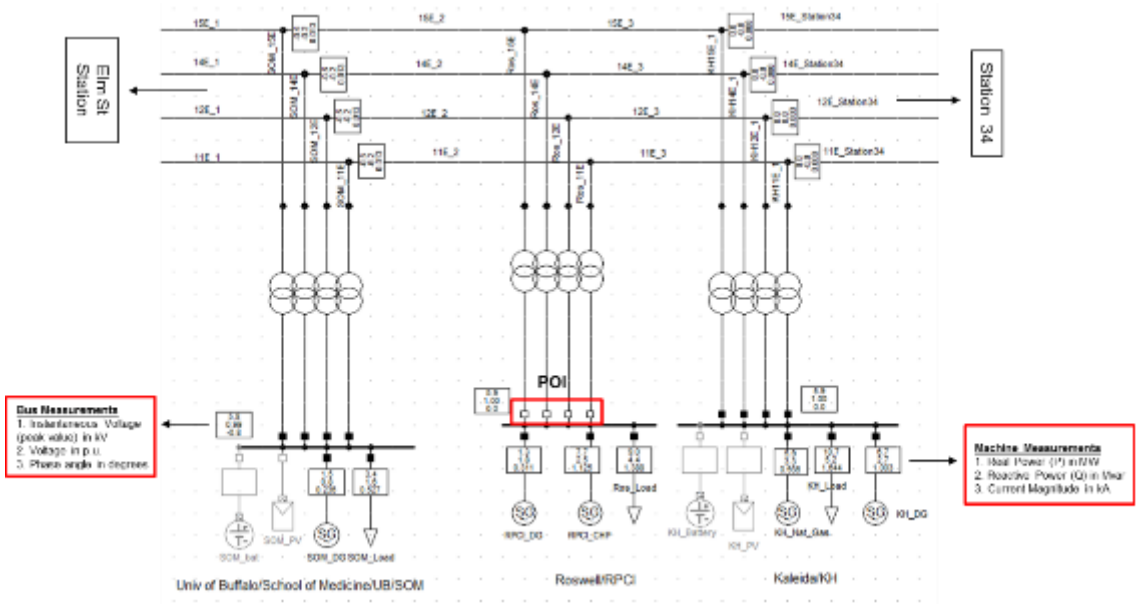

Figure 6-21
Synchronization Case 2: Initial circuit conditions

From Figure 6-21, it may be observed that all the bus voltages are close to 1 pu. The voltage at UB/SOM is a little less than the voltage at KH because the load at UB/SOM consumes both real

and reactive power from generators at KH (1.9 MW and 0.6 Mvar). The frequency of the system was also observed to be 1 pu which shows the system is stable in its present state before synchronization.

Breaker Timing

For connecting RPCI with rest of Group 1 microgrid, the four three-phase breakers present between the secondary of distribution transformers (connecting the feeders and RPCI) and RPCI are to be closed. Similar to Synchronization Case 1, the breakers are timed such that each phase of a three-phase circuit breaker closes one after the other. The three-phase circuit breakers present in 11E, 12E, 14E, and 15E operate one after the other in a similar manner as explained above. Table 6-3 shows the specified time for each breaker operation command.

Table 6-3
Synchronization Case 2: Breaker operation timings

Breaker Closing Operation	Time (seconds)
Ros_11E_T Breaker – Phase A	0.04
Ros_11E_T Breaker – Phase B	0.06
Ros_11E_T Breaker – Phase C	0.08
Ros_12E_T Breaker – Phase A	0.10
Ros_12E_T Breaker – Phase B	0.12
Ros_12E_T Breaker – Phase C	0.14
Ros_14E_T Breaker – Phase A	0.16
Ros_14E_T Breaker – Phase B	0.18
Ros_14E_T Breaker – Phase C	0.20
Ros_15E_T Breaker – Phase A	0.22
Ros_15E_T Breaker – Phase B	0.24
Ros_15E_T Breaker – Phase C	0.26

Event Analysis

Phase A of Ros_11E_T breaker is timed to close at 0.04 seconds. Unlike the previous case, the system at the POI is wye connected. Hence, current starts flowing in each phase as soon as their respective breakers are closed. This may be seen in Figure 6-22 and Figure 6-23.

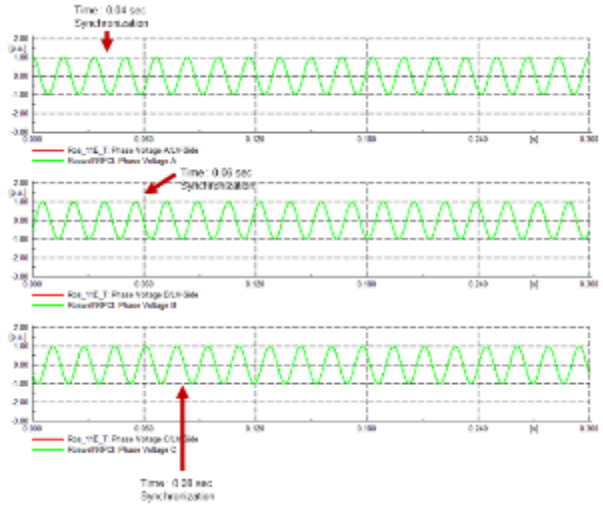

Figure 6-22
Synchronization Case 2: Instantaneous voltages in kV during islanding at 11E breaker

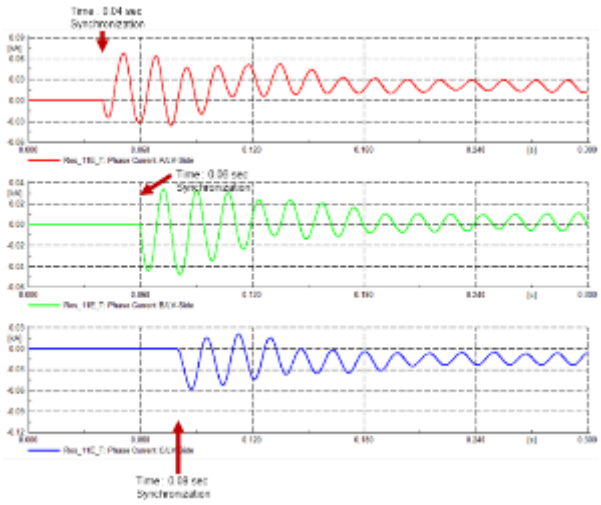

Figure 6-23
Synchronization Case 2: Instantaneous current in kA during islanding at 11E breaker

As seen in Synchronization Case 1, similar current and voltage waveforms are observed while closing other breakers as well. Instantaneous voltages and current waveforms measured at Ros_12E_T, Ros_14E_T and Ros_15E_T breakers are similar to waveforms observed at Ros_11E_T breaker except that the time of operation of each breaker is different.

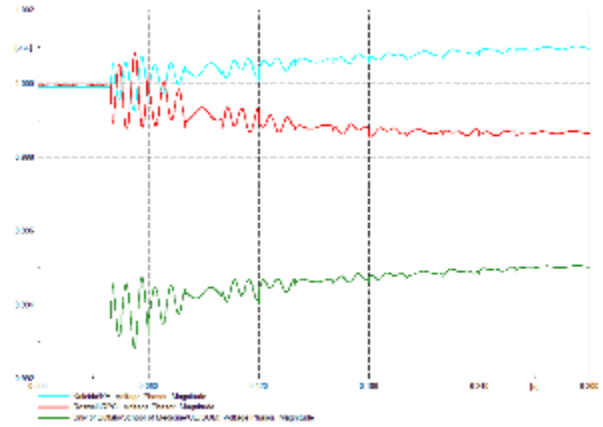

Figure 6-24
Synchronization Case 2: Voltages in pu during synchronization at different buses

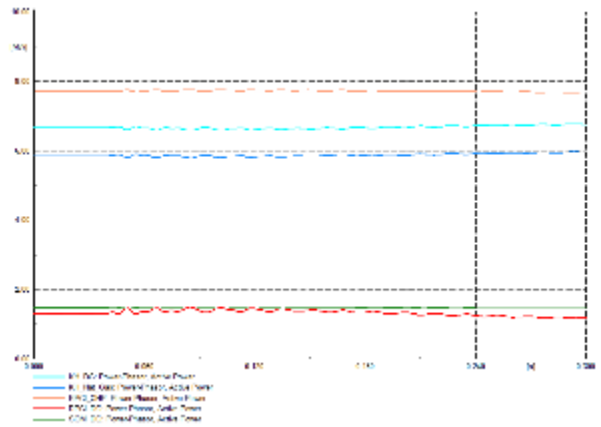

Figure 6-25
Synchronization Case 2: Active power supplied by various machines in MW during synchronization

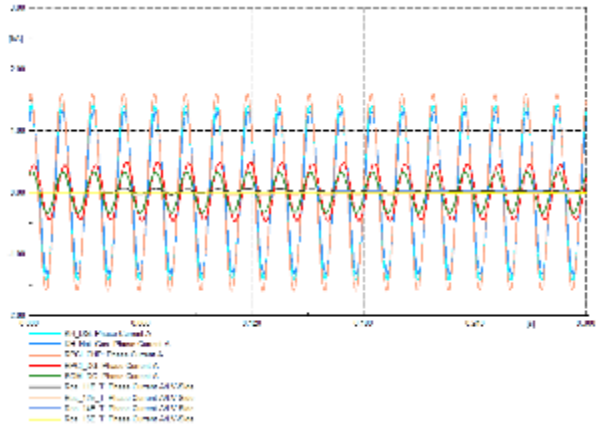

Figure 6-26
Synchronization Case 2: Instantaneous Phase A current in kA during synchronization

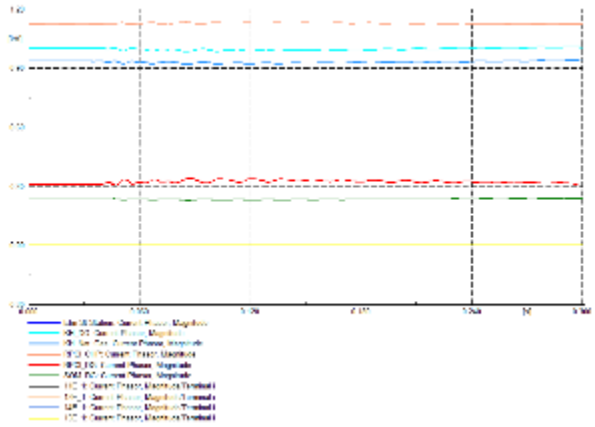

Figure 6-27
Synchronization Case 2: RMS current in kA during synchronization

The variation in the voltage as seen in Figure 6-24 is less than 0.004 pu when synchronization process occurs. Similar to voltage, the variation in frequency shown in Figure 6-28 is also minimal (0.998 pu - 1.002 pu). Figure 6-26 shows instantaneous phase A current and Figure 6-27 shows RMS current of different machines and at the POI. It may be seen that the variation in current is also negligible during synchronization. The transient appears small in magnitude and hence, the synchronization process appears to be successful without any disturbance. Before synchronization, each island had sufficient generation to match its own load and maintain voltage close to 1 pu as well. So, during synchronization, with no deficit or excess power at any location, no large current flows occur through the breakers when they close.

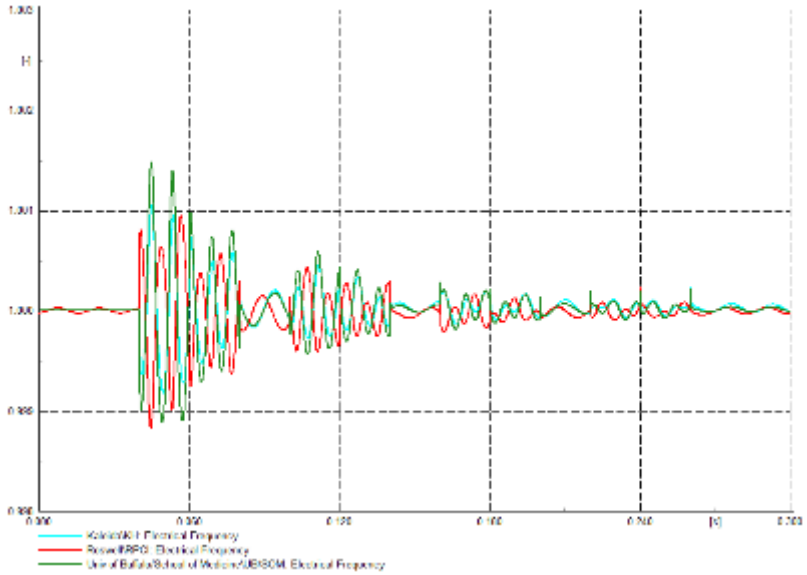

Figure 6-28
Synchronization Case 2: Frequency in pu during synchronization

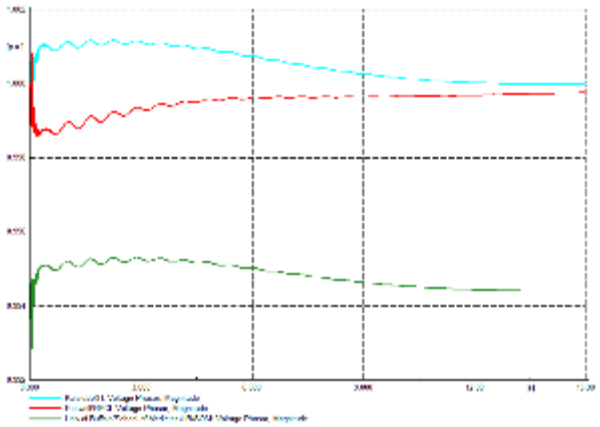

Figure 6-29
Synchronization Case 2: RMS Voltage in pu during synchronization (till steady state)

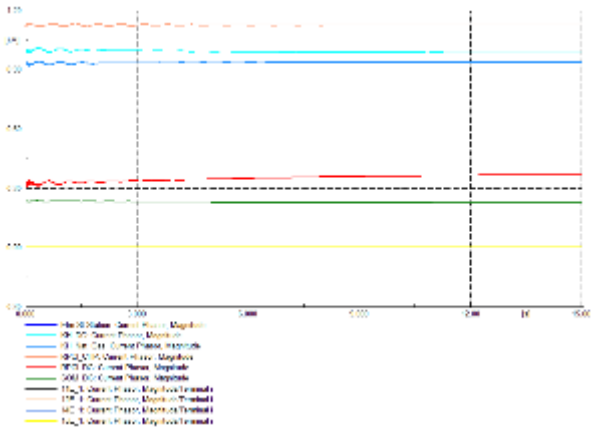

Figure 6-30
Synchronization Case 2: RMS current in kA during synchronization (till steady state)

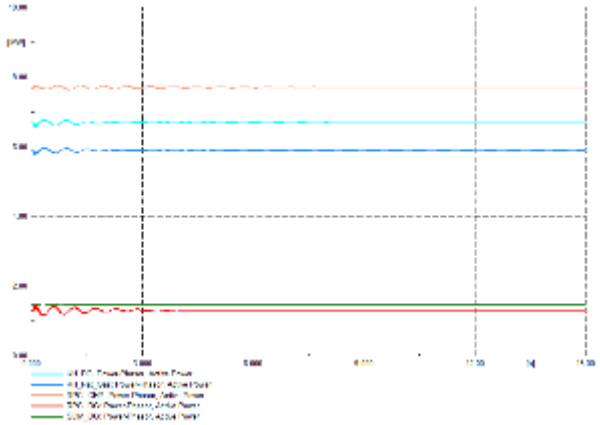

Figure 6-31
Synchronization Case 2: Active Power in MW during synchronization (till steady state)

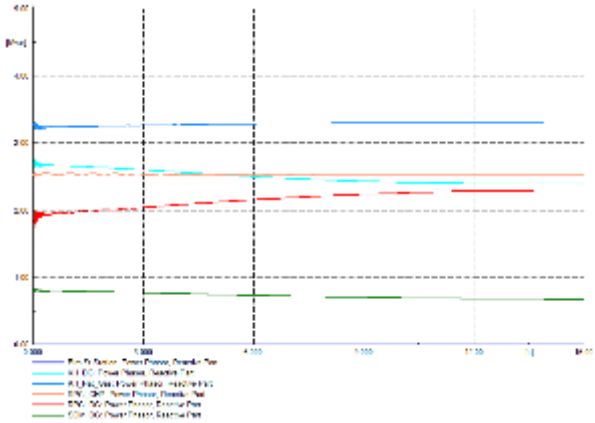

Figure 6-32
Synchronization Case 2: Reactive Power in Mvar during synchronization (till steady state)

Similar to Synchronization Case 1, the loads present in the system remain the same before and after synchronization and the power generated by each machine hasn't changed much from its initial value. Negligible change may be seen in active power produced by different machines before and after synchronization. The small change in current magnitudes in a few machines such as the RPCI_DG result from the change in reactive power produced by that machine. The change in reactive power supplied has led to the voltage of RPCI to increase and the voltage of KH to decrease. The steady-state voltage of KH is higher than the other buses because it supplies reactive power to other buses and SOM has the lowest voltage amongst all the buses because it receives real and reactive power from the other two buildings. After synchronization, the voltage at different buses appear to be closer to 1 pu than they were before synchronization. Figure 6-33 shows the circuit conditions after synchronization on reaching steady state.

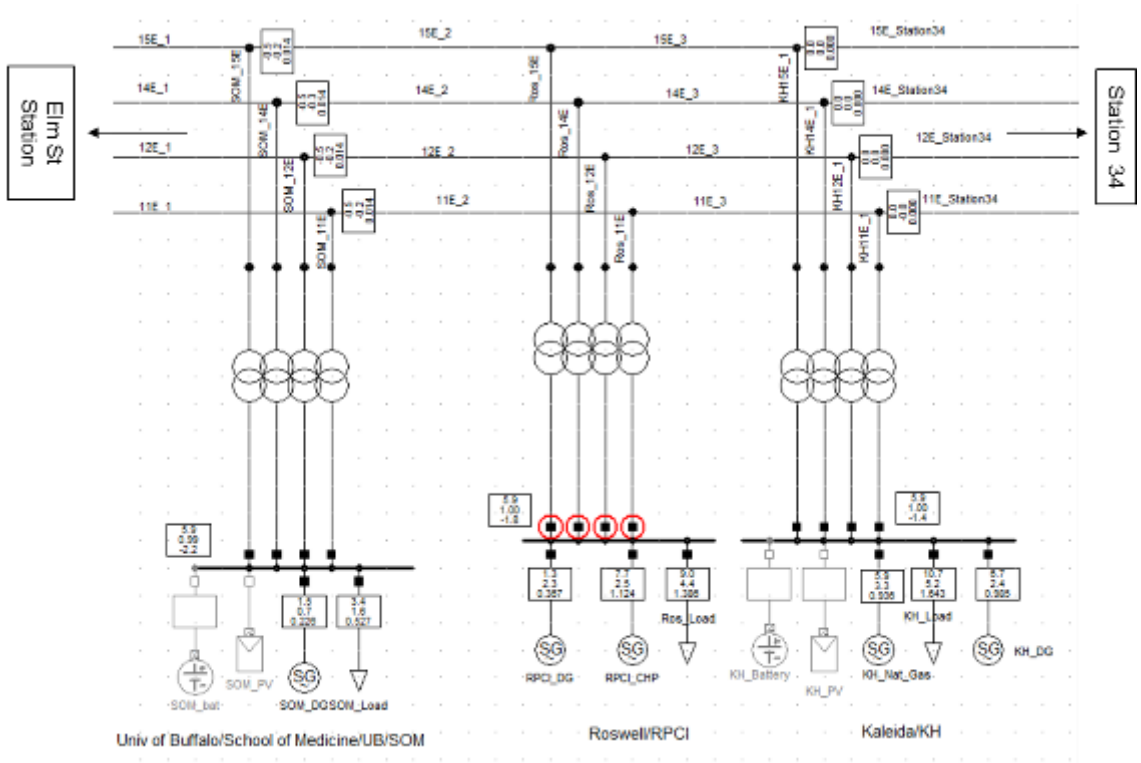

Figure 6-33
Synchronization Case 2: Circuit conditions after synchronization on reaching steady state

From the synchronization cases analyzed, it may be concluded that necessary conditions for smooth synchronization with minimal transients are:

- The two islands which are to be synchronized at the POI must have the same frequency, voltage, and phase angle. It is assumed that there are controllers in each Layer 1 and Layer 2 groups to ensure the above before synchronization is performed.

Islanding

Islanding in a microgrid refers to disconnecting a section of the microgrid. When islanding occurs, a portion of the system separates from the main system. When the islanding is planned, the disconnected section of the microgrid should function independently so that minimal disturbance or interruption affects the loads in the system. Planned islanding occurs for the most part in response to power quality issues which may be within the system or external to the system. This study focuses on demonstrating the ability of the microgrid to form an intentional island as well as to identify the necessary conditions for smooth transitions with minimal disturbance. Table 6-4
presents the different islanding scenarios analyzed.

Table 6-4
Islanding analysis scenarios

Case Number	Scenario
Case 1	Islanding grid-connected Group 1 (connected to Elm Street Station) microgrid Initial condition: Group 1 microgrid is grid-tied with no power flow from Elm Street. Group 1 microgrid changing from grid-connected mode to islanded mode
Case 2	Islanding of Layer 1 (RPCI) from Group 1 microgrid in islanded mode (not connected to Elm Street Station) Initial condition: Group 1 microgrid is in islanded mode. RPCI is then disconnected from the island.

Case 1: Islanding Grid-Connected Layer 2 - Group 1 Microgrid

This case presents the Layer 2 – Group 1 microgrid shown in Figure 4-1 changing from grid-connected mode to islanded mode. The objective is to demonstrate successful islanding of the grid-connected Layer 2 - Group 1 microgrid which is connected to the Elm Street Station. Referring to the circuit description presented in Chapter 4, Layer 2 – Group 1 consists of the State University of New York at Buffalo and the School of Medicine (UB/SOM), Kaleida Health (KH) and Roswell Park Cancer Institute (RPCI). The microgrid connects to the Elm Street Station through 4 feeders (11E, 12E, 14E, and 15E) at the POI as shown in Figure 6-34**.**

Circuit Conditions

The microgrid initially operates in grid-connected mode with the total generation in Group 1 buildings matching the total load in the Group 1 microgrid. Hence, no power is drawn from Elm Street Station before islanding through the POI and no current flows through the breaker connecting Elm Street Station and the four feeders at the POI. The load present in each building of the Layer 2 – Group 1 microgrid corresponds to the load value at the time between 12 pm and 1 pm in islanded mode of operation of the Layer 2 – Group 1 microgrid (analyzed in Chapter 2 while studying load-flow analysis). Only synchronous machines were used for generation. PV and ES were not used as they are relatively very small in size and are also expected to function in a similar manner as the other machines. Hence, they do not impact the islanding process much and are not used. The circuit condition before islanding is presented in Figure 6-34**.**

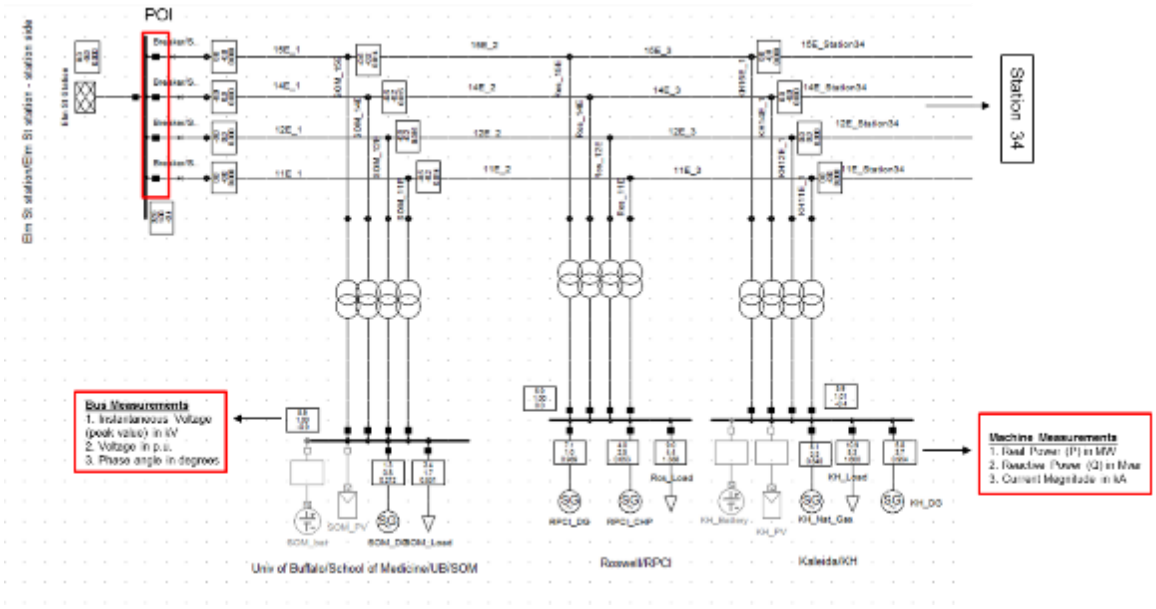

Figure 6-34
Islanding Case 1: Initial circuit conditions

From Figure 6-34**,** it may be observed that all the bus voltages are close to 1 pu because the generation in each building nearly matches the load in their respective buildings, and there is not a very large transfer of power between buildings (UB/SOM imports 2.1 MW and 0.9 Mvar, RPCI exports 2.1 MW and imports 0.9 Mvar and KH exports only reactive power of 1.7Mvar). The frequency of the system was also observed to be 1 pu which shows the system is stable in its present state before islanding.

Breaker Timing

For islanding, the breakers present at the POI need to be opened to island Layer 2 - Group 1 microgrid from Elm Street Station. There are 4 three-phase breakers, each connecting Elm Street Station and one of the 4 feeders (11E, 12E, 14E, and 15E). The opening of each phase of the circuit breaker occurs at the next available zero crossing of current after the specified time in the breaker operation command. The three-phase circuit breakers present in 11E, 12E, 14E, and 15E operate one after the other in a similar manner as explained above. Table 6-5 shows the specified time for each breaker operation command.

Table 6-5
Islanding Case 1: Breaker opening operation timings

Breaker Opening Operation	Time (seconds)
11E Breaker	0.04
12E Breaker	0.10
14E Breaker	0.16
15E Breaker	0.22

Event Analysis:

The 11E breaker is timed to open at 0.04 seconds but the breakers in each phase open only at the next zero crossing of current. This can be observed in Figure 6-35 and Figure 6-36. Of the 3 phases, phase C waveform reaches zero crossing first after time = 0.04 s. Hence, the breaker corresponding to phase C opens first. Then current waveforms in phases A and B reach zero and their breakers open accordingly. The scale on the X axis of the current plots are of the order of 0.0002 kA. Hence, the current flowing through the breaker at the POI before islanding is negligible and almost 0 kA.

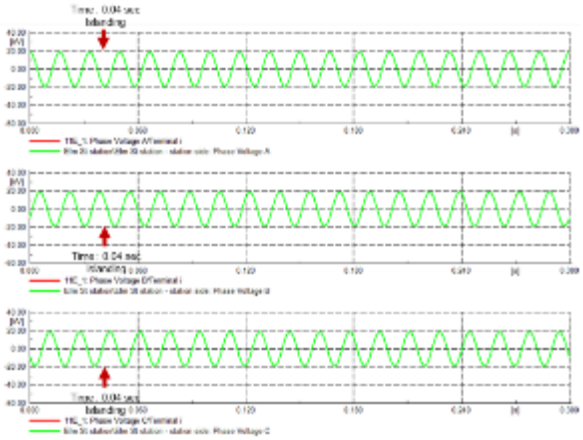

Figure 6-35
Islanding Case 1: Instantaneous voltages in kV during islanding at 11E breaker

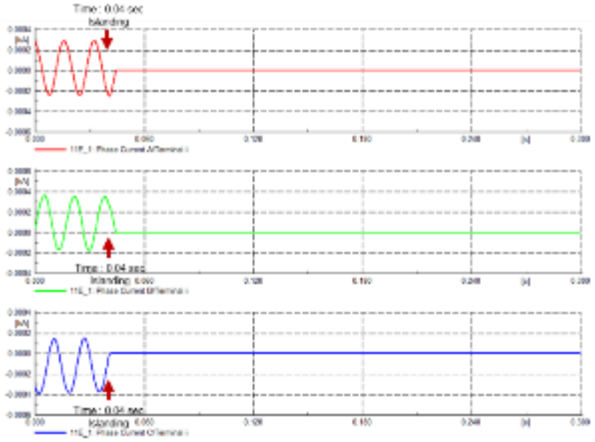

Figure 6-36
Islanding Case 1: Instantaneous current in kA during islanding at 11E breaker

Similar voltage and current waveforms can be observed at 12E, 14E, and 15E breakers at the time of islanding. This can be observed in Figure 6-37 through Figure 6-42. In all these waveforms, it may be observed that the breakers opened only at the immediate next zero crossing of the current waveform past the specified operating time of the breaker.

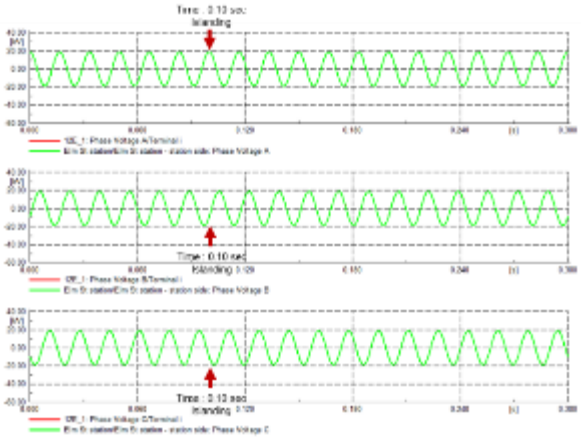

Figure 6-37
Islanding Case 1: Instantaneous voltages in kV

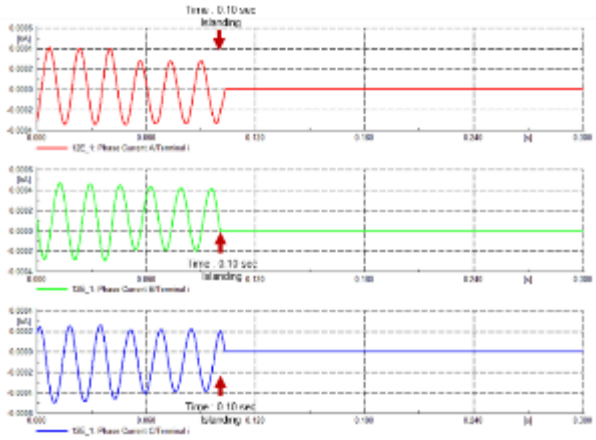

Figure 6-38
Islanding Case 1: Instantaneous current in kA

during islanding at 12E breaker

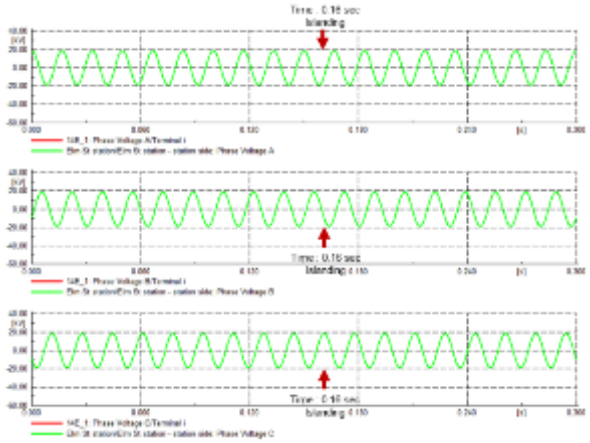

Figure 6-39
Islanding Case 1: Instantaneous voltages in kV during islanding at 14E breaker

during islanding at 12E breaker

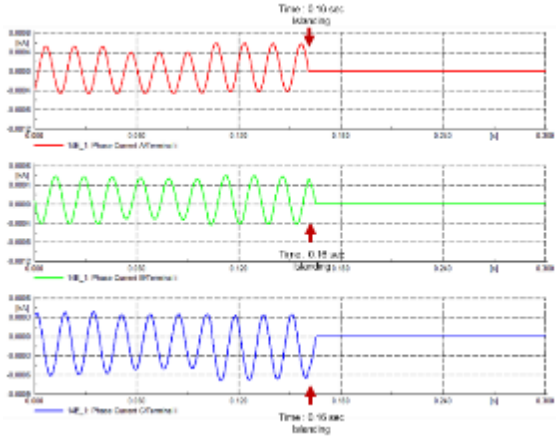

Figure 6-40
Islanding Case 1: Instantaneous current in kA during islanding at 14E breaker

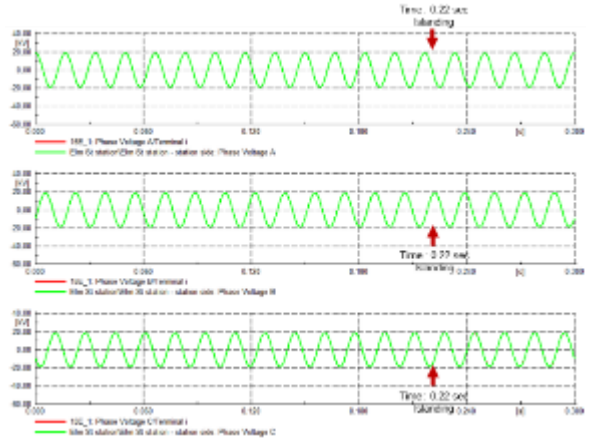

Figure 6-41
Islanding Case 1: Instantaneous voltages in kV during islanding at 15E breaker

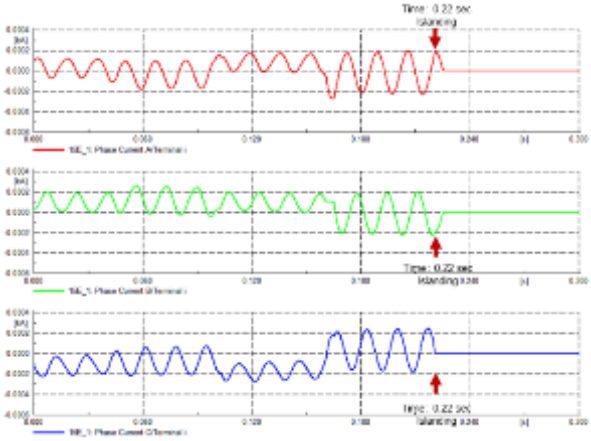

Figure 6-42
Islanding Case 1: Instantaneous current in kA during islanding at 15E breaker

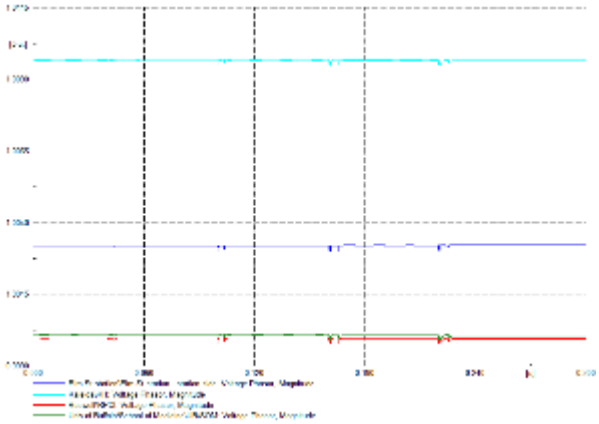

Figure 6-43
Islanding Case 1: Voltages in pu during islanding at different buses

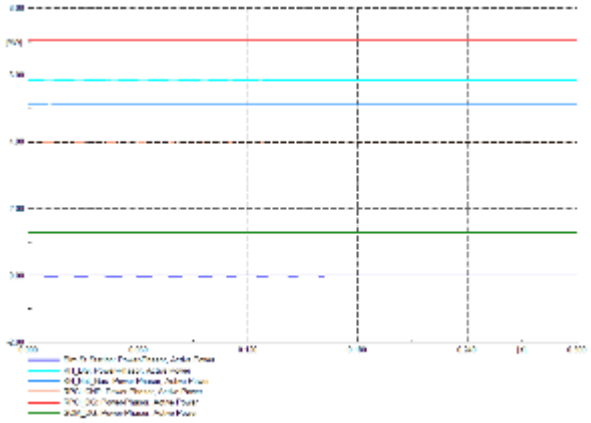

Figure 6-44
Islanding Case 1: Active power supplied by various machines in MW during islanding

The variation in the voltage (shown in Figure 6-43) is negligible when the islanding process occurs. In Figure 6-45, Phase A currents of all the machines and at POI are shown. As the system is balanced, similar waveforms are expected for Phase B and Phase C. From Figure 6-45 and Figure 6-46Figure 6-46, it may be observed that the variation of current during islanding was minimal due to the reason explained below. The change in frequency (shown in Figure 6-47) is less than 0.0005 pu which is negligible. This is because the Layer 2 – Group 1 microgrid did not transfer any power from Elm Street Station before islanding. Hence, the total generation in the Group 1 microgrid was sufficient to meet the load demand and no external power was drawn from Elm Street Station. When the Group 1 microgrid islanded, no change in loading and generation condition resulted. Hence, the voltage at all the buses, current flowing through different elements, and frequency of the system remains the same with negligible transients during the islanding process.

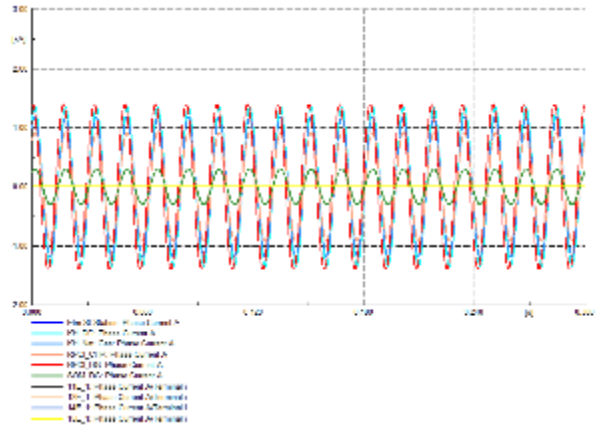

Figure 6-45
Islanding Case 1: Instantaneous Phase A current in kA during islanding

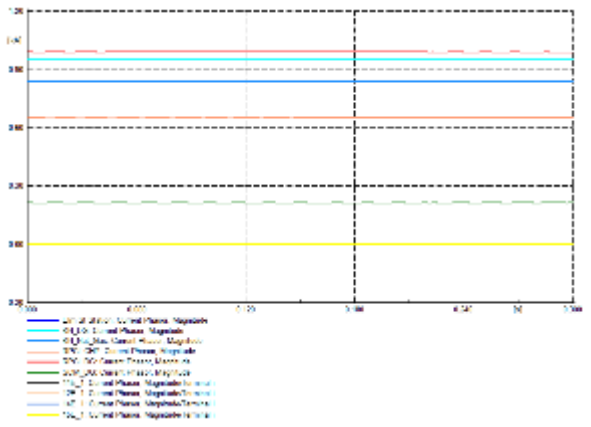

Figure 6-46
Islanding Case 1: RMS current in kA during islanding

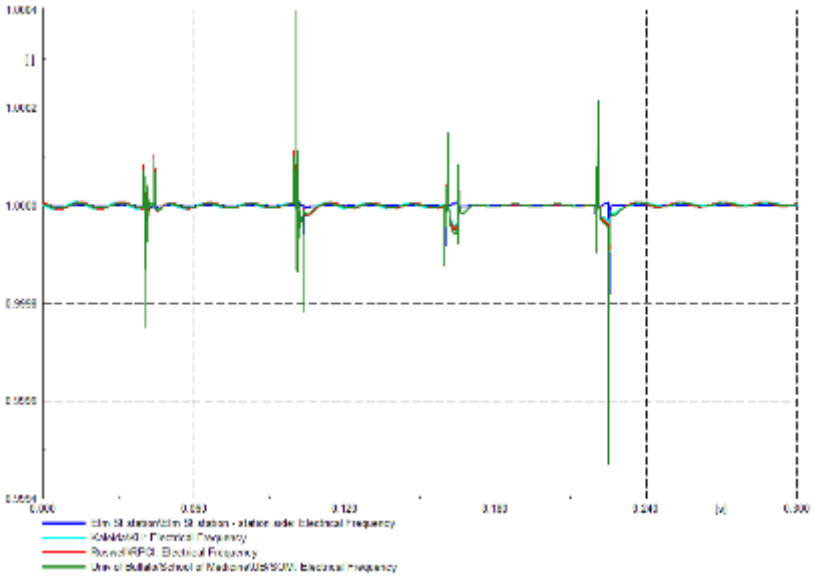

Figure 6-47
Islanding Case 1: Frequency in pu during islanding

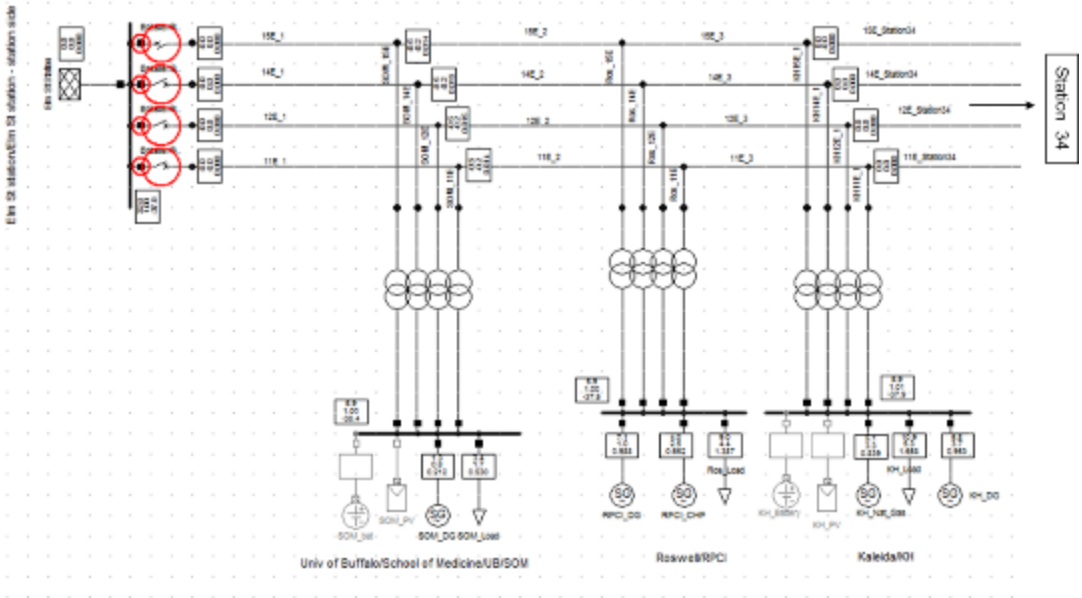

Figure 6-48
Islanding Case 1: Circuit conditions after islanding

Figure 6-48 illustrates the state of the circuit immediately after the four circuit breakers at the POI have been opened. It may be seen in Figure 6-48 that the circuit breakers at the POI have been opened but the system conditions are similar to that of Figure 6-34. The loads at UB/SOM, RPCI and KH are 3.4 MW, 9 MW, and 10.9 MW, respectively. The total load is 23.3 MW. The

generations of SOM_DG, RPCI_DG, RPCI_CHP, KH_DG and KH_Nat_Gas are 1.3 MW, 7.1 MW, 4.0 MW, 5.8 MW, and 5.1 MW, respectively. The total generation is 23.3 MW. So, the total generation is adequate to meet the load before and after islanding. This can ensure that before islanding, the system operating conditions can be adjusted such that no power flows through the breakers at the POI.

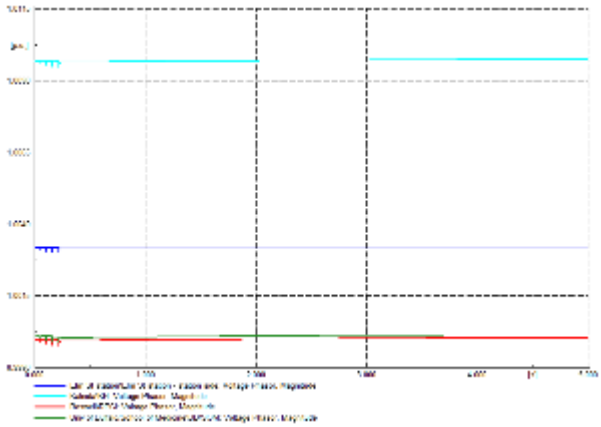

Figure 6-49
Islanding Case 1: RMS Voltage in pu during islanding (until steady state)

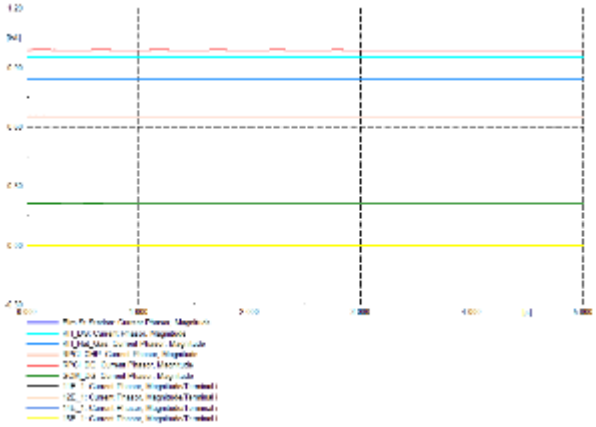

Figure 6-50
Islanding Case 1: RMS current in kA during islanding (until steady state)

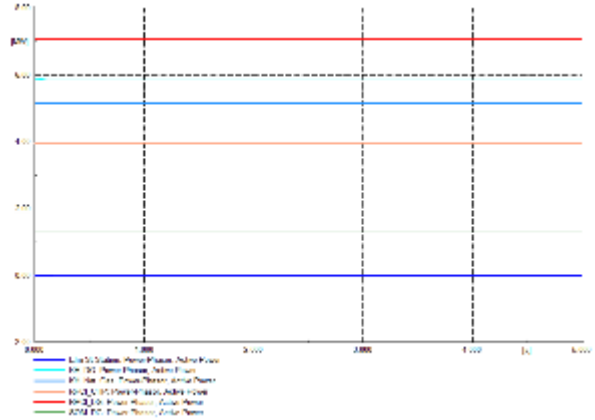

Figure 6-51
Islanding Case 1: Active Power in MW during islanding (until steady state)

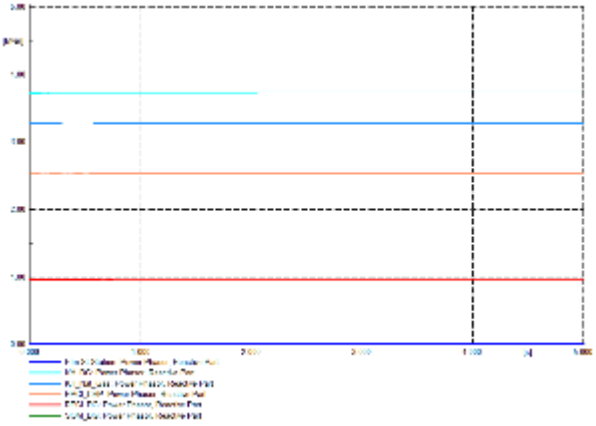

Figure 6-52
Islanding Case 1: Reactive Power in Mvar during islanding (until steady state)

Figure 6-49 through Figure 6-52 show the RMS voltage, current, active and reactive power during the islanding process until steady state is achieved. As discussed earlier in this section, no change in the load or generation condition occurred during the islanding process. Hence, no change occurred in the RMS voltage, current, active, and reactive power plots after islanding. The islanding process was smooth and successful.

From analyzing this case, it may be concluded that the islanding process will be successful and have only minor transients when there is no power flow between the two groups that are to be islanded. This means that there should be no current flow through the breakers at the POI.

Another necessary condition for successful islanding is that each island after the islanding process should have sufficient generation to meet its load demand.

Case 2: Islanding of Layer 1 (RPCI) From Layer 2 - Group 1 Microgrid in Islanded Mode

This case concerns the islanding of a Layer 1 building from Group 1 microgrid itself operating in islanded mode. The objective is to demonstrate successful islanding of a Layer 1 (RPCI) building from islanded Layer 2 - Group 1 microgrid when there is power flow through the POI before islanding. Hence, this case demonstrates unplanned islanding unlike Islanding Case 1 which is planned islanding. The POI in this case is the 4 three-phase breakers present at the low voltage side of the distribution transformers connecting the feeders (11E, 12E, 14E, and 15E) and the RPCI building as shown in Figure 6-53**.**

Circuit Conditions

The Layer 2 – Group 1 microgrid is initially in islanded mode of operation. The total generation in Layer 2 – Group 1 microgrid matches the total load in Layer 2 – Group1 microgrid, but there is transfer of power between the three buildings within Layer 2 – Group 1 microgrid. Unlike Islanding Case 1, here, power flows through POI before islanding. Therefore, current also flows through the breakers connecting RPCI and rest of the Layer 2 – Group 1 microgrid. It may be seen from Figure 6-53 that the load at RPCI is 9.0 MW and 4.4 Mvar but the sum of generation of RPCI_DG and RPCI_CHP is 11.1 MW and 3.5 Mvar. So, real power of 2.1 MW is exported by RPCI but reactive power of 0.9 Mvar is imported. If the islanding was planned as with Islanding Case 1, the system generation would have been adjusted such that there would be no power flow through the POI before islanding.

The load present in each building of Layer 2 – Group 1 microgrid correspond to the load value at the time between 12 pm and 1 pm in islanded mode of operation of Layer 2 – Group 1 microgrid (analyzed in Chapter 4 while studying load flow analysis). Only synchronous machines were used for generation. PV and ES were not used similar to the previous case. The circuit condition before islanding is illustrated in Figure 6-53**.**

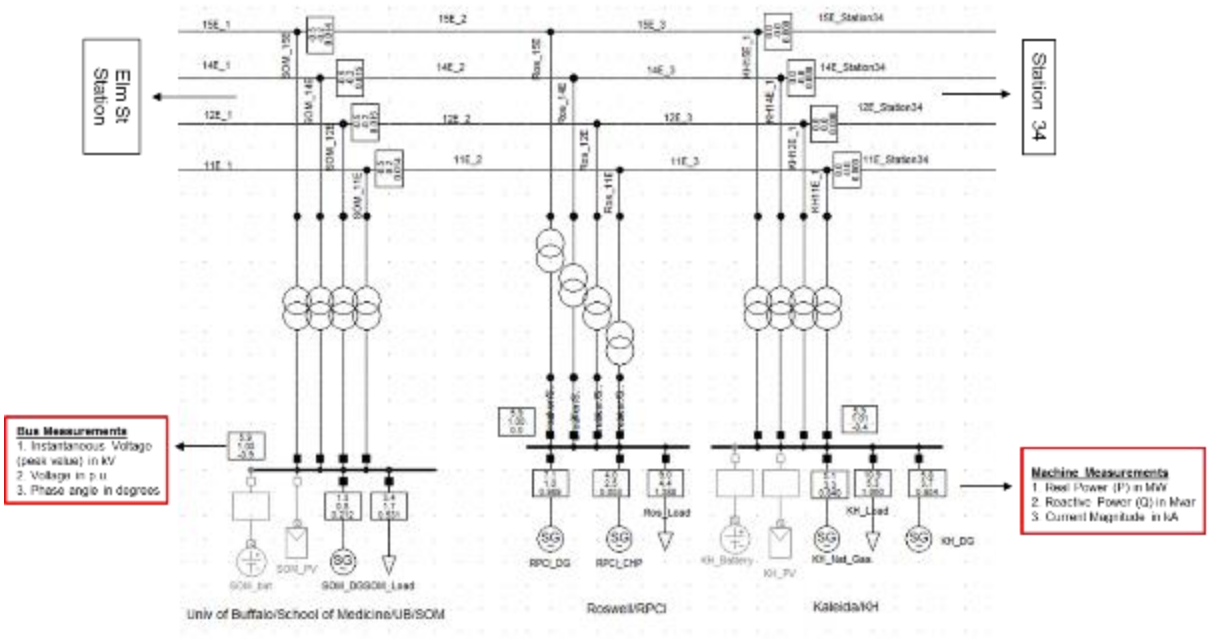

Figure 6-53
Islanding Case 2: Initial circuit condition

From Figure 6-53, it may be observed that all the bus voltages are close to 1 pu. The frequency of the system was also observed to be 1 pu which shows the system is stable in its present state before islanding.

Breaker timing

For separating RPCI from the rest of the Group 1 microgrid, the 4 three-phase breakers present between the secondary of distribution transformers (connecting the feeders and RPCI) are to be opened. Similar to Islanding Case 1, the opening of each phase of circuit breaker occurs at the next available zero crossing of current after the specified time in the breaker operation command. Each of the 4 three-phase circuit breakers present at the end of transformers operate one after the other in a similar manner as explained above. Table 6-6 shows the specified time for each breaker operation command.

Table 6-6
Islanding Case 2: Breaker opening operation timings

Breaker Closing Operation	Time (seconds)
Ros_11E_T Breaker	0.04
Ros_12E_T Breaker	0.10
Ros_14E_T Breaker	0.16
Ros_15E_T Breaker	0.22

Event Analysis

The Ros_11E_T breaker is timed to open at 0.04 seconds but the breakers in each phase opens at the next immediate zero crossing of current. This can be observed in Figure 6-54 and Figure 6-55. Among phase A, phase B, and phase C, phase B reaches zero crossing first past time = 0.04 s. Hence, the breaker corresponding to phase B opens first. Then currents in phase A and C reach zero and their breakers open accordingly.

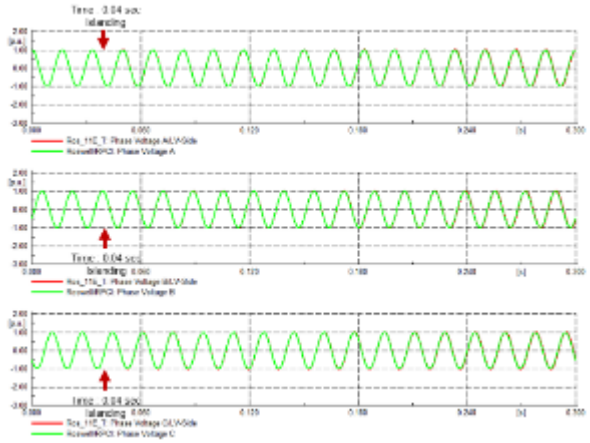

Figure 6-54
Islanding Case 2: Instantaneous voltages in kV during islanding at Ros_11E_T breaker

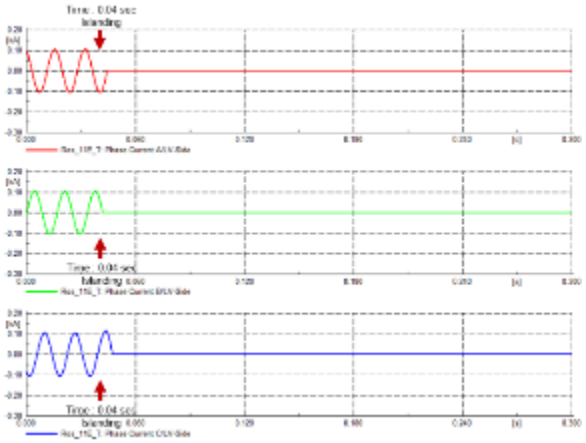

Figure 6-55
Islanding Case 2: Instantaneous current in kA during islanding at Ros_11E_T breaker

As seen in Islanding Case 1, similar waveforms were observed in in other breakers as well. The instantaneous voltages and current waveforms measured at Ros_12E_T, Ros_14E_T and Ros_15E_T breakers are similar to waveforms obtained at Ros_11E_T breaker except that the time of operation of each breaker differs.

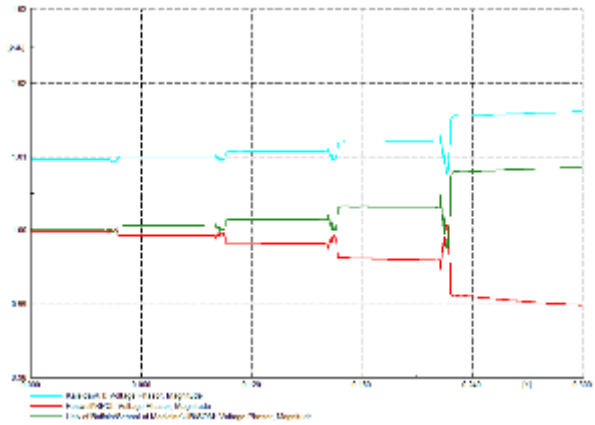

Figure 6-56
Islanding Case 2: Voltages in pu during islanding at different buses

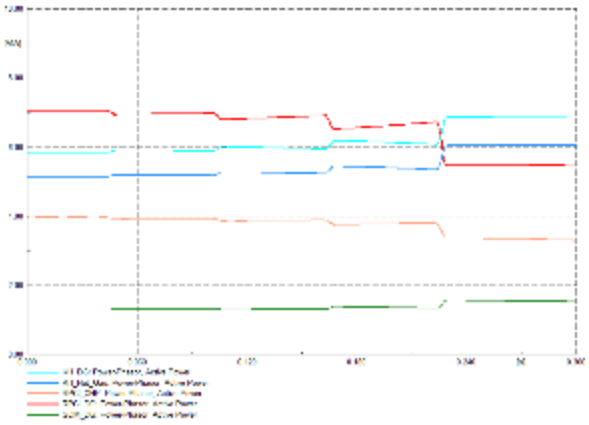

Figure 6-57
Islanding Case 2: Active power supplied by various machines in MW during islanding

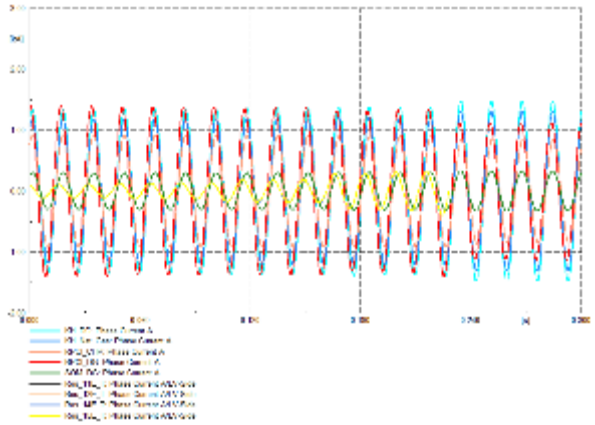

Figure 6-58
Islanding Case 2: Instantaneous Phase A current in kA during islanding

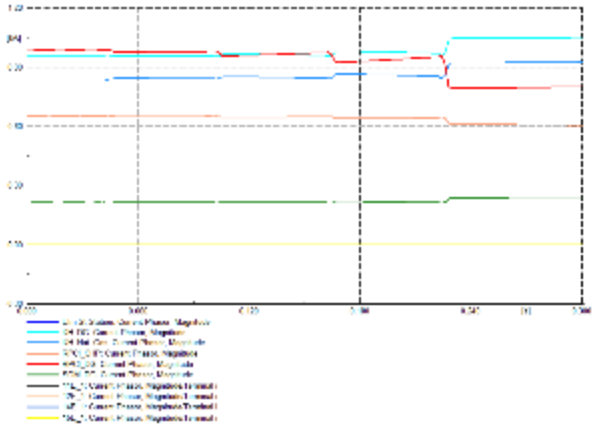

Figure 6-59
Islanding Case 2: RMS current in kA during islanding

As described in the circuit conditions section, RPCI was exporting real power and importing reactive power. During the islanding process, the capability of RPCI to transfer power keeps reducing when each breaker is removed one by one. This is visible in the above waveforms (Figure 6-56 through Figure 6-59). Figure 6-56 illustrates the voltages at UB/SOM, RPCI and KH buildings and Figure 6-57 illustrates the active power generated by various machines. Figure 6-58 and Figure 6-59 illustrate the current waveforms during islanding. When RPCI disconnects from the rest of Layer 2 – Group 1 microgrid, both the islands must adjust their generation to match their load as well as try to maintain near 1 pu voltage and 1 pu frequency. RPCI must reduce its real power generation and increase its reactive power generation according to its load. Similarly, the generators at KH must provide the extra power required by UB/SOM to meet its load. The effect of the imbalance in the generation after islanding can be seen in the frequency waveform as well as shown in Figure 6-60. Immediately after islanding, RPCI has excess active power generation and hence its frequency is slightly higher than 1 pu. The island consisting of KH and UB/SOM have lesser active power generation than their load, hence their frequency is slightly lesser than 1 pu. Once, the generations are adjusted when the system reaches steady state, the frequency of both the islands become 1 pu. Similarly, immediately after the islanding process, RPCI has a deficit of reactive power. Hence, its voltage is slightly less than 1 pu until its generation adjusts to meet the load. The other two buildings have excess reactive power production and as a result, their voltages are higher than 1 pu immediately after islanding.

From Figure 6-56 and Figure 6-57, it may be clearly seen that KH has higher voltage compared to other buses. Also, KH_DG and KH_Nat_Gas are generating more power than they were before islanding whereas RPCI has reduced its generation. The current waveforms also vary according to the generation variation.

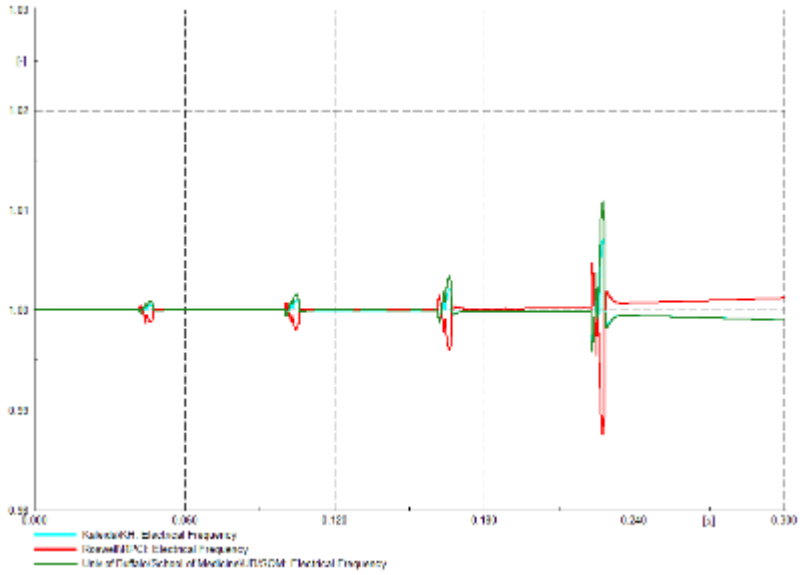

Figure 6-60
Islanding Case 2: Frequency in pu during islanding

From the waveforms presented for this case, it can be seen that there are significant transients present when compared to the previous case. In the previous case, the load on the island which was being formed (23.3 MW, 11.4 Mvar) was balanced by the generation on that island (23.3 MW, 11.4 Mvar). In this case, such a balance was not present during islanding. The generation in RPCI (11.1 MW, 3.5 Mvar) did not match the load at RPCI (9.0 MW, 4.4 Mvar). The mismatch in generation at RPCI after islanding was 2.1 MW and -0.9 Mvar. As a result, in the previous case, there was no generation change after the islanding process and there were negligible transients. Whereas in this case, there was a necessary change in generation and there were more transients.

Another aspect to be noted is that RPCI has the capacity to feed its load entirely without any external support. This is not possible for buildings like UB/SOM because the total generation available at UB/SOM is less than its rated load. If UB/SOM was islanded in a similar manner, the generation cannot keep up with its load and the bus will collapse. In such cases, load shedding is required so that the load can match the generation. Therefore, before islanding, it is essential to verify that each individual island has the capacity to feed its load.

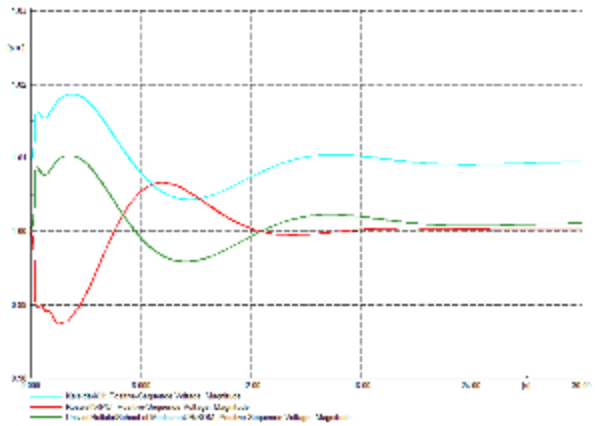

Figure 6-61
Islanding Case 2: RMS Voltage in pu during islanding (until steady state)

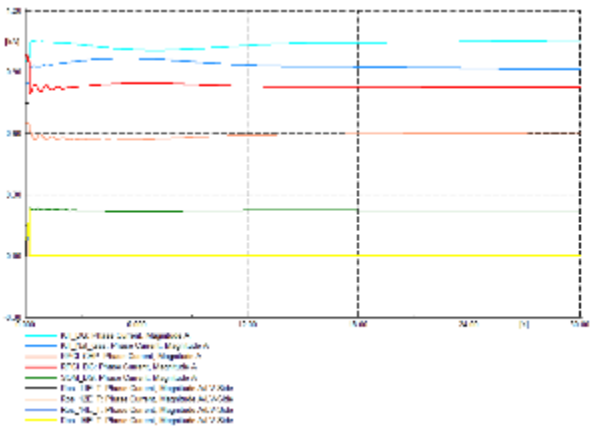

Figure 6-62
Islanding Case 2: RMS current in kA during islanding (until steady state)

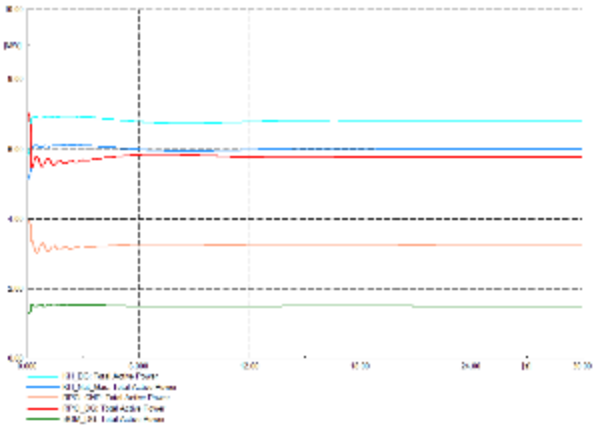

Figure 6-63
Islanding Case 2: Active Power in MW during islanding (until steady state)

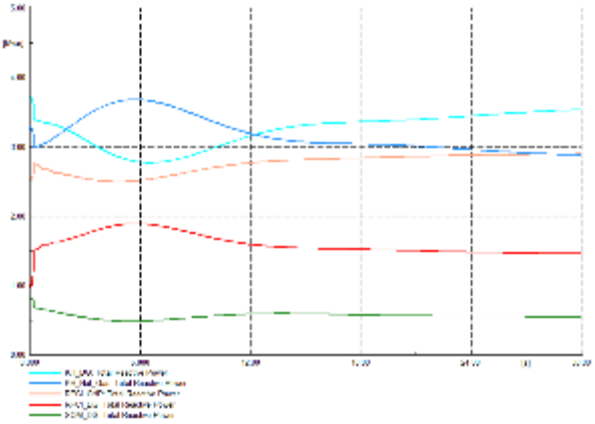

Figure 6-64
Islanding Case 2: Reactive Power in Mvar during islanding (until steady state)

The controllers of each island must try to keep the voltage as close to 1 pu. This can be observed in Figure 6-61 through Figure 6-64 where the system has reached steady state. KH has the highest voltage because it supplies reactive power to UB/SOM. RPCI has a voltage of nearly 1 pu because its total load is met by its own generation. This can be seen in Table 6-7 and Figure 6-65 where the system conditions upon attaining steady state are presented.

Table 6-7
Islanding Case 2
Total load and generation comparison before and after islanding

Equipment	Before Islanding (MW, Mvar)	After Islanding (Steady State) (MW, Mvar)
SOM DG	1.3,0.8	1.5,0.5
KH DG	5.8,3.7	6.8,3.5
KH Nat Gas	5.1,3.3	6.0,2.9
RPCI DG	7.1,1.0	5.8,1.5
RPCI CHP	4.0,2.5	3.2,2.9
Total Generation	23.3,11.3	23.3,11.3
SOM Load	3.4,1.7	3.4,1.7
ROS Load	9.0,4.4	9.0,4.4
KH Load	10.9,5.3	10.9,5.3
Total Load	23.3,11.4	23.3,11.4

The load in the system in this case is similar to that of the previous case. The loads before islanding at UB/SOM, RPCI and KH were 3.4 MW, 9 MW and 10.9 MW respectively. The total load was 23.3 MW. The generations of SOM_DG, RPCI_DG, RPCI_CHP, KH_DG, and KH_Nat_Gas before islanding were 1.3 MW, 7.1 MW, 4.0 MW, 5.8 MW and 5.1 MW. The total generation was 23.3 MW. After islanding and on reaching steady state, the load at RPCI was 9.0 MW and 4.4 Mvar and the generations of RPCI_DG and RPCI_CHP were 5.8 MW, 1.5 Mvar and 3.2 MW and 2.9 Mvar respectively which sums up to 9.0MW and 4.4 Mvar. Hence, on islanding, RPCI generation provides its load individually. Similarly, the total load in the remaining Layer 2 – Group 1 microgrid is 14.3 MW and 7 Mvar and is matched by generation at UB/SOM and KH.

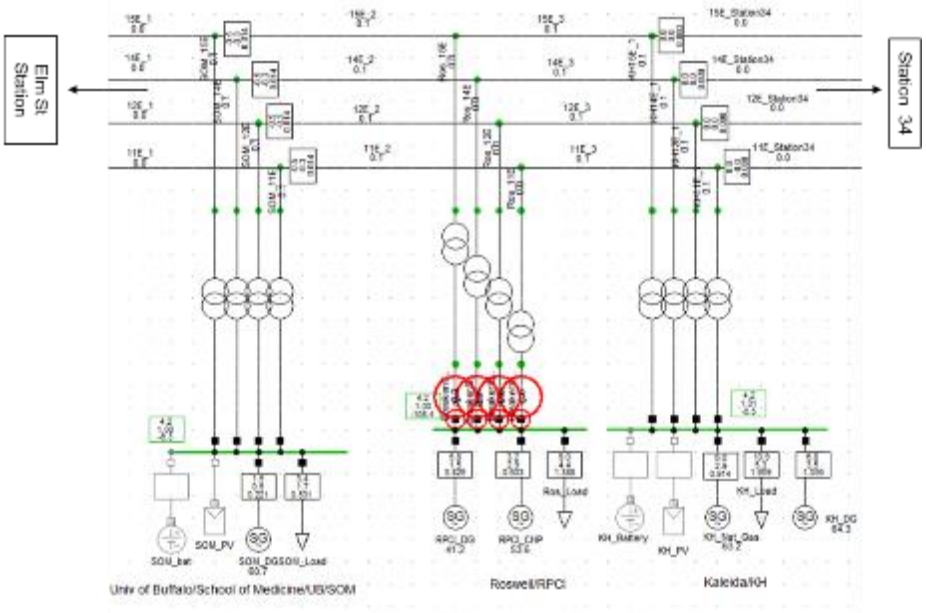

Figure 6-65
Islanding Case 2: Circuit conditions after islanding on reaching steady state

It may be seen that islanding in this case was successful even though power flowed through the breakers at the POI before islanding; however, the transients are larger (compared to Case 1 where there was no power flow at the POI) when there was flow of power at the POI. Each individual island also had the capacity to provide its own load. Hence, after islanding, the machines adjust their generation according to the load because of the generator controllers present in the system. Another point for consideration is that Islanding Case 1 was a planned islanding scenario which was why there was no power flow at the POI before islanding, whereas Islanding Case 2 was unplanned islanding. This is why the islanding process in Islanding Case 1 was smooth and the transients were minimal. There was a transfer of 2.1 MW and 0.9 Mvar through the breakers at POI in Islanding Case 2. If the transfer of power through the POI was much higher, the spikes in voltage and frequency would be much larger than that seen in Figure 6-56 and Figure 6-60. However, the voltage and frequency would eventually settle at a value close to 1 pu at steady state because the generators would adjust the power produced to match the load.

Hence, it can be concluded that necessary conditions for smooth islanding with minimal transients are:

- Each island to be formed should have sufficient generation to meet its load demand.
- The total generation in each individual island to be formed should match the total load in that island before islanding. This will ensure that there is no power/current flow through the breakers at the point of interconnection.

Black Start

Black start is the ability to energize a microgrid from a de-energized state without the help from an external source. The objective of this analysis is to demonstrate energizing a de-energized busbar and then loading it. For this analysis, the Layer 1 University of Buffalo/School of Medicine (UB/SOM) is considered.

Figure 6-66
Black Start: Circuit condition

The 4.16 kV UB/SOM busbar is initially de-energized. There is no machine nor load connected to it. At this stage, SOM_DG has not yet been connected to the busbar. This Layer 1 group is an individual island. The machine parameters are same as those of the previous cases. SOM_DG has governor control (Woodward Diesel Governor) and Automatic Voltage Regulator (AVR) (1968 IEEE Type 1 Excitation System). This helps in regulating the voltage by varying the generation of SOM_DG. Before connecting SOM_DG to the busbar, it is brought to a spinning state using a small external power source such as a diesel generator to excite its field windings.

Black start event analysis consists of connecting the 2.5 MW SOM_DG to the 4.16 kV SOM busbar at 0.05 seconds and subsequently connecting a 1 MW load at 0.2 seconds.

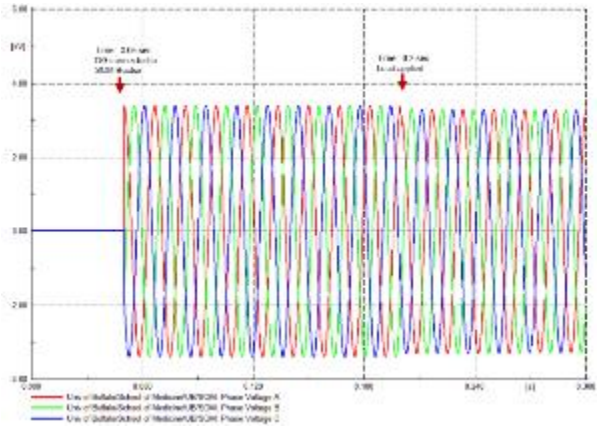

Figure 6-67
Black start: Instantaneous bus voltages in kV

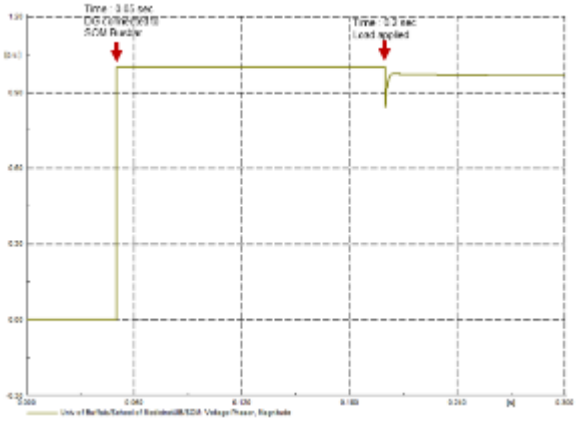

Figure 6-68
Black start: RMS voltage in pu

When the 2.5 MW SOM_DG is connected to the SOM busbar at 0.05 sec, it is immediately energized. The voltage and frequency are 1 pu. There is no active power generated by SOM_DG as there is no load connected to the busbar at this stage yet. At 0.2 sec, a load of 1 MW is added. This results in a small dip in frequency and voltage. The generator which was initially generating 0 MW (spinning) then adjusts its generation to match the load. The voltage and frequency are restored to 1 pu when the system reaches its steady state.

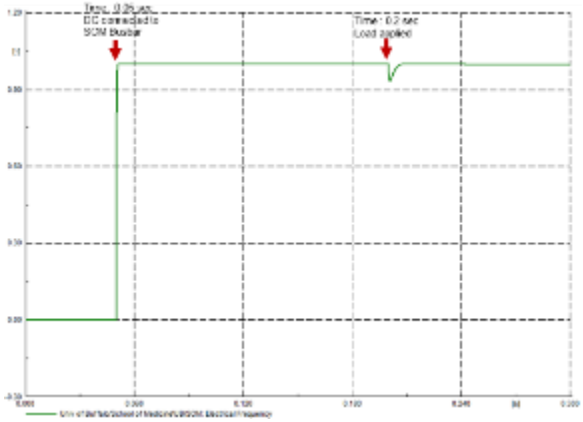

Figure 6-69
Black start: Frequency in pu

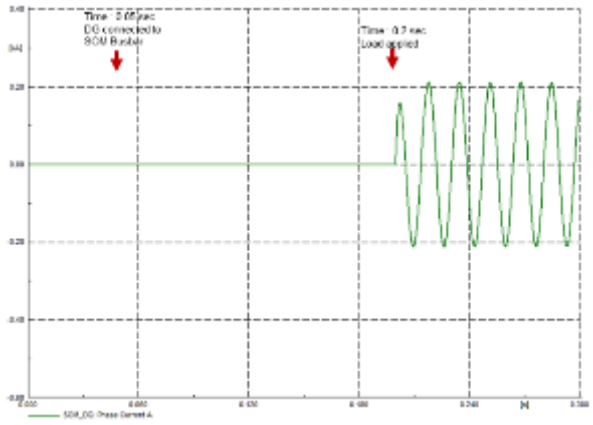

Figure 6-70
Black Start: Instantaneous Phase A current in kA

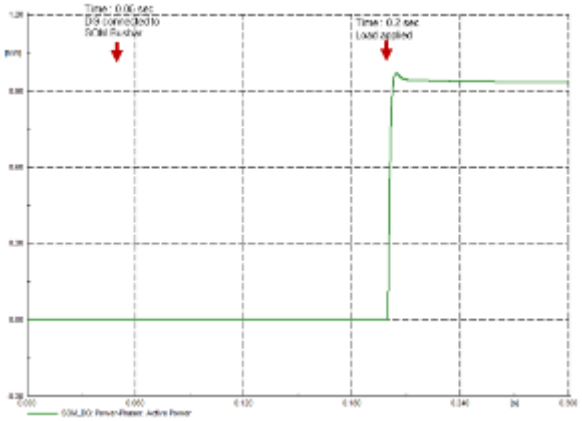

Figure 6-71
Black Start: Active power in MW

Figure 6-70 and Figure 6-71 show the instantaneous current in phase A of the generator and the active power generated by it, respectively. As the system is balanced, similar current waveforms may be expected for phase B and phase C, respectively. Even though the DG is connected to the busbar at 0.05 sec, there is no load connected at that time. Hence, current and active power are 0 MW. At 0.2 sec, the load of 1 MW is connected and the required power is supplied by SOM_SG as can be seen from the plots. Sharp momentary voltage and frequency drop at 0.2 seconds may be observed in Figure 6-68 and Figure 6-69, respectively. The system is not very strong and the addition of large loads (1 MW of load whereas the total load capacity of DG is 2.5 MW) causes

the momentary sharp drop in voltage and frequency. This may be reduced by gradually ramping the load.

Hence, it may be concluded that black start can be performed successfully. The requirements are that the main generator has to be brought to spinning state (normal operation at no load) using an external source of power such as small diesel generator before connecting the generator to the de-energized bus. The load applied to the newly-energized bus must be less than the generating capacity of the generator for the system to remain stable.

Motor Starting

Motor starting analysis evaluates the capability of a microgrid to handle the starting requirements of a motor. Some of the important aspects of motor starting include the high inrush current and low bus voltage during the starting process. The objective is to study the starting characteristics of motors of different sizes in a small and weak microgrid.

For this analysis, the Layer 1 UB/SOM group is chosen as it has the least generating capacity among the different buildings in the Layer 2 – Group 1 microgrid. This means that all the other buildings, or when the individual buildings are connected together to form a microgrid, the microgrid will be able to start motors of much larger capacity than the maximum size of motor which can be started in this case. The Layer 1 – UB/SOM microgrid is taken as an individual island separated from the rest of the microgrid and only SOM_DG is available for generation. Full-voltage motor starting technique is used to start the motor.

Table 6-8 presents the motor parameters used for this motor starting analysis. Motors of different sizes (kW) were obtained by changing the power rating definition of the motor but the other parameters were kept unchanged.

Table 6-8
Motor starting: Motor parameters

Sl. No	Parameter	Value
1	Rated Power Factor	0.942
2	Efficiency at normal operation (%)	97.02
3	No. of pole pairs	1
4	Nominal Speed (rpm)	3580.372
5	Moment of Inertia (kgm^2)	15
6	Locked Rotor Current (pu)	7.595
7	Stator Reactance Xs (pu)	0.05
8	Stator Resistance Rs (pu)	0.023
9	Rotor Resistance Rr (pu)	0.0054
10	Rotor Reactance Xr (pu)	0.08
11	Mag. Reactance Xm (pu)	4.388

Locked Rotor Motor Calculations

This section provides the validation of the expected locked rotor current during motor starting. Locked rotor current is the current drawn by a motor when the rotor is locked or not rotating.

$$Locked\ Rotor\ Current\ Setting\ of\ the\ motor = 7.6\ \text{pu}$$

The locked rotor current depends on the machine parameters, namely, the stator and rotor impedance. Hence, using these parameters, the locked rotor current may be estimated and the locked rotor current setting of the motor can be validated. Locked rotor current calculations assume that the voltage source (V_s) available for starting the motor is 1 pu.

$X_s + X_r = 0.05 + 0.08\,pu \sim 0.13\,pu$

$Starting\ Current \sim \frac{V_s}{X_s + X_r} \sim \frac{1}{0.13}\,pu \sim 7.69\,pu$ (This value is slightly higher than 7.6 because resistance was ignored while calculating the starting current)

Hence, the calculated locked rotor current is close to the locked rotor current setting of the motor.

Analysis

During motor starting, high inrush current is required to accelerate the motor to its rated speed from standstill. The generator (SOM_DG in his case) has to provide this high inrush current and this current causes the voltage drop at the terminals of the generator due to internal reactance of the generator. Hence, the voltage at the bus drops during this period. Starting characteristics of several motor sizes were studied. Figure 6-72 through Figure 6-74 provide the starting characteristics of 1000 kW motor.

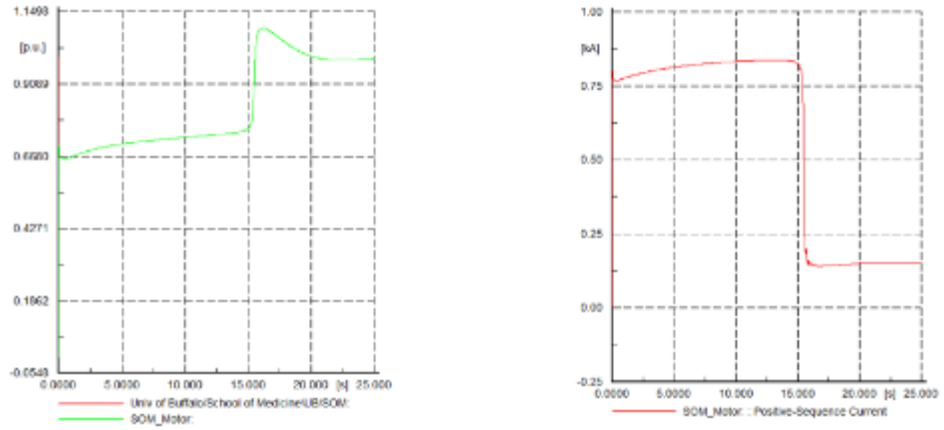

Figure 6-72
Motor starting: RMS voltage in pu (left) and RMS current in kA (right)

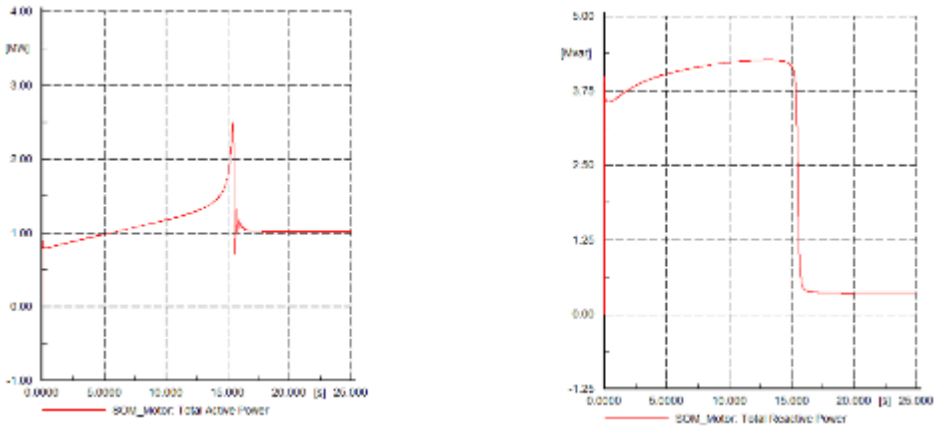

Figure 6-73
Motor starting: Total active in MW (left) and reactive power in Mvar (right)

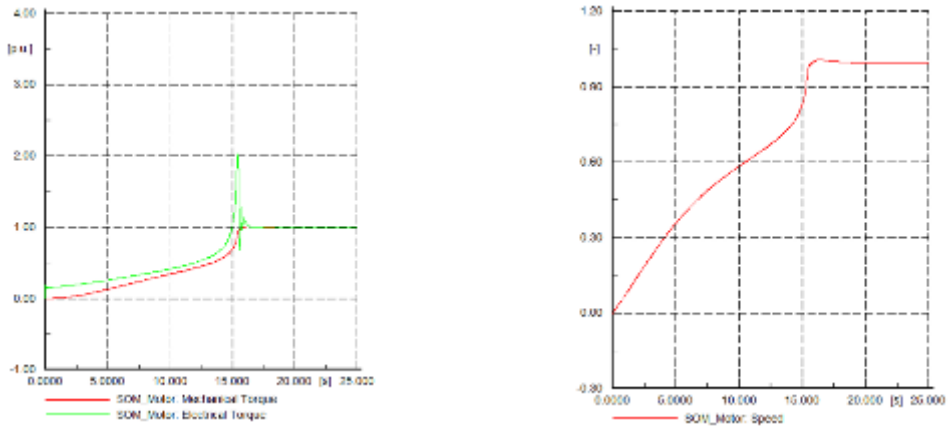

Figure 6-74
Motor starting: Mechanical and electrical torque in pu (left) and motor speed in pu (right)

Motor Starting Validation

The case analyzed below is a motor whose rated mechanical power was 1000 kW. The MVA rating of the motor was 1.093 MVA and the rated power factor of operation was 0.942 lagging. The rated mechanical power will be less than the active power consumed by the motor because of power losses such as copper losses (I^2R losses) in the machine.

$$Short\ circuit\ capacity\ at\ motor\ terminals\ (MVA_{3\emptyset}^{sc}) = 19.782\ MVA$$

$$Motor\ Locked\ Rotor\ Capacity\ (MVA_{LR}) = \frac{MVA_{motor}}{X_{LR}\ (pu)} = \frac{1.093}{0.13} = 8.40\ MVA$$

$$V_{start}^{fv} = \frac{MVA_{3\emptyset}^{sc}}{MVA_{3\emptyset}^{sc} + MVA_{LR}} * V_{applied} \sim \frac{19.782}{19.782 + 8.40} * 1\ pu \sim 0.70$$

The expected starting voltage is 0.70 pu from calculations. This value is close to the observed value of 0.66 pu. There is a small difference between the values because some parameters which may affect the starting voltage calculations, such as stator and rotor resistance, were not considered in the calculation.

Motor Starting Comparison

Table 6-9 and Figure 6-76 show the variation of starting characteristics with different motor sizes. It may be observed that with an increase in motor rating, the starting current increases and the minimum value for the bus voltage during this period also falls.

Table 6-9
Motor Starting: Motor starting characteristics of various motor sizes

Motor Rating (kW)	Min Voltage during starting (pu)	Voltage after starting (pu)	Starting Current (kA)	Start Status
100	0.953	1.000	0.116	Successful
400	0.834	0.999	0.451	Successful
800	0.710	0.998	0.739	Successful
1000	0.659	0.998	0.837	Successful
1100	0.636	0.998	0.879	Successful
1200	0.615	-	0.915	Not successful

It was observed that a motor up to 1100 kW was able to start successfully but motors larger than 1100 kW failed to start. This is because the electrical torque produced is not sufficient to overcome the mechanical torque required. Hence, there is no acceleration torque and the machine fails to accelerate to its nominal speed.

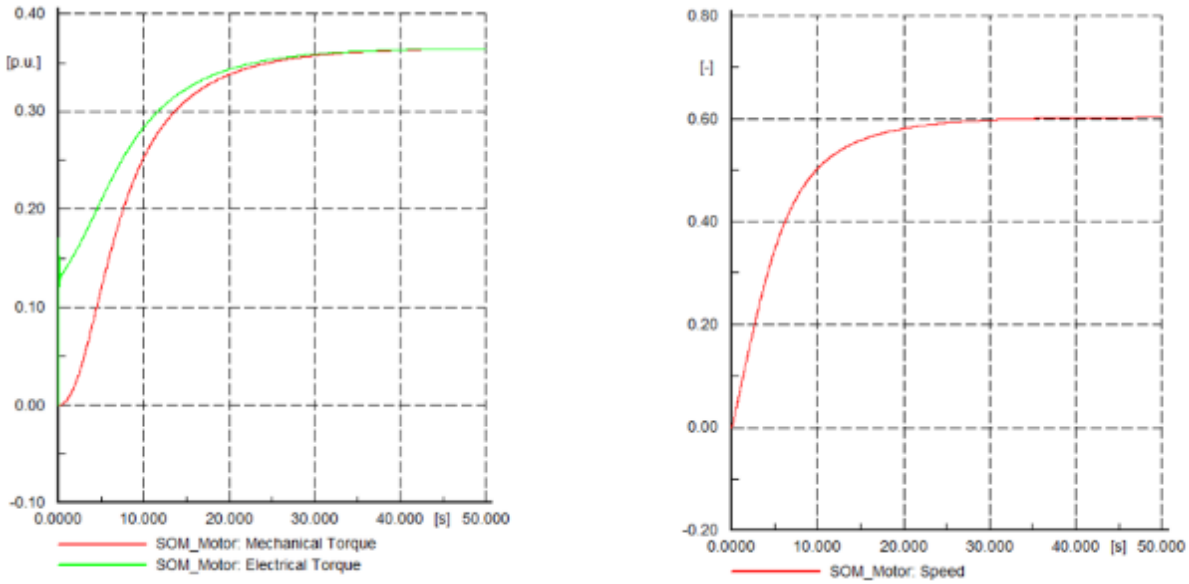

Figure 6-75
Motor starting: Mechanical and electrical torque in pu and motor speed in pu for a 1200 kW motor which failed to start

Figure 6-75 shows the torque and speed plot obtained when attempting to start a 1200 kW motor. From the plot, it may be observed that the motor failed to attain its nominal speed and that the motor has failed to start. Unlike Figure 6-74, the electrical torque is not above the mechanical torque throughout the motor starting period until the machine attains its rated speed. As electrical torque is not higher than mechanical torque during the starting period, the acceleration torque is absent and the machine isn't able to accelerate any further. Hence, the machine can't obtain its rated speed.

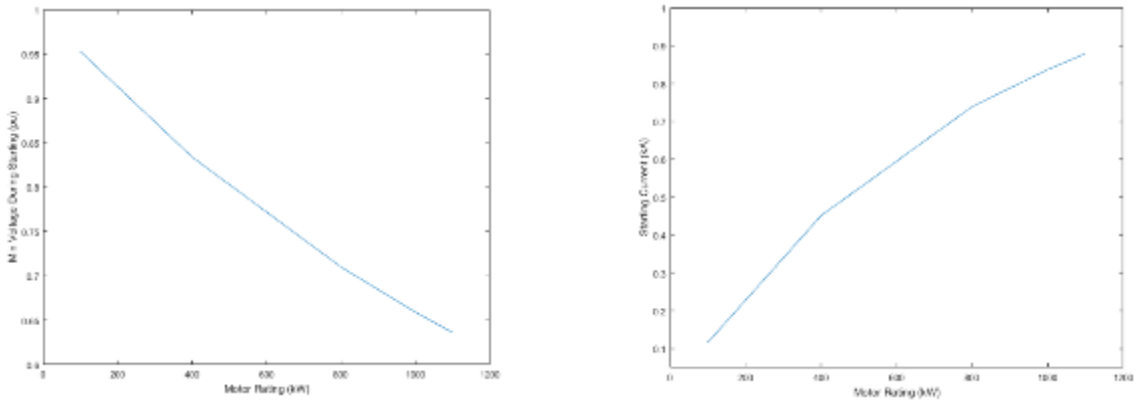

Figure 6-76
Motor starting: Min voltage during starting (pu) vs Motor rating (kW) and Starting current (kA) vs Motor rating (kW)

It may be concluded that, when the motor size is too large, the inrush current requirement will also be large and cannot be provided by the generation available. Another reason a motor may

fail to start may be that the electrical torque produced during motor starting period is less than the torque required to start the motor.

Key Findings

In this chapter, dynamic analysis and transient behavior of the proposed BNMC microgrid were analyzed using various microgrid configurations simulated using DIgSILENT PowerFactory. The major focus of analyses were the synchronization process, the islanding process, black start, and motor starting capability of the microgrid. Based on the analysis, the major conclusions obtained are:

- For successful synchronization with minimal transients, the two islands which are to be synchronized at the POI must have the same frequency, voltage, and phase angle.
- For successful islanding, each island to be formed should have sufficient generation capacity to meet its load demand. For smooth islanding with minimal transients, little or no power should flow through the POI before islanding. The total generation in each individual island to be formed should match the total load in that island before islanding. This will ensure that no power/current flow through the breakers at the POI. In case of unplanned islanding, power may flow through the POI before islanding. The total generation of each island to be formed in this case would not match the total load in that island. The spikes in voltage and frequency would be much larger than that seen in the case with no power flow through the POI before islanding. However, the voltage and frequency would eventually settle at a value close to 1 pu at steady state because the generators would adjust their power produced to match the load.
- The requirements for a successful black start are that the main generator be brought to spinning state (normal operation at no load) using some source of power such as small diesel generator before connecting the generator to the de-energized bus. The load applied to the newly energized bus must be less than the generating capacity of the generator.
- Motor starting will be successful when the microgrid can supply the inrush current required to start the motor without severe voltage drop at the motor terminals. A motor may fail to start should the electrical torque produced during motor starting period be less than the torque required to start the motor.

7 REFERENCES

[1] "Distribution System Feeder Overcurrent Protection," General Electric.

[2] *IEEE Recommended Practice for Utility Interface of Photovoltaic (PV) Systems,* IEEE Std. 929-2000, 2000.

A
IMPLEMENTATION OF A DATA COLLECTION SYSTEM REPORT SUMMARY

Several tasks undertaken as part of the BNMC microgrid project contributed to the initial NYSERDA award and remain relevant to the next phase of the NYSERDA effort. Task 2.3 is one of these tasks.

Task 2.3 involved identifying and analyzing power quality events captured by meters installed in the switchgear of the Buffalo Niagara Medical Campus (BNMC) electrical power system. The intent was to understand the power quality environment of the existing electrical infrastructure that would essentially become the proposed microgrid.

This report summarizes the analysis methods undertaken to assess the PQ events experienced by the BNMC electrical infrastructure, the type of events, their magnitude, duration, and frequency of occurrence.

Power Quality

The electric grid is designed to carry a waveform typically at 60 Hz (in the United States and its territories) or 50 Hz (Europe and elsewhere). The waveform ideally resembles a sine wave and generation systems are designed to produce as nearly perfect a sinewave as possible. However, after being generated, this sinewave experiences any number of perturbations in the electrical transmission and distribution systems. The effects of these perturbations on the generated sine wave may be known as power quality.

The relevance of power quality to a microgrid may be similar to electrical loads in general: the robustness of the microgrid to power quality variations may determine whether or not the microgrid remains in operation in the presence of these events—events both external to the microgrid and within it.

For instance, deviations in the power frequency (from 60 Hz or 50 Hz) may cause the microgrid to island—to separate from the main electrical grid system, or to shut down altogether—to protect the main grid system. Likewise, a voltage deviation of some magnitude and duration whether outside the microgrid or within it may result in the microgrid islanding or shutting down in response. Therefore, understanding those power quality events whether from outside or inside the microgrid becomes important.

EPRI undertook several studies over the years since around 1990 to document and to understand the power quality environment of the electrical system in the continental United States. These studies culminated in three reports known by the general titles DPQ I, DPQ II, and TPQ-DPQ III. These efforts examined power quality characteristics such as system average RMS-variation frequency index (SARFI), voltage distortion, voltage imbalance, and Flicker (both short-term and long-term). The most common voltage variation affecting electrical equipment is the voltage sag, a short-term reduction in voltage.

The above characteristics were examined for the BNMC electrical system.

BNMC Data Summary

Voltage deviation

The BNMC data, as illustrated in Figure A-1, indicated that 5 events occurred over the span of time between 2/4/2016 through June 13, 2016 (around 120 days). These events were momentary reductions in voltage commonly known as *voltage sags*. According to the ITIC and SEMI F47 curves, only one voltage sag should have caused any upset of equipment with the others being within the upper and lower limits. Two events of the same magnitude and duration were measured on different feeders—one in April and one in June.

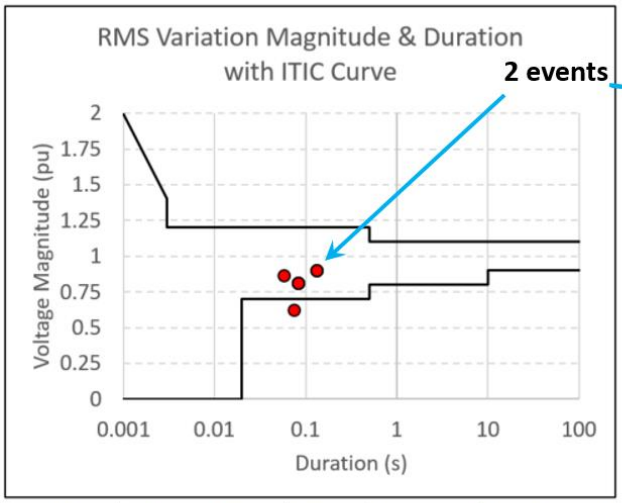

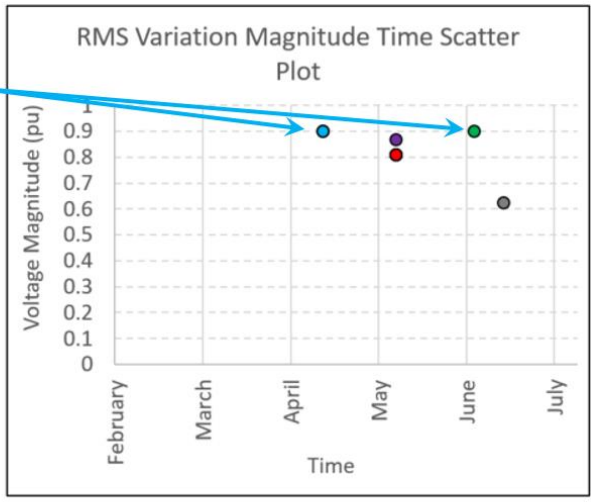

Site	Date and Time	Phase	Duration (s)	Magnitude (p.u.)
BNMC 15E	04/13/2016 01:29:20	CA	0.133	0.898
BNMC 14E	04/13/2016 01:29:20	CA	0.133	0.898
BNMC 12E	05/08/2016 01:16:29	AB	0.083	0.81
BNMC 11E	05/08/2016 01:16:30	AB	0.083	0.81
BNMC 15E	05/08/2016 01:17:14	AB	0.083	0.81
BNMC 14E	05/08/2016 01:17:21	AB	0.083	0.81
RPCI Srvc	05/08/2016 01:17:22	B	0.058	0.865
BNMC 12E	06/03/2016 17:23:08	BC	0.133	0.9
RPCI Panel	06/13/2016 22:16:17	A	0.075	0.621

Site	Monitoring Days
BNMC 11E	120
BNMC 12E	120
BNMC 14E	120
BNMC 15E	120
RPCI Srvc	120
RPCI Panel	120

Figure A-1
BNMC PQ Events

SARFI Events

The SARFI analysis of the BNMC events as recorded by the two meters compared to benchmark comparison data (BCD) taken from EPRI's TPQ-DPQ III study indicates that the BNMC average for this period of time was significant lower than that of the TPQ-DPQ III study. The BNMC/RPCI data ranged from 0 to 5.3 events per 365 days for all seven categories while the TPQ-DPQ III data ranged from 3.2 to 52.2 events for those same categories.

Voltage Distortion (THD)

The BNMC system had a much smaller range (CP 05 to CP 95) of voltage distortion than that of the TPQ-DPQ III study (under 0.8% difference vs. nearly 3.4% for TPQ-DPQ III). CP 50 was less than 1% for feeders 11E, 12E, 14E, and 15. The RPCI measurements were 1.1% for CP 50 while the TPQ-DPQIII data was 1.4%.

Voltage Imbalance

Similarly, the four E feeders had significantly less voltage imbalance than the TPQ-DPQ III data as did the RPCI Service; however, the RPCI_LPsub had a greater incidence of voltage imbalance compared to the TPQ-DPQ III data.

Flicker

For both short-term (Pst) and long-term (Plt) Flicker, the data for CP 05 and CP 50 for the four E feeders were significantly better, almost by half, than the TPQ-DPQ III data. The CP 95 data for the E feeders was one third of that for the TPQ-DPQ III study.

The BNMC monitoring project placed two varieties of power quality meters at two separate locations: the i-Sense (by Allen Bradley) and PQube3 (by Power Standards Labs). These are shown in Figure A-2. The i-Sense devices monitored only voltage at a 480VAC panel while the PQube devices monitored both voltage and current from the PTs and CTs in RPCI's switchgear.

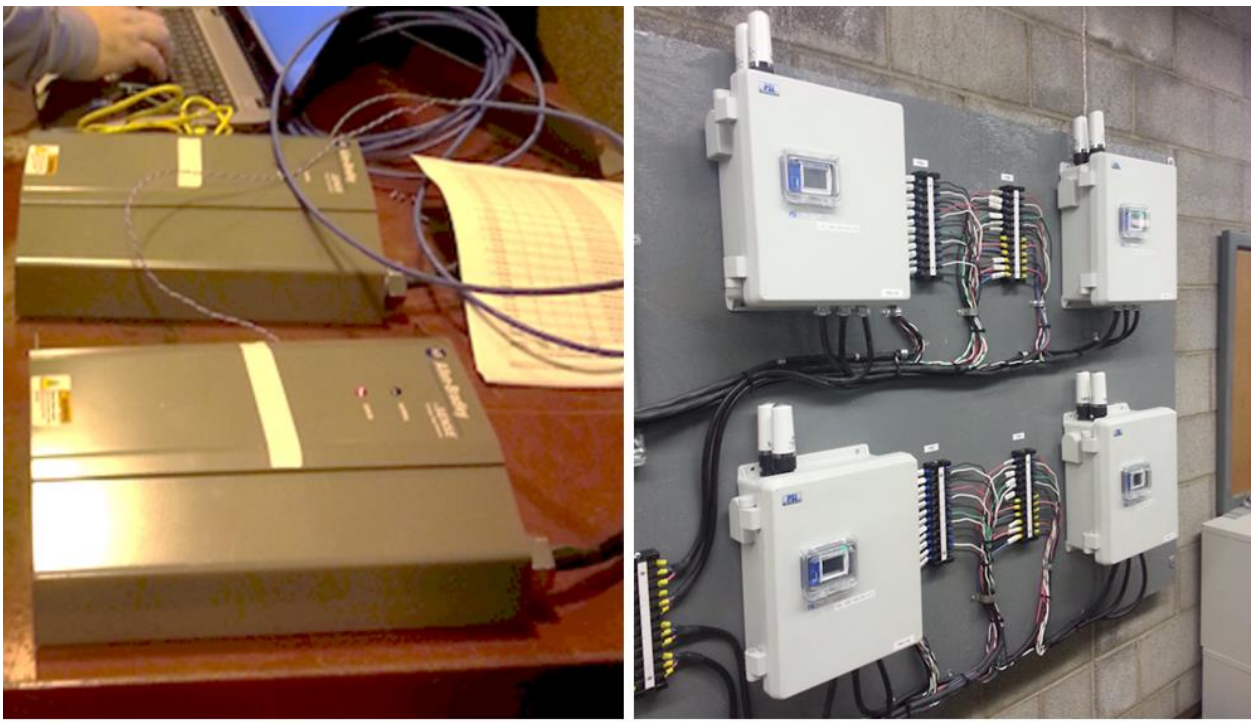

i-Sense at RPCI

Pqube at Elm Street

Figure A-2
Power Quality Monitors Installed at BNMC

The locations of the meters, at the Elm Street Substation and the switchgear for the Roswell Park Cancer Institute (RPCI)—about 1 mile apart—are shown in Figure A-3.

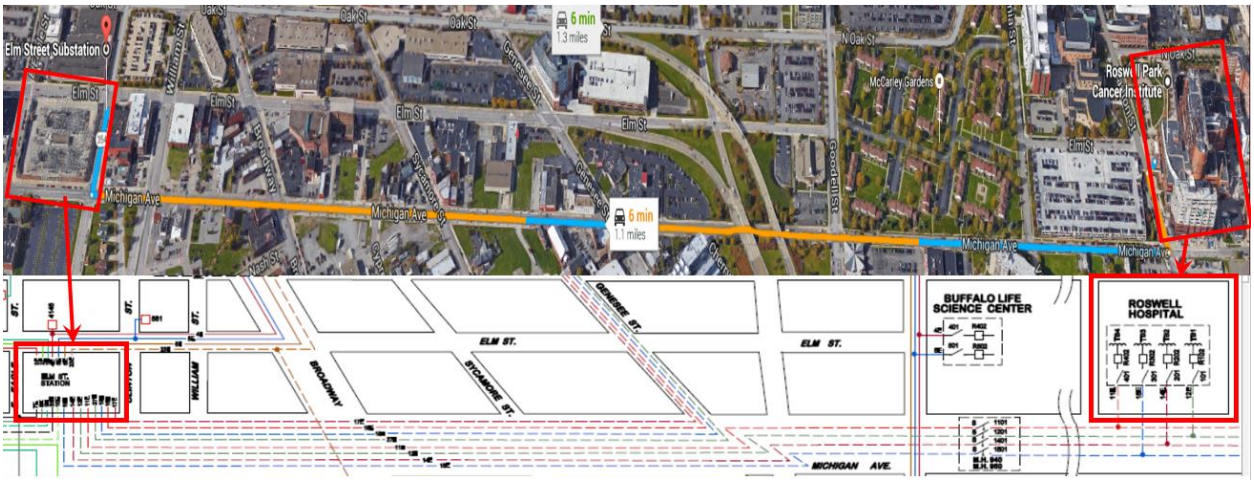

Figure A-3
Locations of Power Quality Monitors

These meters were installed around the 4th of February, 2016 and then monitored the electrical environment at BNMC until around June 13, 2016. The analysis of the data involved making comparisons with standard industry measures such as the ITIC and SEMI F47 curves.

Information Technology Industry Council (ITI or ITIC)

The ITIC curve shown in Figure A-4 basically describes the voltage range within which office machinery should be capable of operating normally. For about 3 cycles, the machines should tolerate up to 120% and down to 70% of nominal voltage and operate normally. From about 3 cycles to 10 seconds, the machines should tolerate up to 110% and down to 80% of nominal voltage, operating normally. Beyond ten seconds—steady-state operation—machines should tolerate up to 110% and down to 90% of nominal voltage and operate normally.

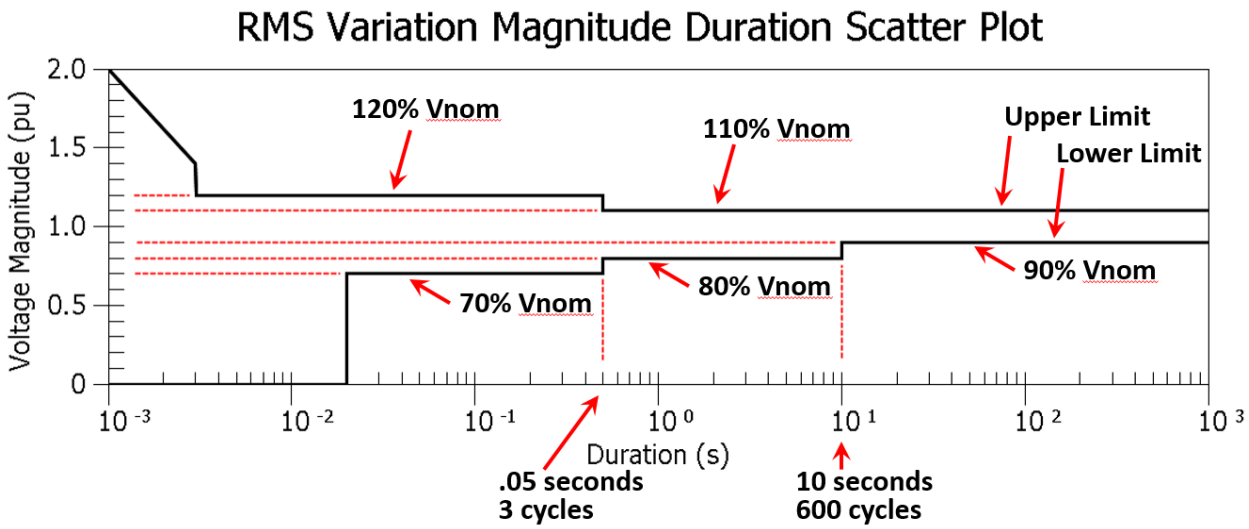

Figure A-4
ITIC Curve

SEMI F47

The SEMI F47 curve is basically the lower limit of the ITIC Curve. It was developed for semiconductor equipment; specifying that the semiconductor equipment was SEMI F47-compliant meant that the equipment could function normally down to the SEMI F47 curve.

During the interval of time the meters were operating, five events were captured as shown in Figure A-5. According to the ITIC and SEMI F47 curves, only one voltage sag, the one at 62% of nominal voltage on June 13th, should have caused any upset of equipment with the others being within the upper and lower limits of the ITIC curve and above the SEMI F47 curve (corresponding to the lower limit of the ITIC curve). Two events of the same magnitude and duration were measured on different feeders—one in April and one in June.

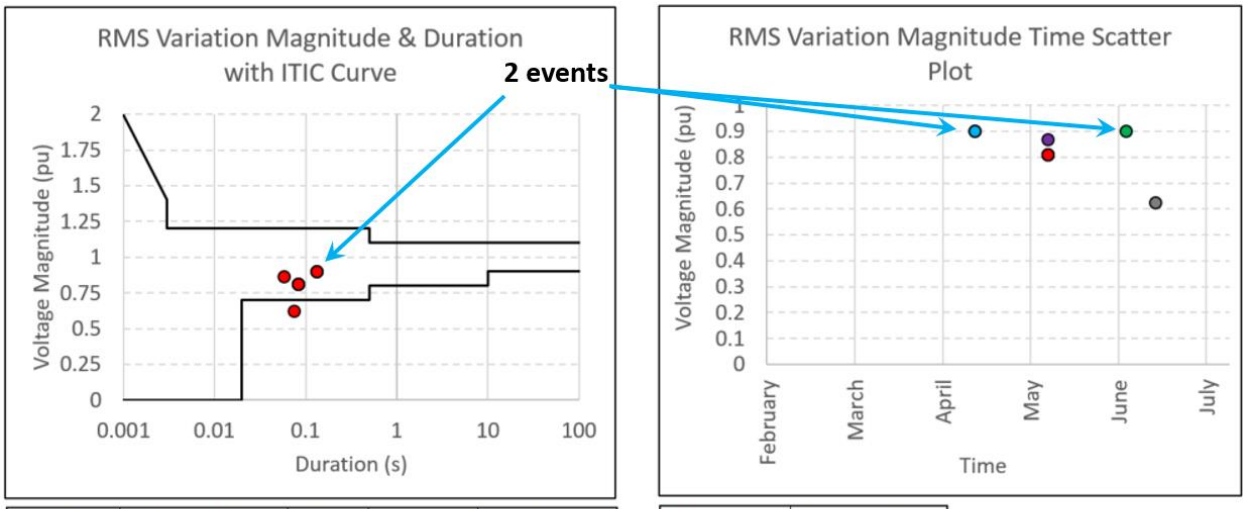

Site	Date and Time	Phase	Duration (s)	Magnitude (p.u.)
BNMC 15E	04/13/2016 01:29:20	CA	0.133	0.898
BNMC 14E	04/13/2016 01:29:20	CA	0.133	0.898
BNMC 12E	05/08/2016 01:16:29	AB	0.083	0.81
BNMC 11E	05/08/2016 01:16:30	AB	0.083	0.81
BNMC 15E	05/08/2016 01:17:14	AB	0.083	0.81
BNMC 14E	05/08/2016 01:17:21	AB	0.083	0.81
RPCI Srvc	05/08/2016 01:17:22	B	0.058	0.865
BNMC 12E	06/03/2016 17:23:08	BC	0.133	0.9
RPCI Panel	06/13/2016 22:16:17	A	0.075	0.621

Site	Monitoring Days
BNMC 11E	120
BNMC 12E	120
BNMC 14E	120
BNMC 15E	120
RPCI Srvc	120
RPCI Panel	120

Figure A-5
PQ Events at BNMC
2/4/2016 to 6/13/2016

All events clustered around 0.1 seconds in duration ranging from 0.75 to 0.133 seconds. The 62% voltage sag may be seen in both waveform and rms voltage in Figure A-6 below. One unfortunate idiosyncrasy of PQ View may be seen between the chart in Figure A-5 and the graph in Figure A-6 for the 62% sag: although the voltage sag involves two phases almost to the same degree, PQ View chose the slightly worst-case phase, Phase A, to assign the voltage sag. However, this was a two-phase sag!

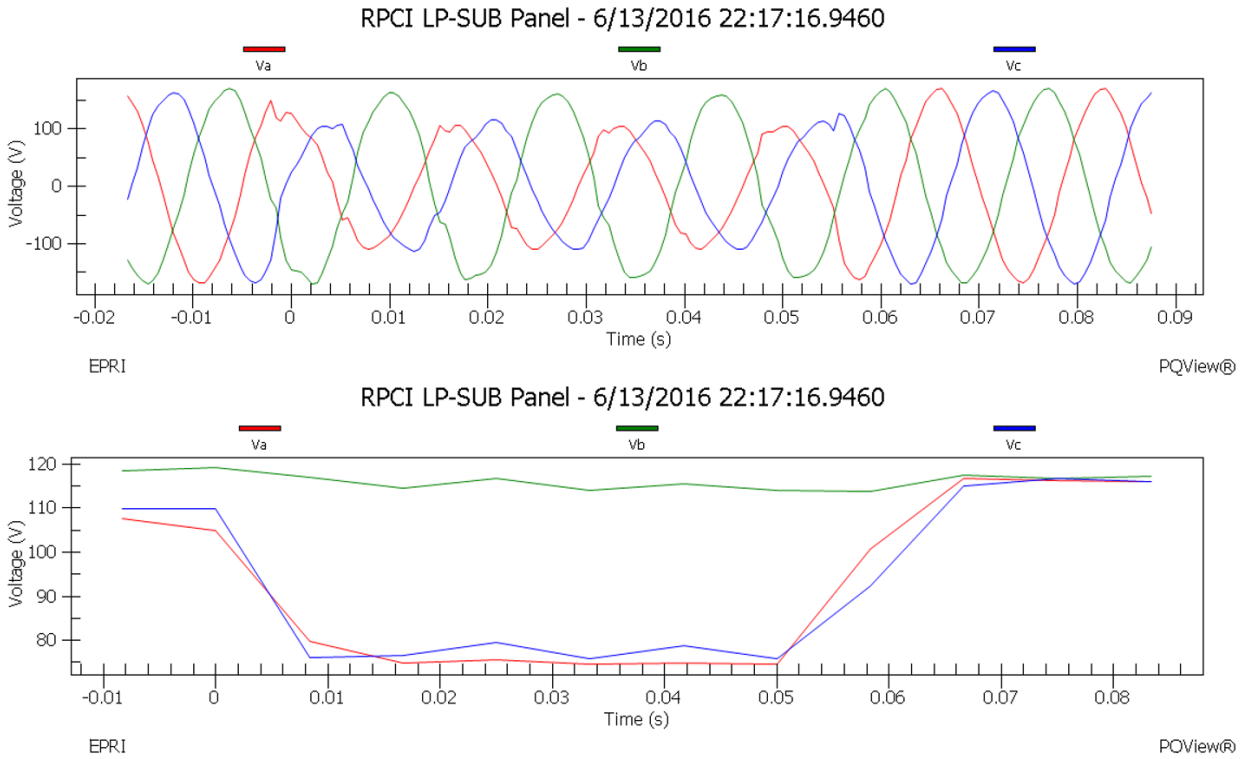

Figure A-6
2-phase, 62% Voltage Sag, ~4.5 cycles
RCPI LP Sub Panel

Another of the five voltage sags may be seen in Figure A-7 for Feeder 15E. barely below 90% of nominal voltage, this sag should not have affected anything in the BNMC network with normal sensitivity.

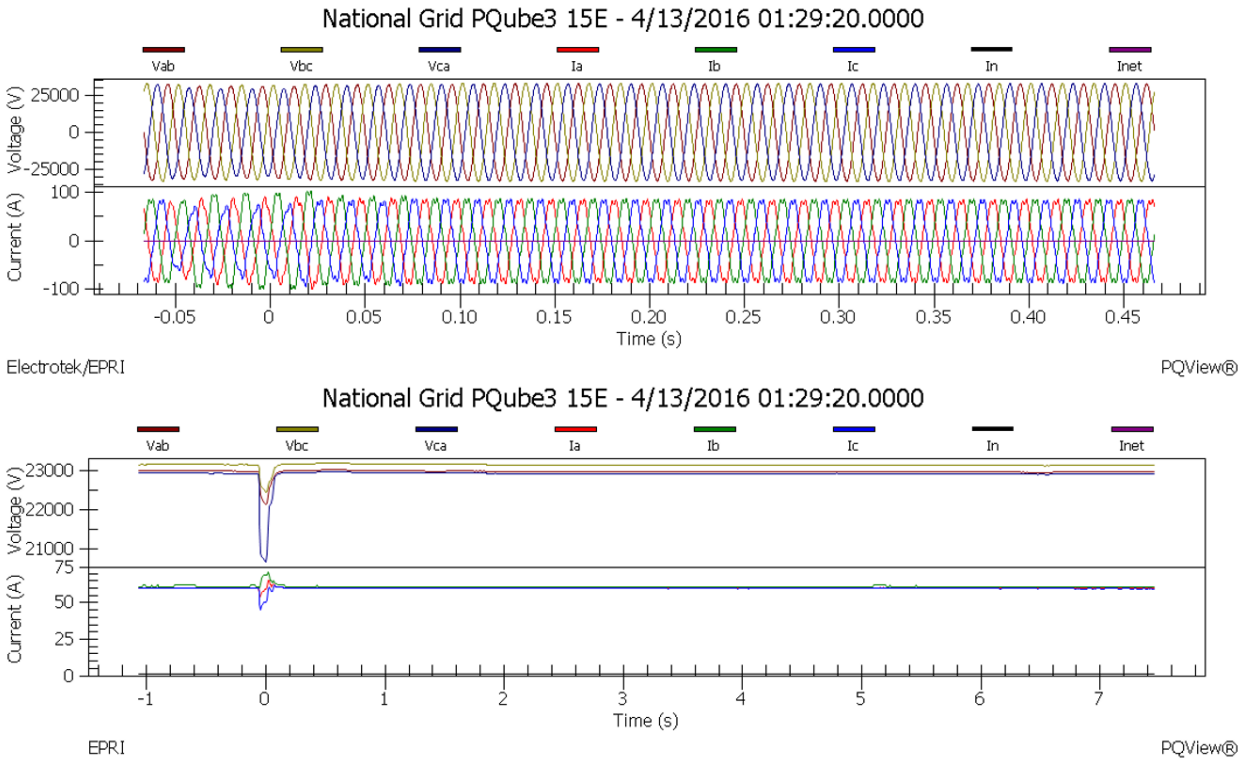

Figure A-7
Voltage Sag on 15E, April 13
89.8% Vnom, 0.133 seconds

TPQ-DPQ III

EPRI undertook several studies over the years since around 1990 to document and to understand the power quality environment of the electrical system in the continental United States. These studies culminated in three reports known by the general titles DPQ I, DPQ II, and TPQ-DPQ III. The last, TPQ-DPQ III provided many insights into the state of the grid on a national basis. One characteristic, shown in Figure A-8, illustrates the frequency of voltage sags of various magnitudes and durations. It may be seen that most voltage sags occur for less than 0.5 seconds, or 30 cycles (red line). It may also be seen that far more occur above 50% of nominal voltage than below.

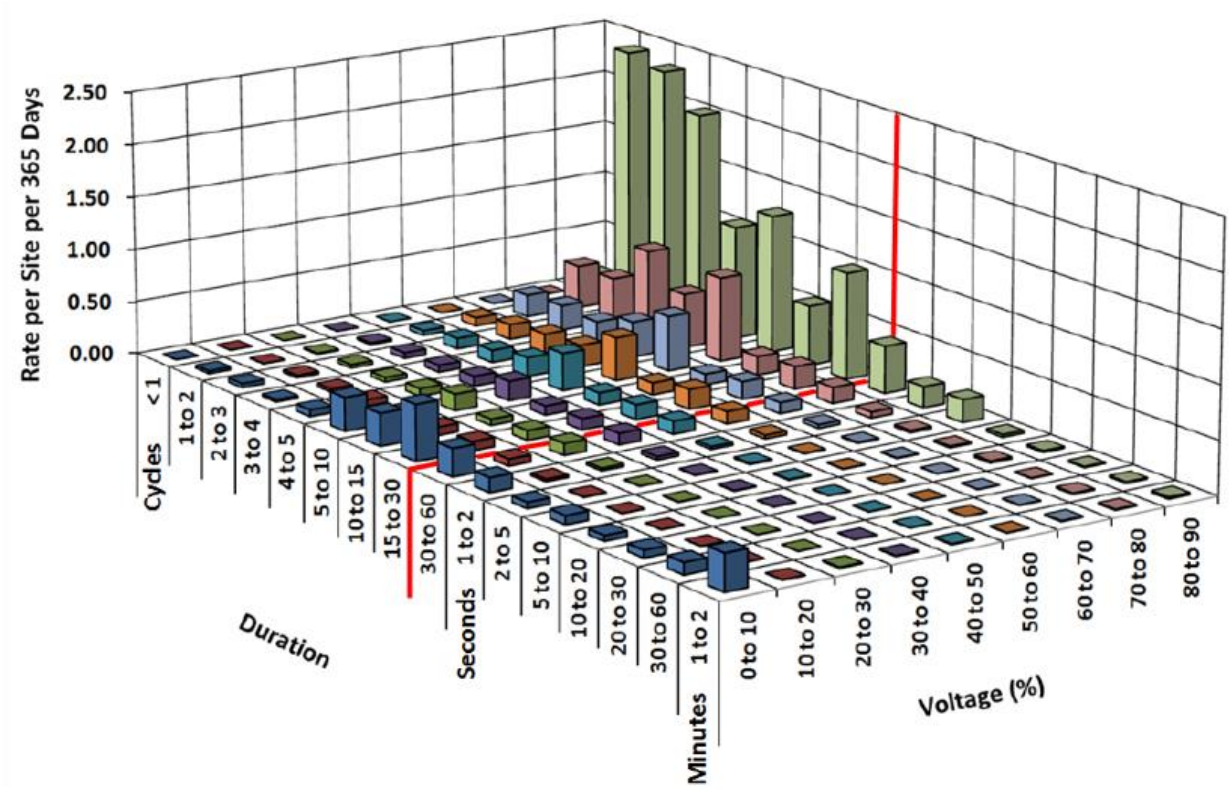

Figure A-8
Voltage Sag Data
Distribution Systems
TPQ-DPQ III

SARFI Events

The SARFI comparison of the BNMC system with the TPQ-DPQ III study (called BCD in the figure for brevity—*benchmark comparison data*) may be seen in Figure A-9. Here, the data for the BNMC system appears significantly better than the earlier study.

The SARFI analysis of the BNMC events as recorded by the two meters compared to benchmark comparison data (BCD) taken from EPRI's TPQ-DPQ III study indicates that the BNMC average for this period of time was significant lower than that of the TPQ-DPQ III study. The BNMC/RPCI data ranged from 0 to 5.3 events per 365 days for all seven categories while the TPQ-DPQ III data ranged from 3.2 to 52.2 events for those same categories.

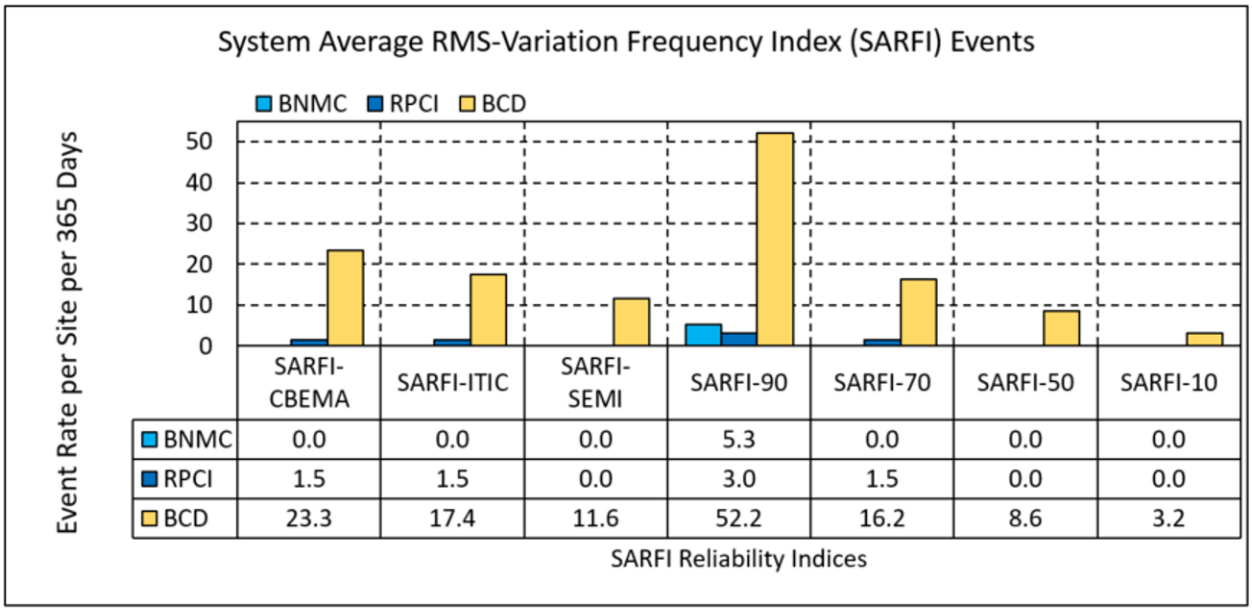

Figure A-9
SARFI Analysis
BNMC and RPCI vs. BCD

Voltage Distortion (THD)

As may be seen in Figure A-10, the BNMC system had a much smaller range (CP 05 to CP 95) of voltage distortion than that of the TPQ-DPQ III study (under 0.8% difference vs. nearly 3.4% for TPQ-DPQ III). CP 50 was less than 1% for feeders 11E, 12E, 14E, and 15. The RPCI measurements were 1.1% for CP 50 while the TPQ-DPQIII data was 1.4%.

Note that typical limits for THD are provided in the chart with red lines: the 5% limit (per IEEE Std 519) at the top of the graph, and the dashed red line at 3.5%—when utilities begin to become concerned.

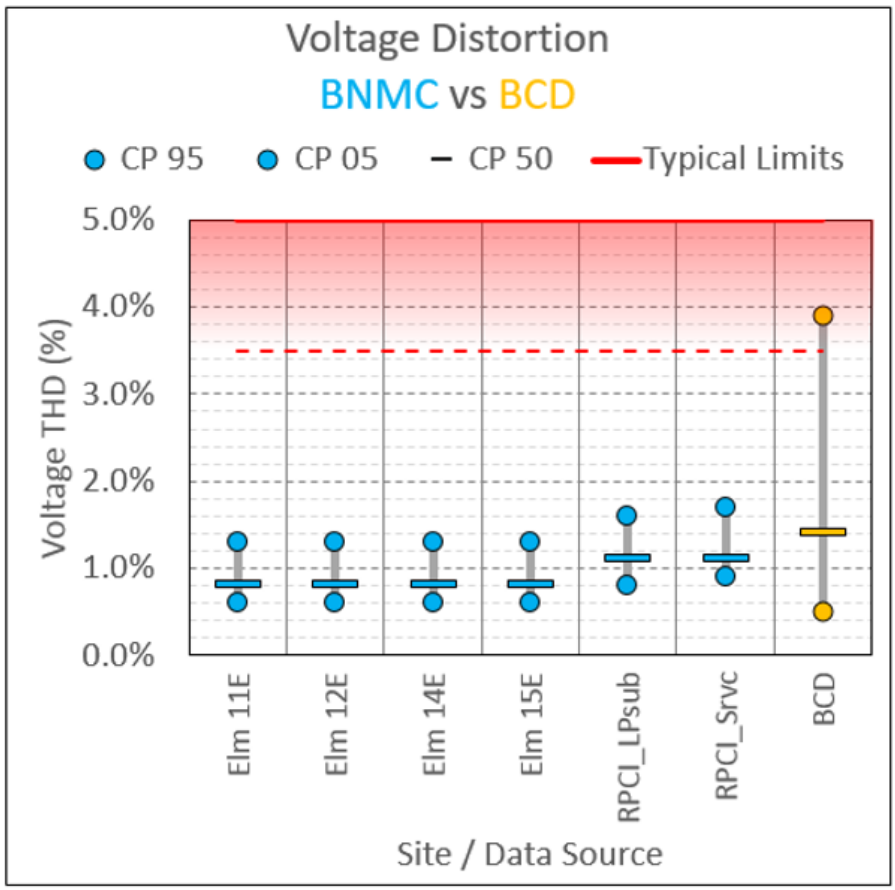

Voltage THD	Elm 11E	Elm 12E	Elm 14E	Elm 15E	RPCI LP	RPCI Srvc	BCD
CP 95	1.3%	1.3%	1.3%	1.3%	1.6%	1.7%	3.9%
CP 05	0.6%	0.6%	0.6%	0.6%	0.8%	0.9%	0.5%
CP 50	0.8%	0.8%	0.8%	0.8%	1.1%	1.1%	1.4%

Figure A-10
Voltage Distortion Comparison

Voltage Imbalance (also called Voltage Unbalance)

As shown in Figure A-11, the four E feeders had significantly less voltage imbalance than the TPQ-DPQ III data as did the RPCI Service; however, the RPCI_LPsub had a greater incidence of voltage imbalance compared to the TPQ-DPQ III data. Here also, the typical maximum voltage imbalance—when motors may suffer damage if not de-rated—is given at the top at 5% (red line) and at 3.5% (dashed red line) at about when motor damage may begin to become a concern should the imbalance worsen.

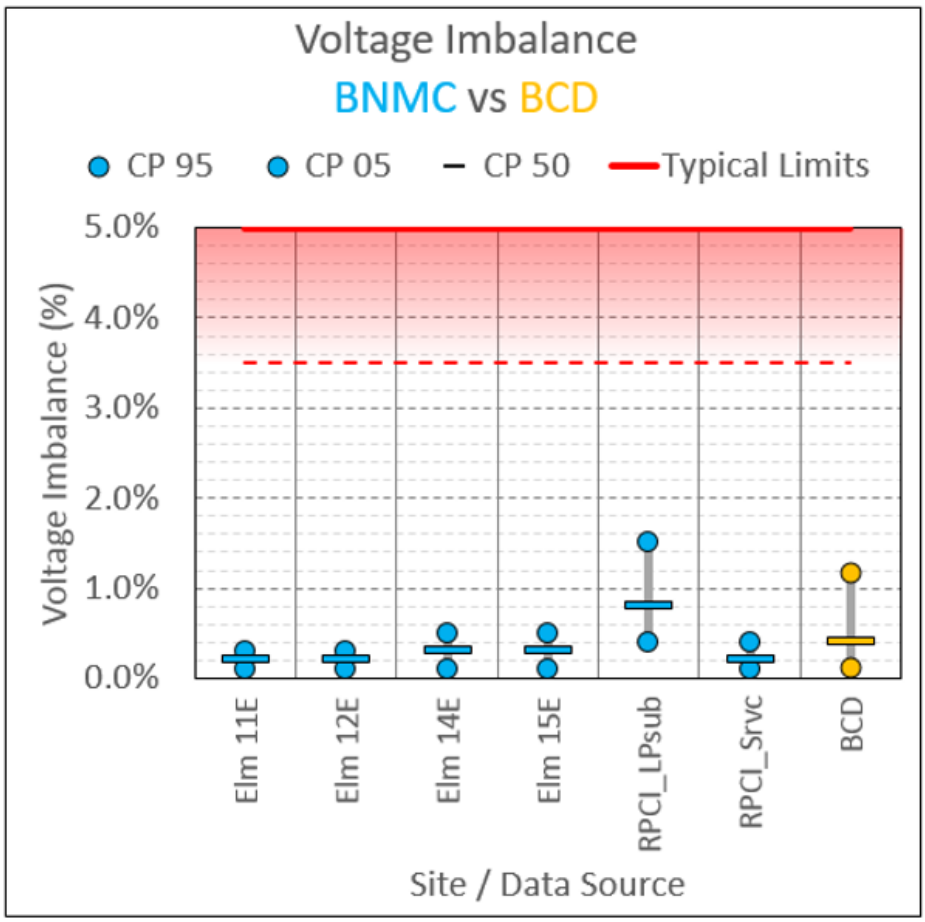

Voltage Imbalance	Elm 11E	Elm 12E	Elm 14E	Elm 15E	RPCI LP	RPCI Srvc	BCD
CP 95	0.3%	0.3%	0.5%	0.5%	1.5%	0.4%	1.2%
CP 05	0.1%	0.1%	0.1%	0.1%	0.4%	0.1%	0.1%
CP 50	0.2%	0.2%	0.3%	0.3%	0.8%	0.2%	0.4%

Figure A-11
Voltage Imbalance

Flicker

Figure A-12 provides the data for Flicker—both short-term (Pst) and long-term (Plt). The data for CP 05 and CP 50 for the four E feeders were significantly better, almost by half, than the TPQ-DPQ III data. The CP 95 data for the E feeders was one third of that for the TPQ-DPQ III study.

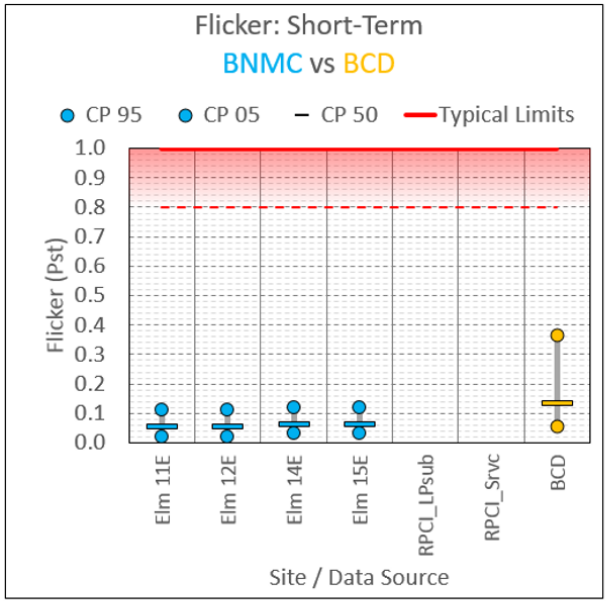

Flicker Pst	Elm 11E	Elm 12E	Elm 14E	Elm 15E	RPCI LP	RPCI Srvc	BCD
CP 95	0.11	0.11	0.12	0.12	NA	NA	0.37
CP 05	0.02	0.02	0.03	0.03	NA	NA	0.05
CP 50	0.05	0.05	0.06	0.06	NA	NA	0.13

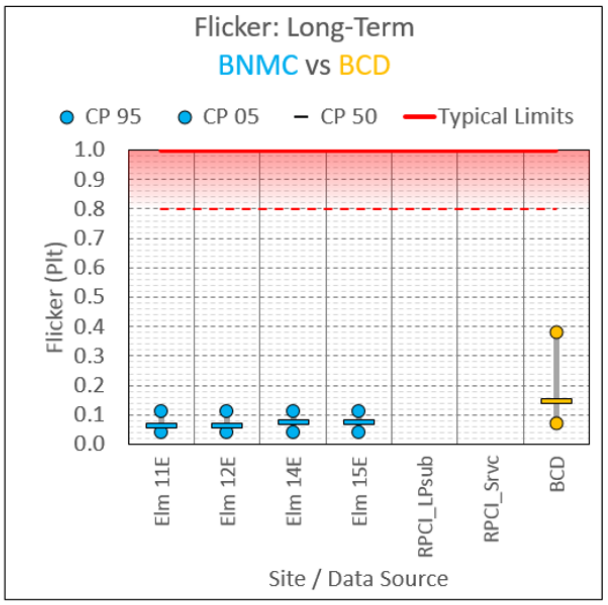

Flicker Plt	Elm 11E	Elm 12E	Elm 14E	Elm 15E	RPCI LP	RPCI Srvc	BCD
CP 95	0.11	0.11	0.11	0.11	NA	NA	0.38
CP 05	0.04	0.04	0.04	0.04	NA	NA	0.07
CP 50	0.06	0.06	0.07	0.07	NA	NA	0.14

Figure A-12
Voltage Flicker, Pst and Plt

Conclusion

The BNMC system appears to be fairly robust on the utility side with no significant events occurring within the system either. Indeed, all the characteristics of the BNMC electrical system appear to be better than those of the TPQ-DPQ III study for the same voltage class.

B
POWER QUALITY AND ENERGY EFFICIENCY: DATA ANALYSIS AND RECOMMENDATIONS REPORT SUMMARY

The concept of the BNMC microgrid consists of several interrelated components—each contributing to the overall functionality and operational success of the microgrid. Power quality and its effects may compromise the effectiveness of a medical campus in that sensitive and critical medical equipment—or even parts of the microgrid—may cease operation due to power quality events experienced during or after the transition to or from the islanded grid. Therefore, understanding the potential sensitivities and possible approaches to mitigating those sensitivities becomes an important activity in the design and implementation of a microgrid.

Task 2.4 involved identifying power quality and energy efficiency optimization possibilities throughout the local power grid and within BNMC customer facilities. Accordingly, EPRI undertook an analysis of member institutes at the Buffalo Niagara Medical Campus (BNMC) to assess two characteristics of the institutes:

- the intrinsic sensitivities of the electrical systems and processes of these institutes to variations in power quality (PQ), and
- the potential for improvements in energy efficiency and the possible energy savings resulting from the implementation of these improvements.

Each member institute received a detailed report of the findings from onsite assessments undertaken for each member institute as a part of this study. These findings included the examination of incoming power equipment, the examination of facility processes such as boilers, compressed air systems, motor and adjustable speed drive (ASD) systems, building management systems, HVAC equipment, etc. Possible sensitivities were identified along with suggested approaches to mitigation of these sensitivities including voltage sag mitigation devices and parameter changes for ASDs. Systems were also examined with the aim of improving their energy efficiency. The cover pages of these reports are shown in Figure B-1.

Figure B-1
Individual Report Cover Pages

This report summarizes the methods and approximate material cost of mitigating the sensitivities identified along with the approximate energy and cost savings for individual member institutes and the group as a whole.

Energy Efficiency

To estimate possible energy efficiency improvements, BNMC member institute sites were examined to identify areas where energy efficiency could be improved. Energy consumption data was obtained directly from member institutes and/or from National Grid or extrapolated from system data provided by National Grid. This data may include electrical consumption and natural gas consumption.

The pattern of energy consumption shown in Figure B-2 was typical of that seen for most member institutions: loads considered *electrical only* tended to be relatively consistent throughout the year while loads having to do with heating or cooling (*Cooling* [kWh] and *Heating* [gas]) tended to fluctuate seasonally. The *heating* and *cooling* loads suggest that energy consumption may be reduced through improvements to the building envelope—that is, through improved insulation and improved sealing around exterior windows and doors.

Small improvements to the energy consumption of *electric only* loads may be accomplished through switching from standard v-belt drives to cogged belt drives for instance, or lowering the system pressure for compressed air systems and fixing leaks. However, greater energy savings in general may be accomplished through the replacement of older equipment *at failure* with newer, more energy efficient equipment.

The member institutes examined were the Kaleida Health facility (including the Gates Vascular Institute, Buffalo General Hospital, Clinical and Translational Research Center, and the Children's Hospital), the Roswell Park Cancer Institute (including its Main Hospital, the Gratwick Basic Science Building, Administrative Services Building, Cell and Virus Building, Grace Cancer Drug Center, and Clinical Sciences Center), the University at Buffalo facilities (consisting of the Gateway Building, the Research Institute on Addictions, the Clinical and Translational Research Center, the Center for Excellence in Bioinformatics, and the new School of Medicine under construction at the time of the assessments), the Buffalo Niagara Medical Campus facilities (consisting of the Innovation Center, and Cleveland BioLabs), and the Hauptman-Woodward Medical Research Institute.

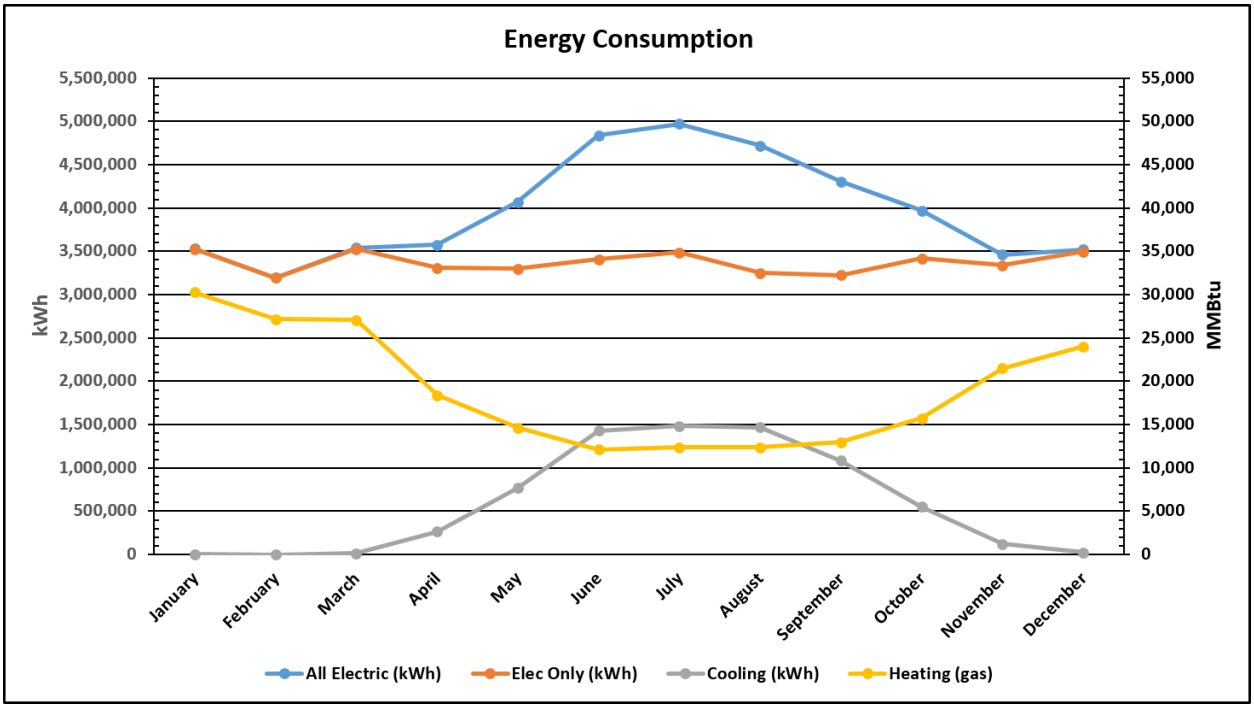

Figure B-2
Example Energy Consumption

Energy Efficiency Findings

Energy conservation measures (ECMs), estimated annual savings, and estimated material costs were identified for specific facility systems or equipment such as lighting, compressed air systems, boilers, application of adjustable speed drives (ASDs), etc. These are shown for each member institute in the Appendix section.

While the annual savings from reducing seasonal thermal losses or gains may be significant, the potential cost of improving the building envelope of an existing structure is not known. Motor efficiencies may be improved by replacing existing motors with premium efficiency motors—*but only at failure*. Therefore, these two options were noted in the individual reports but not included in the estimated costs or savings summaries. However, estimates of costs and savings from improvements to lighting, HVAC, boilers, and other facility processes identified have been summarized in Table B-1. The estimated simple payback represents all identified costs divided by all estimated savings. The simple payback for some individual ECMs may be shorter or longer than that indicated in Table B-1.

Table B-1
ECM Summaries

Member Institute	Estimated Annual Savings	Approximate Material Cost	Simple Payback	Comments

Total for All Members	**$194,649 to $197,884**	**$482,640 to $607,780**	**2.44 to 3.12 years**	
Kaleida Health	**$62,000 to $63,700**	**$66,000**	**12.8 months**	**Many opportunities identified at this site**
Roswell Park Cancer Institute	**$20,584**	**$150,000**	**7.3 years**	**Several measures in effect at time of assessment**
University at Buffalo facilities	**$1,896**	**$13,500 to $16,500**	**7.1 to 8.7 years**	**Some ECMs at no cost**
Hauptman-Woodward Institute	**$94,573 to $96,108**	**$249,000 to $367,000**	**2.6 to 3.9 years**	**Greatest savings and costs associated with HVAC units**
BNMC Properties: Innovation Center	**$4,496**	**$960 to $1,920**	**0.21 to 0.43 yr**	**Small loads**
BNMC Properties: Cleveland BioLabs	**$11,100**	**$3,180 to $6,360**	**0.29 to 0.57 yr**	**Small loads**

Individual Member Institutes

Kaleida Health

EPRI engineers examined the Kaleida Health (KH) facility located in the Buffalo Niagara Medical Campus (BNMC). The KH facility consists of the Gates Vascular Institute (GVI), Buffalo General Hospital (BGH), Clinical and Translational Research Center (CTRC), and the Children's Hospital.

Facility transformers (four at 5 MVA each) receive electricity at 23 kilovolts and provide it at 4,160 volts to the main switchgear. Energy consumption appears to be between 3 million kWh and 5 million kWh per month, and around 48 million kWh per year.

Three 2 MVA, 4,160-volt emergency diesel generators are located on site with a 4th to be installed in the future with future Children's Hospital. Emergency diesel generators at 480 V_{AC} also exists near the 4,160 V_{AC} units.

A seasonal difference of 4,000,000 kWh (~$240,000 per year at an average of $0.06 per kWh) could be identified between the summer and winter electrical energy consumption (identified for cooling). The existing centrifugal chiller compressors should be most efficient. However, the power demand in kW per ton of cooling should be measured and calculated before and after maintenance. For a new unit, this number should be between 0.5 and 0.6 kW/ton. A value over 1 kW/ton may call for major maintenance or replacement of the unit.

Seasonal differences for gas consumption were also identified: ~477,000 therms or $133,500 at $0.28/therm. Both seasonal differences may point to an improved insulation and door/window sealing opportunity in the KH facility to minimize these losses.

Only low temperature waste heat sources were identified at KH. As such, heat recovery for these sources is not generally cost effective.

Roswell Park Cancer Institute

EPRI engineers examined the Roswell Park Cancer Institute (RPCI) facility located in BNMC. The RPCI facility consists its Main Hospital, the Gratwick Basic Science Building, Administrative Services Building, Cell and Virus Building, Grace Cancer Drug Center, Genetics and Pharmacology (not visited), and Clinical Sciences Center.

Four high voltage feeders (11E, 12E, 14E, and 15E), connect to four facility transformers at 23 kilovolts. The transformers provide electricity at 4,160 volts to the main switchgear. RPCI consumes between 3 million kWh and 5 million kWh per month and around 52 million kWh per year. The Genetics and Pharmacology building, currently connected to feeders 4E and 5E, will instead be connected to two of the other high voltage feeders (11E, 12E, 14E, or 15E).

RCPI has three 1250 kW, 4,160-volt emergency diesel generators located on 3rd floor of facility. One generator is 1,100 kW at 480 V_{AC}. Another 4,160-volt, 2000 kW generator on the 4th floor is dedicated for the chiller also located on the 4th floor.

A seasonal difference of 3,655,400 kWh (~$219,300 per year at an average of $0.06 per kWh) could be identified between the summer and winter electrical energy consumption—identified for cooling. A seasonal difference for gas consumption also identified at ~936,928 therms or $262,340 at $0.28/therm. Both may point to an improved insulation and door/window sealing opportunity in the RPCI facilities to minimize these losses.

The efficiency of chiller units should be examined before and after maintenance by calculating the kW/ton.

RPCI is acting upon lighting opportunities with LED replacements where applicable for incandescent, metal halide, etc. inside and outside the buildings. The goal is to replace 4,000 to 5,000 fixtures by year's end (a reduction of ~256,000 kWh to 320,000 kWh per year). 400-Watt outdoor light fixtures will be replaced with 92 W fixtures. Some metal halide may be found in electrical buildings; however, these are left off most of the time. T8 Fluorescent lamps are used throughout buildings.

Buffalo Niagara Medical Campus

EPRI engineers examined two facilities managed by the Buffalo Niagara Medical Campus (BNMC): the Innovation Center (IC), and Cleveland BioLabs (CB). Both are supplied at 5 kV—the IC from Station #49, CB from #34.

The IC consumed between 200,000 and 260,000 kWh/month from January 2014 to March 2015 while CB consumed an estimated 46,000 to 79,000 kWh/month.

A seasonal difference of 13,272 kWh (~$796 per year at an average of $0.06 per kWh—for cooling) could be identified for the IC. Natural gas data was not available.

A seasonal difference of 23,302 kWh (~$1,398 per year at an average of $0.06 per kWh—for cooling) could be identified for CB between the estimated summer and winter electrical energy

consumption. A seasonal difference for estimated gas consumption was also identified: ~1,260 therms or $353 at $0.28/therm although this may vary from year to year.

Both the energy consumption for these facilities as well as the seasonal differences appear relatively small; however, opportunities for improving insulation and door/window sealing in these facilities may further minimize these losses.

Both the IC and CB have T12 lamps that may be replaced largely due to the phasing out of T12 lamps. The energy savings are relatively small.

Existing chillers appear around 10 years of age; the efficiency of these units should be examined before and after maintenance to establish kW/ton of cooling.

The Innovation Center has one 500 kW, 480-volt emergency diesel generators located outside of its facility while Cleveland BioLabs has one 350 kW, 208-volt emergency diesel generator located outside of its facility.

University at Buffalo Facilities

The UB-affiliated facilities consist of the Clinical and Translational Research Center (CTRC), the Gateway Building (GB), the Research Institute on Addictions (RIA), the Center for Excellence in Bioinformatics (CEB), and the new School of Medicine under construction at the time of the assessments.

The CTRC is located in the Kaleida Health building and receives power through the KH transformers connected to feeders 11E, 12E, 14E, and 15E at 23 kV. One of the KH emergency generators supplies CTRC in the event of a loss of electrical power. The GB and CEB are connected to feeders 4E and 5E at 5kV.

Most of the UB facilities appeared to be of small loads. No energy consumption data was made available for the UB buildings although an estimate was possible for the School of Medicine using data from design drawings. Seasonal differences for gas consumption were identified for other, larger facilities on the BNMC campus such that the energy use pattern should also apply to the UB facilities. Therefore, the UB facilities may also have an opportunity to improve insulation and door/window sealing to minimize these losses.

The largest electrical energy uses may include the existing chiller systems. As such, the efficiency of chiller units should be examined before and after maintenance by calculating the kW/ton.

Hauptman-Woodward Medical Research Institute

EPRI engineers examined the Hauptman-Woodward Medical Research Institute (HWI) facility located in the (BNMC). HWI studies biological structures and uses cold temperatures to stabilize these structures for study. Lab space (2/3 of 3-floor facility) temperatures are kept at around 70°F with no fluctuation. Other areas allowed to fluctuate after 6 pm. Some freezers cool to -80°C and others to -20°C.

Facility pad-mounted, 2 MVA transformer receives electricity at 4160 volts and steps it down to 480 V_{AC}. HWI consumes around 2,500,000 kWh per year, and 220,000 average kWh per month. HWI demands an average of 533 kW (minimum 363, maximum 863 from data); $0.09 average

cost per kWh for 2014. A 500 kVA, 480-volt emergency diesel generator is located in a small building at the site.

Energy consumption shows a seasonal difference of 290,000 kWh ($26,000 per year at an average of $0.09 per kWh) that could be identified between summer and winter electrical energy consumption. The difference may point to an improved insulation and door/window sealing opportunity. No natural gas consumption was provided.

An opportunity for energy savings may exist concerning the McQuay 320-ton screw compressor: at failure, it should be replaced with a centrifugal chiller of greater efficiency. Savings of 691,200 kWh per year, 172.8 kW, $ 62,208 at $0.09/kWh are possible. The estimated material cost for this unit ranged from $130,000 to $235,000; simple payback from 2.1 to 3.78 years or 25 to 45.4 months.

Similar opportunities exist for McQuay rooftop units: at failure, replace with newer, more efficient units. Possible savings may be 228,800 kWh per year, 57.2 kW, $ 20,592. Assuming $100,000 material cost of replacing both, the simple payback is 4.9 years or 58.8 months.

A small lighting opportunity with T8 lamps was identified: install LED T8 lamps (lamp replacement—no fixture replacement necessary). Savings range between 42,100 and 59,150 kWh ($3,789 to $5,324) at a material cost of $5,000 to $15,000, with simple payback of 0.9 to 4 years depending on actual cost of LED T8 lamps.

Power Quality

Voltage Sags

In general, power quality problems point to equipment that is intrinsically sensitive to variations in power quality—typically 86% of nominal voltage (for more sensitive equipment) or less. Voltage sags occur at a given magnitude and duration due to short circuits and other events within the electrical distribution system. According to a study performed by EPRI[3] over 97% of all voltage sags (at all magnitudes) in the distribution system endure for 15 seconds or less. For all voltage sags at 50% of nominal voltage or above for up to 2 minutes in duration, those at 50% of nominal voltage and above for about 2 seconds in duration comprise around 93%. In other words, most voltage sags by far tend to be brief and at or above 50% of nominal voltage. Several devices exist that may mitigate such voltage sags while a couple of these may mitigate for temporary interruptions of power. Figure B-3 illustrates a brief but deep example voltage sag. Sensitive 120V controls may very well drop out for a voltage sag of this magnitude.

[3] Transmission-Distribution Power Quality Report (TPQ-DPQ III)

Event	
Worst-Case RMS	53.2V (44.3%)
Nominal Voltage	120.0V
Duration	180ms (10.8 cycles)
IEEE Classification	Instantaneous Sag
Frequency	60.0 Hz

RMS Data

Channel	Min	Max	% Nominal
1	53.2V	118.0V	44.3%
2	56.8V	117.0V	47.4%
3	54.6V	116.5V	45.5%

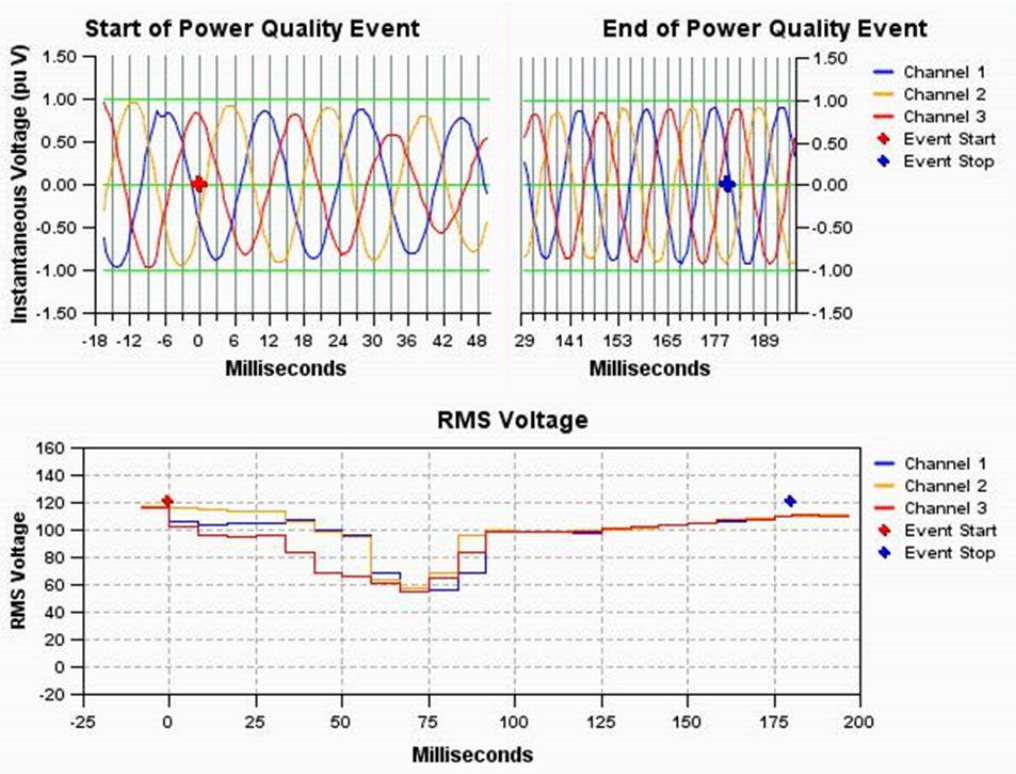

Figure B-3
Example Voltage Sag
Two-phase to Three-phase, 120V System

Thus, sensitive controls systems may cause machinery to drop out due to voltage sags lasting for very brief periods of time. Several mitigation devices designed for $120V_{AC}$ may easily mitigate for this magnitude and duration *with no batteries to maintain*. Several may mitigate for voltage sags down to 50% of nominal voltage for 1 to 3 seconds. One design (the MiniDySC and ProDySC) may support down to 0 volts for periods of 50 milliseconds (standard model) to 200 milliseconds (extended model) due to capacitor storage. The MiniDySC could mitigate any one phase of the brief but deep example voltage sag shown in Figure B-3 while the ProDySC could successfully mitigate all three phases at once. Figure B-4 illustrates the mitigation capabilities of several devices for the control system (the red diamonds represent voltage sags at a given magnitude and duration): the constant voltage transformer (CVT—loaded at 50%), the voltage dip-proofing compensator (VDC), and the two designs of the dynamic sag corrector (MiniDySC—Standard and Extended). Also shown are two devices to mitigate AC “ice cube”

relay sensitivity and/or contactors directly: the Nice Cube and the Coil Lock. The Nice Cube is a direct replacement of the octal relay (other configurations are available) while the Coil Lock is applied to existing contactors.

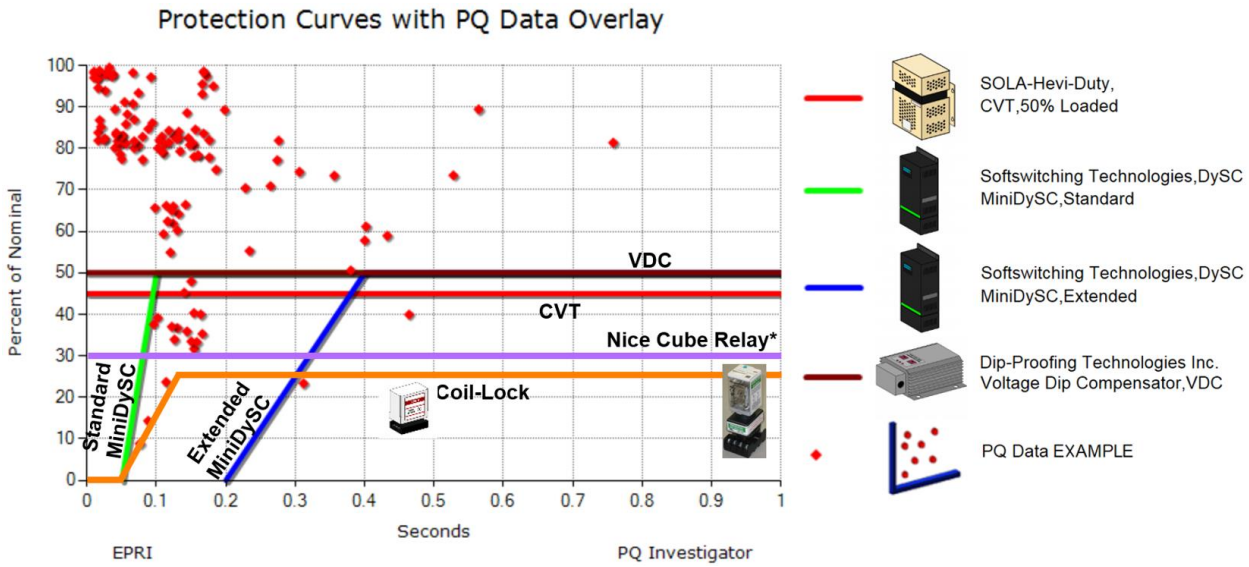

Figure B-4
Voltage Sag Mitigation Devices for Control Systems
Red diamonds represent voltage sags at some magnitude and duration
Colored lines represent the mitigation capabilities of several devices

A double-conversion UPS will provide effective voltage sag mitigation for several minutes to several hours—*if the batteries are maintained*. The main advantage of the battery-less devices is that they do not require maintenance over the life of the device—perhaps 15 to 20 years.

Another option involves protecting multiple controls down to 0 Volts using super capacitor-based UPS units such as a 1 kW or 3 kW unit by Marathon Power. Such an application may be a more economical alternative assuming many sensitive controls cabinets require voltage sag or interruption mitigation until the emergency diesel generators may start and stabilize. This device is capable of supporting loads for 15 seconds at full load and 45 seconds at half load—again, with no battery maintenance required. The 45-second interval could allow for diesel generation to start and stabilize and then have as much as 30 seconds for the transfer of critical loads that cannot be interrupted.

Adjustable Speed Drives (ASD)

ASDs are also known as *variable speed drives* (VSD), *variable frequency drives* (VFD), *inverters*, and simply as *drives*. ASDs may be susceptible to voltage sags; however, many modern ASDs have programming capabilities that may mitigate the effects of voltage sags—specifically, parameter changes that may allow the ASD to ride through the voltage sag by one of several methods. These methods may generally be referred to as *Decel* mode and *Continue* mode.

For *Decel* mode, also called “inertia ride-through,” the ASD attempts to maintain the DC bus voltage at a certain level by regenerating power from the rotating load. More output speed droop

occurs relative to *Continue* mode, yet, for a given sag duration, the DC bus voltage will not droop as much as with *Continue* mode.

For *Continue* mode, the ASD attempts to maintain the rotational speed of the motor load at the expense of the DC bus voltage. Therefore, less output speed droop occurs relative to *Decel* mode while a larger DC bus voltage droop occurs for a given sag duration than for *Decel* mode. The drive is allowed to run at set-speed and load depending on duration of sag and the level of the DC bus voltage droop. However, this option may result in an "undervoltage" fault as the DC bus voltage depletes. Due to the increased output current from the DC bus to maintain load, the ASD may trip on current "Overload." For a given sag duration, the DC bus voltage will not droop as much as with *Continue* mode.

Catch a spinning motor, also called *Flying Restart*, may employ either of the above techniques. In general, the drive releases control of the motor in response to a voltage sag and later synchronizes with the motor at the end of the voltage sag at the rotational speed of the motor at that time, then accelerating the motor back to the operational speed. This capability is illustrated for a two-phase voltage sag at 50% of nominal voltage for 12 cycles in Figure B-5. Default settings may simply drop the motor requiring a manual restart.

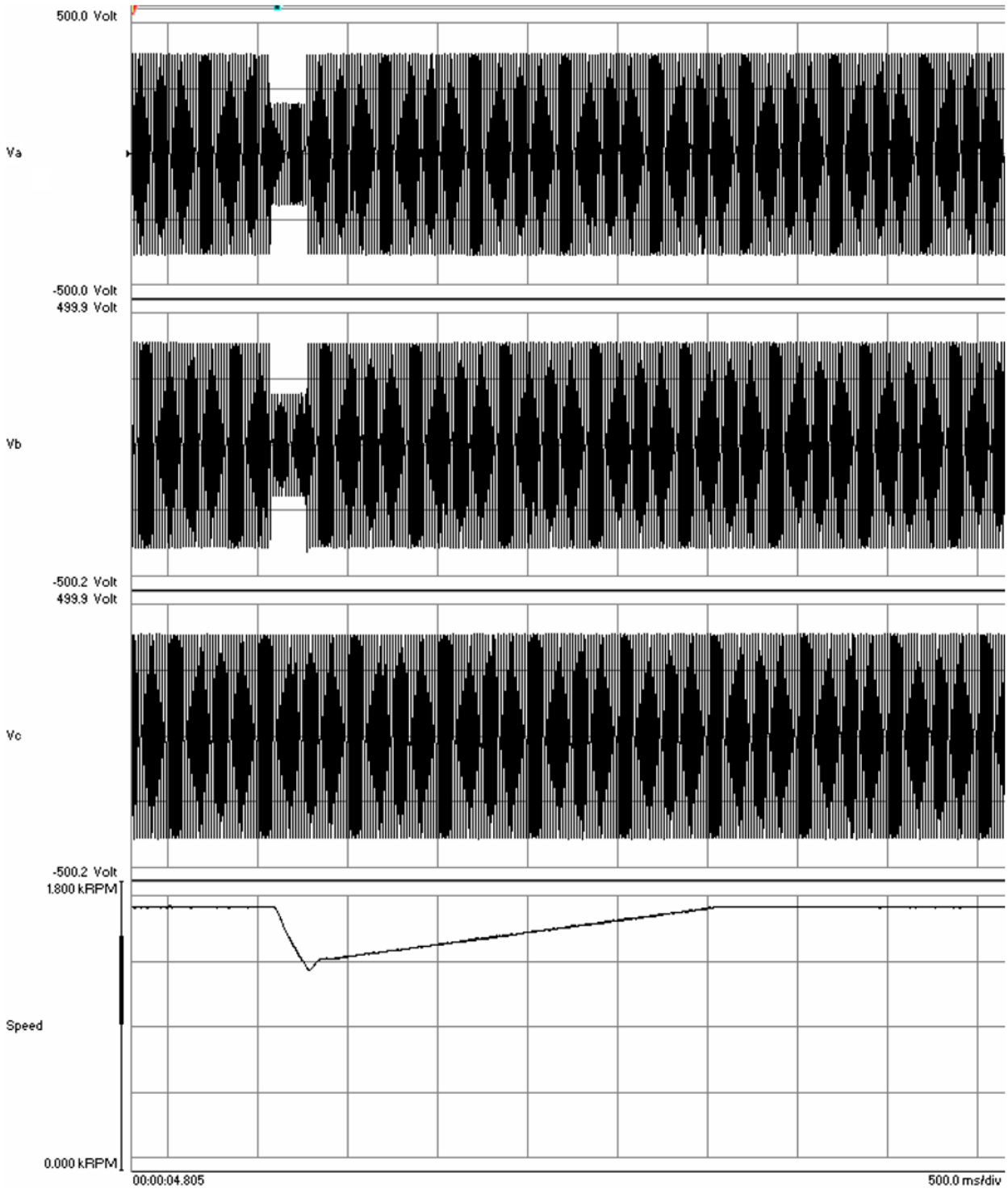

Figure B-5
ASD Settings to Allow Recovery from 2-phase, 12-cycle, 50% Vnom Sag

Other settings may allow the process to recover with little change in speed as indicated in Figure B-6 for the same sag—12 cycles at 50% of nominal voltage. This generally may be called "continue" as the drives continues normal operation.

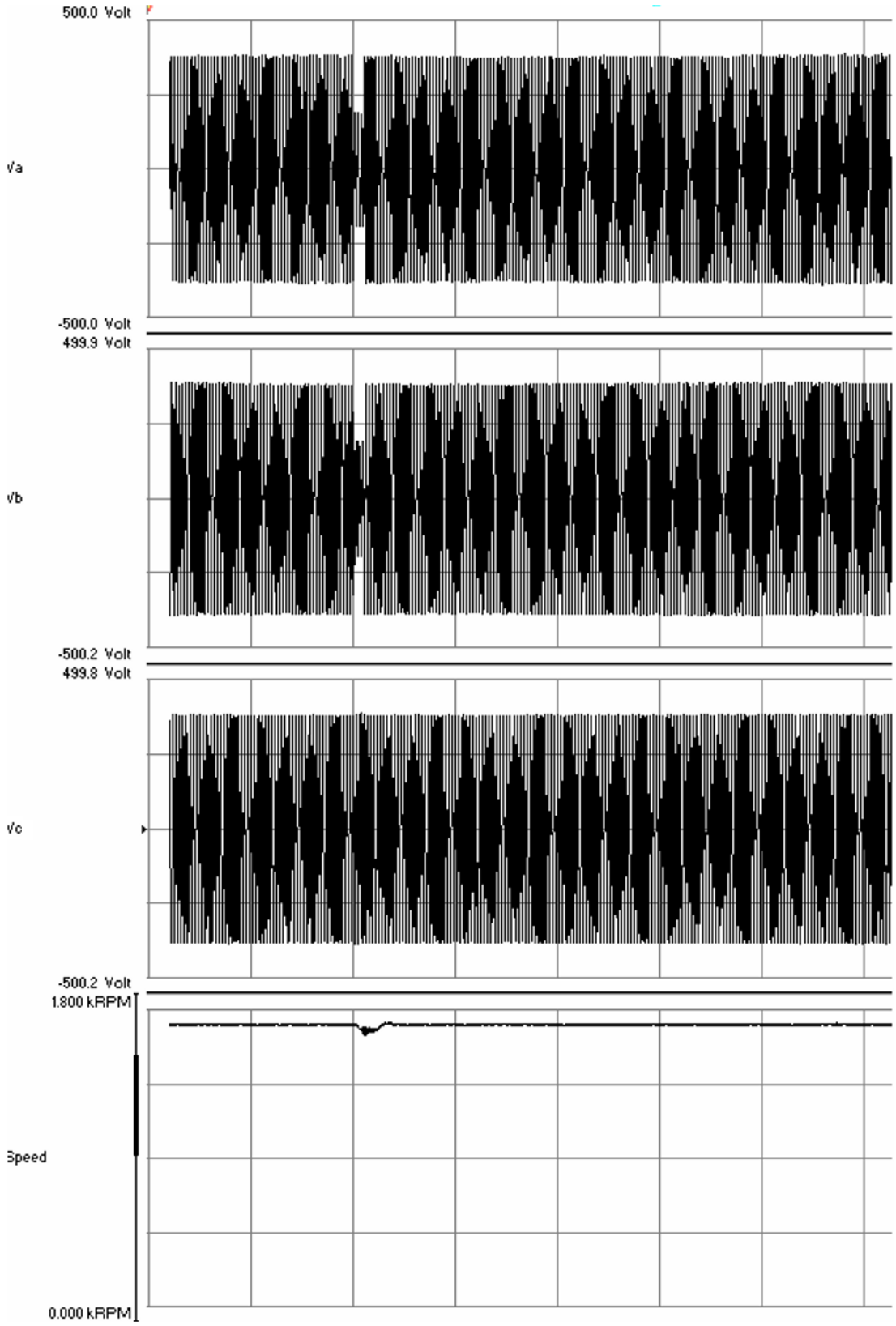

Figure B-6
ASD Settings to Allow Recovery from 2-phase, 12-cycle, 50% Vnom Sag

Where applicable, drive setting changes for specific makes and models of ASDs—as identified by past EPRI investigations and testing involving ASDs—were provided to the member institutions in their site reports.

PQ Mitigation at BNMC

Three possible nonbattery-based options for controls mitigation were suggested for equipment identified as *potentially* being susceptible to voltage sags: application of the MiniDySC, VDC, or CVT. These recommendations may only be necessary for equipment proving itself to be sensitive. The estimated costs for the recommended devices alone[4] may be found in Table B-2.

Table B-2
Mitigation Device Cost Summary

Member Institute	Option 1: MiniDySC	Option 2: VDC	Option 3: CVT
Total for All Members	**$42,398 to $46,915**	**$54,356 to $57,586**	**$41,583 to $42,571**
Kaleida Health facilities	**$16,047 to $20,564**	**$22,548 to $23,678**	**$24,433 to $25,021**
Roswell Park Cancer Institute facilities	**$1,665**	**$4,000 to $6,100**	**$1,800 to $2,200**
University at Buffalo facilities	**$22,493**	**$25,904**	**$14,300**
Hauptman-Woodward Institute	**None identified**	**None identified**	**None identified**
BNMC Properties: Innovation Center	**$2,193**	**$1,904**	**$1,050**
BNMC Properties: Cleveland BioLabs	**None identified**	**None identified**	**None identified**

Individual Member Institutes

Kaleida Health

The controls for several systems were identified that could prove sensitive to voltage sags. Typically, control systems employ small AC or DC relays in emergency off (EMO) and other circuits. DC relays show a far greater level of robustness to voltage sags, whereas AC “ice cube” relays often show significant sensitivity. These “ice cubes” were identified in several controls at KH.

[4] Cost of necessary wiring, labor, conduits, or cabinets not included

Roswell Park

The controls on two processes, the Trane chiller controls and boiler draft fans, were identified that could be sensitive to voltage sags.

Buffalo Niagara Medical Campus

One set of controls was identified at the Innovation Center as possibly being sensitive to voltage sags. None were identified at Cleveland BioLabs; however, most equipment were packaged units that may or may not be sensitive.

University at Buffalo

Some controls were identified as potentially sensitive to voltage sags in the CB (11 air handler controls), CTRC (multiple air handler controls), and RIA (boiler controls and elevator controls).

Hauptman-Woodward Medical Research Institute

Systems at HWI were not found to be particularly susceptible to power quality events such as voltage sags. General suggestions for voltage sag mitigation are provided in all site reports in the event that sensitivities occur in the future.

C
UB PV ASSESSMENT SUMMARY REPORT

One key aspect of the BNMC microgrid concerns the power sources of the microgrid. In the event of a regional emergency resulting in the loss of utility-supplied power for perhaps a long period of time—similar to the effects of Hurricane Sandy in late 2012—the microgrid must be capable of supplying sufficient power to its connected loads. Photovoltaics (PV) may potentially supply a significant proportion of the load during daylight hours thus helping extend the supply of diesel fuel during that period of time.

Thus, the University of Buffalo performed a study of the potential for PV installation in the BNMC environment. *Note that the potential area totals for PV installations provided here may not have been used in their entirety for the ultimate PV analysis provided in the body of this final report*.

UB PV Analysis Report EPRI Final

The software chosen to measure the potential solar panel sites was Google Earth Pro. Utilizing the software's built in measuring tool the areas of the buildings and spaces were measured. Prior to using the software, two test were performed to determine the accuracy of its measurements.

For the first test, the perimeter of the Buffalo General Helipad was measured. The Federal Aviation Administration's information (FFA) for the helipad lists the dimensions as 45 x 45 ft. (13.7m), which is an area of 2,025 ft^2 (188.1 m^2). The Google Earth Pro measurement, shown in Figure C-1, indicates an area of 1,952.96 ft^2 (181.4 m^2), which is an error of 3.56%.

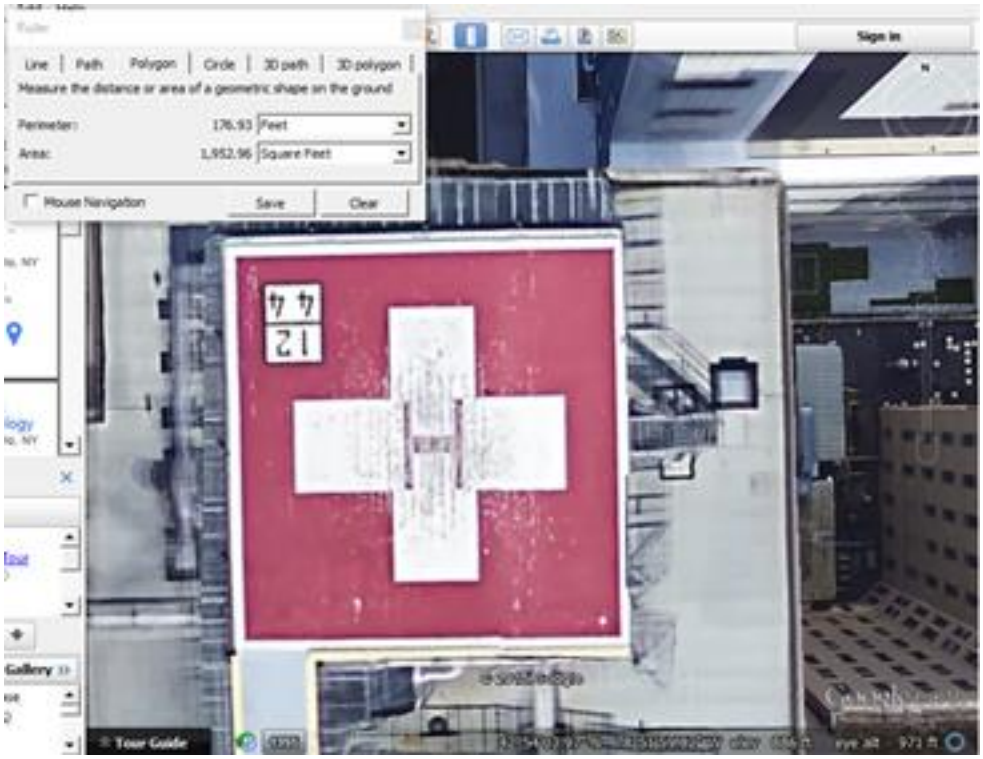

Figure C-1
Buffalo General Helipad on Google Earth Pro

The second test was conducted using Solar Liberty's drawing of the Innovation Center Roof, which can be seen in Figure C-2. The red X in Figure C-2 indicates DIG, which is not included in the area estimation. Solar Liberty lists the area as 20,828 ft^2 (1,935 m^2). Using Google Earth Pro, the area was estimated to be 19,468 ft^2 (1,808.6 m^2), which gives an error of 6.53%. It is unknown whether the Solar Liberty drawing is based upon a site visit, building plans, or a similar software tool.

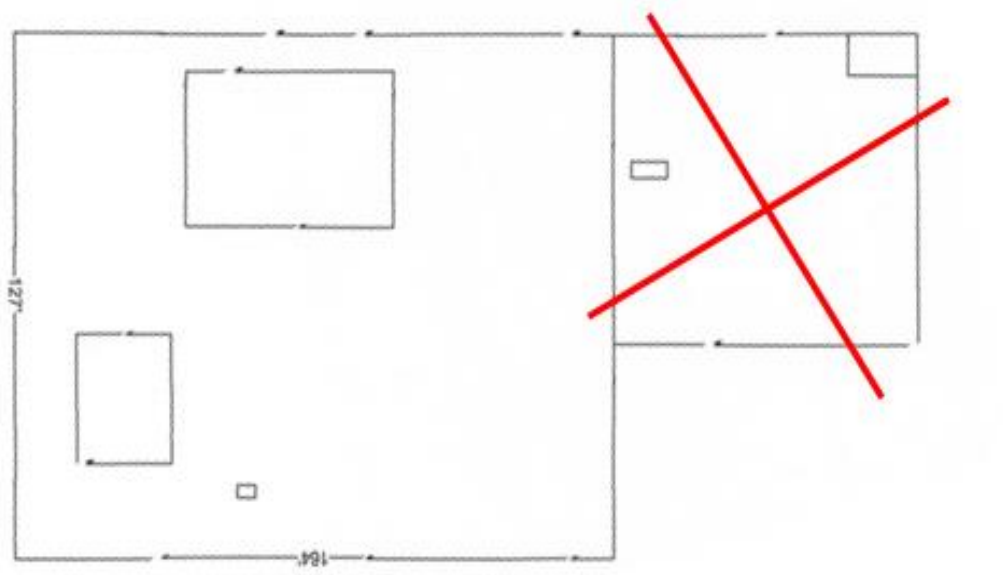

Figure C-2
Solar Liberty's drawing of the Innovation Center's roof area. The red X over DIG is an indication of its non-inclusion of area calculation

Using Google Earth Pro, the usable areas of the rooftops of the BNMC were determined to calculate potential PV generation. Useable area is defined as area on the roof receiving ample sunlight throughout the day and not occupied by rooftop equipment such as: generators, or ventilation equipment. Further calculations in this document only take the rooftop's usable areas into consideration. For the useable area determined for individual buildings, reference the summary in section 5.

To best determine the potential quantity of generated solar energy of each building, a software analysis program was needed. System Advisor Model (SAM), specifically SAM Photovoltaic (detailed) with no financial model, and PV Watts were two software programs tested to determine a reliable and accurate method for solar data acquisition for the Buffalo Niagara Medical Campus (BNMC). The currently implemented and operating solar array at the Innovation Center was used a reference to determine which software would be used. Using Google Earth Pro, the area for the Innovation Center was calculated. Information on the Innovation Center revealed that the current implemented array is using the Sharp NU-U235F1 module and the PV Powered: PVP30KW LV (480) 480V [CEC 2008]. Then using equation 1 and information from the module data sheet, the DC system size was calculated for that specific solar panel.

$$DCSystemSize = Area(m^2) * 1(\frac{kW}{m^2}) * PanelEfficiency$$

Equation 1. DC System Size calculation

With an area of 826.4 m² and a panel efficiency of 14.4% in SAM and 15% in PV Watts, the calculated DC system size was 25.4 kW. The results for the estimated annual energy generated from the Innovation Center solar array model was 27,052 kWh and 28,000 kWh for SAM and PV Watts respectively. According to data provided by the BNMC, the current solar array at the Innovation Center is generating an annual energy of 29.45 MWh. Though the estimation from PV Watts is closer to the actual, PV Watts data did not consider the snowfall losses as SAM did, therefore it does not allow for accurate data acquisition when modeling the solar array. This data reinforces that analysis of sites should be done using SAM. Potential PV calculations are therefore calculated using SAM.

Campus Map Numbering

The campus map used as a reference for all building identification and numbering is included in appendix A. The numbered buildings were then categorized by ownership; i.e. University at Buffalo, Kaleida, BNMC, and Roswell Park Cancer Institute (RPCI). Buildings that are not owned by the previous entities are classified as Other.

Area Estimation

The areas for PV were determined by inspection of the rooftops in Google Earth Pro, as well as site visit data when available. Only spaces that appeared to be clear of equipment, such as vents or generators, and received sunlight throughout most of the day were chosen.

Optimal Tilt and Azimuth

To determine the optimal tilt and azimuth for the BNMC, a parametric analysis was performed in SAM. The DC System Size was set to 250 kWdc, and the tilt was varied from 0-90°, while the azimuth was varied from 0 - 360°. The results for the tilt and azimuth are shown in Figure C-3 and Figure C-4, respectively. The maximum energy was produced at a tilt of 29°, and an azimuth of 180°.

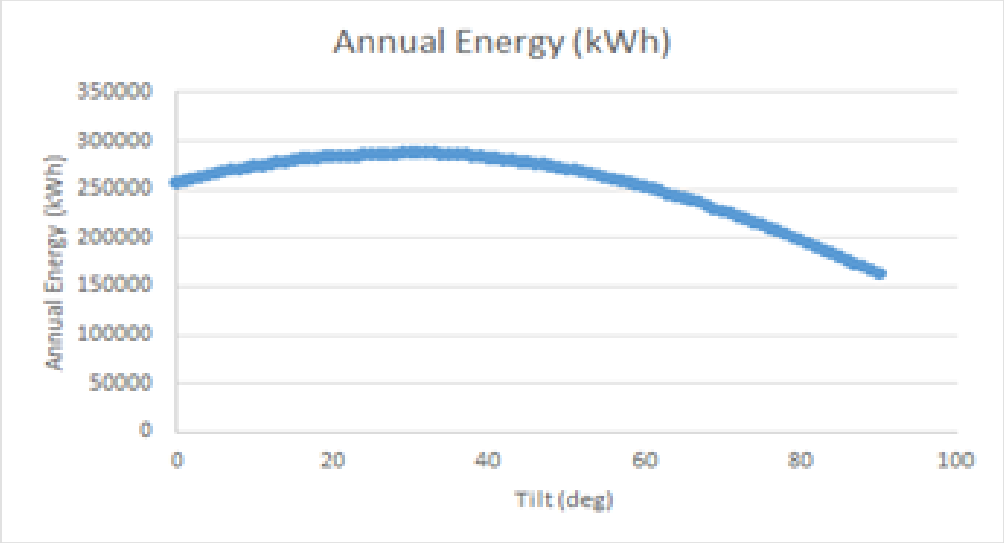

Figure C-3
Annual Energy with respect to the tilt

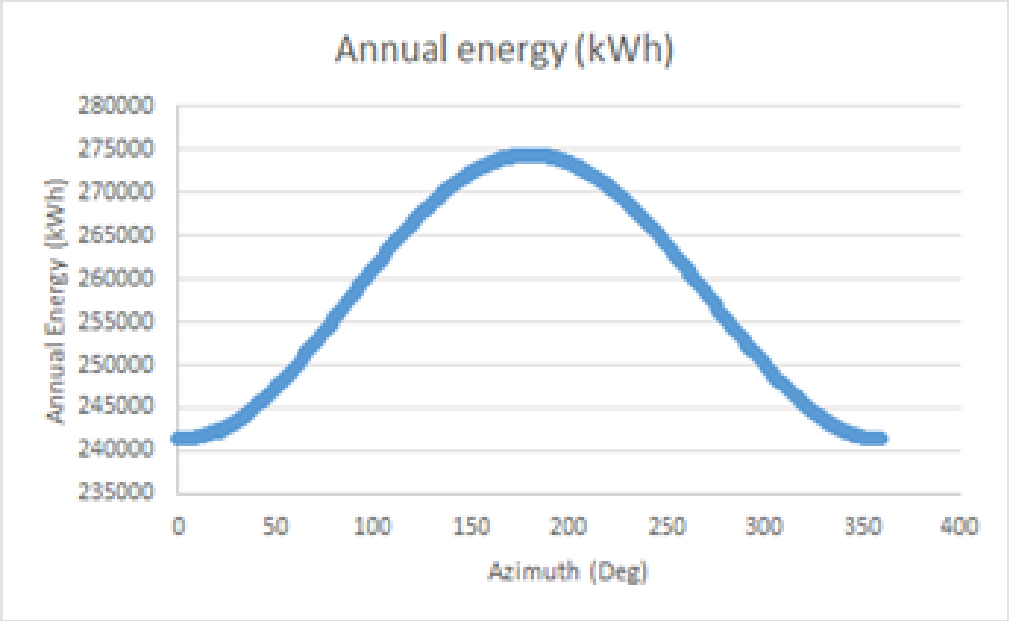

Figure C-4
Annual Energy with respect to the azimuth

Panel Selection

The panel selected for the final PV analysis was decided by choosing a model from the largest manufacturer in the United States, First Solar. The panel chosen was the FS-4105-2 (chosen), which has a maximum output of 105W and an area of 0.72m^2. The datasheet provides power output at 25°C and 45°C. The temperature and efficiency of the panels are inversely related, resulting in less efficiency at higher temperatures, therefore the two temperature values provide an ideal output, at 25°C, as well as a more practical output at 45°C.

Inverter Selection

The inverter was also selected by choosing a model from the largest manufacturer in the United States, SMA America. The Inverter chosen was the STP24000TL-US-10 (480v) (Inverter).

The specific output numbers will change based on the type of panel and inverter selected, but this panel and inverter should give an approximate estimate about the potential energy that could be generated using PV.

Estimating PV capacity

To estimate the capacity for PV based on a given area, an estimation, given by EPRI, was used to calculate the capacity in kWdc. This estimation is shown in equation/eq.

$$Capacity(kWdc) = \frac{\frac{TotalAvailableSpace(m^2)}{2}}{PanelArea(m^2) * PanelRating(kWdc)}$$

Equation 2. Capacity Estimation

Peak Power Estimation

To determine the peak power, hourly values for Array Power (DC) (kW) in SAM were generated for three buildings. The maximum value was shown to be 2% greater than the DC system size. This 2% value was used as an estimate for calculating the peak power for all the buildings.

Final Assumptions

DC-AC Ratio: 1.2

Weather: USA NY Buffalo (TMY2)

Estimated losses due to snow is applied using SAM

All other configurable losses: Default for String Inverters (4.4%)

Analysis performed using SAM PV (detailed)

PV area determined using site visit data and Google Earth Pro

Building Format

In appendix B, each building is provided with the following information: Building number based on the BNMC Map, Name, Entity, Area (m^2), Annual Energy (kWh/yr) at 25°C, Annual Energy (kWh/yr) at 45°C, Peak Power (kWdc) at 25°C, and Peak Power (kWdc) at 45°C. An image of the area from Google Earth Pro is also provided, with a blue polygon used to mark the space considered in this study, along with, when applicable, information about how the area was chosen.

The next section will summarize the results of the individual buildings that were analyzed, using the selected panel and inverter. The buildings are sorted by entity.

Three homes were chosen from the Fruit Belt to show the amount of roof space an average home has on the roof to place solar panels. The roof areas along with annual energy and array size is presented in Table C-1. All of the same SAM analysis methods that were used for the BNMC were used for the Fruit Belt. The area measured in Google Earth Pro is flat. Since the roofs are slanted, the area was multiplied by $\sqrt{2}$, assuming a 45° slanted roof. Detailed information for the Fruit Belt homes is located in appendix C.

Table C-1: Fruit Belt Homes

Address	Area (m^2)	Array Size (kWdc)	Annual Energy (kWh/yr) @25C	Annual Energy (kWh/yr) @45C
248 Peach St	45.1	3.3	3254.6	2115.6
281 Peach St	48.8	3.6	3254.6	2115.6
Orange St	54.6	4.0	4394.2	3254.6

Below in Table C-2 through Table C-6 are summaries of all information obtained. All buildings have been grouped by entity (ownership) displaying the total number of buildings, area, annual energy and peak power respectively for every building that was the analysis was performed on. For information regarding each building individually, see the section following on Comprehensive Building Information. Specific information in regards to all recorded data and equipment consisting of photos, audio files and documents are available.

Table C-2
BNMC

Number	Building	Area (m^2)	Annual Energy (kWh/yr) @25C	Annual Energy (kWh/yr) @ 45C	Peak Power (kWdc) @ 25C	Peak Power (kWdc) @ 45C
1	Innovation Center	881	74,158.7	56,486.3	65.5	48.9
2	DIG	428	35,716.0	27,122.0	31.8	23.7
6	Innovation Center Annex	1,743	148,317.0	110,795.0	129.6	96.7
14	BNMC Green Commons	37.97	2,115.6	2,115.6	2.8	2.1
16	Cleveland BioLabs	190.1	15,777	979.5	14.1	10.5
28	Employee Parking	6,624	573,700.0	424,830.0	492.7	367.4

Table C-3
Kaleida

Number	Building	Area (m^2)	Annual Energy (kWh/yr) @25C	Annual Energy (kWh/yr) @ 45C	Peak Power (kWdc) @ 25C	Peak Power (kWdc) @ 45C
20	Oishei Children's Hospital	1096.75	94,812.0	70,486.0	81.6	60.8
21	Buffalo General Medical Center	2,532.85	217,077	163,453	188.4	140.5
22	Community Mental Health and Service Response Center	962.7	79,785.0	62,103.0	71.6	53.4
25	Patient and Visitor Parking	4,148	356,230	267,897	308.5	230.1
29	Highpointe on Michigan	670	57,616.6	40,619.0	49.8	37.2

Table C-4
RPCI

Number	Building	Area (m^2)	Annual Energy (kWh/yr) @25C	Annual Energy (kWh/yr) @ 45C	Peak Power (kWdc) @ 25C	Peak Power (kWdc) @ 45C
10	Roswell Park Cancer Institute	4,245.7	368,098.0	274,071.0	315.8	235.5
12	Roswell Park Center for Genetics and Pharmacology	311	28,243.2	21,451.0	24.6	18.4
30	Roswell Park Clinical Sciences Center	102.75	7,813.0	5,534.0	7.6	5.7
31	Roswell Park Patient and Visitor Parking	7,531	651,425	484,627	560.1	417.7

Table C-5
UB

Number	Building	Area (m^2)	Annual Energy (kWh/yr) @25C	Annual Energy (kWh/yr) @ 45C	Peak Power (kWdc) @ 25C	Peak Power (kWdc) @ 45C
3	UB Educational Opportunity Center	186	15777	11229	13.8	10.3
4	UB Downtown Gateway	958	79,037.6	62,103.6	71.3	53.1
9	Hauptman-Woodward Medical Research Institute	238	20,317.2	14,640.7	17.7	13.2
9	Parking near Hauptman-Woodward	9,335	808,893	603,290	694.3	517.7
11	UB New York State Center of Excellence in Bioinformatics and Life Sciences	453.1	32,690.5	23,717.1	28.2	21.1
13	UB Jacobs School of Medicine & Biomedical Science	890	75,026.0	57,617.0	66.2	49.4
23	UB Research Institute on Addictions	214.7	22,584.3	16,912.8	19.8	14.7
27	Olmsted Center for Sight/Ross Eye Institute	638.9	55,355.7	39,136.2	47.5	35.4

Table C-6
Other

Number	Building	Area (m^2)	Annual Energy (kWh/yr) @25C	Annual Energy (kWh/yr) @ 45C	Peak Power (kWdc) @ 25C	Peak Power (kWdc) @ 45C
7	ZeptoMetrix	69.3	5,534.0	4,394.2	5.2	3.8
8	Health Clinic	943.8	78,272.3	60,990.8	70.2	52.3
15	Kevin Guest House	38.9	2,115.6	2,115.6	2.9	2.2
17	Buffalo Medical Group	541	42,640.1	34,757.2	40.2	30.0
18	Doubletree Club Hotel	206.2	16,912.8	12,366.7	15.3	11.4
19	Conventus	436	36,633.7	28,243.2	32.4	24.2
24	Buffalo Hearing & Speech Center	856	72,359.1	55,355.7	63.7	47.5
	Parking near 28 & 29	3,975	343,597	253,715	295.6	220.5

Comprehensive Building Information

BNMC Map

This map depicts the Buffalo Niagara Medical Campus. This image was used as reference for all building identification and labeling. Using the Map Key each building was given a respective number and was then later categorized by building ownership; i.e. University at Buffalo, Kaleida, BNMC, and Roswell Park Cancer Institute (RPCI).

Comprehensive Building List

Building Number: 1

Innovation Center

Entity: BNMC

Area (m^2): 881

Annual Energy (kWh/yr) @25C: 74,158.70

Annual Energy (kWh/yr) @45C: 56,486.30

Peak Power (kWdc) @25C: 65.5

Peak Power (kWdc) @45C: 48.9

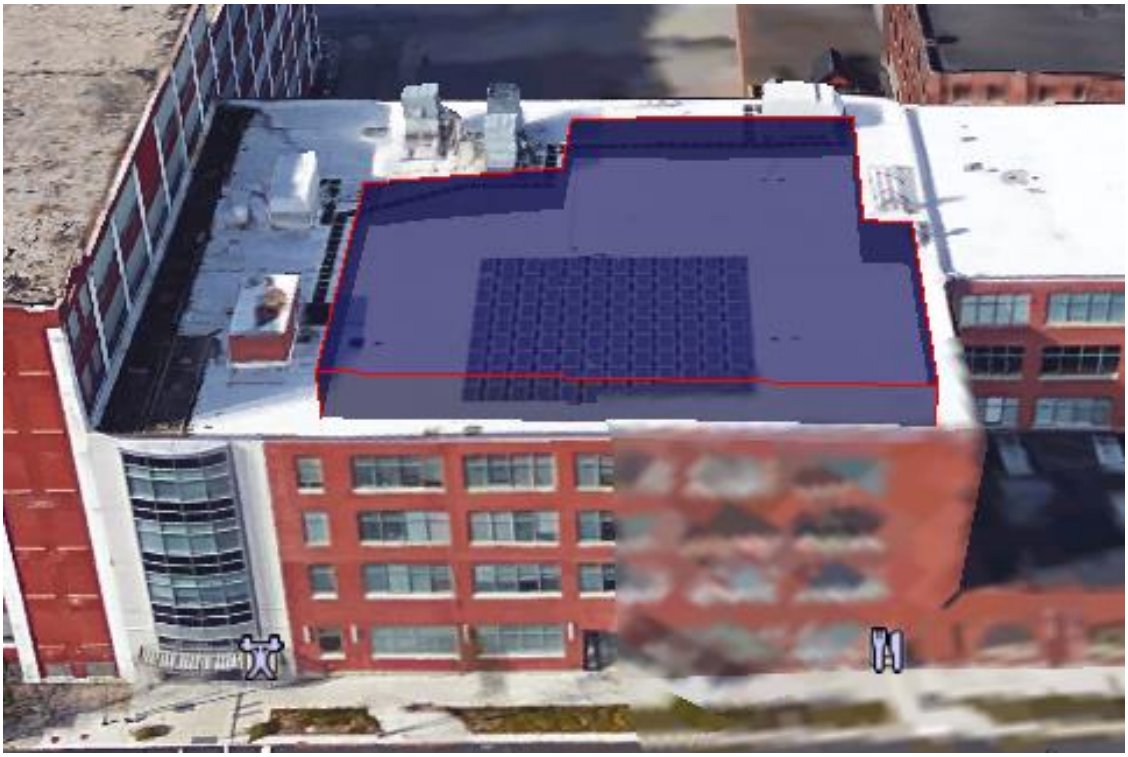

Building Number: 2

DIG

Entity: BNMC

Area (m^2): 428

Annual Energy (kWh/yr) @25C: 35,716

Annual Energy (kWh/yr) @45C: 27,122

Peak Power (kWdc) @25C: 31.8

Peak Power (kWdc) @45C: 23.7

Building Number: 3

UB Educational Opportunity Center

Entity: UB

Area (m^2): 186

Annual Energy (kWh/yr) @25C: 15,777

Annual Energy (kWh/yr) @45C: 11,229

Peak Power (kWdc) @25C: 13.8

Peak Power (kWdc) @45C: 10.3

Building Number: 4

UB Downtown Gateway

Entity: UB

Area (m^2): 958

Annual Energy (kWh/yr) @25C: 79,037.6

Annual Energy (kWh/yr) @45C: 62,103.6

Peak Power (kWdc) @25C: 71.3

Peak Power (kWdc) @45C: 53.1

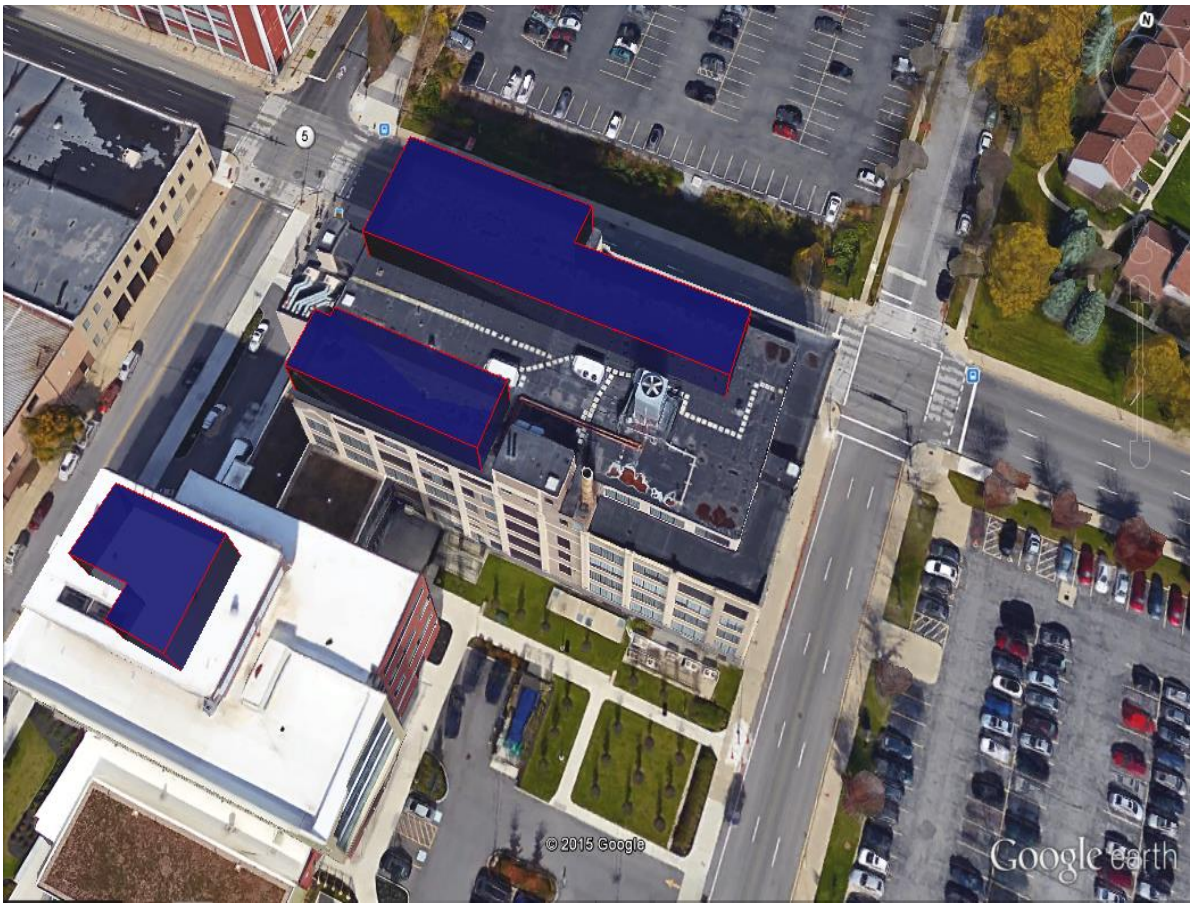

Data was recorded for the 1st through 4th floor mechanical rooms.

Building Number: 5

Visitor and Employee Parking

Entity: BNMC

Area (m^2): 11,157

Annual Energy (kWh/yr) @25C: 965,273

Annual Energy (kWh/yr) @45C: 719,943

Peak Power (kWdc) @25C: 829.8

Peak Power (kWdc) @45C: 618.8

Solar only placed over parking spots.

Building Number: 6

Innovation Center Annex

Entity: BNMC

Area (m^2): 1,743

Annual Energy (kWh/yr) @25C: 148,317.0

Annual Energy (kWh/yr) @45C: 110,795.0

Peak Power (kWdc) @25C: 129.7

Peak Power (kWdc) @45C: 96.7

Equipment sticks out of the roof, which accounts for the shape.

Building Number: 7

ZeptoMetrix

Entity: Other

Area (m^2): 69.3

Annual Energy (kWh/yr) @25C: 5,534.00

Annual Energy (kWh/yr) @45C: 4,394.20

Peak Power (kWdc) @25C: 5.2

Peak Power (kWdc) @45C: 3.8

Building Number: 8

Health Clinic

Entity: Other

Area (m^2): 943.8

Annual Energy (kWh/yr) @25C: 78,272.30

Annual Energy (kWh/yr) @45C: 60,990.80

Peak Power (kWdc) @25C: 70.2

Peak Power (kWdc) @45C: 57.3

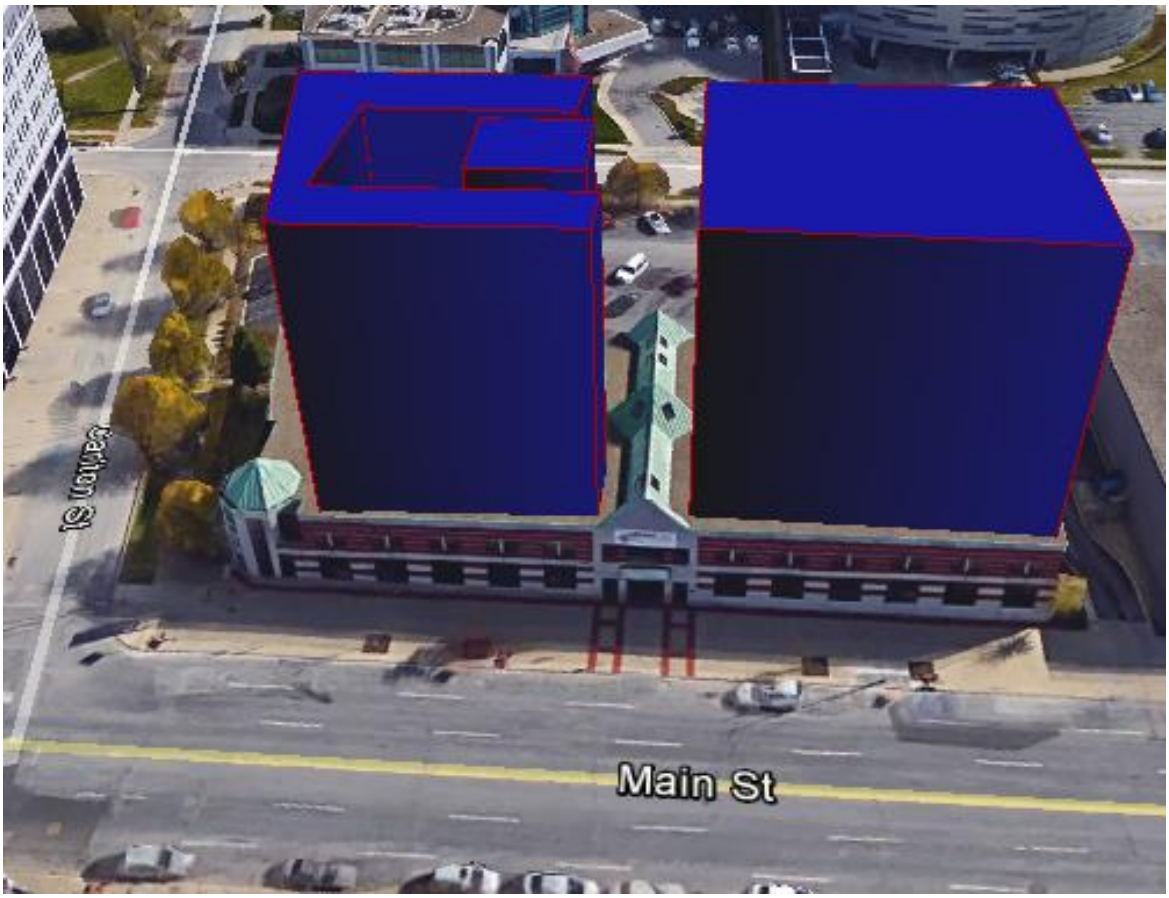

Building Number: 9

Hauptman-Woodward Medical Research Institute

Entity: UB

Area (m^2): 238

Annual Energy (kWh/yr) @25C: 20,347

Annual Energy (kWh/yr) @45C: 14,640

Peak Power (kWdc) @25C: 17.7

Peak Power (kWdc) @45C: 13.2

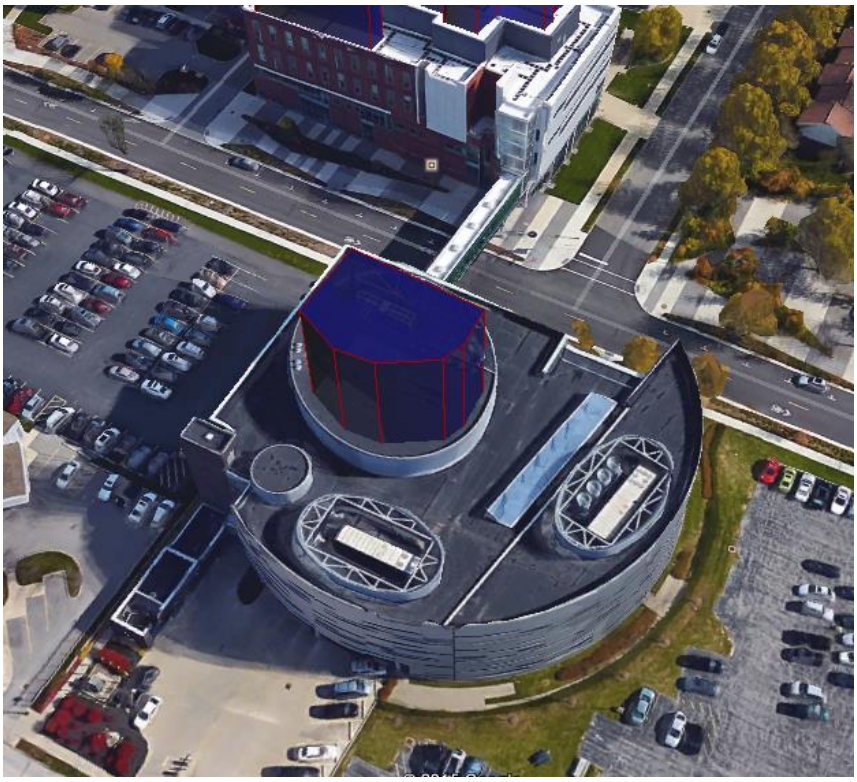

Though the site visit photos and audio indicated there was no space, the area outlined here was not visited, and was chosen solely based on Google Earth images. Labs, offices, maintenance rooms and areas where mechanical and electrical equipment are kept were visited.

Building Number: 9

Parking Lot near HWI

Entity: UB

Area (m^2): 9,335

Annual Energy (kWh/yr) @25C: 808,893.0

Annual Energy (kWh/yr) @45C: 603,290.0

Peak Power (kWdc) @25C: 694.3

Peak Power (kWdc) @45C: 517.7

Building Number: 10

Roswell Park Cancer Institute

Entity: RPCI

Area (m^2): 4,245.7

Annual Energy (kWh/yr) @ 25C: 368,098

Annual Energy (kWh/yr) @ 45C: 274,071

Peak Power (kWdc) @ 25C: 315.8

Peak Power (kWdc) @ 45C: 235.5

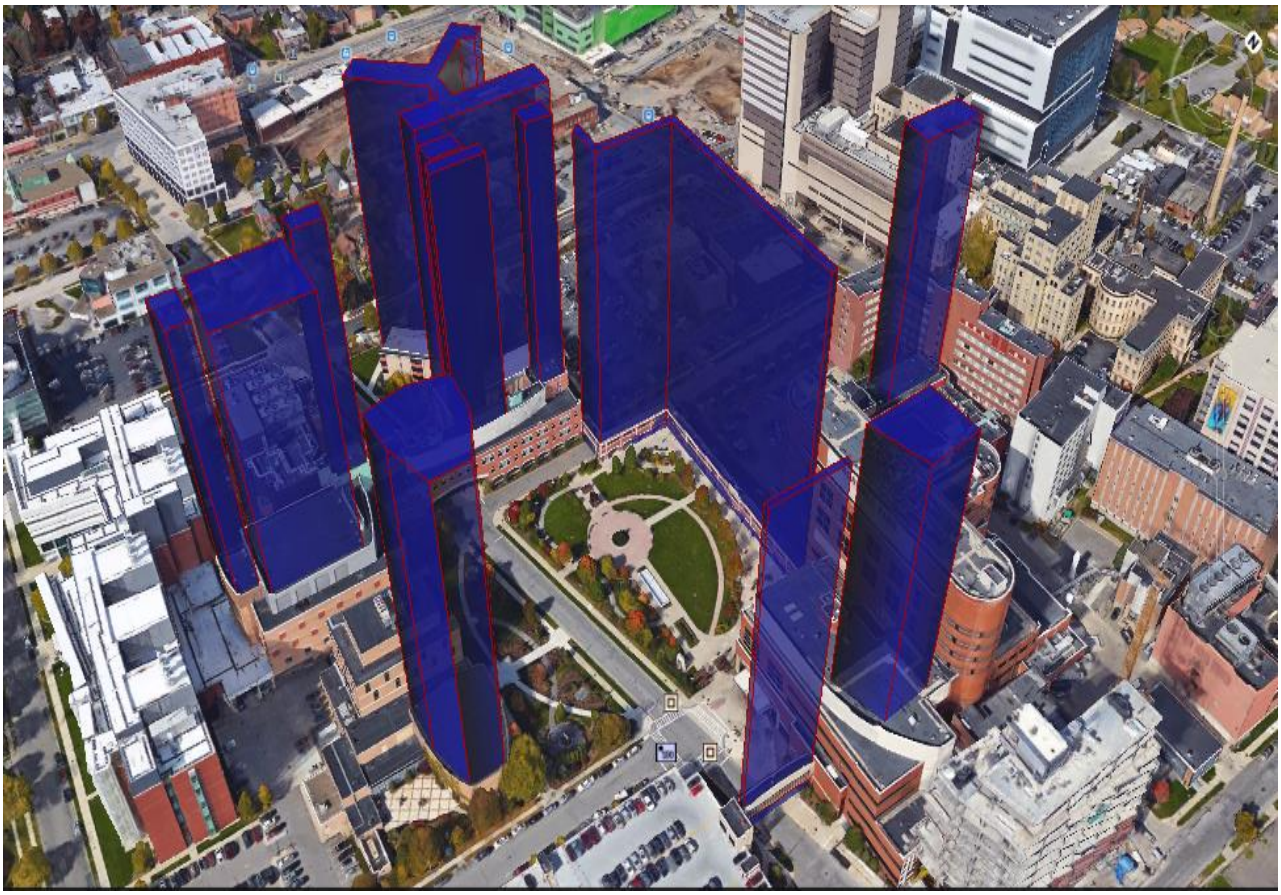

Grace, substation, power plant, and ASB are all shaded or have no roof space. Tall roof of hospital has only a small amount of space in the center, so no space was used for it.

Building Number: 11

UB NYS Center of Excellence for Bioinformatics and Life Sciences

Entity: UB

Area (m^2): 379.6

Annual Energy (kWh/yr) @25C: 32,690.5

Annual Energy (kWh/yr) @45C: 23,717.1

Peak Power (kWdc) @25C: 28.2

Peak Power (kWdc) @45C: 21.1

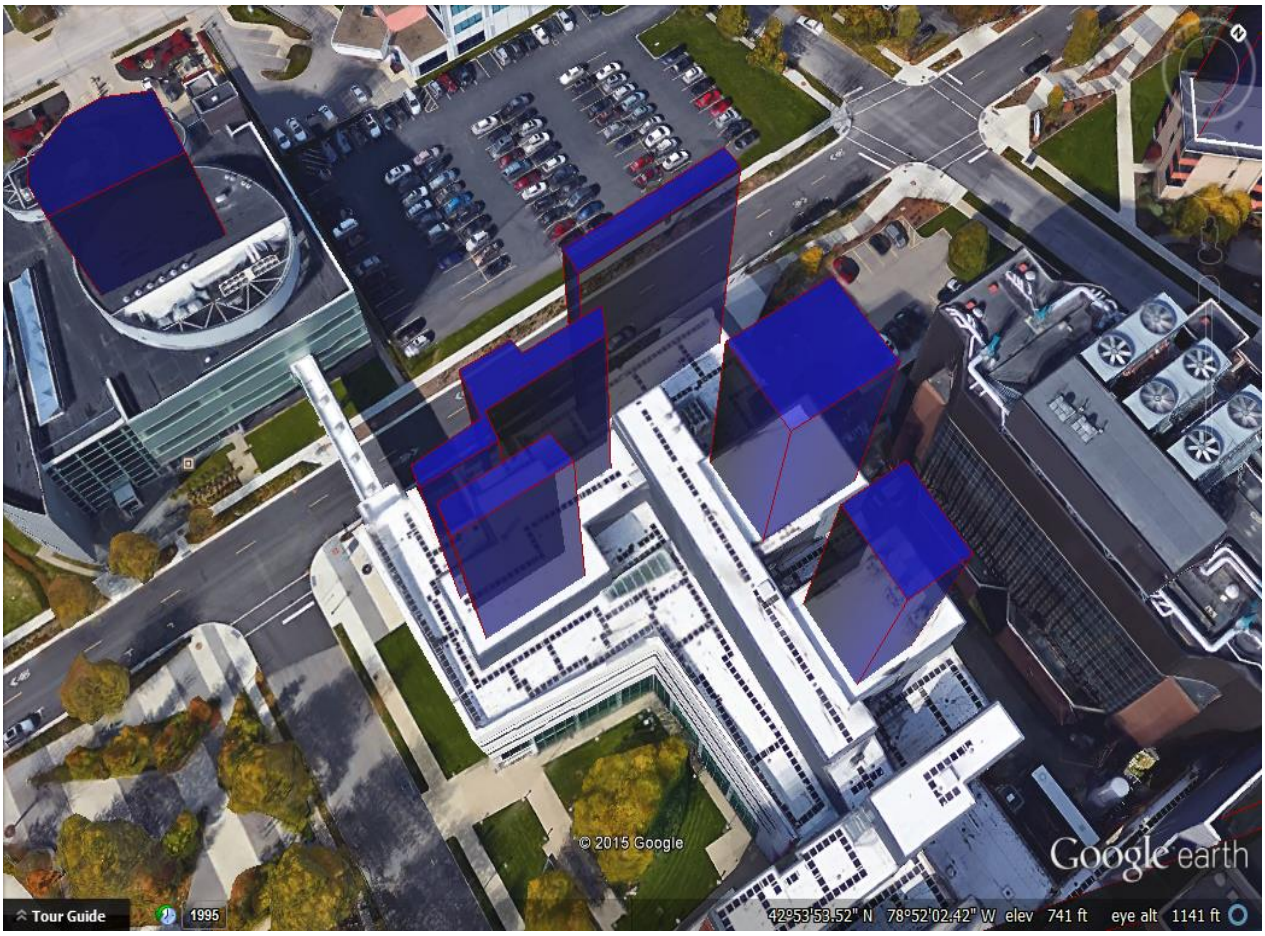

Building Number: 12

Roswell Park Center for Genetics and Pharmacology

Entity: RPCI

Area (m^2): 331

Annual Energy (kWh/yr) @ 25C: 28,243.2

Annual Energy (kWh/yr) @ 45C: 21,451

Peak Power (kWdc) @ 25C: 24.6

Peak Power (kWdc) @ 45C: 18.4

Building Number: 13

UB Jacobs School of Medicine & Biomedical Sciences

Entity: UB

Area (m^2): 890 @ 25% of total area

Annual Energy (kWh/yr) @25C: 75,026

Annual Energy (kWh/yr) @45C: 57,617

Peak Power (kWdc) @25C: 66.2

Peak Power (kWdc) @45C: 49.4

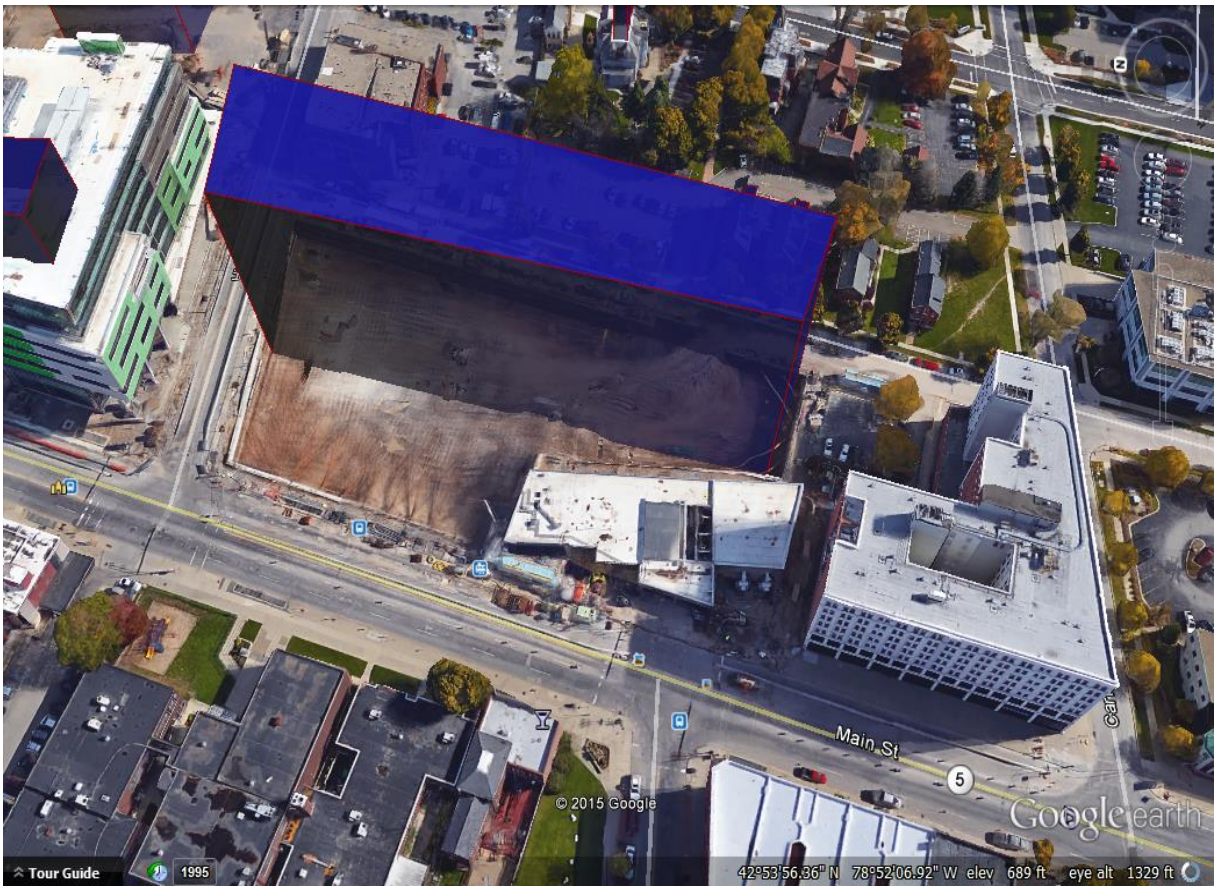

Since the building is still under construction, the area for solar was chosen to be 25% of the ground area.

Building Number: 14

BNMC Green Commons

Entity: BNMC

Area (m^2): 37.97

Annual Energy (kWh/yr) @25C: 2,115.6

Annual Energy (kWh/yr) @45C: 2,115.6

Peak Power (kWdc) @25C: 2.8

Peak Power (kWdc) @45C: 2.1

Building Number: 15

Kevin’s Guest House

Entity: Other

Area (m^2): 38.9

Annual Energy (kWh/yr) @25C: 2,115.60

Annual Energy (kWh/yr) @45C: 2,116.60

Peak Power (kWdc) @25C: 2.9

Peak Power (kWdc) @45C: 2.2

Building Number: 16

Cleveland BioLabs

Entity: BNMC

Area (m^2): 109.1

Annual Energy (kWh/yr) @25C: 15,777

Annual Energy (kWh/yr) @45C: 979.5

Peak Power (kWdc) @25C: 14.1

Peak Power (kWdc) @45C: 10.5

There was a lot of equipment on the roof, so the space chosen were larger areas that did not contain equipment.

Building Number: 17

Buffalo Medical Group

Entity: Other

Area (m^2): 541

Annual Energy (kWh/yr) @25C: 42,640.10

Annual Energy (kWh/yr) @45C: 34,757.20

Peak Power (kWdc) @25C: 40.2

Peak Power (kWdc) @45C: 30.0

Building Number: 18

DoubleTree Club Hotel

Entity: Other

Area (m^2): 206.2

Annual Energy (kWh/yr) @25C: 16,912.80

Annual Energy (kWh/yr) @45C: 12,336.70

Peak Power (kWdc) @25C: 15.3

Peak Power (kWdc) @45C: 11.4

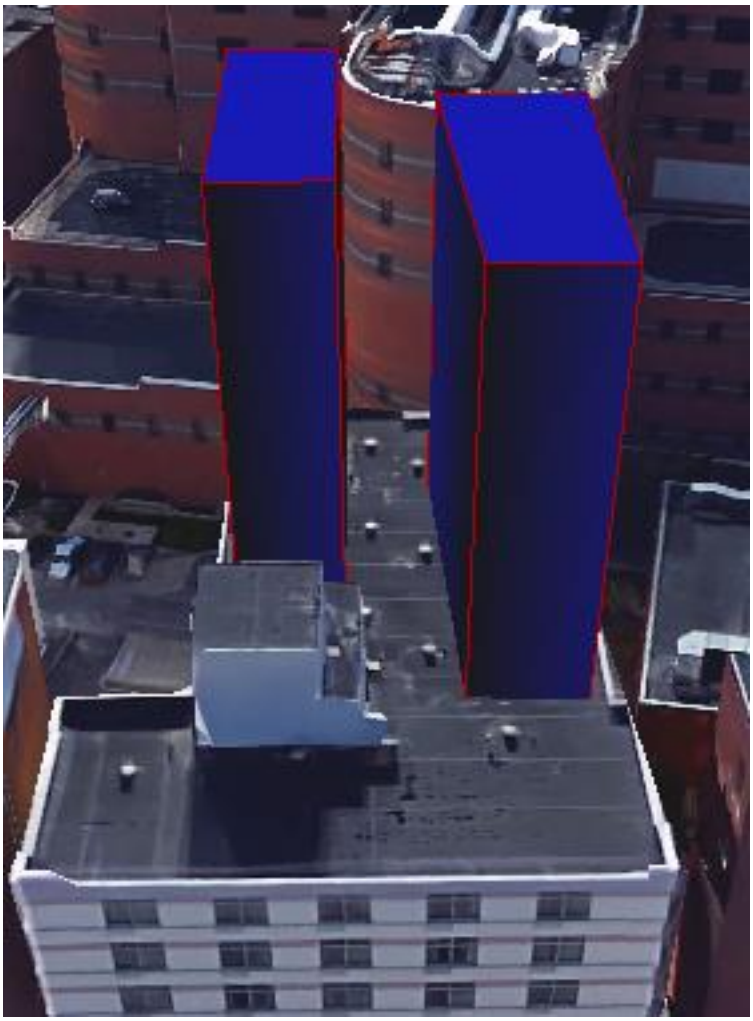

Building Number: 19

Conventus

Entity: Other

Area (m^2): 436

Annual Energy (kWh/yr) @25C: 36,633

Annual Energy (kWh/yr) @45C: 28,243

Peak Power (kWdc) @25C: 32.4

Peak Power (kWdc) @45C: 24.2

Building Number: 20

Oishei Children's Hospital

Entity: Kaleida Health

Area (m^2): 1096.75 @ 25% of total area

Annual Energy (kWh/yr) @25C: 94,812

Annual Energy (kWh/yr) @45C: 70,486

Peak Power (kWdc) @25C: 81.6

Peak Power (kWdc) @45C: 60.8

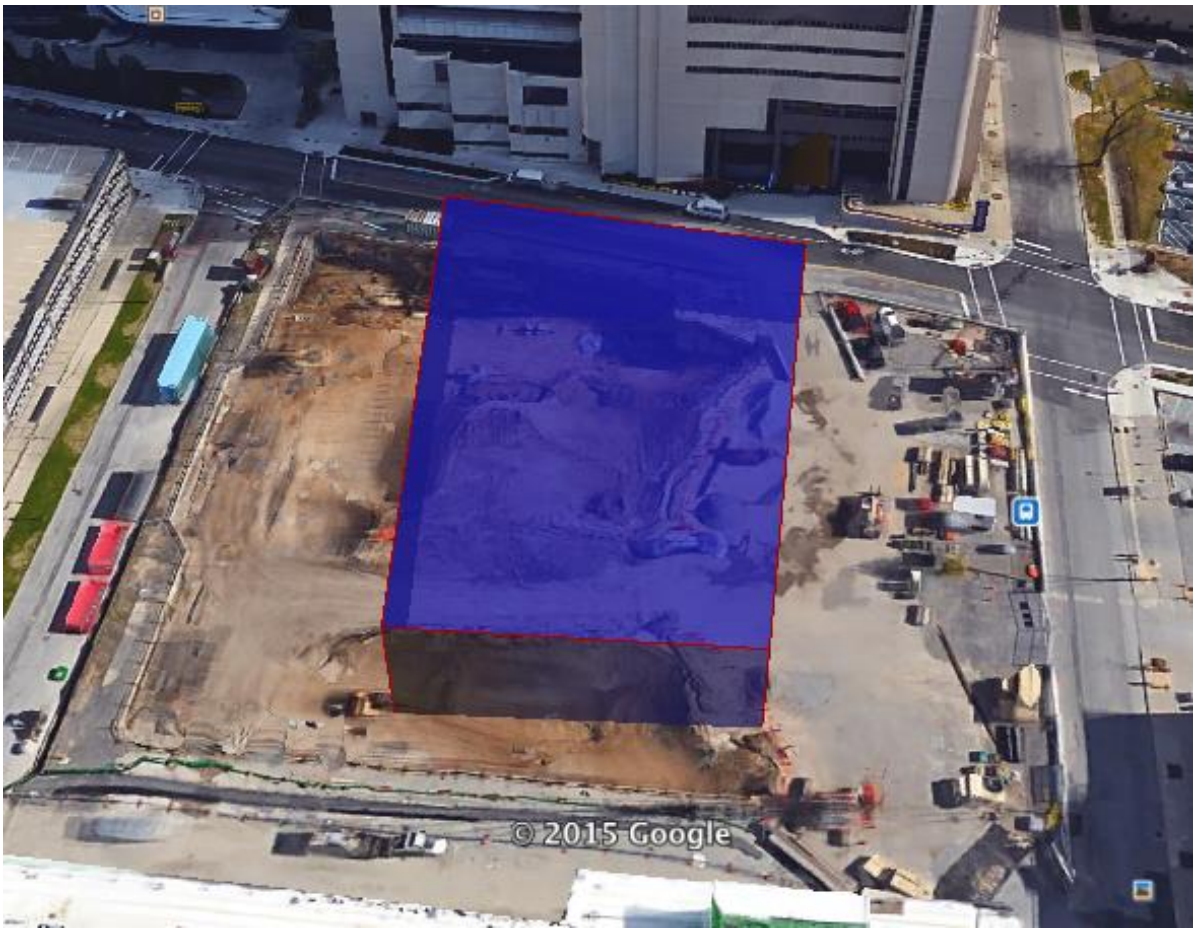

Since the building is still under construction, the area for solar was chosen to be 25% of the ground area.

Building Number: 21

Buffalo General Medical Center

Entity: Kaleida Health

Area (m^2): 2,532.85

Annual Energy (kWh/yr) @25C: 217,077

Annual Energy (kWh/yr) @45C: 163,453

Peak Power (kWdc) @25C: 188.4

Peak Power (kWdc) @45C: 140.5

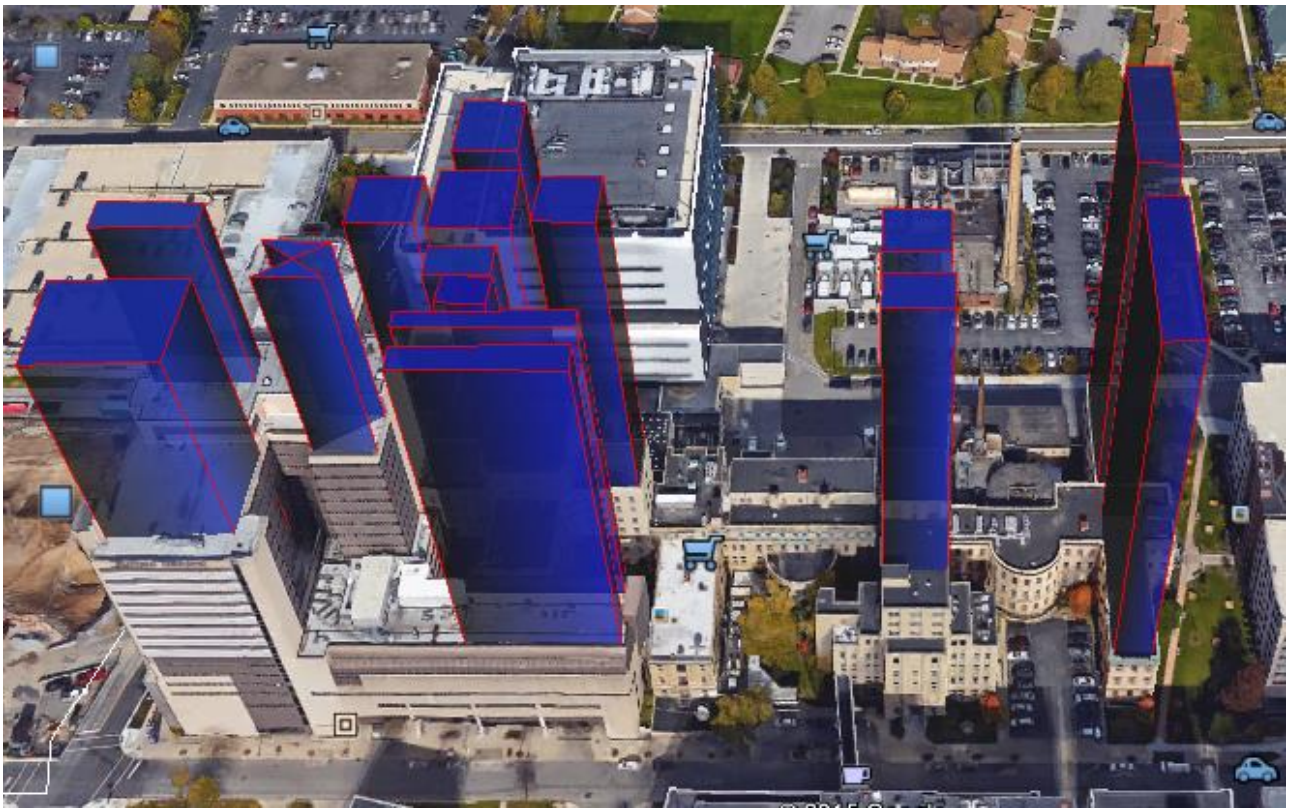

Building Number: 22

Community Mental Health and Service Response Center

Entity: Kaleida Health

Area (m^2): 962.7

Annual Energy (kWh/yr) @25C: 79,785

Annual Energy (kWh/yr) @45C: 62,103

Peak Power (kWdc) @25C: 71.6

Peak Power (kWdc) @45C: 53.4

Building Number: 23

UB Research Institute on Addictions

Entity: UB

Area (m^2): 265.6

Annual Energy (kWh/yr) @25C: 22,584.3

Annual Energy (kWh/yr) @45C: 16,912.8

Peak Power (kWdc) @25C: 19.8

Peak Power (kWdc) @45C: 14.7

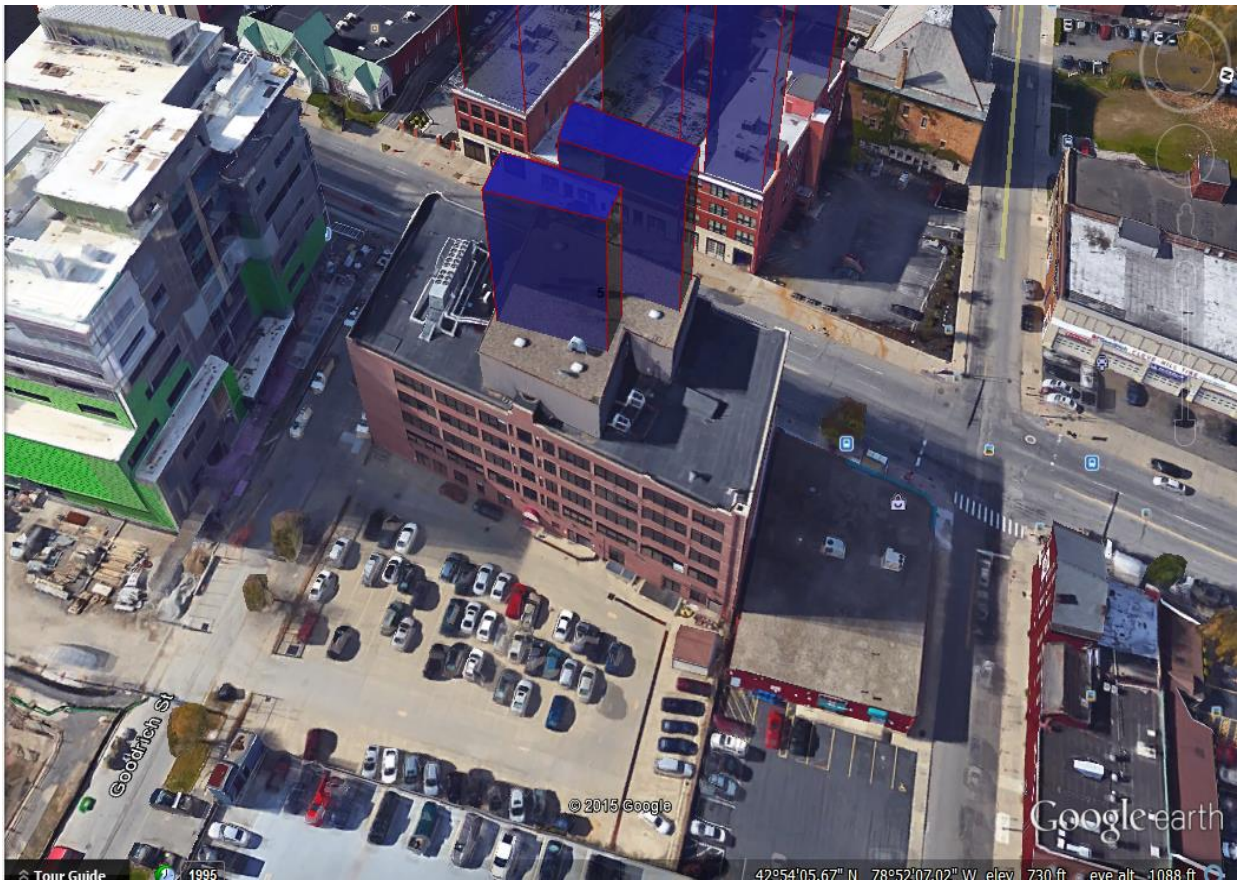

Building Number: 24

Buffalo Hearing and Speech Center

Entity: Other

Area (m^2): 856

Annual Energy (kWh/yr) @25C: 72,359

Annual Energy (kWh/yr) @45C: 55,355

Peak Power (kWdc) @25C: 63.7

Peak Power (kWdc) @45C: 47.5

Building Number: 25

Patient and Visitor Parking

Entity: Kaleida Health

Area (m^2): 4,148

Annual Energy (kWh/yr) @25C: 356,230

Annual Energy (kWh/yr) @45C: 267,897

Peak Power (kWdc) @25C: 308.5

Peak Power (kWdc) @45C: 230.1

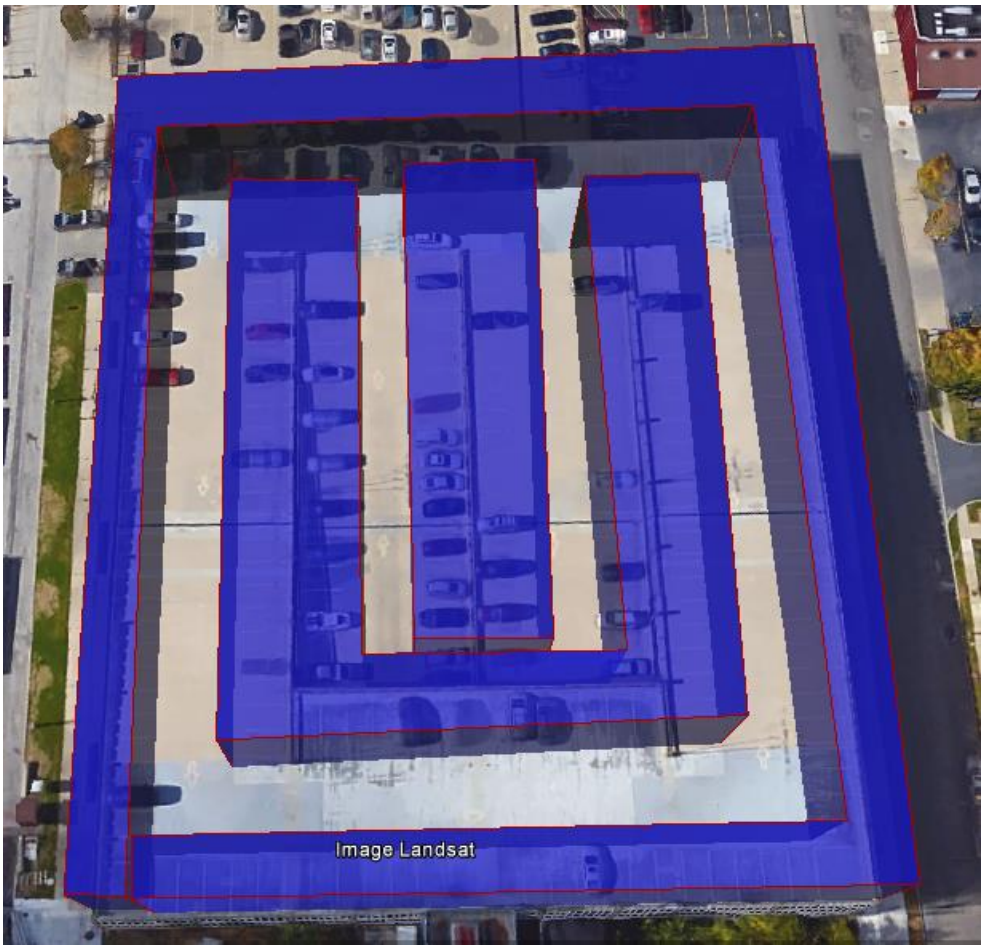

Solar was placed only over parking spots.

Building Number: 26

Gates Vascular Institute, UB Clinical and Translational Research Center

Entity: Kaleida/UB

Area (m^2): 503

Annual Energy (kWh/yr) @25C: 40,619

Annual Energy (kWh/yr) @45C: 31,604

Peak Power (kWdc) @25C: 37.4

Peak Power (kWdc) @45C: 27.9

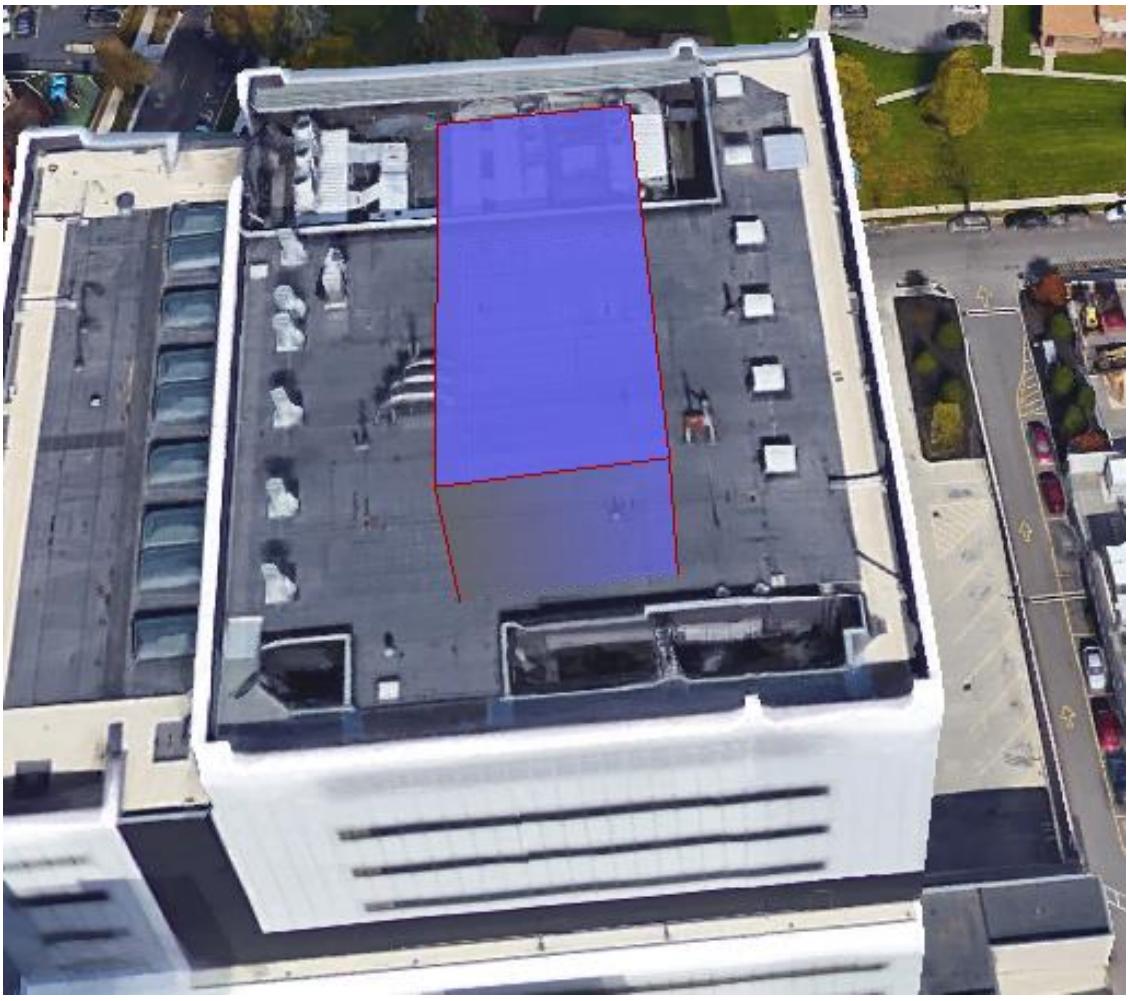

Building Number: 27

Olmsted Center for Sight/Ross Eye Institute

Entity: UB

Area (m^2): 638.9

Annual Energy (kWh/yr) @25C: 55,355.70

Annual Energy (kWh/yr) @45C: 39,136.20

Peak Power (kWdc) @25C: 47.5

Peak Power (kWdc) @45C: 35.4

Building Number: 28

Employee Parking

Entity: BNMC

Area (m^2): 6,624

Annual Energy (kWh/yr) @25C: 573,700

Annual Energy (kWh/yr) @45C: 424,830

Peak Power (kWdc) @25C: 492.7

Peak Power (kWdc) @45C: 367.4

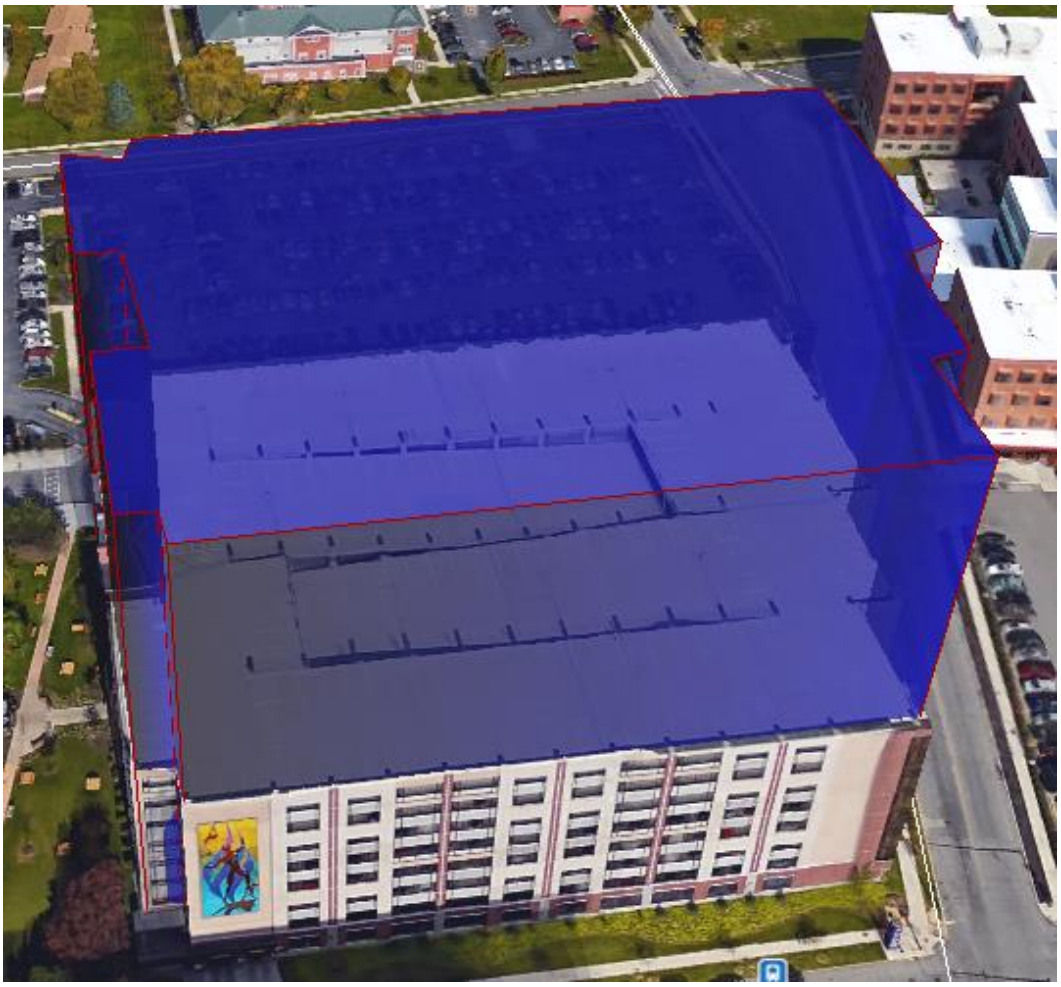

Building Number: 29

Highpointe on Michigan

Entity: Kaleida Health

Area (m^2): 670

Annual Energy (kWh/yr) @25C: 57,616

Annual Energy (kWh/yr) @45C: 40,619

Peak Power (kWdc) @25C: 49.8

Peak Power (kWdc) @45C: 37.2

Building Number: 30

Roswell Park Clinical Sciences Center

Entity: RPCI

Area (m^2): 411

Annual Energy (kWh/yr) @25C: 7,813

Annual Energy (kWh/yr) @45C: 5,534

Peak Power (kWdc) @25C: 7.6

Peak Power (kWdc) @45C: 5.7

Since the building is still under construction, the area for solar was chosen to be 25% of the roof area.

Building Number: 31

Roswell Parking Garage

Entity: RPCI

Area (m^2): 7,531

Annual Energy (kWh/yr) @ 25C: 651,425

Annual Energy (kWh/yr) @ 45C: 484,627

Peak Power (kWdc) @ 25C: 560.1

Peak Power (kWdc) @ 45C: 417.7

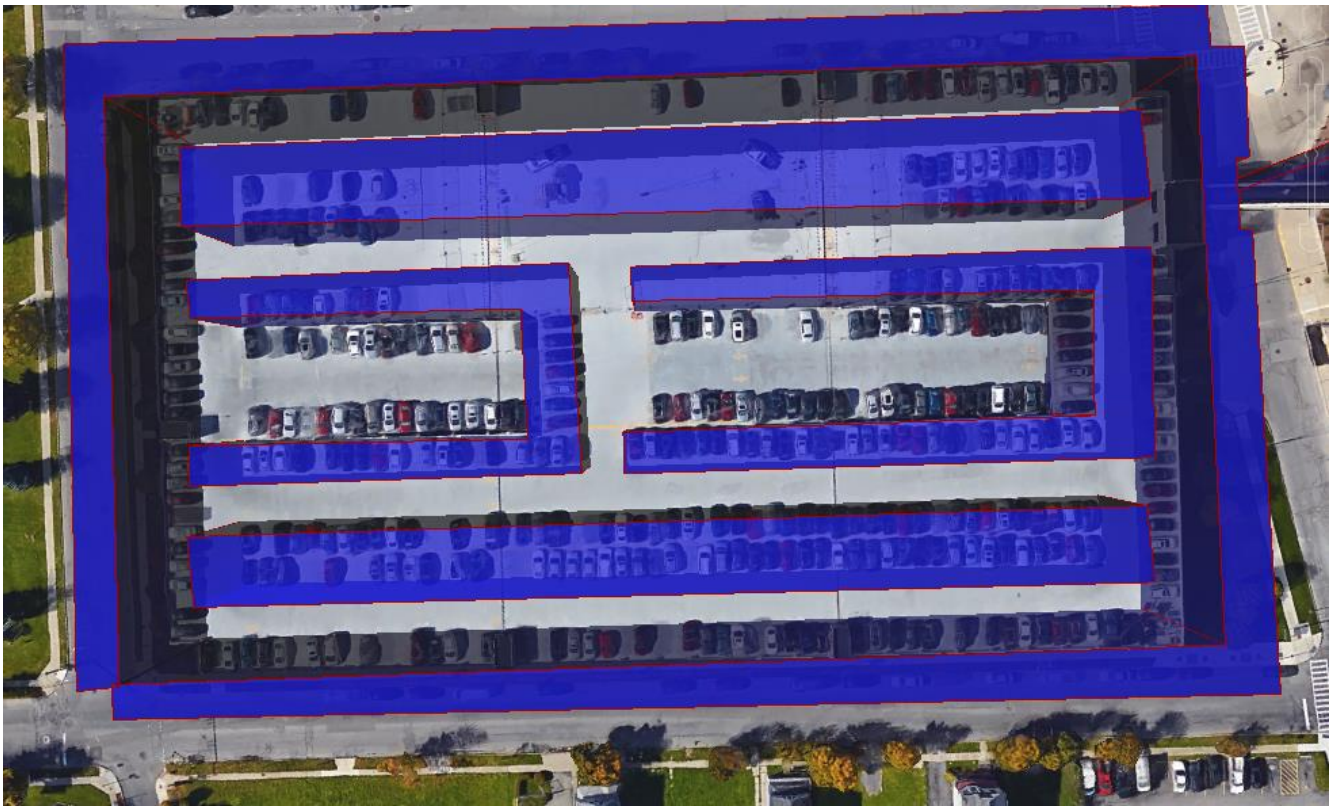

Solar was only placed over parking spaces on the highest level.

Fruit Belt Homes

Address: 248 Peach St.

Area (m^2): 45.1

Array Size (kWdc): 3.3

Annual Energy (kWh/yr) @25C: 3,254.6

Annual Energy (kWh/yr) @45C: 2,115.6

Address: 281 Peach St.

Area (m^2): 48.8

Array Size (kWdc): 3.6

Annual Energy (kWh/yr) @25C: 3,254.6

Annual Energy (kWh/yr) @45C: 2,115.6

Address: 44 Orange St.

Area (m^2): 54.6

Array Size (kWdc): 4.0

Annual Energy (kWh/yr) @25C: 4,394.2

Annual Energy (kWh/yr) @45C: 3,254.6

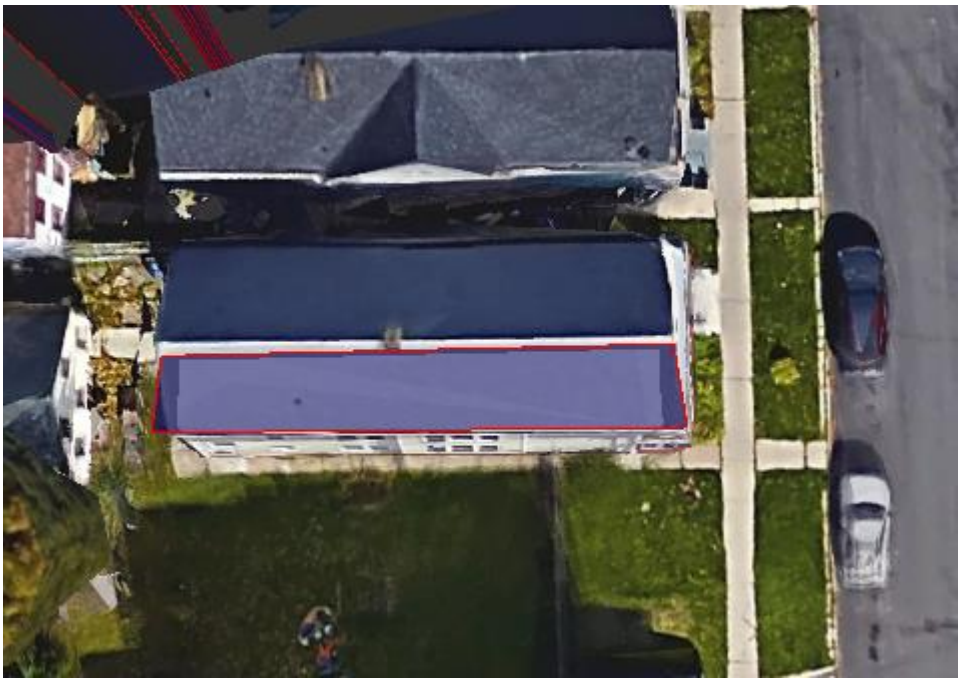

NYSERDA, a public benefit corporation, offers objective information and analysis, innovative programs, technical expertise, and support to help New Yorkers increase energy efficiency, save money, use renewable energy, and reduce reliance on fossil fuels. NYSERDA professionals work to protect the environment and create clean-energy jobs. NYSERDA has been developing partnerships to advance innovative energy solutions in New York State since 1975.

To learn more about NYSERDA's programs and funding opportunities, visit nyserda.ny.gov or follow us on Twitter, Facebook, YouTube, or Instagram.

New York State Energy Research and Development Authority

17 Columbia Circle
Albany, NY 12203-6399

toll free: 866-NYSERDA
local: 518-862-1090
fax: 518-862-1091

info@nyserda.ny.gov
nyserda.ny.gov

State of New York
Andrew M. Cuomo, Governor

New York State Energy Research and Development Authority
Richard L. Kauffman, Chair | Alicia Barton, President and CEO